

***FRZB* gene expression regulation *in vitro* to
restore muscle fibre homeostasis in limb-girdle
muscular dystrophy type 2A (LGMD2A) and *Frzb*^{-/-}
murine model muscle analysis**

Leire Casas Fraile

2018

(c)2018 LEIRE CASAS FRAILE

A dissertation submitted to the Neuroscience Department (Faculty of Medicine and Nursing) of the University of the Basque Country, in partial fulfillment of the requirements for the degree of Doctor of Philosophy.

Autorizacion de la comision academia

Autorizacion del departamento

ACTA DE GRADO DE DOCTOR O DOCTORA ACTA DE DEFENSA DE TESIS DOCTORAL

DOCTORANDA: **Doña Leire Casas Fraile.**

TITULO DE LA TESIS: **FRZB gene expression regulation analysis *in vitro* to restore muscle fibre homeostais in limb-girdle muscular dystrophy type 2A (LGMD2A) and *Frzb*^{-/-} murine model muscle analysis.**

El Tribunal designado por la Comisión de Postgrado de la UPV/EHU para calificar la Tesis Doctoral arriba indicada y reunido en el día de la fecha, una vez efectuada la defensa por el/la doctorando/a y contestadas las objeciones y/o sugerencias que se le han formulado, ha otorgado por _____ la calificación de:
unanimidad ó mayoría

--

SOBRESALIENTE / NOTABLE / APROBADO / NO APTO

Idioma/s de defensa (en caso de más de un idioma, especificar porcentaje defendido en cada idioma):

Castellano _____

Euskera _____

Otros Idiomas (especificar cuál/cuales y porcentaje) _____

En _____ a _____ de _____ de _____

EL/LA PRESIDENTE/A,

EL/LA SECRETARIO/A,

Fdo.:

Fdo.:

Dr/a: _____

Dr/a: _____

VOCAL 1º,

VOCAL 2º,

VOCAL 3º,

Fdo.:

Fdo.:

Fdo.:

Dr/a: _____

Dr/a: _____

Dr/a: _____

EL/LA DOCTORANDO/A,

Fdo.: Leire Casas Fraile

ESKERRAK- AGRADECIMIENTOS- ACKNOWLEDGEMENTS

Ikerketa hau Biodonostia Osasun Ikerketa Institutuko Neurozientzien departamentuan eta Leuveneko unibertsitate katolikoko Rik Lories doktoreak buru duen Tissue Homeostasis and Disease departamentuan garatu da, Amets Sáenz doktorearen gidaritzapean. Ikerlana, Eusko Jaurlaritzako Hezkuntza, Unibertsitate eta Ikerketa Sailaren ikertzaileak prestatzeko dokoretza-aurreko beka bati esker, Osteoarthritis Research Society International (OARSI), Gipuzkoako Eritasun Neuromuskularren Elkarteak (GENE) eta Esapiniako gobernuaren hainbat diru laguntzei esker burutu ahal izan da.

Este proyecto de investigación ha sido realizado en el Departamento de Neurociencias del Instituto de Investigación Sanitaria Biodonostia y en el departamento de Tissue Homeostasis and Disease de la Universidad católica de Lovaina liderado por el Dr. Rik Lories, bajo la dirección de la doctora Amets Sáenz. El proyecto ha sido realizado gracias a una beca para la Formación de Investigadores predoctorales del Departamento de Educación, Universidades e Investigación del Gobierno Vasco, la asociación Osteoarthritis Research Society International (OARSI), la Asociación Guipuzcoana de Enfermos Neuromusculares (GENE) y el Gobierno de España.

This research Project has been conducted in the Neuroscience Department at Biodonostia Health Research Institute and in Tissue Homeostasis and Disease group led by Dr. Rik Lories at Catholic University of Leuven, under the guidance of Doctor Amets Sáenz. The project has been funded by a predoctoral fellowship given by the department of Education, Universities and Research of the Basque Government, and several grants conceded by Osteoarthritis Research Society International (OARSI), Guipuzcoan Association of Neuromuscular Patients (GENE) and the Spanish Government.

INDEX

INDEX	17
INDEX OF FIGURES	20
INDEX OF TABLES	24
ABBREVIATIONS AND ACRONYMS	25
<u>RESUMEN</u>	31
<u>INTRODUCTION</u>	39
1. Muscle	41
1.1 Skeletal muscle	42
1.1.1 Skeletal muscle structure	42
1.1.2 Muscle innervation and muscle contraction	48
1.1.3 Skeletal muscle fibre type	49
2. Myogenesis	51
2.2 Signal regulation in myogenesis	54
2.1.1 Wnt signaling during myogenesis	55
3. Muscular dystrophy	58
3.1 Limb girdle muscular dystrophy	58
3.2 Limb girdle muscular dystrophy type 2A (LGMD2A)	59
3.2.1 Epidemiology	59
3.2.2 Clinical features	59
3.2.3 Genotype-phenotype correlation	63
3.2.4 The current status of therapies for LGMD2A	63
3.2.5 Models for muscular dystrophy studies	64
4. Calpains	67
4.1 Calpain superfamily classification	67
4.2 Calpain structure and functions	68
4.3 Calpain 3	70
4.3.1 Calpain 3 structure	70
4.3.2 Calpain 3 activation and regulation	72
4.3.3 Calpain 3 functions	74
4.3.3.1 Calpain 3 and sarcomere remodelling	74
4.3.3.2 Calpain 3 and apoptosis	75
4.3.3.3 Calpain 3 and mitochondria	76
4.3.3.4 Calpain 3 and calcium mediated signaling	76
4.3.3.5 Calpain 3 and regeneration	77
4.3.3.6 Calpain 3 deregulation in tumour tissue	78

HYPOTHESES AND OBJECTIVES	79
MATERIAL AND METHODS	83
1. Biological material	85
1.1 Human origin samples	85
1.2 Murine origin samples	87
2. RNA isolation	88
2.1 RNA isolation from human or murine skeletal muscle	88
2.2 RNA isolation from human or murine cells	89
2.3 RNA quantification	89
2.4 cDNA synthesis: reverse transcription polymerase chain reaction (RT-PCR)	90
2.5 Real-time quantitative PCR	91
2.5.1 SYBR Green-based detection	91
2.5.2 TaqMan™-based detection	93
3. Protein extraction	95
3.1 Protein isolation from skeletal muscle	95
3.2 Protein isolation from cells	96
3.3 Protein quantification	97
3.4 Protein analyses	97
3.4.1 Western blot analysis	97
3.4.2 Immunofluorescence analyses	99
3.4.2.1 Immunofluorescence analysis of cell cultures	99
3.4.2.2 Immunofluorescence analysis of skeletal muscle	99
3.4.3 Immunohistochemistry	101
3.4.3.1 Hematoxylin and eosin staining	101
3.4.3.2 β -nicotinamide adenine dinucleotide–tetrazolium reductase transferase (NADH-t) staining	101
4. Cell culture	103
4.1 Human primary cells	103
4.2 Murine origin cells	106
4.2.1 C2C12 cell line	106
4.2.2 Murine primary cells	106
4.2.2.1 Satellite cells	106
4.2.2.2 Mesoangioblasts (MABs)	107
5. RNA interference knockdown experiments	110
5.1 Gene silencing in human/murine myotubes	110
5.2 Gene silencing in human/murine myotubes at early and late stage of differentiation....	110
6. LiCl administration experiments	111
7. Foetal bovine serum (FBS) and human heterologous serum (HHS) influence analysis in human primary myotubes	111
7.1 Serum obtaining	111
7.2 Myotubes culture	112
8. <i>Frzb</i>^{-/-} mice functional analysis	112

8.1 Muscle strength analysis	112
8.2 Muscle regeneration analysis	112
8.3 Chronic exercise protocol on a treadmill	112
8.4 Mice gait analysis	113
9. Bioinformatics tools	115
10. Statistical analysis	115
<u>CHAPTER1: <i>In vitro</i> analyses of the pathophysiology of LGMD2A</u>	117
Results	119
Discussion	147
<u>CHAPTER 2: Study of Frzb absence effects in the muscle of a murine model (<i>Frzb</i>^{-/-}) <i>in vitro</i> and <i>in vivo</i></u>	165
Results	167
Discussion	199
<u>CONCLUSIONS</u>	211
<u>APPENDIX</u>	215
APPENDIX I: Material and methods supplementary material	217
APPENDIX II: Product references	221
APPENDIX III: Publications	239
<u>BIBLIOGRAPHY</u>	240

INDEX OF FIGURES

Figure 1	Representative images of skeletal, cardiac and smooth muscle stained with hematoxylin and eosin	41
Figure 2	Skeletal muscle structure	43
Figure 3	Sarcoplasmic reticulum and T-tubule representation	44
Figure 4	Skeletal muscle's sarcomere organization	45
Figure 5	(a) Schematic representation of thin filament. (b) Schematic representation of thick filament	45
Figure 6	Schematic representation of muscle costamere	47
Figure 7	(a) Myosins immunofluorescence analysis of mouse muscle cross-sections. (b) Myosins immunofluorescence analysis of human muscle cross-sections	50
Figure 8	Schematic representation of canonical Wnt signaling	56
Figure 9	(a-b) Immunohistochemical analyses of muscle biopsy of control and LGMD2A patients. (c) Electron microscopy images of subsarcolemmal region in control and LGMD2A patients	61
Figure 10	Regression line between muscle and myoblast/myotubes control samples, based on ΔCT	65
Figure 11	Schematic representation of (a) classical and (b) non-classical calpains structure.....	69
Figure 12	Schematic representations of classical calpain (a) protein and (b) gene	71
Figure 13	Calpain 3 3D structure	71
Figure 14	Schematic representation of calpain 3 activation	72
Figure 15	(a) A model for calpain 3, titin and associated proteins in the sarcomere. (b) Calpain 3 autolytic cleavage avoidance mediated by titin	73
Figure 16	NADH-T staining in <i>Tibialis anterior</i> where different fibre types are visualized	102
Figure 17	Schematic representation of human primary cells (myoblast) isolation	105
Figure 18	Mouse performing muscle strength analysis	112
Figure 19	Schematic representation of mouse step cycle	114
Figure 20	Schematic representation of mouse base of support (mm)	115
Figure 21	Morphology of human (a-b) control and (c) LGMD2A myotubes with FBS or HHS ...	120
Figure 22	Morphology of human (a-b) control and (c) LGMD2A myotubes at 16 days of differentiation grown with FBS or HHS	121
Figure 23	(a) Gene and (b) protein expression analyses of MyH2 in myotubes grown with FBS and HHS	122

Figure 24	(a) Gene expression analysis of <i>ITGB1BP2</i> and <i>DES</i> in myotubes at 16 days of differentiation grown with FBS and HHS. (b) Western blot and densitometry analyses of myogenin, melusin and ITGβ1 in myotubes grown with FBS and HHS123
Figure 25	<i>CD9</i> , <i>ITGB1BP2</i> and <i>FRZB</i> genes expression analysis after gene silencing (si <i>CD9</i> , si <i>FRZB</i> and si <i>ITGB1BP2</i>) in myotubes obtained from distal muscle125
Figure 26	Western blot analyses of integrin β1A and β1D isoforms in myoblasts and myotubes at days 10, 16 and 20 of differentiation125
Figure 27	Western blot and densitometry analyses of integrin isoforms β1A and β1D after silencing (a) <i>ITGB1BP2</i> and (b) <i>FRZB</i> genes126
Figure 28	Immunofluorescence analysis of (a) myosin heavy chain and (b) active β-catenin in myotubes after <i>FRZB</i> silencing (si <i>FRZB</i>)127
Figure 29	Gene expression analysis of <i>COL1A1</i> , <i>COL5A1</i> , <i>FN1</i> , <i>VLDLR</i> , <i>KAL1</i> and <i>FOS</i> genes in human myotubes after <i>FRZB</i> silencing (si <i>FRZB</i>)128
Figure 30	Gene expression analysis of <i>COL1A1</i> , <i>COL5A1</i> , <i>FN1</i> , <i>VLDLR</i> , <i>KAL1</i> and <i>FOS</i> genes where silencing effect is shown129
Figure 31	Western blot and densitometry analyses of (a) P-AKT (Ser473) / AKT, (b) P-GSK3β (Ser9)/GSK3β and (c) P-ERK1/2 (Thr202/Tyr204) / ERK1/2 after <i>FRZB</i> gene silencing (si <i>FRZB</i>) in control and LGMD2A myotubes131
Figure 32	(a) Gene expression analysis of <i>FOS</i> , <i>KAL1</i> , <i>VLDLR</i> , <i>ITGB1BP2</i> , <i>FRZB</i> and <i>MYH2</i> genes in human myoblasts after LiCl 10 mM administration. (b) Western blot and densitometry analyses of ITGβ1D after LiCl 10 mM administration133
Figure 33	Western blot and densitometry analyses of (a) P-AKT (Ser473)/AKT, (b) P-GSK3β (Ser9)/GSK3β and (c) P-ERK1/2 (Thr202/Tyr204)/ERK1/2 after LiCl 10 mM treatment in control and LGMD2A myotubes134
Figure 34	(a) Immunofluorescence analysis of myotubes at day 11 of differentiation after LiCl administration and <i>FRZB</i> gene silencing (si <i>FRZB</i>) at one day or 8 days of differentiation. (b) Total nuclei and fusion index (%) analyses136
Figure 35	(a) Immunofluorescence analysis of myotubes formation and β-catenin nuclear translocation after <i>Frzb</i> gene silencing (si <i>Frzb</i>) in myotubes at 1 day of differentiation and fixed at day 7 post differentiation. (b) Total nuclei and fusion index (%) analyses137
Figure 36	Immunofluorescence analysis of myotubes formation and β-catenin nuclear translocation after <i>Frzb</i> gene silencing (si <i>Frzb</i>) in myotubes at 3 day of differentiation and fixed at day 9 post differentiation. (b) Total nuclei and fusion index (%) analyses138
Figure 37	Gene expression analysis of C2C12 myotubes after <i>Frzb</i> gene silencing (si <i>Frzb</i>) (a) at early and later stages and (b) in non-maintained treatment139
Figure 38	Western blot and densitometry analyses of integrin isoforms β1D and β1A in C2C12 myotubes after <i>Frzb</i> gene silencing (si <i>Frzb</i>) (a) at early and later stages and (b) in non-maintained treatment140

Figure 39	Western blot and densitometry analyses of P-p70S6K (a) (Thr-421/Ser-424) and (b) (Thr-389) in control and LGMD2A patients' skeletal muscles142
Figure 40	Western blot and densitometry analyses of P-RPS6 (Ser-235/Ser-236) in control and LGMD2A patients' skeletal muscles143
Figure 41	Western blot and densitometry analyses of total FoxO1 and phosphorylated FoxO1 (Ser-256) proteins in control and LGMD2A patients' skeletal muscles144
Figure 42	Western blot and densitometry analyses of total FoxO3a and phosphorylated FoxO3 (Ser-253) proteins in control and LGMD2A patients' skeletal muscles144
Figure 43	Western blot and densitometry analyses of phosphorylated FoxO4 (Thr-28) proteins in control and LGMD2A patients' skeletal muscles145
Figure 44	Western blot and densitometry analyses of (a) MuRF1 and (b) atrogin-1 proteins in control and LGMD2A patients' skeletal muscles145
Figure 45	Western blot and densitometry analyses of (a) BNIP3 and (b) beclin 1 proteins in control and LGMD2A patients' skeletal muscles146
Figure 46	Schematic representation of a potential model of the regulation of FRZB, CD9 and melusin in the skeletal muscle151
Figure 47	Schematic representation of a potential model of the regulation of the genes of interest153
Figure 48	Schematic representation of LGMD2A patients' pathophysiological scenario in the skeletal muscle163
Figure 49	(a) WT and <i>Frzb</i> ^{-/-} mice body weight (g) and (b) correlation graph of the hanging time (s)167
Figure 50	Eight and 10 week-old mice paw statistic; stand, swing time, step cycle, swing speed and stride length168
Figure 51	Eight and 10 week-old mice BOS and 10 week-old mice step pattern, step regularity index and step sequence170
Figure 52	Different paw supports in mice171
Figure 53	Four week-old mice (a) body and (b) muscles weight172
Figure 54	(a) Ten and 14 week-old mice hematoxylin and eosin stained <i>Soleus</i> and (b) fibres CSA173
Figure 55	<i>Tibialis anterior</i> and <i>Soleus</i> muscles myosin heavy chain isoforms expression174
Figure 56	(a) NADH transferase staining and (b) NADH transferase staining based fibre-type composition of <i>Tibialis anterior</i>174
Figure 57	Mice body weight (g) while chronic exercise procedure175
Figure 58	<i>Tibialis anterior</i> , <i>Gastrocnemius</i> and <i>Quadriceps</i> weight (mg) after chronic exercise procedure176

Figure 59	(a) Hematoxylin and eosin stained <i>Soleus</i> and (b) fibres CSA after chronic exercise procedure177
Figure 60	(a) NADH transferase staining and (b) NADH transferase staining based fibre-type composition of <i>Tibialis anterior</i> after chronic exercise procedure178
Figure 61	(a) <i>Pax7</i> , (b) <i>Myod</i> , (c) <i>Myog</i> and (d) <i>Myh3</i> gene expression in <i>Gastrocnemius</i> after chronic exercise procedure179
Figure 62	(a) Gene and (b) protein expression analyses of atrogenes (atrogin and MuRF1) in <i>Gastrocnemius</i> after chronic exercise procedure180
Figure 63	Western blot and densitometry analyses of (a) AKT and P-AKT (Ser473), (b) ERK1/2 and P-ERK1/2 (Thr202/Tyr204) and (c) GSK3 β and P-GSK3 β (Ser9) after chronic exercise procedure181
Figure 64	Hematoxylin and eosin stained <i>Tibialis anterior</i> sections after CTX injection experiment183
Figure 65	Hematoxylin and eosin stained <i>Soleus</i> sections after CTX injection experiment184
Figure 66	Immunofluorescence analysis of satellite cells and myotubes185
Figure 67	Percentage of alkaline phosphatase positive and negative cells in WT and <i>Frzb</i> ^{-/-} mice187
Figure 68	FACS data showing CD31, CD45 and CD140A expression187
Figure 69	(a) <i>Cd140a</i> (<i>Pdgfra</i>) and (b) <i>Cd140b</i> (<i>Pdgfrb</i>) gene expression in <i>Tibialis anterior</i> and <i>Soleus</i> of 10 week-old WT and <i>Frzb</i> ^{-/-} mice188
Figure 70	Immunofluorescence staining of <i>Tibialis anterior</i> using PGFR β , alkaline phosphatase, NG2 and α SMA antibodies189
Figure 71	Western blot analyses and protein quantification in (a) <i>Tibialis anterior</i> and (b) <i>Soleus</i> of WT and <i>Frzb</i> ^{-/-} mice where α SMA, NG2, PDGFR β and ALP proteins are analysed190
Figure 72	Representative images of ALP+ cells differentiated into adipocytes. (a-d) Immunofluorescence images and (e-h) bright field images191
Figure 73	Oil red O quantification192
Figure 74	Gene expression analysis of several genes in <i>Tibialis anterior</i> and <i>Soleus</i>193
Figure 75	Gene expression analysis of <i>FRZB</i> , <i>CAPN3</i> , <i>MYOD</i> and <i>MYOG</i> genes in <i>FRZB</i> silencing (<i>siFRZB</i>) experiments196
Figure 76	Gene expression analysis of <i>CAPN3</i> in 3 controls and two LGMD2A patients' myotubes treated with LiCl 10mM196
Figure 77	(a) Western blot and densitometry analyses of MyoD and Calpain 3 in <i>Tibialis anterior</i> . (b) Western blot and densitometry analyses of MyoD, Calpain 3 and Ky in <i>Soleus</i> ...198

INDEX OF TABLES

Table 1	Fibre type classification and characteristics	50
Table 2	Muscle-resident mesenchymal cells	53
Table 3	Human calpain superfamily members' summary	68
Table 4	Control and LGM2A human samples information	86
Table 5	Information of used mice	88
Table 6	Reverse transcription master mix composition and volumes for a final volume of 25µl	90
Table 7	Thermal cycler conditions	90
Table 8	PCR reaction mix components	92
Table 9	Thermal cycling programme	99
Table 10	PCR reaction mix	93
Table 11	Thermal cycling protocol for gene expression analysis	94
Table 12	Nicholson and Paris buffers composition	95
Table 13	RIPA buffer composition	96
Table 14	SDS-polyacrylamide gel composition	97
Table 15	SDS protein sample buffer composition (4X)	98
Table 16	Running (10X) and Transfer (5X) buffers composition	98
Table 17	TBS (10X) and TBST (1X) buffers composition	98
Table 18	Blood donors' information	111
Table 19	Step pattern code and its corresponding step sequence	114
Table 20	A summary of c-Fos, c-Jun and AP-1 transcription factors (TF) binding site prediction for <i>COL1A</i> , <i>COL5A1</i> , <i>FN1</i> , <i>VLDLR</i> and <i>KAL1</i> genes	130
Table 21	Gene expression representation in LGMD2A patients and in FoxO activated models (<i>Lmna</i> ^{-/-} mice and C26 tumour-bearing cachectic mice)	162
Table 22	Mice weights values (g)	168
Table 23	Genotype influence in stand, swing phase, step cycle, swing speed and stride length calculated by two-way ANOVA analysis	169
Table 24	Mice body weight (g), total muscle weight (mg) and obtained cell amount after muscles digestion	185
Table 25	A summary of c-Fos, c-Jun and AP-1 transcription factors binding site prediction for <i>CAPN3</i> gene	197

ABBREVIATIONS AND ACRONYMS

A or a	Adenine
AAV	Adeno-associated virus
Ab	Antibody
Adipoq	Adiponectin
AldoA	Aldolase A
ALP	Alkaline phosphatase
AMPK	5' AMP-activated protein kinase
AP-1	Activator protein 1
APC	Allophycocyanin
APS	Ammonium persulfate, (NH ₄) ₂ S ₂ O ₈
Asn	Asparagine
Aspn	Asporin
Atgs	Autophagy related proteins
ATP	Adenosine triphosphate
BMP	Bone morphogenetic protein
BMSC	Bone marrow stromal cells
BNIP3	Bcl2 interacting protein 3
BOS	Base of support
bp	Base pair
BSA	Bovine serum albumin
C or c	Cytosine
c.	Coding
C2	Protein kinase C conserved domain
C3KO	<i>Capn3</i> knockout mice model
C57BL/6	C57 black 6 mouse
Ca²⁺	Calcium ion
CaM	Calmodulin
CaMK	Ca ²⁺ -calmodulin-dependent protein kinase
CammKII	Calcium-calmodulin-dependent kinase II
CAPN	Calpain
CAPN3 or p94	Calpain 3
Capn6	Calpain 6
CAPNS1	Calpain small regulatory subunit 1
CBSW	Calpain-type beta-sandwich domain
CD	Cluster of differentiation
CD9	CD9 molecule
cDNA	Complementary DNA
CK	Creatine kinase
CKI	Casein kinase I
cm	Centimetres
Col15a1	Collagen, type XV, alpha 1
Col1a1 or COL1A1	Collagen, type I, alpha 1
Col3a1	Collagen, type III, alpha 1
Col5a1	Collagen, type V, alpha 1
C_q	Quantification cycle
CSA	Cross-sectional area
CST	Cell Signaling Technology
CT	Threshold cycle

Cthrc1	Collagen triple helix repeat containing 1
Ctnnb1	Catenin (cadherin associated protein), beta 1
CTX	Cardiotoxin
Cys or C	Cysteine
CysPC	Calpain-like protease domain
D or Asp	Aspartic acid
DES	Desmin
dH₂O	Distilled water
Dkk	Dickkopf
DMD	Duchenne muscular dystrophy
Dmd	Dystrophin
DMEM	Dulbecco's modified eagle medium
DMSO	Dimethyl sulfoxide
DNA	Deoxyribonucleic acid
dNTP	Deoxynucleotide
Dok5	Docking protein 5
DPBS	Dulbecco's phosphate-buffered saline
DSHB	Developmental studies hybridoma bank
Dvl	Dishevelled scaffold protein
dy/dy	Congenital muscular dystrophy mice model
E2f8	E2F transcription factor 8
ECM	Extracellular matrix
EGF	Epidermal growth factor
ERK 1/2	Extracellular signal-regulated kinases 1/2
ESCs	Embryonic stem cells
F or f	Female
FACS	Fluorescence-activated cell sorting
FAK	Focal adhesion kinase
FAPs	Fibro/adipogenic progenitors
Fasn	Fatty acid synthase
FBS	Foetal bovine serum
Fbx32 or FBX32	F-Box protein 32, muscle atrophy F-Box protein and atrogenin-1
FCS	Foetal calf serum
fg	Femto grams
FGF	Fibroblast growth factor
Fhl1	Four and a half LIM domains 1
FITC	Fluorescein isothiocyanate
Fn1 or FN1	Fibronectin 1
FOS	Fos proto-oncogene, AP-1 transcription factor subunit
FoxO	Forkhead box class O
FRZB or Frzb	Frizzled related protein
Frzb^{-/-}	Frizzled related protein knock-out mice model
fs	Frame shift
FSHD	Facioscapulohumeral muscular dystrophy
Fzd	Frizzled
G or g	Guanine
G or Gly	Glycine
Gapdh or GAPDH	Glyceraldehyde-3-phosphate dehydrogenase

gDNA	Genomic DNA
Glu	Glutamic acid
GSK3β	Glycogen synthase kinase-3 β
h	hours
H or His	Histidine
HBSS	Hank's balanced salt solution
HCl	Hydrochloric acid
HDAC	Histone deacetylase
Hepes	4-(2-hydroxyethyl)-1-piperazineethanesulfonic acid
HRP	Horseradish peroxidase
HS	Horse serum
HZ	Hertz
ID	Identification
IGF-1 or Igf1	Insulin-like growth factor-1
IKKβ	Inhibitor of nuclear factor kappa-B kinase subunit beta
ILK	Integrin-linked kinase
IP	Intraperitoneal
IS1/2	Insertion sequence 1/2
Itgb1bp2 or ITGB1BP2	Integrin beta 1 binding protein 2, melusin
ITGβ1A	β 1A integrin
ITGβ1D	β 1D integrin
IκBα	Nuclear factor of kappa light polypeptide gene enhancer in B-cells inhibitor, alpha
JAG1	Jagged 1
KAL1	Anosmin-1
kDa	Kilo Dalton
KO	Knockout
Ky	Kyphoscoliosis peptidase
Leu	Leucine
LF	Left front
LGMD	Limb girdle muscular dystrophy
LGMD2A	Limb girdle muscular dystrophy type 2A
LH	Left hind
<i>Lmna</i>^{-/-}	Laminopathies mice model
LRP5/6	Low density lipoprotein receptor-related proteins 5/6
Lys	Lysine
M or m	Male
m/s	Meters/seconds
M-199	Medium 199
MABs	Mesoangioblasts
MAPK	Mitogen-activated protein kinase
<i>mdx</i>	Duchenne muscular dystrophy mice model
MEF2	Myocyte enhancer factor 2
Mest	Mesoderm specific transcript
Mg²⁺	Magnesium ion
min	Minutes
miRNA	Micro RNA

MIT	Microtubule interacting and transport
ml	Millilitres
mM	Millimolar
Mrf4	Myogenic factor 6
MRFs	Myogenic regulatory factors
mRNA	Messenger RNA
MSCs	Mesenchymal stem cells
mTOR	Mammalian target of rapamycin
Murf1 or MURF1	Muscle-specific RING finger protein 1
Myc	Myelocytomatosis oncogene
Myf5	Myogenic factor 5
Myh1	Myosin, heavy polypeptide 1, skeletal muscle, adult
Myh2 or MYH2	Myosin, heavy polypeptide 2, skeletal muscle, adult
MyH3	Myosin heavy chain 3
Myh4	Myosin, heavy polypeptide 4, skeletal muscle
MyHC	Myosin heavy chain
MyI6b	Myosin, light polypeptide 6B
MyLC	Myosin light chain
MyoD	Myogenic differentiation 1
Myog or MYOG	Myogenin
Myom3	Myomesin family, member 3
Myot	Myotilin
Na⁺	Sodium ion
Na₃O₄V₂	Sodium orthovanadate
NaCl	Sodium chloride
NADH	Reduced nicotinamide adenine dinucleotide
NADH-t	β -nicotinamide adenine dinucleotide-tetrazolium reductase transferase
NaF	Sodium fluoride
NaN₃	Sodium azide
NBT	Nitro blue tetrazolium chloride
N-CAM or CD56	Neural cell adhesion molecule
NCX	Na ⁺ /Ca ²⁺ exchanger
NFAT	Nuclear factor of activated T-cells
NF-κB	Nuclear factor-kappa B
ng	Nano grams
NG2	Neuro-glial 2 proteoglycan
nm	Nanometres
nNOS	Nitric oxide synthase
p.	Protein
P/S	Penicillin/streptomycin
P-AKT	Phosphorylated AKT
Park2	Parkin
Pax3	Paired box 3
Pax7	Paired box 7
PBS	Phosphate-buffered saline
PC1/2	Protease core subdomain 1/2
PCR	Polymerase chain reaction
PCs	Pericytes

PDGFRα	Platelet derived growth factor receptor alpha
PDGFRβ	Platelet derived growth factor receptor beta
PE	Phytoerythrin
PECAM-1	Platelet and endothelial cell adhesion molecule 1
PEF	Penta E-F hand
P-ERK 1/2	Phosphorylated extracellular signal-regulated kinases 1/2
PFA	Paraformaldehyde
P-GSK3β	Phosphorylated glycogen synthase kinase-3 β
PICs	PW1 positive interstitial cells
PINCH	Cysteine-histidine-rich protein
PKC	Protein kinase C
PLC	Phospholipase C
PLEIAD	Platform element for inhibition of autolytic degradation
PMCA	Plasma membrane Ca ²⁺ ATPase
PMSF	Phenylmethane sulfonyl fluoride
P-p70S6K	Phosphorylated p70S6K
Pparg	Peroxisome proliferator activated receptor gamma
Pro	Proline
P-RPS6	Phosphorylated ribosomal protein S6
PSCs	Pluripotent stem cells
PTPRC	Protein tyrosine phosphatase, receptor type, C
Q	Glutamine
R or Arg	Arginine
RF	Right front
RH	Right hind
RNA	Ribonucleic acid
Rora	RAR-related orphan receptor alpha
rpm	Revolutions per minute
RPS6	Ribosomal protein S6
rRNA	Ribosomal RNA
RT	Room temperature
RT-PCR	Reverse transcription polymerase chain reaction
RyR1	Ryanodine receptor 1
Ryr2	Ryanodine receptor 2
s	Seconds
S6K1	S6 Kinase 1
Sca-1	Stem cells antigen-1
SDS	Sodium dodecyl sulphate
Sema3c	Semaphorin 3C
Ser or S	Serine
SERCA	Sarcoplasmic reticulum Ca ²⁺ -ATPase
sFRP	Secreted frizzled-related protein
SHD	Succinate dehydrogenase
Shh	Sonic hedgehog
siRNA	Small interfering RNAs
Six 1/4	Sine oculis homeobox homolog 1/4
Slc16a1	Solute carrier family 16 (monocarboxylic acid transporters), member 1
SOL	Small lobes product homology

Sorbs1	Sorbin and SH3 domain containing 1
SR	Sarcoplasmic reticulum
SRF	Serum response factor
T or t	Thymine
TA	Tibialis anterior
Tbp or TBP	TATA box binding protein
TCF/LEF	T-cell factor/lymphoid enhancer factor
TEMED	N,N,N',N'-Tetramethyl-ethylenediamine
TF	Transcription factors
Tfrc	Transferrin receptor
Thr	Threonin
TLDA	TaqMan low-density arrays
Tm	Melting temperature
Tn	Troponin
Tris	Tris (hydroxymethyl) aminomethane
Trp	Tryptophan
TTN	Titin
UDG	Uracil-DNA glycosylase
VCAM1	Vascular cell adhesion molecule -1
VGM	Walton & Gardner-Medwin
Vldlr or VLDLR	Very low density lipoprotein receptor
Wnt8a	Wingless-related MMTV integration site 8a
Wnt8b	Wingless related MMTV integration site 8b
WT	Wild-type
Zn	Zinc-finger
αSMA	Alpha-smooth muscle actin
μl	Microliters

RESUMEN

Las distrofias musculares son un conjunto heterogéneo de afecciones hereditarias caracterizadas por debilidad muscular y pérdida progresiva del tejido muscular. Están causadas por mutaciones en genes que codifican para proteínas requeridas para el normal funcionamiento del músculo.

Inicialmente las distrofias musculares fueron clasificadas atendiendo a características clínicas sin embargo, debido al avance en técnicas genéticas, hoy en día la clasificación se basa en los genes mutados y sus respectivas proteínas.

Hay diversos tipos de distrofias musculares, la más abundante es la distrofia miotónica tipo 1 seguida por la distrofia facioscapulohumeral y las distrofinopatías. Las distrofias musculares de cinturas (LGMD, de su nombre en inglés limb-girdle muscular dystrophy) son la cuarta forma más común, con una prevalencia estimada de 1,63 casos por 100 000 habitantes.

Las distrofias musculares de cinturas comprenden un grupo heterogéneo de distrofias musculares las cuales comparten características clínicas similares. Se dividen atendiendo a su patrón de herencia, siendo de tipo uno (LGMD1) o tipo dos (LGMD2) cuando su herencia es autosómica dominante o autosómica recesiva respectivamente. Las diversas enfermedades son clasificadas usando un índice alfabético según el orden cronológico de identificación. Según la última revisión de diciembre del año 2017, a día de hoy, hay descritas 8 distrofias musculares con herencia autosómica dominante (LGMD1A-1H) y 26 con herencia autosómica recesiva (LGMD2A-2Z).

Este trabajo se centra en el estudio de la distrofia muscular de cinturas tipo 2A (LGMD2A) también conocida como calpainopatía. Está causada por mutaciones en el gen de la calpaina 3 (*CAPN3*).

Dentro del grupo de distrofias de cinturas es la más frecuente siendo de entre un 20% y un 50% de los casos. Una de las mayores prevalencias mundiales se encuentra en Guipúzcoa con 69 casos por millón de habitantes.

El debut de la enfermedad se da en la segunda década de vida pudiendo ser anterior o posterior en casos aislados. Los primeros síntomas se caracterizan en su mayoría por una debilidad de los músculos proximales de las extremidades. Los pacientes también presentan elevados niveles de creatina quinasa en sangre (entre 5 y 20 veces) los cuales decrecen hasta alcanzar niveles normales en pacientes postrados en silla de ruedas donde la atrofia muscular es muy notoria.

Como se ha comentado, los músculos proximales de las extremidades son los primeramente aparecen afectados, ampliándose el grupo de músculos afectados según la enfermedad avanza. Aun así la afección cardíaca y la debilidad muscular de los músculos respiratorios no es una característica que se observe en este grupo. La progresión de la enfermedad es muy variable pero normalmente los

pacientes acaban confinados en una silla de ruedas después de unos 25 años de evolución de la enfermedad. Ha día de hoy no existe ningún tratamiento.

El espectro de mutaciones en el gen *CAPN3* es altamente heterogéneo, lo cual ha impedido establecer una clara correlación genotipo-fenotipo. Asimismo, el desarrollo de la enfermedad es muy variable, habiéndose observado un similar progreso en pacientes con diferentes mutaciones en el gen y una evolución muy discordante en parientes portadores de las mismas mutaciones.

La calpaina 3 es una cistein-proteasa no lisosomal dependiente de calcio, extracelular, específica de músculo esquelético. Está englobada dentro del grupo de calpainas clásicas debido a su homología de secuencia con las calpainas 1 y 2. Además de las estructuras características de estas dos calpainas, la calpaina 3 posee 3 regiones específicas denominadas región NS, IS1 e IS2 que le confieren unas características específicas como por ejemplo su capacidad autolítica, ausentes en las de más calpainas.

Debido a su capacidad autolítica poco se sabe a cerca de su estructura así como de su regulación. Dentro de la célula muscular la calpaina 3 se une a la zona N2A y C terminal de la titina, localizadas en la zona N2 y línea M del sarcomero (unidad anatómica y funcional del músculo estriado limitado entre dos líneas Z y compuesto en su mayoría por las proteínas actina y miosina). Además también ha sido vista en la línea Z. La unión a titina protege a la calpaina 3 de ser degradada.

Desde la identificación de la calpaina 3 como causante de la LGMD2A en 1995 diversos estudios se han llevado a cabo con el objetivo de estudiar el mecanismo patofisiológico de la enfermedad. Sin embargo, las funciones de la calpaina 3 no han sido completamente elucidadas.

Gracias a diversos estudios llevados a cabo en modelos murinos donde diversas mutaciones han sido introducidas en el gen de la calpaina 3, se han podido descubrir funciones tanto proteolíticas como no proteolíticas de la enzima. Esto llevó a postular que la calpaina 3 además de su función como proteasa, también ejerce un papel estructural en la fibra muscular.

Una de las funciones atribuidas a la calpaina 3 es la remodelación del sarcómero ya que los ratones C3KO, en los cuales se ha eliminado el gen de la calpaina 3, presentan una formación anormal del mismo. También se ha relacionado la falta de calpaina 3 con un aumento de la apoptosis de los mionucleos de la fibra muscular mediada por una alteración de la ruta $\text{I}\kappa\text{B}\alpha/\text{NF-}\kappa\text{B}$. Si bien es cierto que estudios posteriores demostraron que la apoptosis no estaba sucediendo en los mionucleos, un reciente estudio observó una elevada actividad de la ruta $\text{I}\kappa\text{B}\alpha/\text{NF-}\kappa\text{B}$ en músculos de pacientes LGMD2A.

El hecho de que estudios histoquímicos mostrasen mitocondrias alteradas en pacientes y posteriores estudios observasen un aumento de mitocondrias funcionalmente deficientes las cuales

daban lugar a un aumento del estrés oxidativo pusieron de relieve la relación entre la calpaina 3 y las mitocondrias.

También se ha relacionado la calpaina 3 con la liberación de Ca^{2+} en el músculo esquelético. Se ha observado como la falta de esta enzima da lugar a una reducción de AldoA y RyR lo que produce una reducción en la liberación del calcio desde el retículo sarcoplásmico al citoplasma durante la contracción. Así mismo se ha observado una reducción de la recaptación de Ca^{2+} mediada por SERCA al retículo sarcoplásmico. Parece probada también la implicación de la calpaina en la regeneración muscular aunque la relación entre calpaina 3 y células satélite (célula madre muscular) han arrojado conclusiones contradictorias.

Este trabajo ha sido enfocado en el estudio a nivel celular y molecular de la distrofia muscular de cinturas tipo 2A para un mejor conocimiento del mecanismo fisiopatológico subyacente a esta enfermedad.

Estudios previos realizados en nuestro grupo demostraron una tendencia hacia la homogenización de las diferencias entre mioblastos y miotubos de controles y pacientes así como una falta de correlación entre la expresión génica de los modelos *in vitro* y el tejido de origen. Por ello se procedió al uso de suero humano tanto de controles como de pacientes para el cultivo *in vitro* con el objetivo de mejorar la correlación entre la expresión previamente observada en el músculo de los pacientes. Sin embargo el resultado no solo no mejoró el cultivo de miotubos sino que mostró un impacto negativo en la diferenciación de los miotubos.

El hallazgo de genes diferencialmente expresados en músculos de pacientes junto con la observación de que miotubos de pacientes mostraban una morfología anómala con un número excesivo de núcleos, lo cual daba lugar a un aumentado índice de fusión, propició el estudio donde se silenciaron diferentes genes sobre expresados en pacientes con el objetivo de estudiar la implicación de los mismos en la enfermedad. Se escogieron los genes que codifican para las proteínas CD9 y melusina por estar en contacto directo con las integrinas (proteínas esenciales en la fusión de mioblastos la cual se había visto alterada en pacientes donde el necesario recambio de la isoforma de la integrina $\beta 1A$ por la $\beta 1D$ no se producía). También se seleccionó el gen *FRZB* ya que se trata de uno de los más altamente sobre expresados en músculos de pacientes así como en miotubos.

Se postuló que la modulación de estos genes podría rescatar la fisiología de la enfermedad dando lugar al descubrimiento de posibles dianas terapéuticas. Para ello se caracterizó la expresión diferencial de genes y proteínas tras el silenciamiento de estos genes así como se estableció la implicación de los genes desregulados en la patofisiología de la enfermedad.

El estudio confirmó la relación previamente observada de estos tres genes. *CD9* y *FRZB* son reguladores positivos que actúan sobre la expresión de melusina y el gen de la melusina es un regulador negativo de la expresión de *FRZB*. Mientras se observó un efecto nocivo en los miotubos tras el silenciamiento tanto de melusina como de *CD9*, el silenciamiento de *FRZB* dio lugar a un aumento de la isoforma β 1D de las integrinas así como un aumento en la expresión de genes infra expresados en los pacientes. Por este motivo los estudios se centraron en el silenciamiento del gen *FRZB*.

La observación de que el silenciamiento de *FRZB* daba lugar a un aumento de β -catenina nuclear permitió postular que *FRZB* podría mediar en la interacción entre la ruta de Wnt/ β -catenina y las integrinas. Esta idea se apoyó en el hecho de que factores de transcripción como FOS el cual aumentaba su expresión tras el silenciamiento podrían regular la expresión de diversos genes rescatando el nivel de proteínas implicadas en la formación del costámero. El empleo de un mecanismo farmacológico (LiCl) para estimular la ruta de Wnt/ β -catenina también mostro resultados similares a los observados tras el silenciamiento del gen *FRZB*.

Así mismo se procedió al estudio de la miogénesis tras la activación de la ruta Wnt/ β -catenina en estadios tanto tempranos como tardíos de diferenciación mediante tratamiento farmacológico y silenciamiento génico. La necesidad de un correcto control de la ruta Wnt/ β -catenina en la diferenciación muscular hicieron que la inducción temprana mostrase un efecto negativo.

Por todo ello gracias a los resultados obtenidos, se propuso la regulación de la expresión de *FRZB* como potencial diana terapéutica para la enfermedad LGMD2A ya que estudios *in vitro* respaldaron la idea de que podría rescatar la expresión hacia niveles apropiados en músculos de pacientes.

Análisis previos llevados a cabo en músculos mostraron que las rutas de señalización de AKT/mTOR y de MAPK estaban alteradas en pacientes LGMD2A. Por ello, dado que el mejor conocimiento de estas rutas podría llevar a establecer los principales puntos afectados por la falta de calpaina 3, se estudiaron los efectores de estas rutas de señalización.

La elevada fosforilación de AKT previamente observada en los músculos de los pacientes no dio lugar a un incremento de la fosforilación en los efectores S6K1 (residuos Thr-421 y Ser-424) y RPS6 (residuos Ser-235 y Ser-236). Aunque poco se sabe a cerca de la implicación de la fosforilación de RPS6 la ausencia de esta podría ser la causante de la menor área de fibra y de la menor fuerza muscular observada en los pacientes. Este análisis también puso de manifiesto la necesidad de mantener fosforilados estos residuos en estas proteínas para un correcto funcionamiento muscular, ya que pacientes asintomáticos donde la degeneración muscular es mínima, poseían niveles que se asemejan a los de los controles sanos.

Por otro lado también se estudiaron las fosforilaciones de los factores de transcripción FoxO ya que su fosforilación mediada por AKT impide el transporte al núcleo de los mismos donde ejercen su función de transcritores de genes. Se observaron niveles significativamente elevados de FoxO4 fosforilado así como de FoxO3 en menor medida. Esta falta de translocación al núcleo podría ser la causa de la desregulación observada en los genes *EGR1*, *FOS*, *JUNB*, *CITED2*, *MYC*, *DOK5*, *COL1A1*, *COL1A2* and *ITGB1BP2* ya que modelos animales donde una elevada actividad de FoxO fue observada estos genes mostraron una regulación contraria a la observada en los pacientes LGMD2A.

Por último, debido a que los datos previamente obtenidos mostraron un efecto beneficioso tras el silenciamiento del gen *FRZB*, se procedió al estudio más en profundidad la función de esta proteína en el músculo esquelético. Par ello se utilizó el modelo murino transgénico deficiente para el gen *Frzb*. Se realizaron diversas pruebas funcionales, se caracterizó la expresión muscular a nivel de RNA y proteína así como se procedió al análisis de células precursoras miogénicas extraídas del musculo, tanto de ratones transgénicos como no transgénicos.

El análisis a nivel genético mostró una regulación contraria de los genes *Rora*, *Slc16a*, *Tfrc* y *Capn3* en ratones *Frzb*^{-/-} donde el gen *Frzb* está ausente y en pacientes LGMD2A donde *FRZB* se encuentra incrementado. Por ello se pudo establecer la directa implicación de FRZB en la regulación de estos genes.

Junto con estos hallazgos se confirmó la implicación de *Frzb* en la miogénesis ya que este regula la expresión de MyoD tanto a nivel genético como proteico.

La miogénesis también fue estudiada mediante la inyección de cardiotoxina en el tibial anterior y en el sóleo de los ratones ya que esta toxina provoca una degeneración muscular seguida de regeneración, lo cual facilita el estudio. La inyección de cardiotoxina no mostró ninguna alteración en la capacidad regenerativa ni un incremento de fibrosis o tejido adiposo en el modelo transgénico.

Se evaluó la influencia del ejercicio crónico en estos animales ya que diversas distrofias musculares muestran una baja tolerancia al mismo. Para ello se utilizó una cinta de correr. El ejercicio indujo una bajada en la expresión de los atrogenes tanto en ratones transgénicos como no transgénicos. Sin embargo no se observaron diferencias debidas al genotipo.

Finalmete se seleccionaron las células satélite y los mesoangioblastos (células con capacidad miogénica residentes en el músculo) para su posterior análisis. Por un lado, no se observaron diferencias en la capacidad miogénica de las células satélite obtenidas tanto de ratones transgénicos como no transgénicos. Por otro lado la selección de los mesoangioblastos llevada a cabo mediante la selección de las células positivas para el marcador de membrana fosfatasa alcalina mostraron que los ratones *Frzb*^{-/-} poseían un mayor número de células positivas. Estudios posteriores revelaron que los

mesoangioblastos obtenidos de ratones *Frzb*^{-/-} expresaban una menor cantidad del marcador de membrana PDGFR α . Este hecho puede ser el responsable de la observada menor capacidad de diferenciación hacia adipocito mostrada por los mesoangioblastos obtenidos en estos ratones.

INTRODUCTION

1. MUSCLE

The muscular system is a set of soft tissues made up of very specialized cells which are characterized by their contractility and, to a lesser extent, conductivity. Muscles are essential for body movements, circulation and digestion. Muscular tissue could be divided into two main groups attending to their cellular characteristics (**Figure 1**):

- *Striated muscle.*

Striated muscles are characterized by highly ordered ultrastructure unit consisting of sarcomeres which in turn results in a transversal striation of muscular cells perpendicular to the longitudinal axis of the fibre. Fibres are basic contractile units containing a central myosin-rich dark anisotropic (A) band and two actin-dominated light isotropic (I) bands (Hanson and Huxley, 1953; Huxley, 1953). There are two types of striated muscles:

Skeletal muscle: it represents the majority of muscle tissue. These muscles are attached to bones and they are responsible for skeletal movements. They are composed by fast-twitch and slow-twitch fibres and they are under voluntary control.

Cardiac muscle: It forms the muscular wall (myocardium) of the heart and is under involuntary control.

- *Non-striated muscle.*

The cells that compose these muscles lack transversal striation.

Smooth muscle: they are composed by slow-twitch involuntary fibres. They constitute a large part of the musculature of internal organs and the digestive and circulatory system (Paniagua et al., 2007).

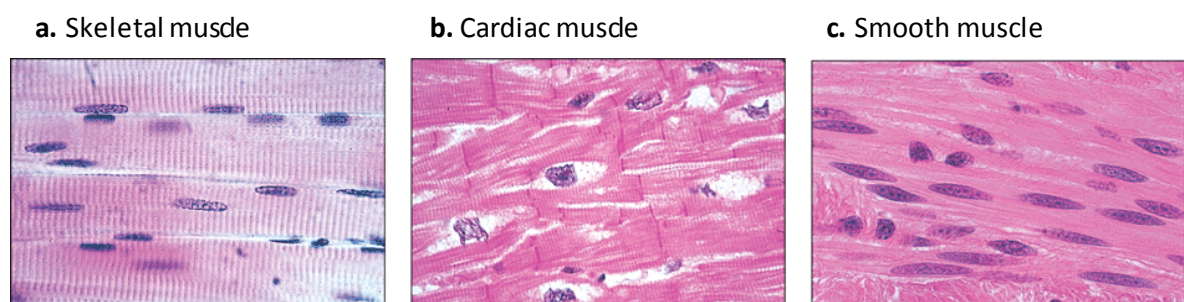


Figure 1. Representative images of skeletal, cardiac and smooth muscle stained with hematoxylin and eosin. Source: The big picture: Medical Biochemistry (2012).

1.1 SKELETAL MUSCLE

Within the muscular system, it is the most abundant muscle. It is inserted into the bones through tendons to allow the movement of the body. It is innervated by axons from motoneurons coming from central nervous system, which enables it to be under voluntary control. It is composed by thousands of fibres, which are the multinucleated individual contractile units of the muscle (Paniagua et al., 2007).

1.1.1 *Skeletal muscle structure*

Each skeletal muscle is surrounded by three connective tissue layers that enclose and provide structure to the muscle. The outer layer is called *epimysium* and it is responsible for wrapping each muscle. Inside the skeletal muscle, muscle fibres are organized into groups called fascicles, or bundles of muscle fibres. Each of them is wrapped by other connective tissue layer named as *perimysium*. Each muscular fibre which is formed when individual muscle cells fuse together, is in turn surrounded by *endomysium*, a thinner layer than *perimysium* and *epimysium*, made up of reticular fibres. Each individual muscle fibre is a postmitotic multinucleated cylindrical and elongated cell enveloped by a basal lamina and cell membrane called sarcolemma. Sarcolemma is similar to a typical plasma membrane but it has specialized functions for muscle cells. Nuclei are eccentrically located in the fibre direction. Apart from fibre's nuclei, there are other nuclei located between the sarcolemma and basement membrane of terminally-differentiated muscle fibres, they belong to satellite cells, small quiescent mononucleated multipotent muscle precursor cells discovered in 1961 by Katz and Mauro (**Figure 2**) (Paniagua et al., 2007).

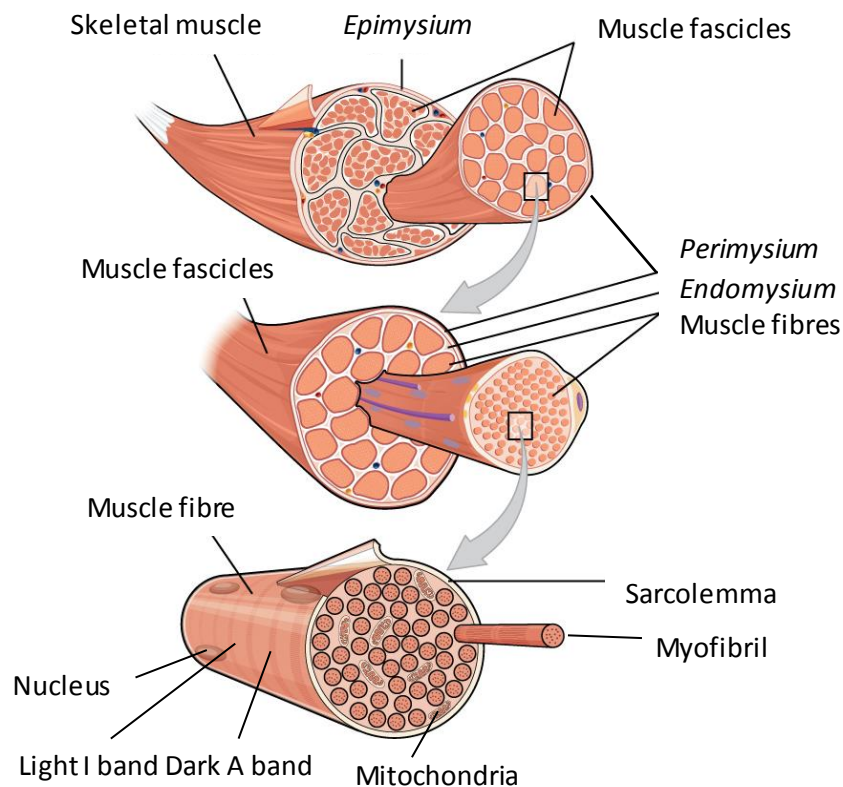


Figure 2. Skeletal muscle structure. Reproduced from *The Hierarchical Structure of the Skeletal Muscle* (2016) creative.

Muscle fibres cytoplasm is named sarcoplasm. Most of the sarcoplasm is occupied by hundreds of myofibrils, the contractile unit of striated muscle. They are oriented with their axes parallel to the length of the fibre. The myofibrils are composed of repeating sections of sarcomeres, which are considered the functional unit of striated muscle. Sarcomere is made up of thick and thin myofilaments mainly composed by myosin and actin proteins respectively, which give the muscle its striated appearance.

Another specialized organelle within sarcoplasm is smooth endoplasmic reticulum, known as sarcoplasmic reticulum (SR). It is located attached to the T-tubules that are infolding of the sarcolemma that penetrate into the cell sarcoplasm forming a tube. T-tubules together with sarcoplasmicreticulum forms sarcotubular system of skeletal muscle (also known as triad), essential structures for excitation-contraction coupling (see muscle contraction) (**Figure 3**).

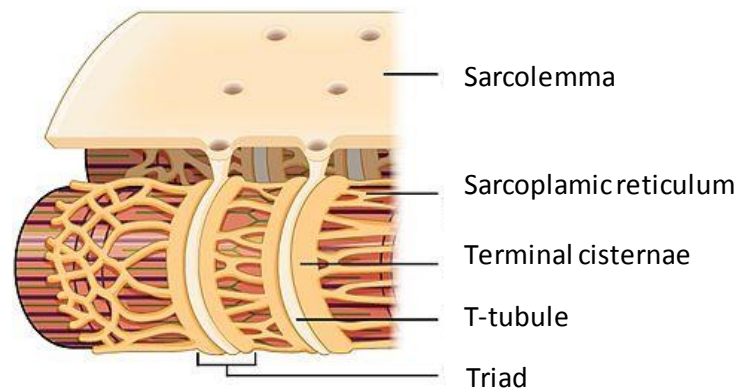


Figure 3. Sarcoplasmic reticulum and T-tubule representation. Reproduced from *The Hierarchical Structure of the Skeletal Muscle* (2016) creative.

Mitochondrion is the most abundant organelle as a result of metabolic needs of skeletal muscle. They are elongated with abundant cristae. They are longitudinally oriented among myofibrils and they could be ramified. Glycogen is also abundant in sarcoplasm and it is located in I bands. It is used as energy source for skeletal muscle. Finally, to a lesser extent, there are also rough endoplasmic reticulum, free ribosomes, slightly developed Golgi complex and some lysosomes (Paniagua et al., 2007).

Due to their different optic features under polarized light microscopy, different bands are observed in myofibrils. These bands have served to delimit sarcomeres, the highly organized contractile functional unit of striated muscle. It extends between two successive Z lines. **Z line** correspond to a transversal dark line which divide into two **I band** that is formed by actin (also called thin filaments). In the middle of sarcomere, within two I bands, **A band** could be observed, which is formed by myosin (also called thick filaments) and has a lighter zone in the middle called **H band** which in turn has a darker central line called **M line** or **M disc**. This H band corresponds to the area where actins are not present. A lighter zone than H band is observed on both sides of M disc called **L line**. The clarity is due to de lack of myosin heads, that are present in the rest of A band (**Figure 4**) (Hanson and Huxley, 1953; Bennett, 1955).

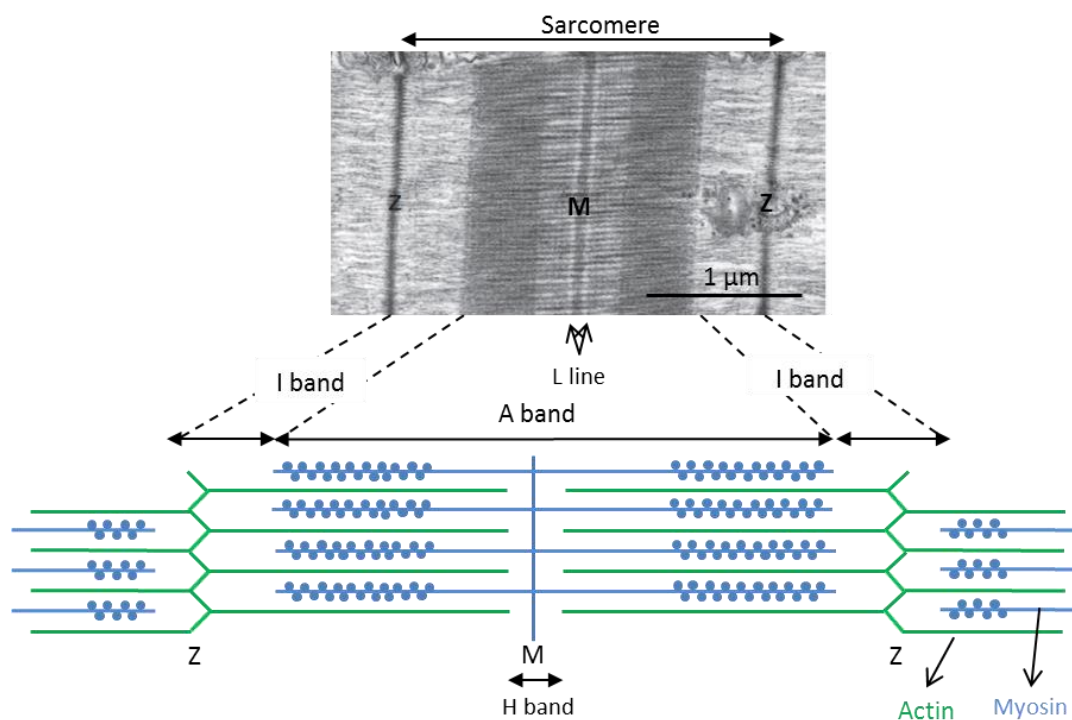


Figure 4. Skeletal muscle's sarcomere organization. Upper image belongs to electron microscopy image of a longitudinal thin section of muscle fibre (Sweeney and Hammers, 2018) .

Thin myofilaments are mainly composed by actin and thick myofilaments are formed by muscle myosin II, a hexameric protein (**Figure 5**) (Hanson and Lowy, 1963; Huxley and Brown, 1967) .

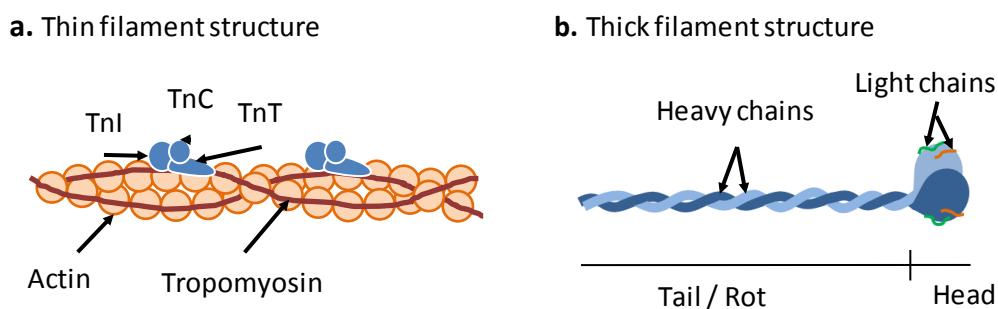


Figure 5. (a) Schematic representation of thin filament. Orange circles represent monomeric G-actin polymerized into long filaments (F-actin). Tropomyosin is represented as marron filament and troponin subunits TnI, TnC and TnT are represented in blue. (b) Schematic representation of thick filament structural unit, myosin II.

Costamere

Costamere is the morphological structure that connects sarcomere with sarcolemma of skeletal muscle and that was described for the first time in 1983 by Pardo and colleagues. It is oriented perpendicularly to the longitudinal axis of the muscle fibre and it is aligned with the myofibril Z disc. Similar structures were found located over the M lines (Porter et al., 1992) and in L domains, oriented parallel to the long axis of the muscle fibre (Bloch et al., 2002). It is composed of several proteins and protein complexes. The main functions of costamere include the assembly and stabilisation of sarcomeres (Pardo et al., 1983; Danowski et al., 1992; Trimarchi et al., 2006), protect the sarcolemma against contraction-induced damage and enable muscle adhesion to the extracellular matrix (Ervasti, 2003) that allows both contractile forces from the sarcomere to the basal lamina and transmits externally applied forces to the extracellular matrix inside de cell (Danowski et al., 1992; Mansour, 2004; Trimarchi et al., 2006).

Costamere is aligned with Z- and M-lines thanks to filamentous proteins of the cytoskeleton, namely intermediate filaments (Pierobon-Bormioli, 1981; Shear and Bloch, 1985; Ku et al., 1999; Omary, 2002). Desmin, together with synemin and paranemin form the intermediate filaments of the Z-lines (Street, 1983; Li et al., 1997).

The assembly of costamere proteins is a highly regulated process that is controlled through transcription factors as well as by mechanical stimuli. Transcription factors involve myocyte enhancer factor-2 (MEF2) required for the terminal differentiation of muscles (Bour et al., 1995; Lilly et al., 1995; Ewen et al., 2011), serum response factor (SRF) which has essential role in the differentiation of muscle among other mesoderm-derived tissues (Miano, 2010) and histone deacetylase (HDAC) (Estrella and Naya, 2014).

Costamere could be divided into two main complexes; dystrophin-glycoprotein complex and the vinculin-talin-integrin system (**Figure 6**).

- **Dystrophin-glycoprotein complex:**

This structural unit binds the intracellular actin fibres with extracellular laminin through dystrophin (Monaco et al., 1986; Matsumura and Campbell, 1994; Suzuki et al., 1994; Campbell, 1995). It is composed by sarcoplasmic proteins dystrophin, dystrobervins and syntrophin and more peripheral components such as nitric oxide synthase (nNOS) and caveolin-3. On the other hand there are two subcomplexes; sarcoglycan subcomplex, consisting of six glycosylated transmembrane proteins (α , β , γ , δ , ϵ and ζ) and dystroglycan subcomplex, consisting of two proteins (α and β). Finally the last member that binds extracellular matrix to the rest of members is laminin α -2 (Kunkel et al., 1986; Ibraghimov-

Beskrovnaya et al., 1992; Wagner et al., 1993; Blake et al., 1995; Ozawa et al., 1998; Watkins et al., 2000).

- **Vinculin-talin-integrin system:**

Vinculin and talin are two sarcoplasmic proteins that bind actin filaments through integrins to extracellular matrix components (Burrige and Mangeat, 1984; Hynes, 1992; Lu et al., 1992; Song et al., 1993).

There are also other costamere associated proteins. One of these is IPP complex formed by integrin-linked kinase (ILK), cysteine-histidine-rich protein (PINCH) and parvin proteins. They interact with cytoplasmic region of $\beta 1$ integrin participating in integrin signaling (Legate et al., 2006). Other protein that binds to $\beta 1$ integrin and acts as biomechanical sensor is melusin (Brancaccio et al., 1999). Kindlin also binds to $\beta 1$ integrin and plays important role in myoblast differentiation (Ussar et al., 2006; Dowling et al., 2008). Finally focal adhesion kinase (FAK) has been found closely associated with integrins. It plays an essential role in signaling pathway necessary for costamere formation (Nadrusz et al., 2005; Quach and Rando, 2006).

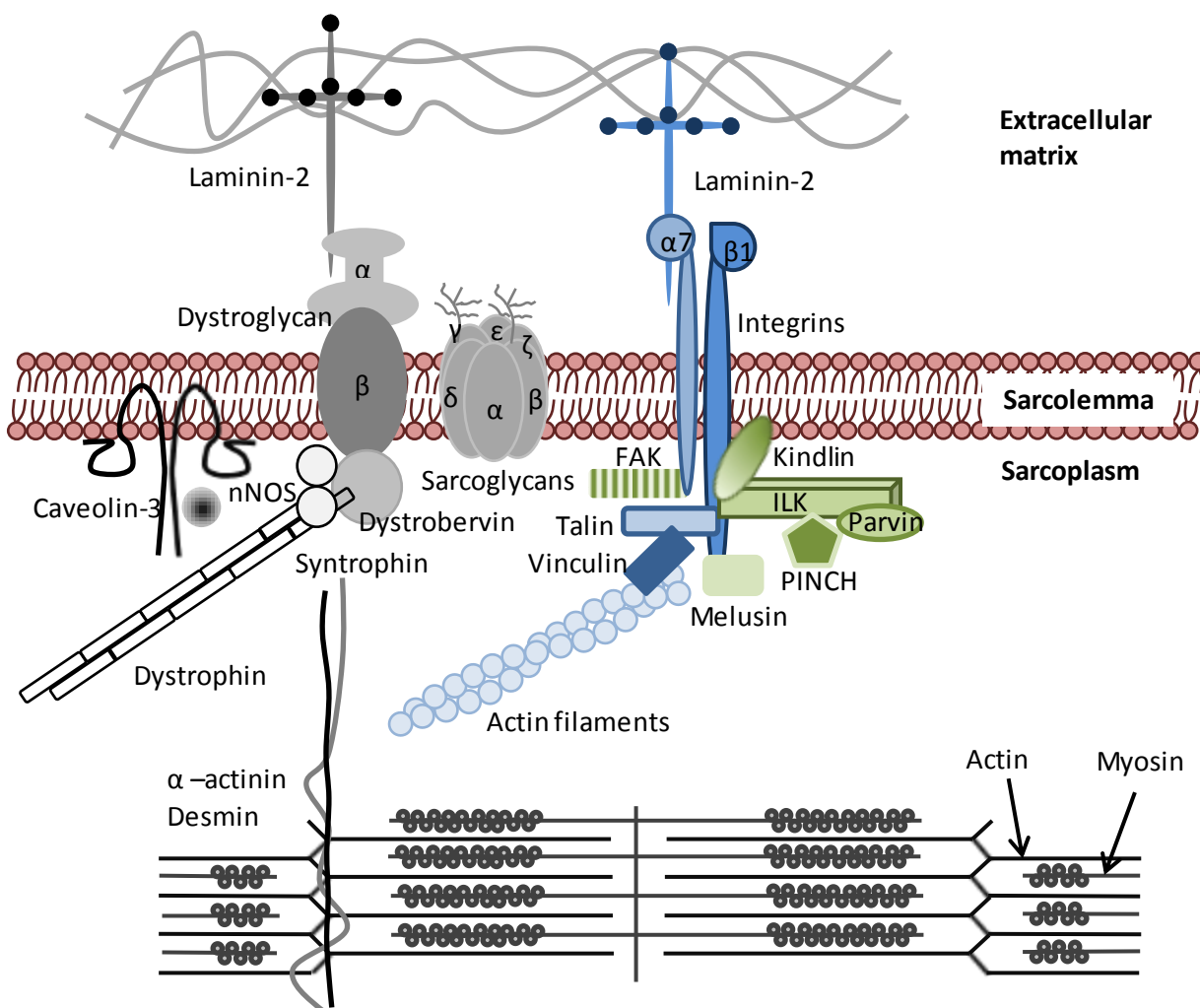


Figure 6. Schematic representation of muscle costamere.

1.1.2 Muscle innervation and muscle contraction

Muscles are innervated by motor neurons whose cell bodies are located in the motor cortex, brainstem or in the anterior horn of spinal cord. The synapse site with muscular fibre is called motor end plate and is formed by several motor neuron axons that branch off into muscle fibre clefts named as neuromuscular junction. At this point, sarcolemma forms invaginations and the basal lamina which surround muscle fibre exhibit some changes.

Muscle contractions start when acetylcholine is released from the axon terminal into neuromuscular junction. Acetylcholine binds to its receptors present in muscle fibre sarcolemma which provoke an action potential due to a rapid opening in the voltage-gate sodium channels leading to an influx of sodium ions into the cell. Sarcolemmal depolarisation reaches the T-tubule causing dihydropyridine receptor (voltage-dependent calcium channel) conformational change that activates ryanodine receptor 1 (RyR1) located in SR, which in turn cause Ca^{2+} release from SR through RyR1. This Ca^{2+} is necessary to begin muscle excitation-contraction coupling (Franzini-Armstrong and Jorgensen, 1994; Stutzmann and Mattson, 2011; Baylor and Hollingworth, 2012).

At this point two different theories have been accepted to explain muscle contraction, the sliding filament theory and the cross-bridge theory. The sliding filament theory proposes that actin filaments slide over myosin filaments causing a shortening of sarcomeres while the cross-bridge theory proposes that sliding of actin filaments is caused by the rotation of cross-bridges (Huxley and Hanson, 1954; Huxley and Niedergerke, 1954).

In any case, contraction is Ca^{2+} and ATP dependent. The Ca^{2+} present in the cytoplasm associates with troponin causing tropomyosin conformational changes that left exposed actin binding site for myosin. Myosin heads then, form a cross-bridge with actin molecules of the thin filaments. ATPase activity that cleaves ATP into ADP and inorganic phosphate is also needed to allow myosin head conformational change that enables the union with actin filaments.

After binding to actin, phosphate is released from myosin head which causes myosin head flexion that pulls the actin filament over myosin towards the M-line of the sarcomere that causes sarcomere shortening. Finally a new molecule of ATP attaches to the myosin head, causing the cross-bridge to detach.

Excitation-contraction cycle finished with Ca^{2+} removal from sarcomere. It could be transferred back to SR by SR Ca^{2+} -ATPase (SERCA) which is responsible of pumping Ca^{2+} back into the SR after Ca^{2+} release (Gunter-Skinner et al., 1988). Ca^{2+} could also be removed to the extracellular space by the sarcolemmal $\text{Na}^+/\text{Ca}^{2+}$ -exchanger (NCX) and the plasma membrane Ca^{2+} -ATPase (PMCA) (Sacchetto et al., 1996).

1.1.3 Skeletal muscle fibre type

Skeletal muscle is composed by different fibre types that lead to specific structural and functional properties of muscles (**Table 1**). Fibre phenotype could change in response to diverse factors such as hormone and neural influences, nerve-activity, exercise, aging and pathological conditions. Main studies classified muscle fibres attending to their contractile response due to myofibrillar proteins (myosin isoforms) and metabolism due to metabolic enzymes (glycolytic or oxidative). Biochemical studies based on glycolytic and oxidative enzymes gave rise to nowadays classification where slow-twitch oxidative (type I), fast-twitch oxidative-glycolytic (type IIa) and fast-twitch glycolytic fibres (type IIb) were named (Peter et al., 1972).

The relative proportions of fibre type vary according to species and anatomical site. Apart from these 3 fibre types, muscles with specific embryological origin and which are highly specialized, present atypical muscle fibres. These muscles are head and neck muscles including the extraocular muscles, jaw muscles, middle ear muscles, laryngeal muscles and muscles in the spindles (Schiaffino and Reggiani, 2011).

Fibre type diversification within muscles has been attributed to functional reasons, as different muscles presented different functions (postural muscles, fast and powerful muscles or long-lasting movements) as well as to an adaptation for body metabolism, as muscle is the main protein reservoir and conducted the plasma glucose disposal (Schiaffino and Reggiani, 2011; Qaisar et al., 2016).

One of the most common classifications of fibre types attends to its myosin heavy chain isoform (**Figure 7**). They are composed by two myosin heavy chains (MyHC) and two pairs of myosin light chains (MyLC) of which are several isoforms. On the one hand, MyHC is coded by different *MYH* genes, which in mammals 11 have been described so far (Berg et al., 2001). First, those that belong to class I myosins (MyHC- α and MyHC- β /Slow, coded by *MYH6* and *MYH7* respectively). Second, three skeletal-specific class II isoforms (MyHC-IIa, MyHC-II_{d/x} and MyHC-IIb coded by *MYH2*, *MYH1* and *MYH4* respectively). Third, two developmental isoforms (MyHC-embryonic and MyHC-perinatal coded by *MYH3* and *MYH8* respectively). Fourth, one specialized eye muscle isoform (MyHC-extraocular, coded by *MYH13*) and finally, 3 more isoforms coded by *MYH7b*, *MYH15* and *MYH16* that are expressed only in some head and neck muscles. Although *MYH4* gene is expressed in the human and mice genome, the protein is not present in humans, which leads to the lack of MyHC-IIb fibres in human skeletal muscles. On the other hand, both MyLC essential (MyLC1) and regulatory (MyLC2) subunits have several isoforms. There are four MyLC2; MyLC2s, MyLC2f, MyLC2m and MyLC2a coded by *MYL2*, *MYL6B*, *MYL5* and *MYL7* respectively and five MyLC1; MyLC1sa, MyLC1sb/sv, MyLC1f and MyLC1g and MyLC1a/emb coded by *MYL6B*, *MYL3*, *MYL1* and *MYL4* respectively (Smerdu et al., 1994;

Ennion et al., 1995; Pereira Sant'Ana et al., 1997; Wu et al., 2000; Horton et al., 2001; Allen et al., 2001).


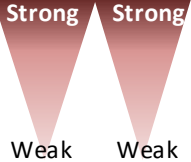
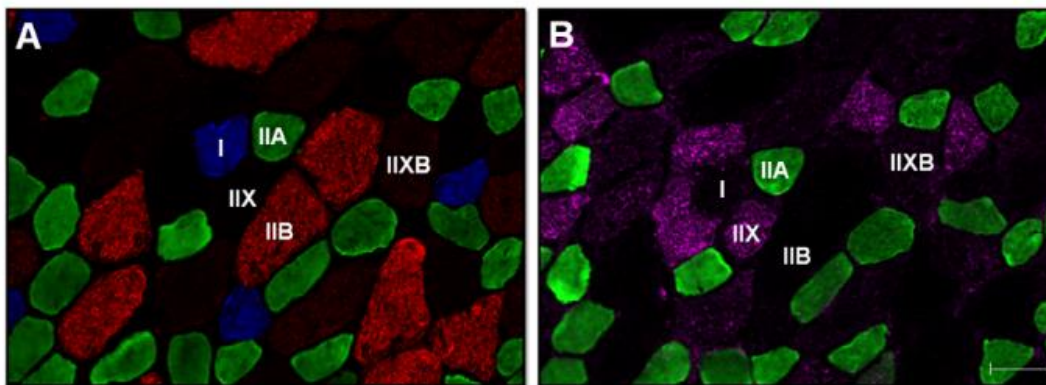
Fibre type	Principal MyHC composition	Twitch duration	Metabolism	Resistant to fatigue	Cross-sectional area	Fibre color	NADH-t staining	SHD staining
I	MyHC β (<i>MYH7</i>)	Slow	Oxidative	High	Small	White	Strong	Strong
IIa	MyHC-IIa (<i>MYH2</i>)	Fast	Oxidative/glycolytic	Fatigable-resistant		Red		
IIx/d	MyHC-IIx (<i>MYH1</i>)	Fast	Glycolytic	Intermediate		Red		
IIb	MyHC-IIb (<i>MYH4</i>)	Fast	Glycolytic	Fatigable/low		Red		

Table 1. Fibre type classification and characteristics. NADH-t = β -nicotinamide adenine dinucleotide-tetrazolium reductase transferase and SHD= succinate dehydrogenase.

a. Mouse



b. Human

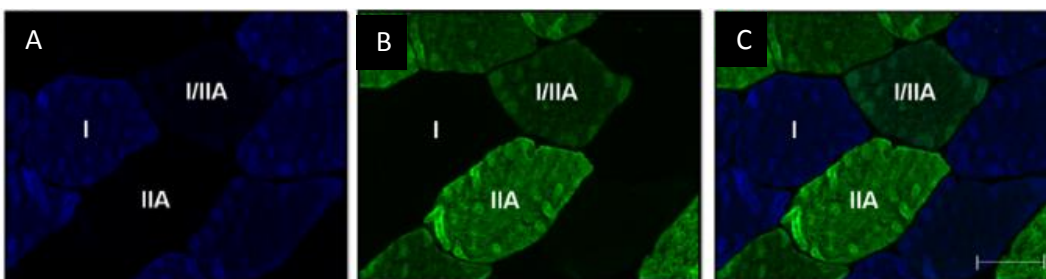


Figure 7. (a) A image represents mouse muscle's serial cross-sections where type I (blue), type IIA (green), type II (red), type IIX (unstained) and type IIXB (intermediate red) fibres are stained with primary antibody cocktail against MHCI (BA-F8), MyHC-IIa (SC-71), and MyHC-IIb (BF-F3). B image confirms the presence of type IIA (green) and that the unstained fibres and intermediate red stained fibres in A image are type IIX (purple) and type IIXB (purple and red) fibres since a primary antibody cocktail against MyHC-IIa (SC-71) and MyHC-IIx (6H1) was used. (b) Human muscle cross-section showing A) type I (blue), B) type IIA (green) and C) type I/IIA (blue and green) fibres. Scale bar 50mm. Adapted from (Bloemberg and Quadrilatero, 2012) .

2. MYOGENESIS

Skeletal muscle is the largest tissue in the body and its development, known as myogenesis, could be divided in embryonic and adult myogenesis (Tajbakhsh, 2009).

Embryonic myogenesis is a highly regulated process that begins in the mesoderm of the embryo which undergoes several divisions to give rise to the postmitotic skeletal muscle cells, myocytes, derived from paired box 3/7 (Pax3/Pax7) or Pax3 positive cells which fuse to form myofibres (Chevallier, 1979; Jacob et al., 1979; Fürst et al., 1989; Babai et al., 1990).

Adult myogenesis occurs when skeletal muscle regeneration is needed. It relies in large part upon the activation, proliferation, migration and differentiation of muscle stem cells, termed satellite cells. They were initially identified in 1961. They are mitotically quiescent cells located between the basal lamina and the sarcolemma of the muscle fibres (Mauro, 1961; Schultz et al., 1978). They can be activated by different signals to allow muscle regeneration. The activation could be ensured by an intrinsic signal, an extrinsic mechanical stretch to the fibre or could be caused by microenvironment-secreted growth factors (Jones et al., 2005; Nagata et al., 2006; Pisconti et al., 2006; Perdiguero et al., 2007; Wozniak and Anderson, 2007).

Satellite cells can be identified by their Pax7 and at less extent Pax3 protein expression or by several cell surface proteins such as M-cadherin, $\alpha7/\beta1$ -integrins, vascular cell adhesion molecule-1 (VCAM1) or neural cell adhesion molecule-1 (NCAM1) among others (Montarras et al., 2005; Fukada et al., 2007; Sambasivan et al., 2011). Genetically ablation of Pax7+ cells has demonstrated the absolute requirement of these cells in myogenesis (Sambasivan et al., 2011).

In contrast to what was initially believed, satellite cells belong to a heterogenic cell population. It was postulated that uncommitted progenitors responsible for the maintenance of the satellite cell population exists (Kuang et al., 2007). They have the ability to undergo symmetric or asymmetric divisions to produce either one daughter stem cell and one daughter committed cell or two identical cells (Conboy and Rando, 2002).

Muscle regeneration could be divided into several stages. The first one starts with the activation of satellite cells. Pax7 and myogenic factor 5 (Myf5) expressing activated satellite cells migrate to damaged site and start proliferating. At this point cells are called myoblasts. They express Pax7 and/or Myf5 and/or myogenic differentiation factor 1 (MyoD). Proliferation stage is influenced by several factors and signaling pathways that increase cell cycle progression and repress differentiation. After proliferation, cells exit the cell cycle and start to differentiate. Myoblast fuse to each other or to pre-existing fibres. At this point the expression of Pax7 and Myf5 decreases and myogenin and myogenic factor 6 (Mrf4) levels increase. Once myotubes appeared MyoD is also

decreased and mature myotubes proteins such as myosin heavy chain and other contractile proteins appear (Le Grand and Rudnicki, 2007; Buckingham and Rigby, 2014; Zammit, 2017).

Although satellite cells are the main responsible of adult myogenesis, other cell types have been shown to have myogenic potential or to contribute to regenerative potential providing correct environmental settings. The first finding of cells with myogenic potential was first described by Gussoni and colleagues (1999). They described muscle-resident side population cells which can give rise to dystrophin-positive myofibres when injected into *mdx* mice (Duchenne muscular dystrophy mouse model) (**Table 2**). They comprise a heterogeneous group expressing Sca-1, CD34 and Pax7 (Uezumi et al., 2006). In addition to this population, another subset of muscle interstitial cells was discovered; PICs (PW1 positive interstitial cells). They express PW1 as well as Sca-1 and CD34, like side population cells, but in this case they do not express Pax7. However they contribute to muscle regeneration and they can generate Pax7-positive satellite cells (Mitchell et al., 2010). More detailed studies showed that PICs could be divided into two subpopulations according to their platelet derived growth factor receptor-alpha (PDGFR α) expression. Those with PDGFR α expression display adipogenic potential while those who do not express PDGFR α are myogenic progenitors (Pannerec et al., 2013).

In addition to these two populations, skeletal muscle vessel-associated stem cells have also been described; pericytes (PCs) and mesoangioblasts (MABs). Microvascular PCs are considered the adult counterpart of the embryonic MABs and they are able to differentiate into a variety of mesoderm tissues including skeletal muscle, both *in vitro* and *in vivo* (De Angelis et al., 1999; Minasi et al., 2002; Sampaolesi, 2003). PCs are characterized by the expression of several cell-surface markers such as neuro-glial 2 proteoglycan (NG2), PDGFR α , platelet derived growth factor receptor-beta (PDGFR β), alpha-smooth muscle actin (α SMA) and alkaline phosphatase (ALP). However, none of them are pericytes specific markers since their expression is dynamic and varies between organs and developmental stage (Hellström et al., 1999; Gerhardt and Betsholtz, 2003; Hughes and Chan-Ling, 2004; Chan-Ling et al., 2004; Dellavalle et al., 2007). As happened with PICs cells, pericytes also were further subdivided into two different populations. They were first subdivided according to the expression of nestin, being type I negative and type II positive for nestin expression. Together with this finding it was also noted that they have different cell fate potential. Type I pericytes are profibrotic and adipogenic, and type 2 pericytes, have myogenic potential (Birbrair et al., 2013a). Further studies from the same group discovered that the adipogenic progenitor marker PDGFR α was only expressed by type I pericytes (Birbrair et al., 2013b).

In addition to these myogenic muscle-resident mesenchymal progenitors, other cells have been described. These cells do not display myogenic differentiation potential but they have important roles during myogenesis. Two different populations were described at the same time by two different groups, both of them located at the muscle interstitium; fibro/adipogenic progenitors (FAPs) and

mesenchymal stem cells (MSCs). The first one was isolated based on Sca-1 cell-surface antigen and further characterized by negative expression of CD45, CD31 and $\alpha 7$ -integrin together with positive expression of CD34 markers and the second one based on its PDGFR α expression. Both of them display *in vivo* and *in vitro* adipogenic differentiation potential (Joe et al., 2010; Uezumi et al., 2010). It is important to note whether those cell populations could overlap, since different techniques were employed in their discovery. Unlike previously mentioned cells, these cells do not contribute to regenerate myofibres even so, they promote myotube formation and differentiation of muscle progenitors (Joe et al., 2010).

This feature has also been observed for muscle-resident fibroblast. Apart from their structural functions on muscle they are key component of the satellite cells niche and are critical regulators of myogenesis. It has been shown that the loss of skeletal muscle fibroblast leads to premature satellite cell differentiation and depletion of the early pool of satellite cells, highlighting the importance of reciprocal interactions between fibroblasts and satellite cells to proper muscle regeneration (Mathew et al., 2011; Murphy et al., 2011).

Cell type	Positive markers	Subtypes	Cell fate
Myogenic potential			
<i>Satellite cells (SC)</i>	M-cadherin, $\alpha 7$ - $\beta 1$ integrin, VCAM1 and NCMA1		
<i>Muscle-resident side population cells</i>	Sca-1, CD34 and Pax7		
<i>PW1 positive interstitial cells (PICs)</i>	PW1, Sca-1 and CD34	PDGFR α +	Adipogenic potential
		PDGFR α -	Myogenic potential
<i>Mesoangioblasts (MABs)</i>	NG2, PDGFR α , PDGFR β , α SMA and ALP		
<i>Perycytes (PCs)</i>	NG2, PDGFR β , α SMA and ALP	Nestin - PDGFR α +	Type 1: Fibrotic and adipogenic potential
		Nestin + PDGFR α -	Type 2: Myogenic potential
Non-myogenic potential			
<i>Fibro/adipogenic progenitors (FAPs)</i>	Sca-1 and CD34 (negative expression of CD45, CD31 and $\alpha 7$ integrin)		Adipogenic potential
<i>Mesenchymal stem cells (MSCs)</i>	PDGFR α		Adipogenic potential
<i>Muscle-resident fibroblasts</i>			Adipogenic potential

Table 2. Muscle-resident mesenchymal cells.

2.1 SIGNAL REGULATION IN MYOGENESIS

Myogenesis is a tightly regulated process that has been thoroughly studied. Several myogenic regulator factors and different signaling pathways have been described to be involved in its regulation.

Paired-homeobox family transcription factors composed by Pax3 and Pax7 which are upstream regulators of myogenesis are one of the most important (Seale et al., 2000). Both, Pax3 and Pax7, seems to be able to compensate each other during embryonic myogenesis (Relaix et al., 2005) and their functional differences in postnatal myogenesis appeared to attend to post-transcriptional modifications of proteins and the association with cofactors (Miller et al., 2008). Pax3 is crucial during embryonic development since it regulates Myf5 expression. In adulthood, Pax3 is restricted to trunk muscles such as diaphragm and some limb muscles satellite cells (Relaix et al., 2006). By contrast, Pax7 acts activating MyoD and other targets genes in satellite cells including genes involved in cell growth, cell adhesion and signaling pathways (Hu et al., 2008; Soleimani et al., 2012).

Furthermore, myogenic regulatory factors (MRFs) also regulate myogenesis. They are basic helix-loop-helix muscle specific transcription factors namely Myf5, MyoD, Mrf4 and myogenin (Davis et al., 1987; Braun et al., 1989; Rhodes and Konieczny, 1989; Braun et al., 1990; Edmondson and Olson, 1990; Miner and Wold, 1990). Myf5 is the first MRF expressed during embryonic development and together with it, Mrf4 and MyoD are responsible of myoblast development while myogenin is important in myoblast differentiation (Ott et al., 1991; Hasty et al., 1993; Rudnicki et al., 1993; Tajbakhsh et al., 1996; Kassir-Duchossoy et al., 2004).

Together with Pax transcription factors and MRF, several molecules have been described to be involved in myogenesis regulation: MEF2 family members (Black and Olson, 1998; Spitz et al., 1998) that act together with MRF to control gene expression (Molkentin et al., 1995; Junion et al., 2005; Sandmann et al., 2006), Six1/4 transcription factors and Eva1/2 cofactors, required for correct expression of Myf5 and MyoD (Heanue et al., 1999; Tapscott, 2005; Relaix et al., 2013), as well as Pitx2 and Pitx3 transcription factors present in myogenic progenitors and in differentiating muscles respectively (L'Honoré et al., 2007).

Finally, post-transcriptional regulation through microRNAs (miRNAs) also have shown an important role during myogenesis. miR-1, miR-27, miR-206 and miR-486 downregulate Pax3 and Pax7 expression as well as miR-31 targets Myf5 (Chen et al., 2010; Hirai et al., 2010; Dey et al., 2011; Goljanek-Whysall et al., 2011; Crist et al., 2012).

Wnt, Notch, Sonic hedgehog (Shh) and bone morphogenetic protein (BMP) signaling pathways are the major players that regulate embryonic myogenesis. Since the beginning, spatiotemporal somitogenesis involves Notch and Wnt pathways. From early stages, Wnt signaling effectors are

secreted to promote somite patterning (Parr et al., 1993). Along with Wnt, Shh pathway is also involved in early specification of muscle progenitors. It is essential for the maturation of dermomyotomal cells into MyoD/Myf5-expressing cells (Johnson et al., 1994; Borycki et al., 1998; Feng et al., 2006; Hammond et al., 2007). Finally, in contrast to Wnt and Shh, BMP inhibits expression of some myogenic genes with the aim of expand the pool of myogenic progenitors (Pourquié et al., 1995).

2.1.1 Wnt signaling during myogenesis

The etymological origin of Wnt is derived from the mixture of the gene known as Wingless found in *Drosophila* and its homologous gene *int1* discovered in mice (Uzölgöyi et al., 1988).

Wnt signaling pathway is a signal transduction cascade activated by Wnt ligands that binds to seven-transmembrane Frizzled (Fzd) receptors which in turn could activate different downstream effectors that result in regulation of several gene expressions. 19 Wnt genes in humans and 10 Fzd receptors in vertebrates have been described so far. The Wnt signaling pathway could be divided in to canonical (β -catenin dependent) or non-canonical (β -catenin independent) pathways.

Canonical Wnt signaling begins with the binding of the Wnt ligand to its Fzd receptor and its co-receptor LDL-receptor-related proteins 5/6 (LRP5/6) (Bhanot et al., 1996; Pinson et al., 2000). In the absence of Wnt ligand binding, cytosolic β -catenin is degraded via phosphorylation-dependent ubiquitination and proteolysis. This β -catenin is within a complex formed by scaffold protein axin, adenomatous polyposis coli (APC), glycogen synthase kinase 3 beta (GSK3 β), dishevelled scaffold protein (Dvl) and casein kinase I (CKI) that allows its phosphorylation and its subsequent destruction by the proteasomal pathway. Once Wnt binds to its receptor, Dvl is recruited causing β -catenin dissociation from the complex and preventing it from being degraded. Thus, β -catenin accumulates in the cytoplasm and translocates to the nucleus where it binds members of the T-cell factor/lymphoid enhancer factor (TCF/LEF) family of transcription factors which control different genes transcription (**Figure 8**) (Amit, 2002; Niehrs, 2012).

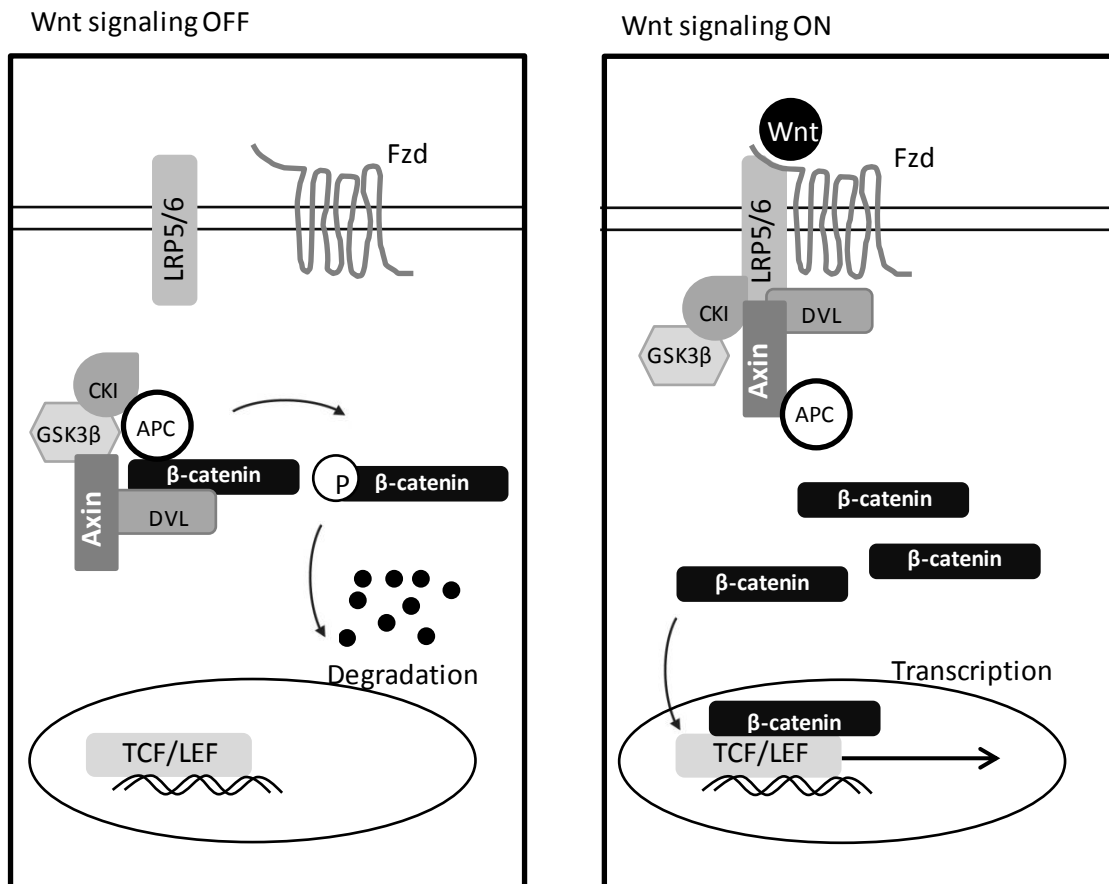


Figure 8. Schematic representation of canonical Wnt signaling.

On the other hand, non-canonical pathways do not act through β -catenin. Two pathways have been described so far. The first one is Planar Cell Polarity Pathway. In this case Wnt-Fzd binding activates small GTPases proteins which in turn activate c-Jun N-terminal kinase. It is responsible of cytoskeletal organization for migration and cell polarization (Tomlinson et al., 1997). The second one is Wnt/ Ca^{2+} pathway where Wnt-Fzd binding leads to heterotrimeric G proteins and phospholipase C (PLC) activation that evoke intracellular Ca^{2+} release which in turn activates Ca^{2+} dependent different enzymes such as calcium-calmodulin-dependent kinase II (CamKII) or protein kinase C (PKC) (Slusarski et al., 1997).

Wnt signaling could be inhibited by different ways. First, a family of secreted proteins containing homology to the cysteine-rich ligand-binding domain of Fzd receptors called secreted frizzled-related proteins (sFRPs) were found (Rattner et al., 1997). Due to their ability to bind to Wnt receptors and Wnt molecules they are able to inhibit Wnt signaling (Leyns et al., 1997; Wang et al., 1997). Along with sFRPs, Dickkopf (DKK) protein also inhibits Wnt signaling. It probably forms a negative feedback of the signaling since it is a TCF target gene that potently inhibits Wnt signaling (Glinka et al., 1998; Niida et al., 2004).

The increased interest in modulating Wnt pathway for different purposes has given rise to a range of new molecules or drugs that could act modulating this pathway. One example of this is lithium chloride (LiCl), which has been shown to inhibit GSK3 β and mimic the active effects of the canonical Wnt signaling on gene expression and cell proliferation (Klein and Melton, 1996).

As it has been previously mentioned, Wnt signaling has importance in prenatal myogenesis, since together with Shh pathway, Wnt1, Wnt3, Wnt4, Wnt6 and Wnt7 could initiate somite myogenesis in chicken embryos (Münsterberg et al., 1995). In addition, different Wnts have been shown to induce expression of MRFs in the embryo (Tajbakhsh et al., 1998; Borello, 2006; Brunelli et al., 2007). Finally it has also been reported that transplacenta delivery of a Wnt inhibitor molecule, frizzled related protein (FRZB), reduced skeletal myogenesis in mouse embryos (Borello et al., 1999).

Despite the knowledge of Wnt signaling during embryonic myogenesis, the role of Wnt pathway during adult myogenesis or muscle regeneration is not completely clear. Evidence suggests that Wnt pathway plays an important role in myogenesis but its regulation is not completely well defined. The activation of Wnt signaling in satellite cells during proliferation with opposite effects has been reported. Wnt1, Wnt3 and Wnt5a induced cell proliferation while Wnt4 and Wnt6 inhibited it (Otto et al., 2008). On the other hand, other works suggested that aberrant expression of Wnt signaling during aging in satellite cells is the responsible of increased fibrosis, leading to a myogenic-to-fibrogenic conversion which result in impaired muscle regeneration (Brack et al., 2007).

The temporal switch from progenitor cell proliferation to differentiation is essential for effective adult tissue repair. The role of Notch signaling in the proliferative expansion of myogenic progenitors is critical in mammalian postnatal myogenesis. It has been shown that the onset of differentiation is due to a transition from Notch signaling to Wnt signaling in myogenic progenitors and is associated with an increased expression of Wnt in the tissue. Crosstalk between these two pathways occurs via GSK3 β , which is maintained in an active form by Notch but is inhibited by Wnt in the canonical Wnt signaling cascade. These results demonstrate that the temporal balance between Notch and Wnt signaling orchestrates the precise progression of muscle precursor cells along the myogenic lineage pathway (Brack et al., 2008).

Related to the possibility that the activation of the Wnt pathway might be beneficial for patients with muscular dystrophy, Vieira and colleagues (2015) showed two exceptional Golden Retrievers, since being natural models of Duchenne muscular dystrophy, they escaped gravity derived from the absence of dystrophin expression in muscle. After analysing the complete genome of these dogs, it was observed that overexpression of the jagged 1 (*JAG1*) gene, which is an inhibitor of the Notch pathway, was responsible for the improvement of the dystrophic phenotype.

3. MUSCULAR DYSTROPHY

The muscular dystrophies are a heterogeneous group of inherited genetic disorders characterized by progressive weakness and muscle degeneration. They are caused by mutations in genes encoding proteins required for normal muscle function (Emery, 2002).

Initially, muscular dystrophies were classified attending to their clinical features but through the emergence of genetic technics nowadays, classification is based on mutated genes and their respective proteins' function.

There are many different types of muscular dystrophies, being the most common, myotonic dystrophy type 1 followed by facioscapulohumeral dystrophy and dystrophinopathies. Limb girdle muscular dystrophies (LGMD) are the fourth most common dystrophies, even if the prevalence of each LGMD subtypes vary geographically, it is estimated at 1.63 per 100,000 (Mah et al., 2016).

3.1 LIMB GIRDLE MUSCULAR DYSTROPHY

Limb girdle muscular dystrophy term was coined in 1954 by Walton and Nattrass (Walton and Nattrass, 1954). They comprise a group of heterogeneous muscular dystrophies that share common clinical features. They are characterized by chronic progressive weakness and atrophy of hip and shoulder girdles, elevated creatine kinase (CK) levels and dystrophic findings on muscle biopsy. Their inheritance is either autosomal dominant (LGMD1) and autosomal recessive (LGMD2). Diseases are classified using alphabetic index according to the chronology of identification of their genetic loci (Bushby and Beckmann, 1995). According to the latest review, to date there are 8 autosomal dominant (LGMD1A-1H) and 26 autosomal recessive types (LGMD2A-2Z) (Bonne et al., 2017).

The age at onset ranged from the first decade to late adult life. Pattern of muscle involvements also have a wide range of symptoms. Proximal limb muscles are the most affected and muscle weakness typically starts in the proximal muscles of the lower limbs. Ocular muscles are always preserved and facial weakness is only present in later stages of some subtypes as well as cardiac involvement is not common in recessive forms. Even if predominantly muscle affection present symmetric patten, asymmetry could be present (Vissing, 2016).

3.2 LIMB GIRDLE MUSCULAR DYSTROPHY TYPE 2A (LGMD2A)

Limb girdle muscular dystrophy type 2A, also known as calpainopathy, is an autosomal recessive disorder caused by mutations in calpain 3 (*CAPN3*) gene (Richard et al., 1995).

3.2.1 Epidemiology

Within LGMD, calpainopathy is the most frequent disorder, it is estimated to account about 20-50% of total LGMD cases (Bushby and Beckmann, 2003). Epidemiology studies of LGMD2A vary depending on the geographic origin. Some founder mutations have been found in different regions with high inbreeding rates. The highest prevalence has been found in some small genetically isolated communities: in Reunion Island is 48 per million (Fardeau et al., 1996a), 69 per million in Guipuzcoa, Basque Country (Urtasun et al., 1998), 1,990 per million cases in the 'Mòcheni' people in the Italian Alps (Fanin et al., 2012) and 13,000 per million in the Amish population of Indiana, USA (4,000 inhabitants) (Jakson G., personal communication).

The particular calpain 3 mutation predominant in Basque chromosomes (p.(Arg788Serfs*14)) (Urtasun et al., 1998) is linked to a specific haplotype and it is also shared by Brazilian patients (Cobo et al., 2004).

3.2.2 Clinical features

The age at onset could be divided into early (< 12 years), typical (between 12 and 30 years) or late (> 30 years) (Fanin and Angelini, 2015), but most of the cases presented with weakness in the second decade of life (Fardeau et al., 1996a; Urtasun et al., 1998). The first clinical symptoms are mostly characterized by proximal muscle weakness which goes along with muscle atrophy and fatty replacement of muscles as the disease progresses (Fardeau et al., 1996a; van der Kooi et al., 1996; Urtasun et al., 1998). CK level are markedly raised (5 – 20 fold) in the early stages and decreased to reach normal levels in wheelchair-bound patients with marked muscle atrophy (Urtasun et al., 1998). Eosinophilic myositis is an early histopathological manifestation of LGMD2A found also in childhood with circulating eosinophilia which disappears once muscle weakness appears (Krahn et al., 2006a, 2011). Together with these symptoms, the onset of the disease could present with a phenotype resembling metabolic myopathy with exercise intolerance, myalgia and muscle stiffness (Pénisson-Besnier et al., 1998; Pollitt et al., 2001; Fanin et al., 2004; Krahn et al., 2006b; Hermanová et al., 2006; Lahoria and Milone, 2016).

Regarding muscle involvement *Hip adductors* and *Gluteus maximus* are the earliest clinically affected muscles. The upper girdle involvement give rise to scapular winging condition that is often

developed in calpainopathy. As the disease progresses, more muscles appeared affected such as *Quadriceps*, *Triceps brachii* and some distal muscles such as *Tibialis anterior* and some forearm muscles (Fardeau et al., 1996b). Cardiac involvement and respiratory muscle weakness are not clinical features of LGMD2A although some cases with cardiac dysfunction or respiratory failure were reported (Fardeau et al., 1996a, 1996b; Urtasun et al., 1998; Groen et al., 2007; Quick et al., 2015; Nemes et al., 2017; Mori-Yoshimura et al., 2017).

Hypertrophy is not a hallmark of the disease but it has been observed calf hypertrophy in Brazilian population (De Paula et al., 2002; Albuquerque et al., 2015). Although symmetric affection of limb muscles is considered, asymmetry may also be present in calpainopathy (Mercuri et al., 2005; Guglieri et al., 2008).

The disease progression is also variable but patient became wheelchair-bound after no more than 25 years of disease progression. No intellectual disability was noticed in these patients (Fardeau et al., 1996a; Urtasun et al., 1998).

The heterogeneous nature of LGMD2A makes it difficult to establish a prognosis to predict the clinical evolution of the disease. There are different functional scales for the evaluation of neuromuscular patients. The most widely used is the modified Walton & Gardner-Medwin (WGM) scale.

In computed tomography and magnetic resonance imaging, posterior compartment impairment of the thighs, which is a hallmark of LGMD2A patients, is observed (Fardeau et al., 1996a; Urtasun et al., 1998; Mercuri et al., 2005; Degardin et al., 2010).

The histopathological features of LGMD2A patients' muscle biopsies present differences in their dystrophic pattern in early stage or late stages of the disease. In early stages of the disease, active necrosis and regenerating process is observed (**Figure 9 a**). Eosinophilic myositis, which is characterized by eosinophilic infiltration of the skeletal muscle, peripheral blood and/or bone marrow hypereosinophilia, associated with inflammatory lesions of the muscle tissue could be also present (Guerard et al., 1985; Krahn et al., 2006a; Keira et al., 2007; Rosales et al., 2013) (**Figure 9 b**). In later stages, the muscle pathology is characterized by the presence of lobulated fibres and there is also fibre size variation and interstitial fibrosis. On electron microscopy, misaligned myofibrils and accumulation of mitochondria could be observed (**Figure 9 c**) (Guerard et al., 1985; Keira et al., 2007).

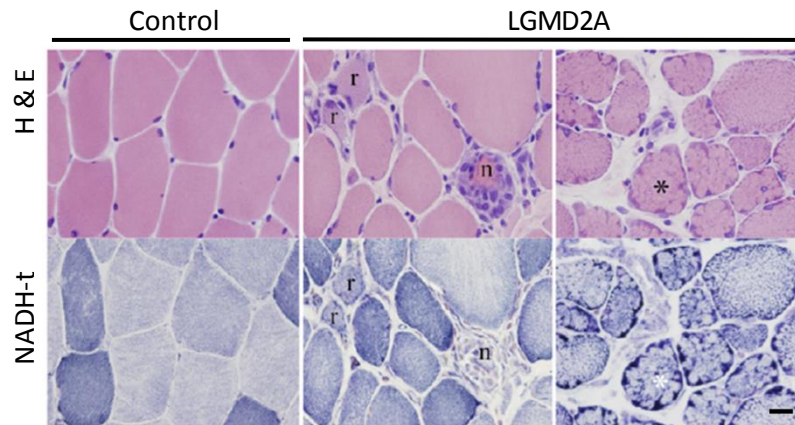
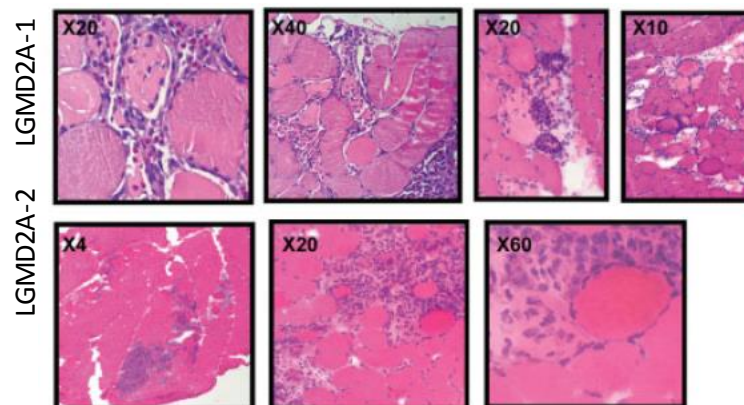
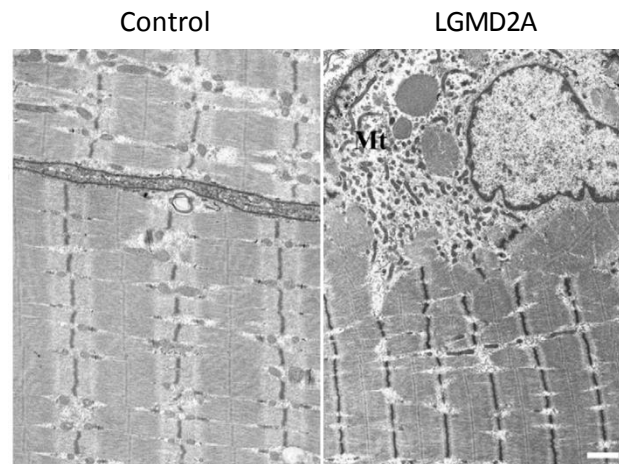
a. Immunohistochemical analysis**b****c. Electronmicroscopic analysis**

Figure 9. (a) Immunohistochemical analyses of muscle biopsy of one control and two LGMD2A patients. Upper images are stained with hematoxylin and eosin while lower images are stained with β -nicotinamide adenine dinucleotide–tetrazolium reductase staining (NADH-t). r = regenerative fibres, n = necrotic fibres and * = lobulated fibres. Scale bar 20 μ m. From (Keira et al., 2007). (b) Immunohistochemical analyses of muscle biopsy stained with hematoxylin and eosin of two LGMD2A patients. LGMD2A-1 patient has focal inflammatory lesions with abundant eosinophilic infiltration involving necrotic fibres. LGMD2A-2 patient has irregular fibre size and focal inflammatory infiltration with necrosis of involved fibres. Adapted from (Krahn et al., 2006a). (c) Electron microscopic images of subsarcolemmal region in control and LGMD2A patients. Mt = mitochondria. Scale bar: 1 μ m. From (Keira et al., 2007).

Protein testing has also been used for diagnostic purposes. However, calpain 3 protein detection in muscle biopsies by western blot could give both, false positive and false negative results (Fanin et al., 2004; Piluso, 2005; Sáenz et al., 2005). On the one hand, false negative result could be obtained when normal levels of calpain 3 protein are detected in muscle but, due to specific mutations the protein is not functional (Fanin et al., 2003, 2004). On the other hand, secondarily calpain 3 protein reduction has been found in other muscular dystrophies such as LGMD2B, LGMD2I, titinopathy, sarcoglycanopathies and merosin deficient patients which would lead to a false positive result (Anderson et al., 2000; Sáenz et al., 2005; Charton et al., 2015; Magri et al., 2017).

LGMD2A diagnosis is established by identification of biallelic pathogenic variants (mutations) in *CAPN3* gene. To date almost 500 mutations in *CAPN3* gene have been identified (Leiden Open Variation database, at <http://www.dmd.nl/>).

Diagnosis based on routine blood sample could be performed given that the blood cells express *CAPN3* mRNA (De Tullio et al., 2003; Blázquez et al., 2008). Since in 10-22% of patients considered as LGMD2A, only 1 pathogenic mutation in *CAPN3* gene has been found (Richard et al., 1999; De Paula et al., 2002; Chrobáková et al., 2004; Sáenz et al., 2005; Zatz and Starling, 2005; Stehlíková et al., 2007), Jaka and colleagues (2014) proposed a strategy as the safest diagnostic approach for LGMD2A.

LGMD2A was considered as a recessive inherited disease so far. However, recent findings have suggested a dominant form of calpainopathy (Vissing et al., 2016; Martinez-Thompson et al., 2018). Authors reported heterozygous carriers of an inframe 21-bp deletion in *CAPN3* gene in European origin families. There has, however, been a controversy with the first study and other authors have criticised some points, although the original authors rebutted the critique (Sáenz and López de Munain, 2017; Vissing and Duno, 2017).

This scenario is not unique since several myopathies with both dominant and recessive model of inheritance have been reported. This dual model of inheritance has been reported in desminopathies, in *RYR1* gene mutations associated central core myopathy, in myopathies caused by mutations in the titin (*TTN*) gene, in myotonia congenita, in collagen 6-related muscle diseases, in carnitine palmitoyltransferase II deficiency and in glutaryl-CaA dehydrogenase deficiency (Hackman et al., 2002; Dunø et al., 2004; Udd et al., 2005; Ørngreen et al., 2005; Foley et al., 2009; Bross et al., 2012; Nigro and Savarese, 2014; Snoeck et al., 2015).

3.2.3 Genotype-phenotype correlation

The spectrum of mutations in the *CAPN3* gene is highly heterogeneous thus, a clear genotype-phenotype correlation has been difficult to establish. Moreover, the clinical course of the disease is also highly heterogeneous. Similar clinical course in patients with different *CAPN3* gene mutations or discordant phenotype in affected sibs carrying the same mutation could be observed (Zatz et al., 2000; Sáenz et al., 2005).

Some authors have suggested that patients with early onset of the disease are most severely affected and usually have two null mutations with a total absence of calpain 3 protein. Conversely, in moderately to severe affected patients, calpain 3 protein could be absent or reduced, while patients with later onset of the disease, usually have milder phenotype with normal level of calpain 3 protein (Fanin et al., 2004; Sáenz et al., 2005).

In line with these findings, Sáenz and colleagues (2011) described two patients with benign phenotype who had compound heterozygous missense mutations (pG222R and pR748Q). It was postulated that autolyzed fragments of mutant proteins co-associate to reconstitute an intact wild-type (WT) calpain 3 molecule.

3.2.4 The current status of therapies for LGMD2A

There is no any treatment for LGMD2A so far, nevertheless, different molecular strategies have been conducted to restore *CAPN3* expression. The first study used adeno-associated virus (AAV) vectors expressing *CAPN3* that were injected in calpain 3 - deficient mice (Bartoli et al., 2006; Roudaut et al., 2013). The second study, however, was focused on *CAPN3* gene mutations correction. Authors carried out *in vitro* correction of a pseudoexon-generating deep intronic mutation by antisense oligonucleotides (Blázquez et al., 2013).

Moreover, today there are two research projects ongoing funded by coalition to cure calpain 3 organization. One of these projects is focused on DNA-mediated gene therapy. Without AAV-mediated gene delivery, this project proposes *CAPN3* gene introduction by employing 'naked' plasmid DNA. The aim of the second project is to genetically correct mutations in the *CAPN3* gene in LGMD2A iPS cells by CRISPR-CAS9 technology which further could be transplanted into the muscles of models of muscular dystrophy (<http://www.curecalpain3.org/research/>).

3.2.5 Models for muscular dystrophy studies

- *In vitro* models

Several attempts to improve *in vitro* models have been done since the first successful cultivation of normal human skeletal muscle was done by Pogogeff and colleagues in 1946. However, it was not until 1957 when first progressive muscular dystrophy derived cells were cultured (Geiger and Garvin, 1957).

In vitro studies limitations due to their finite life-span and slow growth rate (Swim and Parker, 1957) has been solved with the immortalization of primary cells proposal (Miranda et al., 1983).

However, it is known that results obtained from *in vitro* models not always recapitulate result obtained from tissues of origin (Smith et al., 1994; Cornelison and Wold, 1997; Hawke and Garry, 2001; LaFramboise et al., 2003). A uniform myotubes culture was observed from different origin muscles when cultured in identical conditions, suggesting a myotube culture homogenization (LaFramboise et al., 2003). It is known that in *in vitro* experiments the extracellular matrix (ECM) is absent, which is responsible to provides support and creates microenvironmental niche that influences endogenous cell behaviour and phenotype (Bissell et al., 1982; Bissell and Aggeler, 1987; Ingber, 1991; Boudreau et al., 1995). A more recent study found out that more than thousand genes displayed differential expression when human cultured myotubes and skeletal muscle tissue were compared. Cultures showed reduce metabolic and muscle-system transcriptome adaptations, augmented tissue remodelling transcriptome and induction of genes involved in the apoptosis or anoikis process. Among others, one interesting finding was that *CAPN3* gene was downregulated in cultured myotubes (Raymond et al., 2010).

Analysis carried out by our group also showed evidences of discrepancies between tissue (muscle) and cell culture (myoblasts and myotubes). Myoblast/myotubes gene expression did not show a good correlation with genes expressed in muscle, but myotubes at 16 days of differentiation showed the best correlation (**Figure 10**). Moreover, within deregulated genes in LGMD2A patients' muscles (Sáenz et al., 2008), only the *FRZB* gene showed the same deregulation pattern in myotubes at 16 days of differentiation (Jaka, 2014).

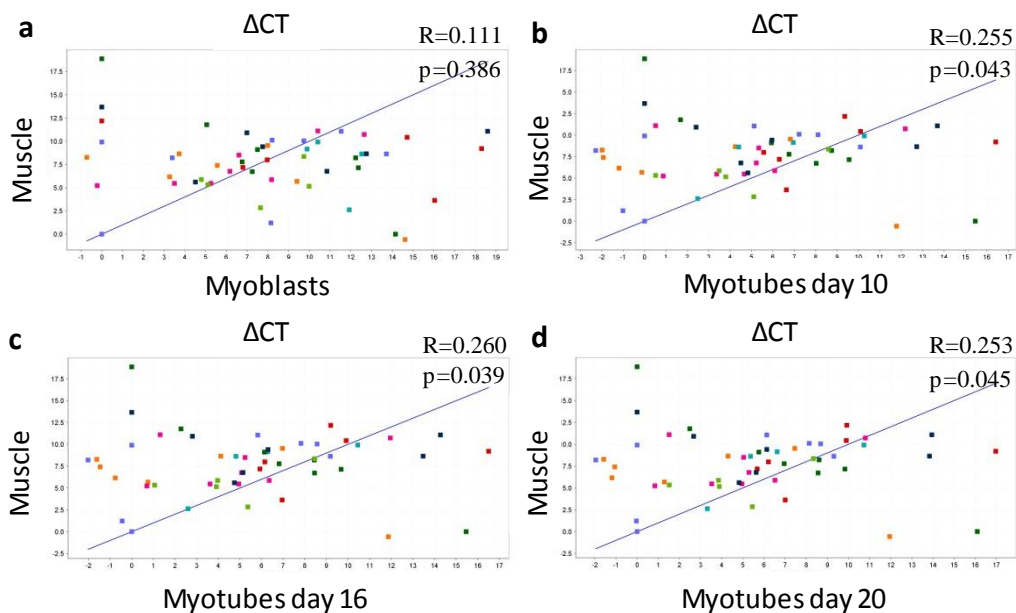


Figure 10. Regression line between muscle and myoblast/myotubes control samples, based on ΔCT . (a) Regression line between muscle and myoblast. (b) Regression line between muscle and myotubes at 10 days of differentiation. (c) Regression line between muscle and myotubes at 16 days of differentiation. (d) Regression line between muscle and myotubes at 20 days of differentiation (Jaka, 2014).

For skeletal muscle cellular models studies, diverse animal origin myoblast cell lines are also available. C2C12 and L6 cell lines, derived from mouse and rat respectively, are widely used. Nonetheless, to avoid inter-species differences, diverse approaches have been employed to obtain myotubes culture. Embryonic stem cells (ESCs) and pluripotent stem cells (PSCs) have been used though direct reprogramming as well as directed differentiation to produce skeletal muscle in the dish (Barberi et al., 2007). Finally, Yamanaka factors have made possible the production of iPS derived myoblast (Darabi et al., 2012).

With regard to studies in LGMD2A, in order to create a proper cellular model, different approaches have been used to modulate *CAPN3* gene expression such as shRNA-lentivirus (Toral-Ojeda et al., 2016). The newly found CRISPR/Cas9 gene-editing technology provides a solution for phenotypic differences found within different mutation carriers patients since the desired mutation combinations could be set into the same background cells to study mutations' phenotype precisely. This approach has already been carried out for Duchenne muscular dystrophy (Shimo et al., 2018).

- *In vivo* models

Several *in vivo* murine models have been developed to study LGMD2A disease. Based on a chronological order, the first one was developed by Tagawa and colleagues (2000). They created three lines of transgenic mice (S62, S44 and S21) that expressed together with fully active *Capn3*, an inactive mutant of *Capn3* gene, in which the active site Cys129 was replaced by Ser (C129S). In these mice,

even if fully active calpain 3 was expressed, some disease features were present such as motor function alterations and some lobulated fibres with centrally located nuclei.

In the same year, a murine model where *Capn3* gene was absent was developed (Richard et al., 2000). This *Capn3* gene deficient mice (*Capn3*^{-/-}) showed LGMD2A typical features in muscle analysis. Histology analysis showed necrotic and regenerative areas together with muscle fibres with centrally located nuclei. Mononuclear cells infiltrations were also present. The second murine model with *Capn3* gene absence was a *Capn3* knock-out (C3KO) model reported by Kramerova and colleagues (2004). These mice showed dystrophic phenotype in their muscles as is observed in LGMD2A patients where reduced cross-sectional area of muscle fibres, rare and small foci of necrosis and regeneration are present (Kramerova et al., 2004; Keira et al., 2007). Further studies showed an unstructured sarcomere with accumulation of abnormal shape mitochondria (Kramerova et al., 2006). However, when identification of differentially expressed genes was carried out in LGMD2A patients and C3KO mice, different results were obtained (Sáenz et al., 2008; Jaka et al., 2012). The comparison between control and LGMD2A patients showed 74 differentially expressed genes (Sáenz et al., 2008). By contrast, only 6 genes were differentially regulated between adult WT and C3KO mice, moreover, none of these were deregulated in human LGMD2A patients (Jaka et al., 2012).

Later, through a different approach to knock-out the gene, another *Capn3* deficient mouse model was created (Laure et al., 2009). In this work other mice model were used together with *Capn3* deficient mouse for the search of muscle wasting targets.

Ojima *et al.*, (2010) developed a knock-in mouse model (p94KI or *Capn3CS/CS*) where the mutation previously used by Tagawa and colleagues, in the active site of the protein, was homozygously expressed. Thus, mice showed more severe phenotype. Their muscles also displayed centrally located nuclei but in this case muscle degeneration worsened with age. Moreover, exercise induced muscle fibres breakdown was observed.

Finally, Ermolova and colleagues (2011) reported two different mice models. The first one consisted on two transgenic mice which overexpressed mutated *Capn3* (C3-R448H or C3-D705G) in which the proteolytic activity was not altered and they were further crossbred with C3KO mice. In parallel, *Capn3* overexpression was induced in WT mice. Calpain 3 was not detected in C3-D705G mutation carrier mice, while in C3-R448H mutation carrier mice it was detected. The calpain 3 overexpression showed muscular force and growth improvement in C3KO mice. By contrast, its overexpression in WT mice seemed to be detrimental.

4. CALPAINS

Calpain superfamily members are intracellular Ca^{2+} -dependent non-lysosomal cysteine proteases that share a common primary sequence which is the calpain-like protease domain (CysPc) (Croall and DeMartino, 1991; Goll et al., 2003; Suzuki et al., 2004; Sorimachi et al., 2011a). The first calpain was identified in 1964 and later 14 more calpain homologs have been identified in humans. Some are ubiquitously expressed while others are tissue specific (Guroff, 1964; Macqueen et al., 2010).

4.1 CALPAIN SUPERFAMILY CLASSIFICATION

Calpain 1 (CAPN1 or μ CL) and calpain 2 (CAPN2 or mCL) were the first calpains to be discovered. Both of them are composed by two subunits: an 80 kDa subunit, where the active site is located and a 28 kDa regulatory subunit, small regulatory subunit 1 (CAPNS1) (Hosfield, 1999).

Based on these calpains' domain structure, the rest of the superfamily members were further classified as classical (if they share the same domain structure as CAPN1 and CAPN2) and non-classical calpains. In humans there are 9 classical calpains and 6 non-classical calpains. Non-classical calpains, in turn, are further divided attending to structural characteristics. On the other hand, according to their expression pattern, 7 calpains are considered ubiquitous while the rest are tissue-specific (**Table 3**) (Sorimachi et al., 2011b).

<i>Gene</i>	<i>Chromosome</i>	<i>Protein names</i>	<i>Tissue-specificity</i>	<i>Classification</i>	<i>References</i>
<i>CAPN1</i>	11q13	CAPN1, μ cl	Ubiquitous	Classical	(Malik et al., 1983)
<i>CAPN2</i>	1q41-q42	CAPN2, Mcl	Ubiquitous	Classical	(Malik et al., 1983)
<i>CAPN3</i>	15q15.1-q21.1	CAPN3, p94	Skeletal muscle	Classical	(Sorimachi et al., 1989)
<i>CAPN5</i>	11q14	CAPN5, hTRA-3	Ubiquitous (abundant in testis and brain)	Non-classical	(Dear and Boehm, 1999; Dear et al., 1997)
<i>CAPN6</i>	Xq23	CAPN6, CAPNX	Embryonic muscles, placenta	Non-classical	(Dear et al., 1997; Dear and Boehm, 1999)
<i>CAPN7</i>	3p24	CAPN7, PalBH	Ubiquitous	Non-classical	(Franz et al., 1999)
<i>CAPN8</i>	1q41	CAPN8, nCL-2	Gastrointestinal tracts	Classical	(Sorimachi et al., 1993a)
<i>CAPN9</i>	1q42.11-q42.3	CAPN9 nCL-4	Gastrointestinal tracts	Classical	(Sorimachi et al., 1993a)
<i>CAPN10</i>	2q37.3	CAPN10	Ubiquitous	Non-classical	(Horikawa et al., 2000)
<i>CAPN11</i>	6p12	CAPN11	Testis	Classical	(Dear and Boehm, 1999; Dear et al., 1999)
<i>CAPN12</i>	19q13.2	CAPN12	Hair follicle	Classical	(Dear et al., 2000)
<i>CAPN13</i>	2p22-p21	CAPN13	Ubiquitous	Classical	(Dear and Boehm, 2001)
<i>CAPN14</i>	2p23.1-p21	CAPN14	Esophagus	Classical	(Dear and Boehm, 2001; Kottyan et al., 2014)
<i>CAPN15</i>	16p13.3	CAPN15	Ubiquitous	Non-classical	(Kamei et al., 1998)
<i>CAPN16</i>	6q24.3	CAPN16	Testis	Non-classical	(Hoogewijs et al., 2012)

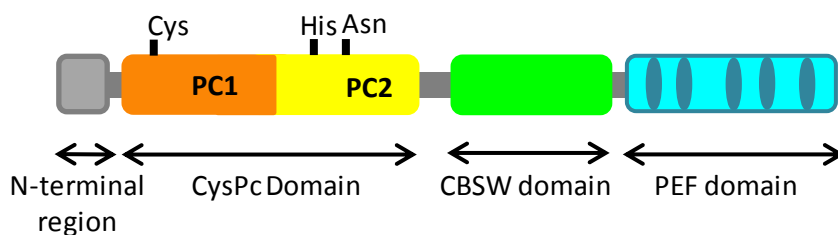
Table 3. Human calpain superfamily members' summary.

4.2 CALPAIN STRUCTURE AND FUNCTIONS

Classical calpains structure is composed of four domains:

- N-terminal anchor helix region.
- Calpain-type cysteine protease conserved domain (CysPc) which in turn is divided in two protease cores subdomains (PC1 and PC2). Three key amino acids that constitute the active site, Cys-105 (in PC1) and His-262 and Asn-286 (in PC2) are within this domain.
- Calpain-type beta-sandwich domain (CBSW) (previously known as C2L domain).
- Penta E-F hand (PEF) domain.

The structure of non-classical calpains, however, could present some of the aforementioned domains with or without different specific domains (**Figure 11**) (Ohno et al., 1984; Maki et al., 1997; Sorimachi et al., 2011a, 2011b; Campbell and Davies, 2012).

a. Classical calpains:

CAPN1
CAPN2
CAPN3
CAPN8
CAPN9
CAPN11
CAPN12
CAPN14

b. Non-classical calpains:

CAPN5
CAPN6
CAPN7
CAPN10
CAPN15
CAPN16

Figure 11. Schematic representation of (a) classical and (b) non-classical calpains structure. C2, protein kinase C conserved domain; MIT, microtubule interacting and transport motif; Zn, zinc-finger motif; SOL, small lobes product homology domain; IQ, calmodulin-interacting motif. Adapted from (Ono and Sorimachi, 2012).

Calpains are Ca^{2+} dependent proteases, they required Ca^{2+} ions for their activation. Calpain protease domain has two Ca^{2+} binding sites (CBS-1 and CBS-2) within PC1 and PC2. Once Ca^{2+} is bound, it provokes a conformational change that approaches PC1 and PC2 domains which in turn induce the activation of the protease domain (Hosfield, 1999; Strobl et al., 2000; Moldoveanu et al., 2008; Hanna et al., 2008).

For its activation conventional calpains CAPN1 and CAPN2, required to form a heterodimeric protein with CAPNS1 through EF-hand motif (Hosfield, 1999). However, CAPN8 and CAPN9 together form a hybrid complex called G-calpain for their activation (Hata et al., 2010).

4.3 CALPAIN 3

Skeletal muscle specific calpain 3 protein, also known as p94, was described in 1989 and later it was localized in chromosome 15q15-1-15.3 in human (Sorimachi et al., 1989; Ohno et al., 1990). But it was not until 1995 when mutations in this gene were associated with limb-girdle muscular dystrophy type 2A (Richard et al., 1995).

The human calpain 3 gene is composed by 24 exons and 2466 nucleotides. The calpain 3 protein has 94 kDa and is formed by 821 amino acids (Sorimachi et al., 1993a; Richard et al., 1995). Even if calpain 3 was firstly discovered to be skeletal muscle specific protein, its mRNA which produces several splicing variants, has been found in diverse human tissues such as heart, eye, peripheral blood mononuclear cells and astrocytes (Azuma et al., 2000; Ma et al., 2000; Fougousse et al., 2000; De Tullio et al., 2003; Kawabata et al., 2003; König et al., 2003). However, the functions of these splicing variant forms are largely unknown. In skeletal muscle, its expression is higher in type II fibres (Jones et al., 1999) and during development appears later than other skeletal muscle proteins (Fougousse et al., 1998).

4.3.1 *Calpain 3 structure*

Calpain 3 is categorized as a classical calpain since it shows significant sequence homology with both human CAPN1 (54%) and CAPN2 (51%) large subunits (Sorimachi et al., 1989). However, it contains three additional regions: **a**) NS, located in the N-terminal region, **b**) Insertion Sequence 1 (IS1), within PC2 domain which contains the autocatalytic activity of the enzyme (Kinbara et al., 1998) and **c**) Insertion Sequence 2 (IS2) between the CBSW and PEF domains, which contains a nuclear localization motif. These additional regions confer to calpain 3 specific features, such as autocatalytic capacity (**Figure 12**).

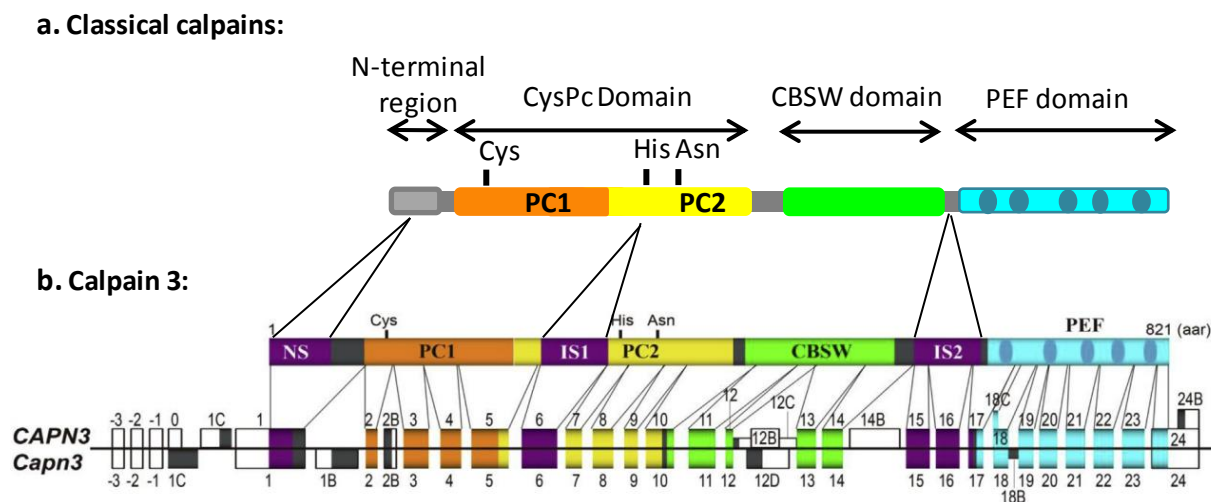


Figure 12. (a) Schematic representation of classical calpains. (b) Schematic representation of calpain 3 protein and gene representation for human and mouse. Adapted from (Ono et al., 2016).

Calpain 3 has short half-life due to its autocatalytic capacity (Sorimachi et al., 1993b), thus, its 3D crystal structure has not been entirely solved. Nevertheless, based on its similarities to calpain 2 and since its structure without Ca^{2+} have already been determined by X-ray crystallography, a 3D model has been proposed for calpain 3. This model lacks NS, IS1 and IS2 regions (**Figure 13**) (Strobl et al., 2000; Jia et al., 2001).

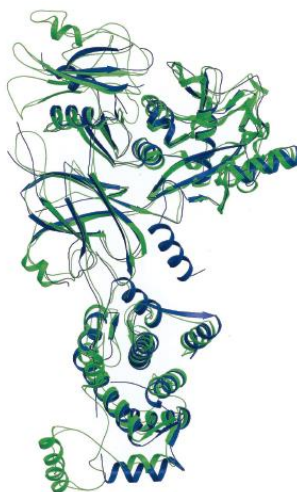


Figure 13. Calpain 3 3D structure proposed by Jia and colleagues (2001). Calpain 3 crystal structure is represented in green and calpain 2 in blue.

4.3.2 Calpain 3 activation and regulation

Knowledge based on truncated calpain 3 mutants and conventional calpains have been used to better understand calpain 3 activation. The amino acid sequence have revealed that calpain 3 also has residues involved in Ca^{2+} binding within the proteolytic domain; however whether calpain 3 is a Ca^{2+} -dependent protease has remained controversial. It was postulated that calpain 3 was not activated by Ca^{2+} but it was activated by Na^+ (Sorimachi et al., 1993b). However, further studies showed how calpain 3 is activated in the presence of Ca^{2+} (Rey and Davies, 2002; García Díaz et al., 2006).

Two-step activation mechanism for calpain 3 activity has been suggested. Upon Ca^{2+} binding to PC1 and PC2 domains, the realignment of the catalytic triad leads to its activation which in turn leads to an autolytic cleavage that has been proposed as follows. Intermolecularly, a rapid cleavage in the N-termini of NS domain occurs. The second step involves a second intermolecular cleavage at C-termini end of IS1 domain leading to two fragments that remain together forming the active enzyme (García Díaz et al., 2006). Calpain 3 could also be cleaved at IS2 leading to its inhibition (Ono et al., 2006). Intramolecularly, IS1 is cut rapidly, followed by a relative slow cut in IS2, whereas a cut in NS does not happen significantly (**Figure 14**).

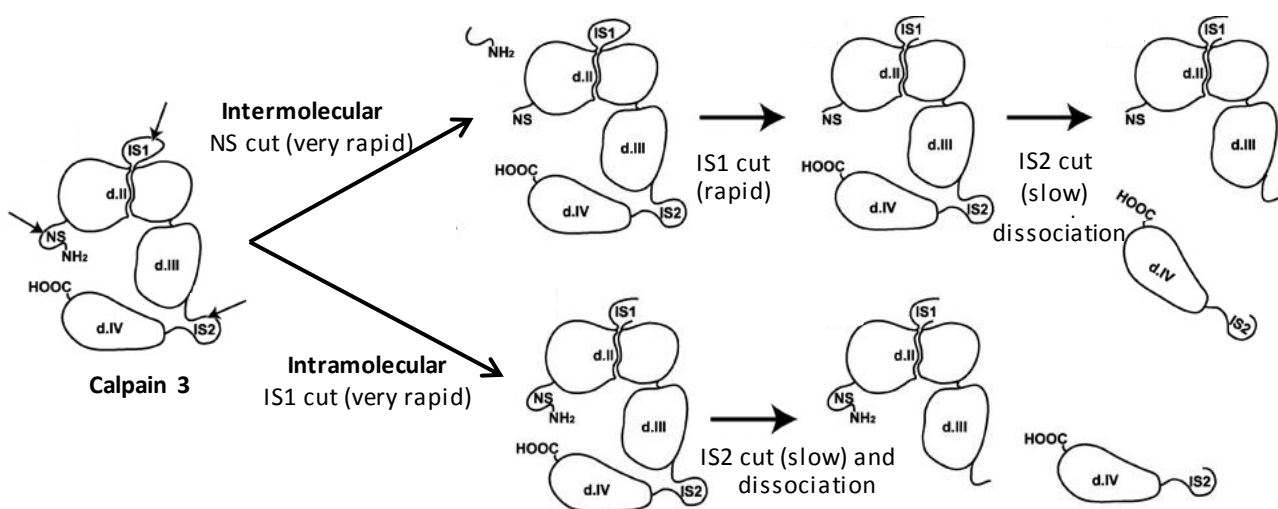


Figure 14. Schematic representation of calpain 3 activation. Arrows indicate the autolytic sites in the NS, IS1, and IS2 regions. d.II, d.III, and d.IV, domain are CysPc, CBSW and PWF domains respectively. Figure adapted from (Ono et al., 2006).

Even if little is known about calpain 3 regulation, its interaction with titin protects calpain 3 from being degraded. Calpain 3 is located in the sarcomere interacting with titin (which spans from the M- to Z- lines of sarcomere) (Sorimachi et al., 1995; Kinbara et al., 1997; Kramerova et al., 2004; Ojima et al., 2007). Within the sarcomere, calpain 3 has been also found in the Z-line (Sorimachi et al.,

1995; Ojima et al., 2007). Calpain 3 binds to two different sites of titin, the N2A and C terminus regions, which are located in the sarcomeric N2- and M-lines (Sorimachi et al., 1995; Kinbara et al., 1997). The proximity of the calpain 3 IS2 domain to titin N2A region (Val⁵⁷³ and Leu⁵⁸⁰ upstream of the IS2 region), suppresses IS2-autolysis (**Figure 15**) (Ono et al., 2006).

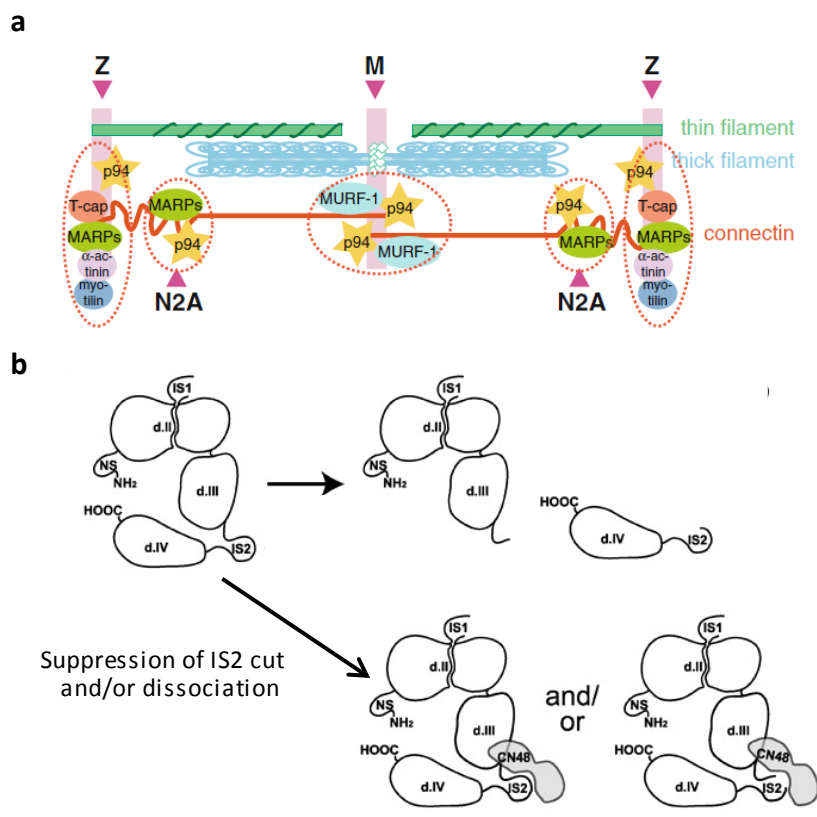


Figure 15. (a) A model for calpain 3, titin and associated proteins in the sarcomere. p94= calpain 3 and connectin= titin. (b) Calpain 3 autolytic cleavage avoidance mediated by titin. CN48= titin cDNA clone encoding N2A region. (Ojima et al., 2006).

As it has been previously mentioned, conventional calpains act as heterodimers formed by calpains and the small regulatory subunit (Hosfield, 1999). However, calpain 3 does not required the small regulatory unit to be active, but even so, some authors have suggested that calpain 3 may homodimerize (Ravulapalli et al., 2005, 2009; Partha et al., 2014).

More recently it has been reported that calpain 3 has two Ser residues in the IS2 region that could be phosphorylated. Phospho-calpain 3 is preferentially located in myofibril fraction and it has been shown that phosphorylation leads to slighter slower autolysis. All these data suggest a new regulation mechanism for calpain 3 location and for its autolysis prevention (Ojima et al., 2014).

On the other hand the endogenous inhibitor for conventional calpains, calpastatin, does not inhibit calpain 3 (Todd et al., 2003; Ono et al., 2004). However, at least two regulators of calpain 3

activity have been identified. The first one is PLEIAD (platform element for inhibition of autolytic degradation) protein. PLEIAD reduces calpain 3 autolytic activity and regulates its substrate-proteolyzing activity (Ono et al., 2013). The second one is calmodulin (CaM). In this case CaM acts as a positive regulator of calpain 3 activity by promoting its autolytic cleavage (Ermolova et al., 2015).

4.3.3 Calpain 3 functions

Since the identification of the implication of calpain 3 in LGMD2A in 1995, several studies have been carried out with the aim of clarifying the pathophysiological mechanism of the disease. However, calpain 3 functions are not fully elucidated.

Together with proteolytic functions, non-proteolytic functions have also been attributed to calpain 3. These findings arose from studies comparing *Capn3*-null and *Capn3* knocking mice. C129S mutation carrier mice, which lead to a proteolytically inactive but structurally intact calpain 3, showed less severe dystrophic symptoms, suggesting that calpain 3 also has a non-proteolytic function.

4.3.3.1 Calpain 3 and sarcomere remodelling

Calpain 3 is located in the sarcomere interacting with titin (Sorimachi et al., 1995; Kinbara et al., 1997; Kramerova et al., 2004; Ojima et al., 2007) and it has also been found in the Z-line (Sorimachi et al., 1995; Ojima et al., 2007). Both proteins are bounded together through IS2 domain of calpain 3 and N2A zone of titin (Ono et al., 2006). It has been proposed that calpain 3 plays a role in titin-based mechanosensory transduction pathway, since the dynamic and distinct localization of calpain 3 has been reported depending on sarcomere length (Ojima et al., 2007). Changes in its location from M-line to N2A region as sarcomere lengthened is allowed by its protease activity. All these findings suggested a possible physical stress sensor that acts in a stretch-dependent manner (Ojima et al., 2011).

This was also described with the studies carried out in C3KO mice where abnormal sarcomere formation was observed in the absence of calpain 3. Authors suggested that calpain 3 is necessary for sarcomere formation since it would be responsible of replacing non-muscle myosins II during myofibrillogenesis. It also could mediate sarcomere remodelling through its protease activity which in turn could be facilitated by placing calpain 3 in the correct proximity of its substrates when it is bounded to titin (Sanger et al., 2002; Kramerova et al., 2004).

Concerning the functions mediating sarcomere remodelling, it has been shown that calpain 3 promotes myofibrillar protein turnover by promoting ubiquitination of muscle proteins. The lack of

calpain 3, leads to accumulation of damaged or misfolded proteins that could be the responsible of muscle pathology (Kramerova et al., 2007).

Moreover, together with abnormal sarcomere formation, abnormal myofibrillogenesis was observed in C3KO myotubes. A study has revealed that M-cadherin and β -catenin accumulation are the responsible of this problem (Kramerova et al., 2004). M-cadherin is involved in myogenic fusion and its deregulation cause fusion problems (Zeschnigk et al., 1995; Charrasse et al., 2006). β -catenin together with M-cadherin plays a role in later stages of myogenic differentiation within cadherin cell adhesion complex (Krauss, 2005). Calpain 3 could cleave both proteins and when it is absent, both accumulates, leading to enhanced fusion of myotubes (Kramerova et al., 2006).

4.3.3.2 Calpain 3 and apoptosis

LGMD2A patients' muscles showed myonuclear apoptosis mediated by the disruption of $\text{I}\kappa\text{B}\alpha/\text{NF-}\kappa\text{B}$ pathway (Baghdiguian et al., 1999). Nuclear factor-kappa B (NF- κB) protein is maintained in the cytoplasm due to its inhibitor $\text{I}\kappa\text{B}\alpha$, after the complex activation, $\text{I}\kappa\text{B}\alpha$ is degraded and NF- κB translocates to the nucleus to activate the expression of anti-inflammatory and cell survival genes.

$\text{I}\kappa\text{B}\alpha$ degradation could be mediated by calpain 3, thus, in the absence of calpain 3, $\text{I}\kappa\text{B}\alpha$ is not degraded what leads to the NF- κB sequestration in the sarcoplasm. This feature was observed in LGMD2A patients' muscles where an accumulation of $\text{I}\kappa\text{B}\alpha$ together with a sarcoplasmic retention of NF- κB was observed. This situation resulted in a failed expression of antiapoptotic genes activation mediated by the lack of NF- κB nuclear translocation, increasing cellular apoptosis (Baghdiguian et al., 1999, 2001). Further studies carried out by Richard and colleagues (2000) in a *Capn3*-deficient mice model, supported these previous findings. Additionally, an impairment of membrane permeability in C3KO mice was suggested together with perturbation of the $\text{I}\kappa\text{B}\alpha/\text{NF-}\kappa\text{B}$ pathway to produce myonuclear apoptosis. They showed normal pattern of NF- κB in half of the fibres, suggesting that alternative mechanisms would be acting to produced myonuclear apoptosis.

Subsequent studies corroborated $\text{I}\kappa\text{B}\alpha/\text{NF-}\kappa\text{B}$ pathway impairment in LGMD2A patients. A NF- κB -dependent expression of some antiapoptotic factors such as c-FLIP, BclII and Bcl- X_L was observed, concluding that calpain 3 participates in the regulation of the expression of NF- κB -dependent survival genes to prevent apoptosis in skeletal muscle (Benayoun et al., 2008).

However, contrary to what was postulated, another study carried out in C3KO mice, found out that the apoptotic positive nuclei were located outside of the sarcolemmal membrane. It was reported that these nuclei corresponded to immune cells since they co-stained with CD11b (Kramerova et al., 2004).

Despite the controversy in the implication of I κ B α /NF- κ B pathway in LGMD2A disease another study reported that oxidative stress and I κ B α /NF- κ B signaling pathway were increased in muscles from LGMD2A patients. They suggested that it could contribute to the increased protein ubiquitinylation and muscle protein loss (Rajakumar et al., 2013).

4.3.3.3 *Calpain 3 and mitochondria*

Histochemical analyses of human LGMD2A patients as well as calpain 3 deficient mice models have shown abnormalities in mitochondrial structure and distribution in lobulated fibres (Kawai et al., 1998; Chae et al., 2001; Kramerova et al., 2009). Kramerova and colleagues (2009) reported that C3KO mice have more but functionally deficient mitochondria which produce elevated reactive oxygen species leading to oxidative stress and energy deficit. Authors suggested that these important pathological features could represent a secondary effect of the absence of calpain 3. Conversely, in a study carried out in human LGMD2A samples, even oxidative damage was present, mitochondrial enzymes dysfunction was not detected (Nilsson et al., 2014). Finally, the latest studies carried out in a *Capn3* null mice has showed attenuated mitochondria biogenesis in muscle regeneration process induced by cardiotoxin (CTX) injection (Yalvac et al., 2017).

4.3.3.4 *Calpain 3 and calcium mediated signaling*

Several studies have described calpain 3 as key protein in regulating calcium release in skeletal muscle. Calpain 3 has been found next to the membrane, in association with triads. Calpain 3 is necessary for the proper recruitment of aldolase A (AldoA; glycolytic enzyme) and ryanodine receptor (RyR; calcium release channel) to the triads. Loss of calpain 3 leads to the reduction of AldoA and RyR which in turn leads to reduced calcium release from the SR to cytoplasm during muscle activation. Calpain 3 plays a structural role stabilizing RyR associated protein complexes in the SR (Kramerova et al., 2008; Ojima et al., 2011; DiFranco et al., 2016).

During muscle activity, Ca²⁺ accumulates in the sarcoplasm, leading to the activation of Ca²⁺-mediated signaling pathways. Given that in the absence of calpain 3 there is a reduced release of Ca²⁺, two Ca²⁺-calmodulin dependent pathways have been widely studied; calcineurin/nuclear factor of activated T-cells (NFAT) pathway and Ca²⁺-calmodulin-dependent protein kinase (CaMK) pathway.

Studies carried out in C3KO mice showed that only CaMK-mediated signaling is decreased. This was proven by reduced total and activated CaMK as well as nuclear accumulation of class II HDAC (Potthoff et al., 2007; Kramerova et al., 2012). The impaired CaMK signaling led C3KO mice to fail in muscle adaptation after exercise since exercise training increases slow fibres proportion mediated by

CaMK signaling. (Talmadge, 2000; Bassel-Duby and Olson, 2006). Impaired CaMK pathway also leads to altered transcriptional response in C3KO mice. Gene expression activation of genes related to lipid metabolism, energy production and sarcomere maintenance are deregulated (Kramerova et al., 2016).

In LGMD2A patients RyR1 downregulation also was observed, however no conclusive data regarding CaMK or calcineurin were observed (Kramerova et al., 2012). Another group studied Ca²⁺ mediated signaling in human myotubes where calpain 3 has been silenced. Ca²⁺ release and SERCA mediated Ca²⁺ uptake into the SR, was reported also to be impaired. This myotubes displayed reduced SERCA1/2, RyR1 and small ankyrin 1 (sAnk1) protein levels that led to significant increased of basal intracellular Ca²⁺ levels. However, in LGMD2A muscles only SERCA2 downregulation was observed in LGMD2A patients' muscles (Toral-Ojeda et al., 2016).

4.3.3.5 Calpain 3 and regeneration

A study carried out in C2C12 cell line demonstrated that calpain 3 participates in the establishment of the pool of reserve satellite cells by downregulation of MyoD via proteolysis, thus promoting renewal of the satellite cell compartment (Stuelsatz et al., 2010). However, when these findings were analysed in human LGMD2A skeletal muscles, a significant increase of Pax7 positive satellite cells were observed (Rosales et al., 2013). Authors attributed satellite cells increase to downregulation of muscle specific microRNAs: miR-1, miR-133a and miR-206. Since it has been proven that miR-1 and miR-206 facilitate satellite cells differentiation and their downregulation increase Pax7 levels (Yuasa et al., 2008; Chen et al., 2010; Dey et al., 2011). A recent study carried out in *Capn3* deficient mice showed that muscle regeneration is impaired after a single CTX injection. *Capn3* null mice showed a downregulation of muscle-specific microRNAs (miR-206) through TGF- β signaling pathway, which is a potent myogenic differentiation inhibitor (Winbanks et al., 2011; Rosales et al., 2013; Yalvac et al., 2017).

When muscle regeneration was assessed in LGMD2A patients, based on developmental markers such as neonatal myosin heavy chain, vimentin, MyoD and myogenin, negative impact on regenerative response was observed. Regeneration was more severely impaired when patients have *CAPN3* null-alleles (Hauerslev et al., 2012).

In addition to all of these findings, *in vitro* studies carried out in both C3KO and human cells have reported that myoblast fusion is defective when calpain 3 is absent (Kramerova et al., 2006; Jaka et al., 2017). Furthermore, perturbed AKT/mTOR signaling pathway has been observed in *Capn3* null regenerating muscles (Yalvac et al., 2017).

4.3.3.6 Calpain 3 deregulation in tumour tissue

Different studies have related calpain 3 expression regulation to cell cycle progression, however the results were contradictory. On the one hand, calpain 3 downregulation was observed after treatment in melanoma cell lines (Huynh et al., 2009) while also calpain 3 downregulation have been related to a highly invasive metastatic phenotype in the same cell line (Moretti et al., 2009; Ruffini et al., 2013). Moreover, calpain 3 upregulations has been found in papillomavirus-associated urothelial tumours (Roperto et al., 2010).

All these studies related calpain 3 with cell cycle regulation however no studies indicating presence of tumours in LGMD2A patients have been described so far. Furthermore, whether this function is implicated in the pathophysiology of LGMD2A disease has not been studied yet.

HYPOTHESES AND OBJECTIVES

HYPOTHESES

CHAPTER 1: *In vitro* analyses of the pathophysiology of LGMD2A

- I. The tendency towards the homogenization between controls and LGMD2A patients' cell cultures, together with a lack of correlation between myoblast/myotubes and their tissue of origin are a methodological limitation for cell analysis. Thus the use of sera obtained from healthy controls as well as LGMD2A patients to grow cells *in vitro*, will improve the recapitulation of the observed events in muscle.
- II. Although lack of calpain 3 is the responsible of the disease, several genes are deregulated in patients' muscles. Modulation of the deregulated genes could rescue the normal function of the muscle and unveil potential therapeutic targets.
- III. The analysis of protein regulation in LGMD2A patients' muscles could characterize essential signaling pathways that are impaired in the muscle fibre of LGMD2A patients.

CHAPTER 2: *Study of Frzb absence effects in the muscle of a murine model (Frzb^{-/-}) in vitro and in vivo*

- IV. The characterization of *Frzb^{-/-}* mice muscle, at functional as well as at molecular/cellular level, could contribute to the knowledge of the mechanisms involved in LGMD2A pathophysiology.

OBJECTIVES

CHAPTER 1: *In vitro* analyses of the pathophysiology of LGMD2A

- I. To establish use of human serum as an *in vitro* strategy to obtain a better correlation between cultures and muscle tissue.
- II. To establish the implication of the deregulated genes in the pathophysiology of the disease.
- III. To characterize the effect of gene expression control by means of siRNA to rescue the deregulated expression observed in LGMD2A muscle.
- IV. To identify perturbations in signaling pathways in the skeletal muscle of LGMD2A patients to shed some light on the pathways implicated in the muscle homeostasis.

CHAPTER 2: *Study of Frzb absence effects in the muscle of a murine model (Frzb^{-/-}) in vitro and in vivo*

- V. To establish possible muscle dysfunctions (strength or gait pattern alterations) due to *Frzb* gene absence in *Frzb^{-/-}* mice.
- VI. To analyse muscle regeneration capacity in *Frzb^{-/-}* mice after induced injury.
- VII. To characterize cell types with myogenic potential (satellite cells and mesoangioblasts) in *Frzb^{-/-}* mice muscles.
- VIII. To characterize the differential expression of genes and proteins between *Frzb^{-/-}* and WT mice muscle.

MATERIALS AND METHODS

1. BIOLOGICAL MATERIAL

1.1 HUMAN ORIGIN SAMPLES

For this study skeletal muscle biopsy samples were obtained from Donostia University Hospital after all subjects gave informed consent, using forms approved by the Ethics Committee on the Use of Human Subjects in research.

Biopsies from LGMD2A patients were collected after disease diagnosis have been confirmed genetically by the identification of both mutations in the *CAPN3* gene. Control healthy samples were chosen from patients that underwent surgery due to bone fractures.

Proximal limb muscles were most used muscle samples (Fardeau et al., 1996a; Urtasun et al., 1998) but distal limb muscles were also used.

Human primary myoblast obtained from proximal muscles biopsies (*Tibialis anterior*) were kindly provided by Dr. Schneiderat from the Muscle Tissue Culture Collection, Munich (Germany).

Muscle biopsies were used for different purposes, protein extraction as well as muscle cell (myoblasts) isolation for cell culture experiments. Depending on the sample availability for each of them different sets of muscles were used. All samples details are listed in the next table (**Table 4**).

Sample	Status	Age	Gender	Origin tissue	Ambulation	CAPN3 mutations	
						Mutation 1	Mutation 2
1: Foetal Bovine Serum Vs human heterologous serum experiment							
09-21	P	19	M	<i>Biceps brachii</i>	Ambulant	p.(His690ArgfsX9)	p.(His690ArgfsX9)
13-05	C	14	M	Quadriceps	-	-	-
2: Proximal muscles for myoblast isolation							
09-21	P	19	M	<i>Biceps brachii</i>	Ambulant	p.(His690ArgfsX9)	p.(His690ArgfsX9)
09-25	P	28	M	<i>Deltoid</i>	Ambulant	p.(Lys254Glu)	p.(Pro637HisfsX25)
10-39	P	29	M	<i>Deltoid</i>	Wheelchair bound	p.(Lys254del)	p.(X822Leuext62X)
10-36	C	23	M	<i>Biceps brachii</i>	-	-	-
13-05	C	14	M	<i>Quadriceps</i>	-	-	-
13-07	C	36	F	<i>Biceps brachii</i>	-	-	-
3: Distal muscles for myoblast isolation							
2009Ca11	P	27	M	<i>Tibialis anterior</i>	Ambulant	p.(Thr184Argfs*36)	p.(Thr184Argfs*36)
2009Ca13	P	21	F	<i>Tibialis anterior</i>	Ambulant	p.(Thr184Argfs*36)	p.(Arg490Trp)
2009Ca14	P	12	M	<i>Tibialis anterior</i>	Ambulant	c.1992+1G>T	p.(Thr679Serfs*20)
08-08	C	34	M	<i>Tibialis anterior</i>	-	-	-
4: Muscles for protein analysis							
5	P	13	M	<i>Deltoid</i>	Asymptomatic	p.(Arg788SerfsX14)	p.(Arg788SerfsX14)
9	P	14	F	<i>Biceps braquii</i>	Asymptomatic	p.(Arg490Trp)	p.(Gly691TrpfsX7)
36	P	26	M	<i>Quadriceps</i>	Ambulant	p.(Lys254Glu)	c.1910delC
114	P	49	M	<i>Deltoid</i>	Ambulant	p.(Pro637HisfsX25)	p.(Asp665LeufsX18)
168	P	*	M	*	Ambulant	p.(Ser479Gly)	p.(Asp665LeufsX18)
169	P	51	M	<i>Deltoid</i>	Ambulant	p.(Ser479Gly)	p.(Asp665LeufsX18)
352	P	19	M	<i>Deltoid</i>	Ambulant	p.(Arg788SerfsX14)	p.(Arg788SerfsX14)
27	C	50	M	<i>Quadriceps</i>	-	-	-
31	C	46	M	<i>Quadriceps</i>	-	-	-
33	C	51	M	<i>Deltoid</i>	-	-	-
38	C	31	M	<i>Quadriceps</i>	-	-	-
42	C	52	M	<i>Quadriceps</i>	-	-	-

Table 4. Control and LGMD2A human samples information. Status; P= LGMD2A patient and C= Control. Gender; M= male and F= female. *= Not available information.

Sample processing started at operating room at the hospital where muscle piece is removed and conserved in a sterile phosphate-buffered saline (PBS; Gibco- Thermo Fisher Scientific; Whatman, MA, USA) containing wet gauze until procedure room in the laboratory. At this point, muscle pieces were cleaned in a $\text{Ca}^{2+}/\text{Mg}^{2+}$ containing Hank's balanced salt solution (HBSS; Thermo Fisher Scientific) supplemented with 1% of penicillin/streptomycin (P/S) and fungizone (amphotericin B) (Thermo Fisher Scientific). Blood vessels and fat tissue present in muscle biopsy were removed.

Once muscle piece was clean, could be processed for different purposes, RNA or protein extraction and cells (myoblast) isolation. When muscle biopsy was used for RNA or proteins extraction, muscle piece was directly frozen into liquid nitrogen and further stored in -80°C freezer. By comparison, for myoblast isolation muscles had to be processed in a different way (see myoblast isolation).

1.2 MURINE ORIGIN SAMPLES

The generation of *Frzb* knockout (*Frzb*^{-/-}) mice was carried out at Skeletal Biology and Engineering Research Centre (Katholieke Universiteit Leuven, Belgium). Cre/loxP strategy was employed to inactivate *Frzb* gene (exon 1 was floxed). Mice were back-crossed into two different backgrounds (Swiss/CD1 and C57BL/6) for over 10 generations (Lories et al., 2007). In the experiments reported here, C57BL/6 mice were at least in the 19th -20th generation of backcrossing. WT C57BL/6 mice were purchased from Janvier (Le Genest St Isle, France). Mice with normal immune status were housed in groups of 4-5 mice in Static micro-insulator cage with Macrolon filter with bedding material (composed of spruce particles of approximately 2.5 - 3.5 mm, type Lignocel® BK 8/15), under conventional laboratory conditions (14 h light – 10 h dark; 23±/-2°C), with standard mouse chow food (Sniff, Soest, Germany) and water provided ad libitum. All studies were performed with the approval from the Ethics Committee for Animal Research (P034/2016; KU Leuven, Belgium).

Mice were genotyped by PCR using DNA obtained from ear biopsy tissue. WT and knockout (KO) alleles were amplified using forward primer p1 (5'-TGAACCTTGCCCGACCTCTGAG-3') and reverse primer p2 (5'-GATCGCTCGGATCACTTGTGG-3') or using forward primer p3 (5'-CTGATGTCTCTGCCAGAGCGAG-3') and reverse primer p4 (5'-TGGACGTAACTCCTCTCAGACC-3'), respectively (Lories et al., 2007).

Several sets of mice were used with different purposes (**Table 5**). For more detailed information, **appendix II, table 1**.

<i>Experimental procedure</i>	<i>Genotype</i>		<i>Age (weeks)</i>
	WT	<i>Frzb</i> ^{-/-}	
Muscle strength analysis	9	13	5 - 6
Catwalk analysis			
8 week-old mice	20	16	8
10 week-old mice	19	17	10
	-----	-----	
	39	33	
RNA and protein extraction			
	15	15	10 - 11
Chronic exercise protocol			
Not-trained	4	3	
Trained	5	4	
	-----	-----	
	9	7	5
Cardiotoxin injection			
CTX + 3 days	4	3	
CTX + 7 days	4	3	
CTX + 14 days	4	6	
CTX + 28 days	7	8	
	-----	-----	
	19	20	10
Satellite cells isolation			
	7	7	4
ALP+ cells isolation			
	8	8	3 - 4

Table 5. Information of used mice.

2. RNA ISOLATION

2.1 RNA ISOLATION FROM HUMAN OR MURINE SKELETAL MUSCLE

RNA isolation from skeletal muscle was based on mechanical disruption of the tissue through stainless steel beads in plastic RNase free tubes with the TissueLyser (QIAGEN, Hilden, Germany).

For each muscle or muscle piece, one bead was introduced in rounded bottom eppendorf. Five hundred microliters of cold trizol (QIAzol®, QIAGEN) were added before frozen muscle introduction. After that, samples were set into the TissueLyser where a first cycle of 30 s at 30 Hz was performed. Next, an incubation step was performed; one minute on ice where more cold trizol, 500 µl were added. Following, another cycle of 30 s at 30 Hz was performed. This step could be repeated if big undisrupted muscles were observed.

Finally, samples were centrifuged at 8,000 rpm for 3 min at 4°C. Supernatant was collected in a new RNase free tube. At this point samples could be stored at -80°C or continue with RNA extraction.

2.2 RNA ISOLATION FROM HUMAN OR MURINE CELLS

For RNA isolation cell plates were washed twice with cold PBS once medium was removed. After that, 700 μ l of cold trizol was added. Cells were detached with cell scrapers and collected on an RNase free eppendorf. Samples were subjected to a vortex for one minute. At this point samples could be stored at -80°C or continue with RNA extraction.

Total and small RNAs were purified using miRNasy mini kit (QIAGEN) following the company's protocol. Trizol samples were placed at room temperature (RT) for 5 min. One hundred and forty microliters of chloroform (Merck KGaA) was added. All samples were shaken vigorously for 15 s followed by an incubation of 3 min at RT. Next, tubes were centrifuged at 1,2000 g for 15 min at 4°C . When finished, RNA containing supernatant (upper clear aqueous phase) was collected, avoiding white interphase (that contains proteins) and lower organic phase (that contains DNA and lipids). From here the protocol was carried out in a QIACube (QIAGEN) where next steps were carried out, as informed in the company's protocol:

- 1.5 volumes of 100% ethanol were added followed by mixing thoroughly by pipetting.
- 700 μ l of this mixture were placed into an RNeasy[®] Mini column placed in a 2 ml collection tube.
- Samples were centrifuged at 8,000 g for 15 s at RT. Flow-through was discarded. This step was repeated using the remainder of the samples.
- 700 μ l of buffer RWT buffer was added to the RNeasy[®] Mini column and samples were centrifuged at 8,000 g for 15 s at RT. Flow-through was discarded.
- 500 μ l of buffer RPE was added to the RNeasy[®] Mini column and samples were centrifuged at 8,000 g for 2 min at RT.
- RNeasy[®] Mini column was placed in a new 1.5 ml collection tube. Thirty microliters of RNase-free water was pipetted directly onto the column membrane. Next, samples were centrifuged at 8,000 g for 1 min to elute RNA.

The obtained RNA was eluted in 30 μ l of RNase-free water. At this point samples could be stored at -80°C .

2.3 RNA QUANTIFICATION

NanoDrop spectrophotometer ND-1000 was used to measure RNA concentration (ng/ μ l) and purity (absorbance ratio at 260 nm/280 nm and 260 nm/230 nm). If the absorbance ratio at 260 nm and 280 nm were lower than 1.8, samples were discarded due to the presence of protein or phenol

contamination. Similarly, if the absorbance ratio at 206 nm and 230 nm were diverse form 2.0, samples were discarded due to the presence of contaminants which absorb at 230 nm.

2.4 cDNA SYNTHESIS: REVERSE TRANSCRIPTION POLYMERASE CHAIN REACTION (RT-PCR)

RNA obtained either from skeletal muscles or cell cultures was reversed transcribed with High-Capacity cDNA Reverse Transcription Kit (Thermo Fisher Scientific) following the company's protocol. All species of RNA molecules present, including mRNA and rRNA were transcribed due to random primers.

In a final volume of 50 μ l, 25 μ l of RNA at 50 ng/ μ l and 25 μ l of reverse transcription master mix were mixed. The reverse transcription master mix was performed following manufacturer recommendations (**Table 6**).

Reverse transcription master mix	
Component	Volume per reaction
10X RT buffer	5 μ l
25X dNTP mix (100 mM)	2 μ l
10X random primers	5 μ l
MultiScribe™ reverse transcriptase	2.5 μ l
RNase inhibitor	2.5 μ l
Nuclease-free H ₂ O	8 μ l
Total volume	25 μl

Table 6. Reverse transcription master mix composition and volumes for a final volume of 25 μ l.

Tubes were centrifuged and introduced into a thermal cycler. The used program on the thermal cycler is detailed below (**Table 7**). Obtained cDNA was stored at -20°C.

	Step 1	Step 2	Step 3	Step 4
Temperature	25°C	37°C	85°C	4°C
Time	10 min	120 min	5 min	∞

Table 7. Thermal cycler conditions.

2.5 REAL-TIME QUANTITATIVE PCR

Real-time quantitative PCR was used to analyse gene expression levels. Two different approaches were used for this purpose: **a)** SYBR Green-based detection and **b)** TaqMan™ probes-based detection.

2.5.1 SYBR Green-based detection

A custom-designed SYBR Green panel was used (Bio Rad) to test a series of 38 genes in murine samples. Genes were selected base on previous knowledge (Sáenz et al., 2008; De la Torre et al., 2009; Lories et al., 2009; Lodewyckx et al., 2012). For a more detailed information; **appendix II, table2.**

- **Muscle specific genes:** *Myh1, Myh2, Myh4* and *Pax7*.
- **Deregulated genes in LGMD2A patients' muscles:** *Canp3, Capn6, Col1a1, Dok5, Fhl1, Itgb1bp2, Myl6b, Myom3, Myot* and *Vldlr*.
- **Deregulated genes in *Frzb*^{-/-} mice articular cartilage and LGMD2A patients' muscles:** *Aspn, Col3a1, Col5a1, Col15a1, Cthrc1, Ctnnb1, E2f8, Fasn, Fn1, Frzb, Igf1, Mest, Myc, Rora, Sema3c, Slc16a1, Sorb1* and *Tfrc*.
- **Genes coding for proteins participating in Wnt signaling pathway:** *Lrp5, Lrp6, Wnt8a* and *Wnt8b*.
- **Endogenous controls:** *Gapdh* and *Tbp*.

The primePCR custom plates was designed in a 384-well plate panel to test three different samples in each plate. Panels already had lyophilized primers in each well and PCR reaction mix and samples were added.

Each plate contains four different experimental control assays designed to assess the quality of samples, the reverse transcription reaction and quantitative PCR reaction. Only samples that fulfil the required criteria were analysed.

- **Positive PCR control assay:** a synthetic DNA template (not present in human and mouse genome) was added to test possible inhibitors. For that purpose 0.5 µl of PrimePCR PCR control buffer was added. The obtained result from this analysis was accepted when $\Delta C_q > 1$, being $\Delta C_q = \text{PCR } C_q \text{ control sample} - \text{PCR } C_q \text{ for sample}$ (quantification cycle C_q).
- **Reverse transcription control assay:** a synthetic RNA template was introduced into the cDNA synthesis reaction to evaluate its performance. In this case lyophilized retrotranscription control assay template was diluted in 200 µl of RNase-free water. For each sample 1 µl of this control RNA template was added to each 20 µl of cDNA synthesis reaction. The obtained result

could compromise gene expression when $\Delta C_q > 1$, being $\Delta C_q = \text{PCR } C_q \text{ control sample} - \text{PCR } C_q \text{ for sample}$.

- **DNA contamination assay:** was used to assess whether genomic DNA was present in the samples. If samples $C_q > 35$; no genomic DNA was present. Otherwise if $C_q < 35$ indicated the presence of it. RNA control template was added to this well too.
- **RNA quality:** was used to study the possible RNA degradation. The obtained result demonstrated minimal degradation when $\Delta C_q \geq 3$. However values of $\Delta C_q < 3$ indicated that RNA integrity may compromise gene expression.

PrimePCR custom plates were allowed to reach room temperature and iTaq universal SYBR Green supermix (Bio Rad), cDNA samples and positive PCR control DNA template were thawed on ice protected them from light.

PCR reaction mix was made following company's protocol adding all required components. One PCR reaction mix for each cDNA sample was prepared using 8.78 ng of cDNA (**Table 8**).

PCR reaction mix		
Component	Volume per reaction	Final concentration
PrimePCR assay	Dried in well	1x
iTaq™ Universal SYBR® Green Supermix	5 µl	1x
cDNA sample	0.5-2 µl	100 ng-100 fg
Nuclease-free water	Variable	
Total volume	10 µl	

Table 8. PCR reaction mix components.

Plates were sealed prior to centrifuge to remove possible bubbles. For gene quantification CFX384 Touch Real-Time PCR Detection System (Bio Rad) was used with a specific thermal cycling programme (**Table 9**). Data processing was made using CFX Manager Software.

Thermal cycling programme			
Step	Temperature	Time	Number of cycles
Activation	95°C	2 min	1
Denaturation	95°C	5 seconds	40
Annealing/extension	60°C	5 seconds	
Melt curve	65-95°C (0.5°C increments)	5 seconds/step	

Table 9. Thermal cycling programme.

The expression of all transcripts was determined relative to the internal housekeeping gene in the plate, *GAPDH* or *TBP*, for which no alterations in expression were detected. For relative gene expression comparisons between WT mice and *Frzb*^{-/-} mice muscles, 2^{- $\Delta\Delta$ CT} method was applied.

2.5.2 TaqMan™-based detection

Individual TaqMan real-time PCR assays and custom-designed TaqMan Low-Density Arrays (TLDA) (Applied Biosystems) were used. 7900HT Fast Real-Time PCR System (Applied Biosystems) was used to perform gene expression analysis.

For the experiments where individual assays were performed, TaqMan™ Gene Expression Master Mix (Thermo Fisher Scientific) and cDNA samples diluted in RNase-free water were mixed. Twenty-five nanograms of cDNA were added per well together with 1 μ l for 96 well-plate or 0.5 μ l for 384 well-plate of TaqMan™ probes in a final reaction volume of 20 μ l or 10 μ l for 96 well-plates and 384 well-plates respectively. All the components were maintained on ice and protected from light. Plates were sealed prior to centrifugation to remove possible bubbles. Used TaqMan™ probes are listed on **appendix II, table 3**.

By comparison, TLDA custom-designed plates were used to test a series of 64 genes based on the validation of the 74 genes that were found to be deregulated in the muscle of LGMD2A patients (Sáenz et al., 2008). TLDA custom-plate was provided as 384 well-plate to test 64 genes in triplicate for two different samples. TLDA TaqMan™ probes are listed on **appendix II, table 4**.

TLDAs were maintained at room temperature prior to their use. All the components were maintained on ice. For each sample the PCR reaction mix was prepared as follow (**Table 10**).

PCR reaction mix	
<i>Component</i>	<i>Volume per reaction</i>
PrimePCR assay-probes	Dried in well
TaqMan™ Gene Expression Master Mix	200 μ l
cDNA simple (1000 ng)	200 μ l
Nuclease-free water	Variable
Total volume	400 μl

Table 10. PCR reaction mix.

To distribute all the samples homogeneously to the reaction wells, the TLDA plates had to be centrifuged following manufacturer recommendations, 1,200 rpm for one minute, twice. Finally, TLDA plates were sealed as instructed and were inserted into the real-time PCR machine.

The following programme was used for single assays as well as for TLDA.

Thermal cycling programme

	UDG incubation	AmpliTaq Gold, UP enzyme activation	PCR	
	Hold	Hold	40 cycles	
			Denature	Anneal/Extend
Time	2 min	10 min	15 seconds	1 min
Temperature	50°C	95°C	95°C	60°C

Table 11. Thermal cycling protocol for gene expression analysis. UDG= Uracil-DNA glycosylase.

The expression of all transcripts was determined relative to the internal housekeeping gene in the same plate (*GAPDH* or *TBP* genes). For relative gene expression levels between samples, $2^{-\Delta\Delta CT}$ method was applied. DataAssist v3.01 and RQ Manager from Applied Biosystems programs were used for that purpose.

3. PROTEIN EXTRACTION

3.1 PROTEIN ISOLATION FROM SKELETAL MUSCLE

The same procedure was carried out for human or murine origin samples. It was based on mechanical disruption of the tissue through stainless steel beads in plastic tubes with the TissueLyser (QIAgen).

For protein extraction two different buffers were used Nicholson (Anderson and Davison, 1999) and Paris protein extraction buffers (**Table 12**).

Nicholson buffer for protein extraction		Paris buffer for protein extraction	
<i>Compound</i>	<i>Final concentration</i>	<i>Compound</i>	<i>Final concentration</i>
Tris hydrochloride pH 6.8	1.25 M	Tris hydrochloride pH 6.8	4.5 mM
Urea	4 M	SDS	15%
Sodium dodecyl sulfate (SDS)	4%	Glycerol	20%
2-mercaptoethanol	5%	Bromophenol blue	0.5%
Glycerol	1%	2-mercaptoethanol	5%
Bromophenol blue	0.001%	Protease inhibitor cocktail	1 tablet for 10 ml
Protease inhibitor cocktail	1 tablet for 10 ml	β -glycerophosphate	50 mM
β -glycerophosphate	50 mM	Sodium pyrophosphate	5 mM
Sodium pyrophosphate	5 mM	dH ₂ O	
dH ₂ O			

Table 12. Nicholson and Paris buffers composition. dH₂O= distilled water.

For muscle disruption each muscle was introduced in a rounded bottom tube containing 20 μ l of elected buffer for each milligram of tissue and one stainless steel bead. Samples in Nicholson buffer were maintained on ice while those in Paris buffer were maintained at RT because Paris buffer solidifies at low temperatures. Next, samples were set into the TissueLyser where a first cycle of 30 s at 30 Hz was performed. Following, another cycle of 30 s at 30 Hz was performed. For those samples which were in Nicholson buffer, 1 min incubation on ice was performed between two TissueLyser cycles. TissueLyser cycles could be repeated if big undisrupted muscles were shown.

Finally, proteins were denatured at 100°C for 5 min on a thermoblock and centrifuged at 8,000 rpm for 3 min. Supernatant was collected on a new tube and samples were stored at -80°C.

3.2 PROTEIN ISOLATION FROM CELLS

The procedure carried out was the same for human or mice and for myoblasts or myotubes samples.

For protein extraction two different buffers were used, Paris (the same as for muscles) and RIPA protein extraction buffers (**Table 13**). The composition of PARIS did not allow quantifying protein amount with any of the available methods while proteins extracted with RIPA buffer could be quantified by diverse techniques.

RIPA buffer for protein extraction	
Compound	Final concentration
Tris hydrochloride pH 7.8	50 mM
Sodium chloride (NaCl)	150 mM
SDS	0.10%
Na·Deoxycholate	0.50%
Triton X-100	1%
Protease inhibitor cocktail tablets	1 tablet for 10 ml
Sodium fluoride (NaF ¹)	5 mM
Activated sodium orthovanadate (Na ₃ O ₄ V ²)	1 mM
E-64 ³	10 µM
Phenylmethane sulfonyl fluoride (PMSF ⁴)	1 mM
dH ₂ O	

Table 13. RIPA buffer composition. (1) NaF was used as protein phosphoserine and phosphothreonine phosphatases inhibitor. (2) Activated Na₃O₄V was used as protein phosphotyrosine phosphatases inhibitor. It should be activated since depolymerized vanadate has maximal inhibition activity. For that purpose a stock solution of Na₃O₄V (1 mM or higher concentrations) was prepared in dH₂O. The pH had to be adjusted at 10.0. To ensure the presence of vanadate monomers, the solution was boiled until translucent and the pH was readjusted to 10.0 again. This procedure had to be repeated until the solution remains colourless (orange colour observed before boiling was due to decavanadate) and the pH stabilized at 10.0. To adjust the pH solution had to be at room temperature. Activated Na₃O₄V could be stored at -20°C. (3) E-64 is a cysteine protease inhibitor. It was required to be prepared in ethanol. (4) PMSF is a serine protease inhibitor. It was required to be prepared in ethanol.

For protein extraction, cultured cell medium was removed and plates were washed twice with cold PBS. Next, 8 µl/cm² of protein extraction buffer was added. Cells were detached with cell scrapers and collected samples were subjected to a vortex for 10 s. At this point proteins extracted with RIPA buffer were stored at -80°C while proteins extracted with Paris buffer were denatured at 100°C for 5 min previous to store them at -80°C.

3.3 PROTEIN QUANTIFICATION

Proteins extracted with RIPA buffer were quantified with Bradford method. This method is based on the ability of coomassie brilliant blue G-250 dye to bind to proteins and convert in a stable unprotonated form (with blue colour) that absorbs at 595 nm.

The assay was performed in microplates where 5 μ l of sample and 250 μ l of Bradford 1X dye reagent (Bio Rad) were mixed. Prior to absorbance measure, plates were incubated at RT for 5 min in darkness. Absorbance at 595 nm was measured in a microplate reader. The obtained measure results were the mean of three different measures.

3.4 PROTEIN ANALYSES

3.4.1 Western blot analysis

Homogenised samples were loaded into homemade SDS-polyacrylamide gel (**Table 14**).

Western blot gel composition for one gel		
Component	Resolving (%8)	Stacking (3%)
Tris-HCl 1.875 M, pH 8.8	2 ml	
Tris-HCl 1.25 M, pH 6.8		325 μ l
Acrylamide 29:1 30%	2.65 ml	325 μ l
Glycerol 50%	2 ml	325 μ l
dH ₂ O	3.294 ml	2.095 ml
SDS 25%	80 μ l	25 μ l
TEMED	5 μ l	5 μ l
APS (15 mg/ml)	150 μ l	150 μ l

Table 14. SDS-polyacrylamide gel composition. Resolving was made at 8% while Stacking was made at 3% of acrylamide/bis solution. TEMED= N,N,N',N'-Tetramethyl-ethylenediamine and APS= ammonium persulfate.

When RIPA buffer was used, 15 μ g of total proteins were loaded per well. SDS proteins sample buffer (**Table 15**) was added to allow protein solubilisation and samples were further denatured for 5 minutes at 100°C.

4X SDS Protein sample buffer

<i>Component</i>	<i>Final concentration</i>
Glycerol	40%
SDS	8%
Bromophenol blue	0.04%
2-mercaptoethanol	5%
Tris-HCl pH 6.8	240 mM

Table 15. SDS protein sample buffer composition (4X).

A mixture of multi coloured recombinant proteins was loaded as protein standard (Bio Rad). Proteins were separated by electrophoresis in Running buffer 1X at 50 mA for 2 hours and transferred to a 0.45 µm nitrocellulose blotting membranes (GE Health care life science) performed in cold Transference buffer 1X at 400 mA for one hour (**Table 16**).

Running buffer 10X		Transfer buffer 5X	
<i>Component</i>	<i>Grams per one litre</i>	<i>Component</i>	<i>Grams per one litre</i>
Tris	30.3	Tris	30
Glycine	144	Glycine	144
SDS	15	SDS	0.05

Table 16. Running (10X) and Transfer (5X) buffers composition, both were made in dH₂O. For 1X concentration 100 ml of Running buffer (10X) were added to 900 ml of dH₂O and 200 ml of Transfer buffer (5X) + 200 ml of methanol were added to 600 ml of dH₂O.

The protein transference was verified by membrane staining with Ponceau solution (Sigma-Aldrich). After this verification, proteins were blocked for one hour at RT in 5% skim milk (Sigma-Aldrich) containing TBST solution (**Table 17**). After that, membranes were washed once in TBST for 10 min.

TBS pH 8.0 10X		TBST 1X	
<i>Component</i>	<i>Grams per one litre</i>	<i>Component</i>	<i>Millilitres per one litre</i>
Tris	24	TBS pH 8.0 10X	100
NaCl	180	dH ₂ O	900
Prepared in dH ₂ O		Tween®20	2

Table 17. TBS (10X) and TBST (1X) buffers composition.

Primary antibody hybridisation was performed in 5% BSA (Biowest) containing TBST solution at 4°C in a roller overnight. After membranes were washed three times in TBST, secondary antibody hybridisation was performed in 5% skim milk containing TBST solution for one hour at RT in a roller. Several washings steps also were carried out after secondary antibody hybridisation. Immunoreactive bands were visualised with SignalFire™ Plus ECL Reagent (Cell Signaling) and the chemiluminescent signal was obtained by both, the iBright FL1000 Imaging System (Thermo Fisher Scientific) and manually. Finally, the obtained results were analysed with ImageJ program.

A complete antibodies list and working dilutions are shown in the **appendix II, table 5**.

3.4.2 Immunofluorescence analyses

Immunofluorescence detection of different proteins was performed in cells cultures as well as in skeletal muscles cryosections.

3.4.2.1 Immunofluorescence analysis of cell cultures

Cells grown on coverslips or directly on the plate were fixed with 4% paraformaldehyde (PFA) (Electron Microscopy Sciences) for 10 min at RT. Then, they were washed in PBS, and permeabilised by addition of 0.2% of Triton-X (Sigma-Aldrich) in PBS with 1% bovine serum albumin (BSA) (Biowest) for 10 min at RT. After that, samples were blocked in a solution containing 1% BSA for 1h at RT. For the immunostaining, fixed cells were incubated with the primary antibody diluted in 1% BSA containing PBS solution overnight at 4°C. After several washes with PBS, samples were incubated with the corresponding secondary antibody diluted in 1% BSA containing PBS solution for 1 h at RT. Cells were further washed with DPBS and coverslips mounted on glass slides in a drop of ProLong mounting medium with DAPI (Life Technologies). For immunofluorescences carried out in plates, 1 µg/ml Hoechst solution (Thermo Fisher Scientific) was used for nuclear staining. Plates were maintained with PBS. All samples were maintained at 4°C until analysis.

3.4.2.2 Immunofluorescence analysis of skeletal muscle

All analyses were made in murine *Tibialis anterior* and *Soleus*. *Tibialis anterior* were directly frozen into 2-methylbutane (Thermo Fisher Scientific) cooled by liquid nitrogen. *Soleus* were frozen using tissue-Tek O.C.T Compound (Sakura Finetek USA INC) filled 10 mm x 10 mm x 5 mm cryomolds (Sakura Finetek USA INC) also into cooled 2-methylbutane. Samples were stored at -80°C until immunostaining was performed.

Seven micrometres width sections of frozen muscles were cut using a 34° cutting angle blade in a Leica CM 1950 cryostat. At this point cryosections containing slides could be stored before use at -80°C.

Below is detailed the followed protocol for cryosection immunostainings.

- Slides were tempered at RT for 10 min or until they dried.
- Fixation: 4% PFA for 10 min at RT.
- Permeation (not necessary for all antibodies): 0.3% Triton X-100 (Sigma-Aldrich) containing PBS solution for 20 min at RT.
- Washing: 5 min PBS washes for three times.
- Blocking step: 5% BSA containing PBS solution for 45 min at RT.
- Primary antibody hybridisation: overnight at 4°C with primary antibody diluted in 1% BSA containing PBS solution. Washing: 5 min PBS washes for three times.
- Secondary antibody hybridisation: one hour at RT in a 1% BSA containing PBS solution, protected from light.
- Washing: 5 min PBS washes for three times.
- Nuclear staining: 1 µg/ml Hoechst solution for 2 min at RT.
- Washing: several washing steps with PBS, dH₂O and milli-Q H₂O.
- Samples were let air-dry and mounted with Fluoro-Gel (Electron Microscopy Sciences). Slides were stored at 4° upon analysis.

All the samples (belonging to cell culture or cryosections) were examined using Nikon 80i microscope and ECLIPSE Ti-S/L100 inverted microscope (Nikon) together with NIS-Element software. A complete antibodies list and working dilutions are shown in the **appendix II, table 5**.

Fusion index quantification:

Immunofluorescence analysis was used to calculate the fusion index of cultured myotubes. It was calculated as the percentage ratio of the number of nuclei inside MyHC positive myotubes to the total number of nuclei. The number of nuclei was estimated by calculating the average number of nuclei counted in 9-13 independent and randomly chosen microscope fields of view.

3.4.3 Immunohistochemistry

3.4.3.1 Hematoxylin and eosin staining

Hematoxylin and eosin staining was performed to analyse skeletal muscle structure. Hematoxylin stains cell nucleus in blue and eosin stains eosinophilic structures in a range of red, pink and orange.

Frozen muscle cryosections were tempered at RT for 10 min or until they dried. Slides were introduced in different boxes to perform tissue fixation, hematoxylin eosin staining and dehydration in the above order.

- 96% ethanol (made from absolute ethanol from VWR Chemiclas)
- Tap water
- Filtered hematoxylin (PanReac AppliChem ITW Reagents) for 1 min.
- Rinsing with warm tap water until water was clear
- Eosin (PanReac AppliChem ITW Reagents)
- 96% ethanol (2X)
- 100% ethanol (2X)
- Xylene (Oppac s.a) (2X)

Finally samples were mounted and stored at RT. Muscle structure was analysed using Nikon 80i microscope and the NIS-Element software.

Hematoxylin and eosin stained muscle sections were used to measure muscle fibres cross-sectional area (CSA) through ImageJ software. *Soleus* fibres CSA from two different experiments were measured. On one side, 10 week-old 7 mice and 14 week-old 7 mice muscles were studied. Between two and three hundred fibres from randomly selected 4 or 5 different fields of view were measured. Conversely, for trained and not-trained mice fibres, 100 fibres from 4 different fields of view were measured.

3.4.3.2 β -nicotinamide adenine dinucleotide–tetrazolium reductase transferase (NADH-t) staining

NADH transferase enzymatic activity was used to stain fibres with different intensity purple-blue pigment. The standard protocol was followed where water-insoluble purple-blue formazan dye (NTBH₂) is detected due to its reduction from tetrazolium blue (NTB) because of the presence of NADH in cells mitochondria.

Muscle fibre classification was performed in murine *Tibialis anterior*. Frozen muscle cryosections were firstly re-hydrated in PBS before working solution was added on the top of the samples (Tris-HCl 0.1M, 0.4 mg/ml NADH, 0.8 mg/ml NBT) for 10 min at 37°C. After washing them twice in dH₂O, nuclear staining was performed with hematoxylin for 1 min at RT followed by dehydration performed as follow: 96% ethanol (4 times), 96% ethanol (4 times), 100% ethanol (4 times), 100% ethanol (4 times), xylene (4 times) and xylene (4 times). To conclude, muscles were mounted and stored at RT. Muscle pictures were taken using Nikon 80i microscope and analysed by the NIS-Element software.

For fibre type analysis ImageJ software was used. The fibres were assigned to four different groups depending on the intensity (in pixels) value obtained with the ImageJ program (strongly coloured < 100 pixels, medium-strongly coloured 100-150 pixels, medium-weakly coloured 150-200 pixels and weakly coloured > 200 pixels) (**Figure 16**). All fibres of one section of *Tibialis anterior* were measured.

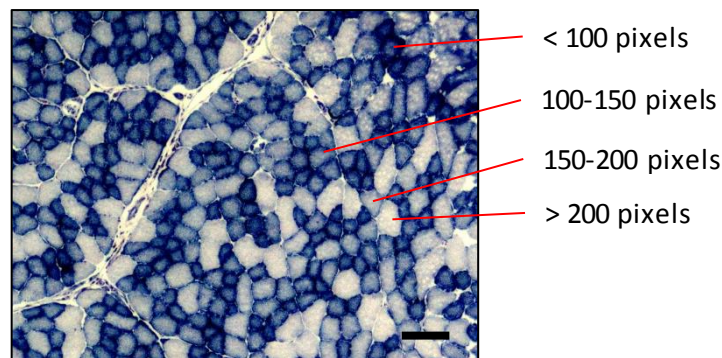


Figure 16. NADH-t staining in *Tibialis anterior* where different fibre types are visualized, glycolytic (pale > 200 pixels), oxidative (dark < 100 pixels) and intermediate (100-200 pixels). Scale bar 100 μ m

4. CELL CULTURE

4.1 HUMAN PRIMARY CELLS

Human origin primary myoblasts were obtained from skeletal muscle biopsy samples (**Figure 17**). Muscle pieces were cut maintaining fibre orientation in smaller pieces and were placed on a dish containing **conditioned medium** composed of medium 199 (M-199; Lonza, Basel, Switzerland) supplemented with 37.5% of foetal bovine serum (FBS; Thermo Fisher Scientific) and 1.25% of P/S and fungizone (9:1) and incubated overnight at 37°C and 5% CO₂.

At this point muscle pieces could be freeze for long term storage or continue with myoblast isolation. For long term storage muscle pieces (5-8) were introduced into cryo vials with **freezing medium** composed of Dulbecco's modified eagle medium (D-MEM; Lonza) supplemented with 10% FBS, 1% P/S + fungizone (9:1) and 8% dimethyl sulfoxide (DMSO; Thermo Fisher Scientific). Cryo vials were placed into a freezing container filled with isopropyl alcohol which was in turn introduced in a -80°C freezer for at least 6 h. For storage, cryo vials were stored in liquid nitrogen.

For myoblast isolation frozen muscles were thawed and cleaned in Ca²⁺/Mg²⁺ containing HBSS supplemented with antibiotics. Muscles were further cut until 1-2 cm size in a **conditioned medium** containing plate. After that muscle pieces were placed in a 58.95 cm² surface plate containing filtered (0.22 µm pore size) **conditioned medium** supplemented with 20% human plasma. Plates were incubated for 30 min at RT and then in a cell culture incubator for 6-7 days at 37°C and 5% CO₂.

After incubation, muscles pieces were chopped again (1mm³) in a plate with Ca²⁺/Mg²⁺ containing HBSS supplemented with antibiotics. The small muscle pieces were plated in plasma treated dishes (11.78 cm²) coated with filtered 1.5% gelatine supplemented with human plasma 2:1 solution. Plates were incubated for 30 min at 37°C and 5% CO₂ to allow muscles to attach and after that, **proliferation medium** was added (DMEM and M-199 supplemented with 10% FBS, 1% insulin 1 mg/ml, 1% glutamine 200 mM, 0.5% fibroblast grow factor (FGF) 5 µg/ml, 0.1% epidermal grow factor (EGF) 10 µg/ml and 1% P/S + fungizone (9:1)). Medium was replaced twice a week. The required time to grow could range between 7 and 12 days.

When proliferating cells were observed procedure was repeated. Muscle pieces were plated again and cells were collected. Myoblasts were isolated from all the different cell types using MACS® Column technology based on the use of magnetically labelled MACS Microbeads with LS columns (Miltenyi Biotec; Bergisch Gladbach, Germany). Microbeads for neural cell adhesion molecule (N-CAM or C56) (Illa et al., 1992) were used.

For the isolation, cells were collected through trypsinization and resuspended in the protocol recommended buffer (AutoMACS Running Buffer–MACS Separation Buffer, Miltenyi Biotec). LS columns were rinsed with this buffer before separation. Samples were incubated with MACS Microbeads before cells suspensions were loaded onto the LS columns. Columns were washed three times with buffer to remove unlabelled material. Finally columns were removed from the magnetic field and cells were eluted in **proliferation medium**. Later they were plated in an appropriate 0.5% gelatine coated plate (25 cm²).

Myoblasts were maintained there until 70-75% confluence was achieved. Then, they were plated in two 75 cm² area flask to amplify them. Once 70-75% confluence was achieved, cells were frozen. For long term storage myoblasts were stored at a concentration of 5×10^5 cell/cryo vial in a **freezing medium** into liquid nitrogen.

Human primary myoblasts obtained from proximal muscles biopsies (*Tibialis anterior*) were grown as myoblasts obtained from distal muscles.

- **Human plasma**

Human plasma was collected from healthy donors after they gave informed consent using forms approved by the Ethics Committee of the Use of Human Subjects in research. Blood was collected in Vacutainer® K2E (EDTA) 18.0 mg plus blood collection tubes (BD Bioscience, San Jose, California, USA) and centrifuged at 2,000 rpm for 10 min. Supernatant, plasma, was collected and stored at -20°C.

All mediums compositions are detailed in the **appendix II, table 6**.

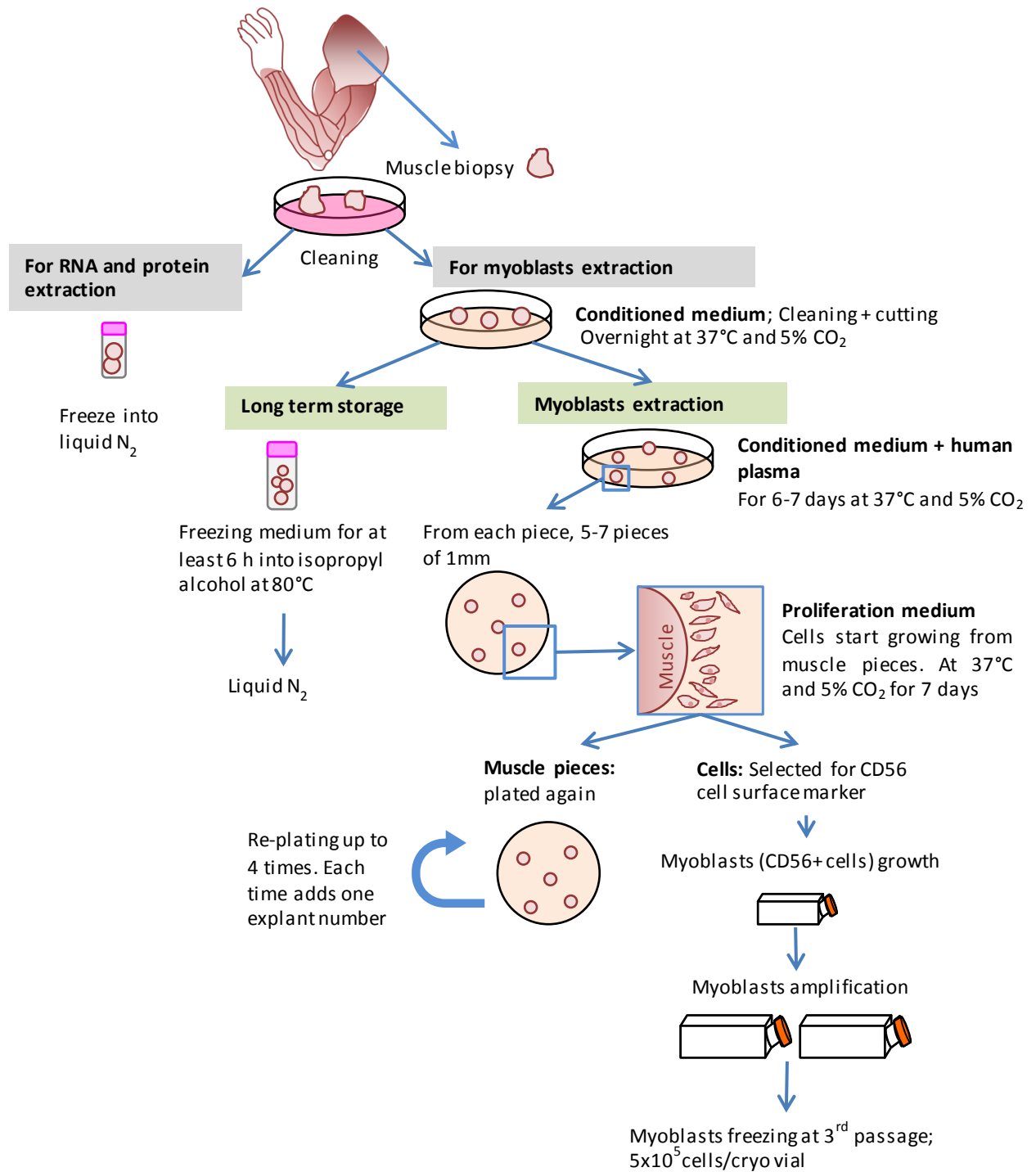


Figure 17. Schematic representation of human primary cells (myoblast) isolation.

4.2 MURINE ORIGIN CELLS

4.2.1 C2C12 cell line

C2C12 cell line is a subclone produced by H. Blau and collaborators (1985) from *Mus musculus* myoblast cell line established by D. Yaffe and O. Saxel (1977). It is widely used as skeletal muscle cell line model. It was purchased from ATCC (ATCC-CRL[®]-1772[™]).

For proliferation C2C12 myoblasts were grown in a **proliferating medium** composed of DMEM supplemented with 10% FBS and 1% P/S + fungizone (9:1). For myotubes, once myoblast achieve 80-90% confluence proliferating medium was switched to medium containing DMEM supplemented with 2% of horse serum (Thermo Fisher Scientific) and 1% P/S + fungizone (9:1).

4.2.2 Murine primary cells

4.2.2.1 Satellite cells

Murine skeletal muscle satellite cells were extracted from 4 week-old WT and *Frzb*^{-/-} mice (Biressi et al., 2013). Mice were euthanized by cervical dislocation and *Gastrocnemius*, *Tibialis anterior*, *Quadriceps* and *Biceps* from both legs were extracted. Muscles were introduced in a petri dish containing warm PBS + 25% antibiotics (P/S + gentamicin 9:1) to be cleaned.

Muscles were digested in 0.002% D collagenase (Hoffmann-La Roche, Basel, Switzerland) and 0.006% pancreatin (Sigma-Aldrich) containing solution placed at water bath at 37°C, shaking, for one hour. After sample sedimentation, supernatants were filtered through 70 µm filters. A second digestion was made in the same conditions for 30 min. Supernatant was filtered as before and samples were centrifuged at 1,200 rpm for 5 min. Supernatants were discarded and samples were further washed with PBS and filtered again through 40 µm filters followed by a centrifugation at 1,200 rpm for 5 min. Finally, supernatants were discarded and cells were resuspended in PBS and counted.

Cells were grown in DMEM-high glucose (FBS; Gibco-Thermo Fisher Scientific) supplemented with 20% FBS, 1% chicken embryo extract (Bio-connect BV, Huissen, The Netherlands), 1 mM sodium pyruvate, 100 U/ml penicillin and streptomycin, 2 mM L-glutamine (ThermoFisher Scientific) and 0.1% gentamicin (Sigma-Aldrich). Once high confluence was achieved, the differentiation was induced by switching medium to DMEM high glucose supplemented with 2% horse serum (Gibco-Thermo Fisher Scientific) and 1 mM (100 mg/ml) sodium pyruvate, 100 U/ml penicillin and streptomycin and 2 mM L-glutamine. Cells were incubated at 37°C, 5% CO₂, 5% O₂.

4.2.2.2 Mesoangioblasts (MABs)

MABs were isolated from 4-5 week-old mice. Muscles were extracted as previously described for satellite cells.

Muscles were chopped in small pieces around 1 mm² and attached to a collagen coated P12 dish with **MABs medium** (DMEM-high glucose GlutaMAX™ supplemented medium supplemented with 20% FBS, 1 mM (100 mg/ml) sodium pyruvate, 100 U/ml penicillin and streptomycin + gentamicin 1:20, 2 mM L-glutamine, 1% non-essential amino acids (Thermo Fisher Scientific) and 1% 2-mercaptoethanol 1:100 (Thermo Fisher Scientific)). Cells were incubated at 37°C, 5% CO₂, 5% O₂.

Cells grown from muscle pieces were sorted using fluorescence-activated cell sorting (FACS)-antibody technique targeting alkaline phosphatase (ALP) (Quattrocchi et al., 2012). For that purpose cells were trypsinized and collected in a PBS containing tube. At this point, cell amount was counted using trypan blue in an automated cell counter.

For cell sorting different round bottom polystyrene test tubes (Corning) were prepared:

- a) Blank sample: 100,000 cells diluted in 200 µl of PBS.
- b) Isotype control: 100,000 cells supplemented with 0.2 µg of the appropriate isotype (monoclonal mouse IgG1, κ (Affymetrix eBioscience, Thermo Fisher Scientific) diluted in 200 µl of PBS.
- c) Samples: mixed with 2 µl per 100,000 cells of ALP-phycoerythrin-conjugated antibody (R&D Systems a Biotechne brand) diluted in 200 µl of PBS.

All of them were incubated for 30 min at RT protected from light. After incubation samples were washed with PBS and centrifuged at 1,200 rpm for 5 min at RT. Supernatants were discarded and more PBS was added to cells. Next, samples were filtered through round bottom polystyrene test tube with cell strainer snap cap (Corning) and centrifuged at 1,200 rpm for 5 min at RT and washed again once with PBS. Finally, samples were resuspended in 200 µl of PBS and sorted.

Positive and negative fractions were collected in a round bottom high clarity polypropylene test tubes containing 500 µl of MABs medium + antibiotics. Both fractions were seeded in a collagen coated plate at a density of 50 000 cell/cm² with MABs medium supplemented with antibiotics. Plates were incubated at 37°C in a 5% CO₂, 5% O₂ and medium was changed every two days.

Cells were amplified and stored in liquid nitrogen at passages between 4 and 7.

Cells characterization through flow cytometry analysis

MABs characterization was carried out through the analysis of different cell surface markers. Protein tyrosine phosphatase receptor type C (PTPRC or CD45), platelet and endothelial cell adhesion molecule 1 (PECAM-1 or CD31) and platelet derived growth factor receptor alpha (PDGFR α or CD140 α) cell surface markers amount was studied in 3 WT and 7 *Frzb*^{-/-} samples.

500,000 cells were fixed in 4% PFA for 10 min at RT. After fixation cells were centrifuged at 1,200 rpm for 5 min at RT and pellets were stored in PBS at 4°C until the analysis was carried out.

Each sample was divided to obtain 100,000 cells/ tube. They were centrifuged at 1,200 rpm for 5 min at RT and pellets were resuspended in 1 ml of **staining medium** (HBSS with Ca²⁺/Mg⁺ supplemented with 2% FBS, 10 mM HEPES pH 7.2 and 10 mM NaN₃). Then, another centrifugation was carried out and pellets were resuspended in 100 μ l of staining medium. FACS analysis samples were stained as follow:

- a) Blank: 100,000 cells/150 μ l PBS. Only one blank tube was used for all analyses.
- b) Sample 1: 100,000 cells/100 μ l staining medium supplemented with 0.1 μ g of APC labelled CD140 α monoclonal antibody (Thermo Fisher Scientific) and 0.1 μ g of PE labelled CD140 β monoclonal antibody (Thermo Fisher Scientific).
- c) Isotype control 1: 100,000 cells/100 μ l staining medium supplemented with 0.1 μ g of PE Rat IgG2a, κ isotype control (BD Bioscience) and 0.1 μ g APC rat IgG α , κ isotype control (BD Bioscience).
- d) Sample 2: 100,000 cells/ 100 μ l staining medium supplemented with 0.1 μ g of APC labelled CD31 monoclonal antibody (Thermo Fisher Scientific) and 0.1 μ g of FITC labelled CD45 monoclonal antibody (Thermo Fisher Scientific).
- e) Isotype control 2: 100,000 cells/100 μ l of staining medium supplemented with 0.1 μ g APC rat IgG α , κ isotype control and 0.1 μ g of FITC mouse IgG2a, κ isotype control (BD Bioscience).

Samples were incubated protected from light for 25 min. Next, PBS was added to each tube and after centrifugation at 1,200 rpm for 5 min, another one washing step was carried out. Finally cells were mixed in 150 μ l PBS, analysed and quantified by flow cytometry (BD FACS Canto I or II with HTS; BD Biosciences) and FlowJo Software (FlowJo LLC).

Adipogenic induction of ALP+ cells

For the adipogenic induction of ALP+ cells 3 WT and 3 *Frzb*^{-/-} samples were used. Each sample was seeded in triplicate on a collagen coated dish at 66,000 cell/cm² density in MABs medium until 100% confluence was achieved. Then MABs medium was switched to StemPro[®] adipogenesis

differentiation basal medium supplemented with StemPro® Adipogenesis supplement (Thermofisher Scientific), for adipogenic induction. Medium was change every day and after 10 days cells were fixed in 4% PFA for 10 min. Next, cells were stored in PBS at 4°C.

Non-induced cells were used as a negative control of adipogenic differentiation.

- **Oil red O stain for *in vitro* adipogenesis analysis**

Oil red O fat-soluble dye was used for the visualization of fat cells. Working solution was 0.5% Oil Red O (Sigma-Aldrich) in 65% propan-2-ol solvent (Fisher chemicals) in milli-Q water.

Samples were stained for 30 min with the solution and after that several PBS washes were performed. Cells were examined using the Eclipse Ti inverted microscope (Nikon) and the NIS-Element software.

After immunofluorescence analysis Oil red O was quantified in our samples. For that purpose lipid vacuoles were lysed with a solution made of petroleum ether and propan-2-ol (Fisher chemicals) in a 3:2 proportion. The different colour intensities were measured in a spectrophotometer at 490 nm. Different samples' Oil red O quantity was measured as triplicates and was compared to values obtained from a known Oil Red O quantity standard curve.

- **Immunofluorescence for *in vitro* adipogenesis analysis**

In vitro adipogenesis was also measured with the presence of perilipin, a protein which is present in the surface of lipid droplets, by immunofluorescence. For immunofluorescence oil red O stained cells were blocked in a donkey serum solution 1:10 for 30 min before the incubation with polyclonal rabbit anti-perilipin A/B 1:300 (Sigma-Aldrich) overnight at 4°C. Samples were washed several times with PBS and incubated with anti-rabbit antibody conjugated to Alexa-Fluor 488, 1:500 for 1 h at RT. After more PBS washes nuclear staining was performed with a Hoechst solution 1:10,000 in PBS for 2 min. Finally after several washes with PBS, cells were maintained in PBS upon microscope analysis. Cells were examined using an Eclipse Ti inverted microscope (Nikon) and the NIS-Element software.

5. RNA INTERFERENCE KNOCKDOWN EXPERIMENTS

5.1 GENE SILENCING IN HUMAN/MURIN MYOTUBES

The siRNA for human *CD9* (s2598), *ITGB1BP2* (s25536) and for human and mice *FRZB* (s5369) knockdown (in this work identified as si*CD9*, si*ITGB1BP2* and si*FRZB*) were purchased from Life Technologies. A scramble siRNA was used as negative control (AM4611; has no significant sequence similarity to mouse, rat, or human gene sequences).

Myoblast (primary human and C2C12 myoblasts) were plated at 24,000 cells/cm² and maintained in **proliferation medium** until 80% confluence was achieved. At this time, medium was switched toward **differentiation medium**. *CD9*, *ITGB1BP2* and *FRZB* genes silencing were carried out at day 8 and day 3 of differentiation in human and murine origin myotubes respectively. Myotubes were transfected with the siRNA at a concentration of 5 nM using RiboCelling transfection reagent (Bulldog Bio; Portsmouth, NH, USA) following the manufacturer's instructions. For RNA analysis, its extraction was performed 48 h post-silencing. Likewise, for protein analysis, its extraction was performed 72 h post-silencing.

5.2 GENE SILENCING IN HUMAN/MURIN MYOTUBES AT EARLY AND LATE STAGE OF DIFFERENTIATION

si*FRZB* transfection was carried out as a previously described, however silencing was performed at day 1 and at day 8 of differentiation and the effect was maintained until day 11 of differentiation in human origin samples. Finally, silencing was analysed at day 11 of differentiation through immunofluorescence.

In murine origin myotubes silencing was performed at day 1 and day 3 of differentiation and maintained until day 7 and day 9 of differentiation respectively for immunofluorescence analysis. For RNA analysis, its extraction was performed 4 days post-silencing. Likewise, for protein analysis, its extraction was performed 5 days post-silencing.

To keep the silencing effects during several days, avoiding transitory loose of it, silencing was performed every time the medium was changed.

6. LiCl ADMINISTRATION EXPERIMENTS

LiCl (Sigma-Aldrich) was administered at a 10 mM concentration to the myotubes at day 8 of differentiation. LiCl was prepared in dH₂O diluted from an 8 M stock solution. At 48 h after administration of the drug, RNA and proteins were extracted for further analyses.

LiCl administration also was analysed in early and late stage of myotube differentiation. Drug was added at day 1 and at day 8 of differentiation and the effect was maintained until day 11 of differentiation. To keep the silencing effects during several days, avoiding transitory loose of it, drug was added every time the medium was changed. Finally, the effect was analysed at day 11 of differentiation through immunofluorescence.

7. FOETAL BOVINE SERUM (FBS) AND HUMAN HETEROLOGOUS SERUM (HHS) INFLUENCE ANALYSIS IN HUMAN PRIMARY MYOTUBES

7.1 SERUM OBTAINING

FBS was externally purchased from Gibco. Before use it was heat-treated at 56°C for 20 min.

Human serum was obtained from healthy control and LGMD2A patients' blood after they gave informed consent using forms approved by the Ethics Committee of the Use of Human Subjects in research (**Table 18**). Blood was collected in coagulation activator and gel separator containing Vacutainer® SST II Advance plus blood collection tubes (BD Bioscience). For serum collection blood was centrifuged at 3,000 rpm for 10 min. Supernatant was collected and stored at -20°C. Sera were heat-treated at 56°C for 20 min before use.

Sample	Status	Age	Gender	Ambulation	CAPN3 mutations	
					Mutation 1	Mutation 2
1	LGMD2A	19	Female	Ambulant	p.(*822Leuext62*)	HG19, chr15:42,630,844-42,704,125
2	LGMD2A	21	Female	Ambulant	p.(*822Leuext62*)	HG19, chr15:42,630,844-42,704,125
3	Control	43	Female	-	-	-

Table 18. Blood donors' information. HG19, chr15: 42,630,844-42,704,125= break points of the deletion. Comprises part of the *GANC* gene (starting point in intron 16) and the entire *CAPN3* gene locus (endpoint in the 3'UTR region)

7.2 MYOTUBES CULTURE

Control or LGMD2A patients' myoblast were seeded on 0.5% gelatine coated dish at 20,000 cell/cm² density on **proliferating medium** supplemented with 10% FBS or HHS. Once 80% confluence was achieved medium was switched toward **differentiation medium** supplement with 2% FBS or HHS. For RNA and protein analysis, their extraction was performed at 16 days of differentiation.

8. *Frzb*^{-/-} MICE FUNCTIONAL ANALYSES

8.1 MUSCLE STRENGTH ANALYSIS

To monitor muscle strength and condition over time four limb hanging test was used (Standard operating procedure: DMD_M.2.1.005 (Carlson et al., 2010)). Five to 6 week-old mice were placed in a crosslinked wire grid (every 12 mm). The grid was inverted over a cylinder with a diameter of 314 cm² at a height of 20 cm and the 'time to fall' was monitored. Each mouse weight was also measured.



Figure 18. Mouse performing muscle strength analysis.

8.2 MUSCLE REGENERATION ANALYSIS

Ten week-old mice were anesthetized by intraperitoneal (IP) injection of ketamine (10 mg/ml; Nimatek, Eurovet animal healthcare)/xylazine (0.1%; MVD) in a dosage of 10 µl/g. Muscle degeneration was induced by 3 µl of 50 µM cardiotoxin (CTX; Latoxan, Portes-lès-Valence, France) into *Tibialis anterior* and 3 µl of 16.7 µM of cardiotoxin into *Soleus* injection (Duchen et al., 1973). After sewing the wound, 50 µl of buprenorphine (0.03mg/ml; Vetergesic, Ecuphar) was injected subcutaneously for analgesia.

8.3 CHRONIC EXERCISE PROTOCOL ON A TREADMILL

Five to 7 week-old mice were caged together and housed in the same facility and acclimated at standard cage conditions for at least 72h before exercise treatment. Mice were subjected to a 5

weeks chronic exercise treadmill on a 4 lane modular treadmill (Columbus Instruments). The WT and *Frzb*^{-/-} mice belonging to the exercised groups ran 30 min on a horizontal treadmill at 12 m/min twice a week (Granchelli et al., 2000; De Luca, 2003) before a warm-up exercise consisting in 2 min at 4.2 m/s followed by 8 min at 7.8 m/s. All mice weight was monitored every training day. Mice were euthanized by cervical dislocation.

Mice *Tibialis anterior*, *Quadriceps*, *Gastrocnemius* and *Soleus* from both legs were extracted and weighed. *Tibialis anterior* were directly frozen in 2-methylbutane and one *Soleus* of each mouse was frozen into cryomolds in 2-methylbutane as previously described. Remaining muscles were frozen through immersion into liquid nitrogen. All of them were stored at -80°C.

8.4 MICE GAIT ANALYSIS

CatWalk™ XT (Noldus, CatWalk 7.1, The Netherlands) was used to assess gait and locomotion (Vandeputte et al., 2010) of WT and *Frzb*^{-/-} mice. The analysis was carried out in two study groups; 8 week-old and 10 week-old mice. Mice were placed into the walkway for three consecutive runs. Runs were analysed separately and an average of this three runs was used as an individual value. All given parameters are explained below.

CatWalk™ XT walkway was fixed as 730 mm far and 72 mm wide with the camera set 40 cm far from the walkway. The following parameters were evaluated:

- **Paw statistics (Figure 19):**
 - **Stand or stance phase:** paw contact time with the glass plate during the step cycle in seconds.
 - **Swing phase:** paw time in the air during the step cycle in seconds.
 - **Step cycle:** the sum of stand and swing phase in seconds.
 - **Stride length:** the distance covered by a paw in mm.
 - **Swing speed:** measure of the speed of the moving limb during the swing phase of the step cycle in m/s. Is calculated as follow,

$$\text{Swing speed (m/s)} = \frac{\text{Stride length}}{\text{Stand} + \text{Swing}}$$

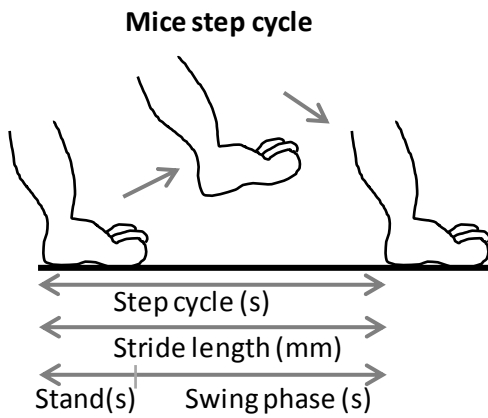


Figure 19. Schematic representation of mouse step cycle. Step cycle (s), stride length (mm), stand (s) and swing phase(s) are represented on a step cycle.

- *Step sequence analysis*: it analysed the order in which mice paws were placed.
- **Step pattern**: counts the number of patterns that can be assigned to one given step sequence which in turn measure the order in which paws were place during the gait. A specific code is given by de program to each step pattern (**Table 19**).

Step pattern abbreviation	Step sequence
AA	RF-RH-LF-LH
AB	LF-RH-RF-LH
CA	RF-LF-RH-LH
CB	LF-RF-LH-RH
RA	RF-LF-LF-RH
RB	LF-RF-RH-LH

Table 19. Step pattern code and its corresponding step sequence. RF= right front paw, RH= right hind paw, LF= left front paw and LH= left hind paw.

- **Step regularity index**: the amount of normal step patterns within the total number of paw placements.
- **Paw support**: the relative duration of all combinations of number of paw in contact with the glass plate was assessed. Possible combinations are one, two, three or four paws in contact with the glass at the same time; when two paws are in contact with the glass, 3 the pattern can be used; diagonal support (when front right and hind left or front left and hind right paws are used), girdle support (when front paws or hind paws are used) and lateral support (w hen left paws or right paws are used).
- **Base of support (BOS)**: the average width between both the front and hid paws in mm (**Figure 20**).

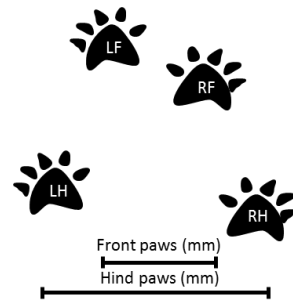


Figure 20. Schematic representation of mouse base of support (mm). LF= left front, RF= right front, LH= left hind and RH= right hind paws.

9. BIOINFORMATICS TOOLS

Online available AliBaba v2.1 program (<http://gene-regulation.com/pub/programs/alibaba2/>) was used to predict transcription factor binding sites by contrasting matrices on the fly form TRANSFAC 4.0 sites. Min mat. conservation was set in 80% (high).

10. STATISTICAL ANALYSIS

All statistical analyses along the study were made with Student's t-test for two means comparison and two-way ANOVA study for multiple means comparisons. Further post hoc analyses were made based on Tukey's and Sidak's criterion for significance. Significance was set when p value was lower than 0.005.

CHAPTER 1:

***In vitro* analyses of the pathophysiology of**

LGMD2A

CHAPTER 1: RESULTS

1. APPROACH TO THE OPTIMIZATION OF CELL CULTURE FOR THE INVESTIGATION OF MECHANISM UNDERLYING MUSCULAR DYSTROPHIES

Previous studies carried out by our group, showed a tendency towards the homogenization of the differences between controls and LGMD2A patients' myoblasts and myotubes cell cultures. These previous studies showed also a lack of correlation between *in vitro* skeletal muscle model (myoblast and myotubes) and their tissue of origin (muscle). When gene expression pattern of the *in vitro* cellular model and the skeletal muscle were compared, only one gene, *FRZB*, showed the same deregulation pattern in muscle and in myotubes at 16 days of differentiation of LGMD2A patients (Jaka, 2014)

To try to overcome this issue, the following analyses were carried out in two controls' and one LGMD2A patient's samples.

1.1 Effect of FBS and human heterologous serum in myoblast proliferation

The use of different origin sera showed that growing media conditions affected myoblast shape under optical microscope. Myoblast grown with HHS showed a more elongated shape and a higher rate of multiplication than myoblasts grown with FBS (**Figure 21**). Myoblasts cultivated in HHS containing proliferation medium required 7, 8 (2 controls) and 12 (LGMD2A) days to achieve 90% of confluence while 12 and 21 days (controls and patient respectively) were required for myoblast grown with FBS ($p=0.0591$ paired t test).

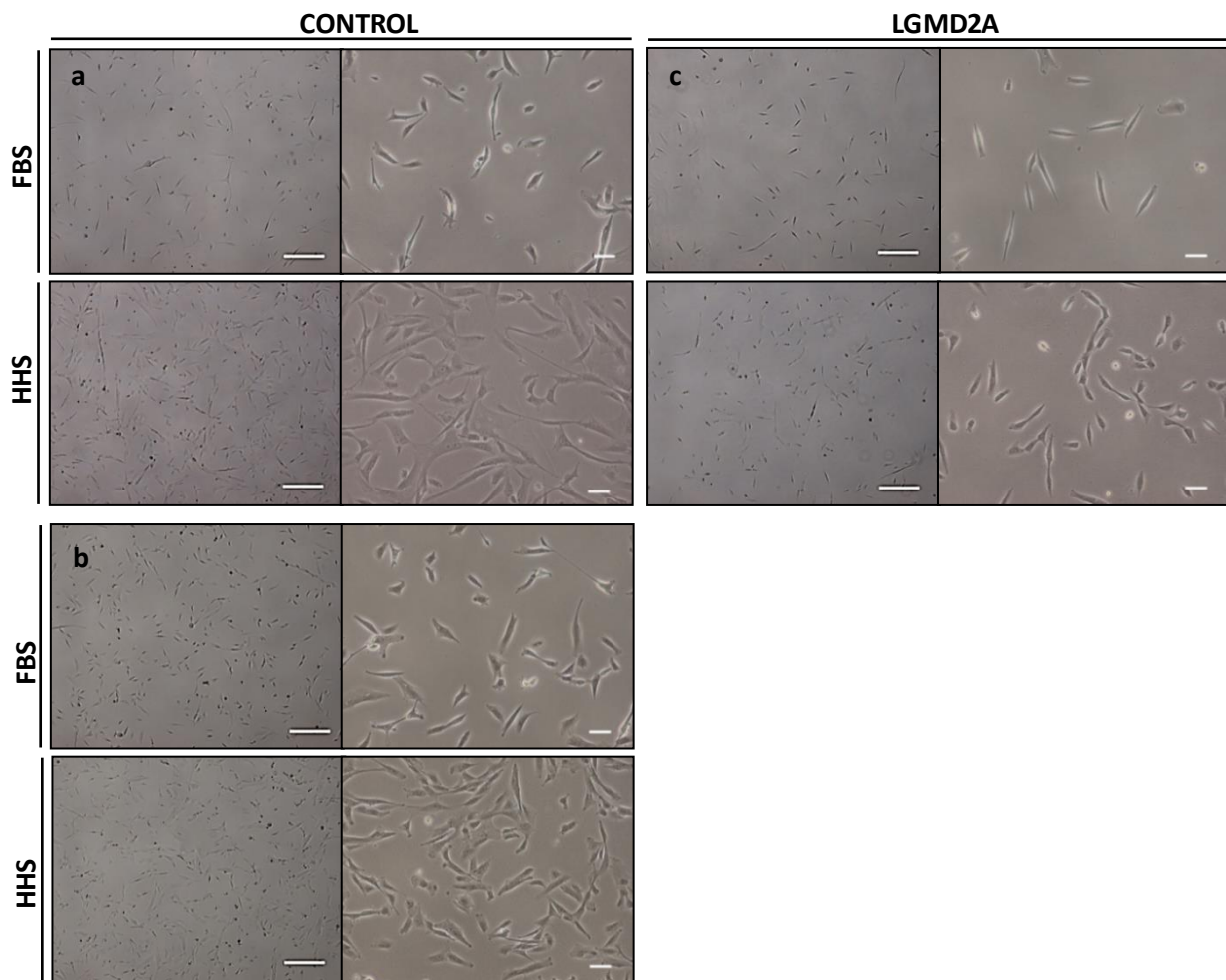


Figure 21 . Morphology of human (**a** and **b**) control and (**c**) LGMD2A myoblasts after 5 days in culture with FBS or HHS. Scale bar 250 μ m.

1.2 Effect of FBS and human heterologous serum in myoblast differentiation

The influence of different origin serum in myoblast differentiation was also analysed. Myotubes at 16 days of differentiation were analysed (under optical microscope) and a decline of the efficiency of myotubes formation was shown when HHS was used. The presence of uninucleated and rounded cells, which did not form myotubes, was more evident in control samples. By contrast, LGMD2A myotubes formation appeared to be similar in both conditions (**Figure 22**).

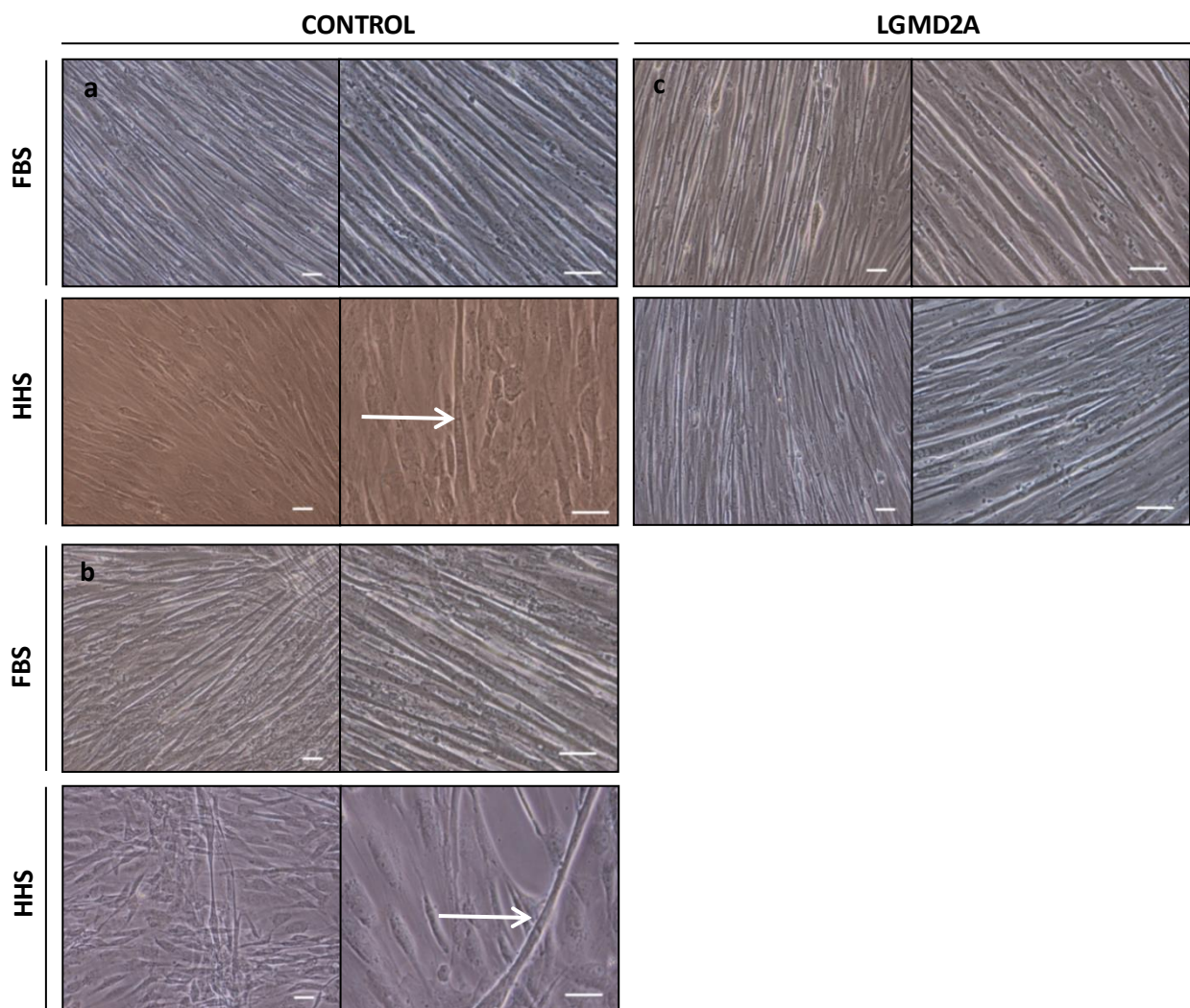


Figure 22 Morphology of human (**a** and **b**) control and (**c**) LGMD2A myotubes at 16 days of differentiation grown with FBS or HHS. White arrows highlight myotubes. Scale bar 250 μ m.

1.3 Myotube maturity analyses

To evaluate differentiation and maturity level of myotubes, myosin heavy chain 2 (*MYH2*) gene expression was evaluated and it was downregulated in HHS cultured myotubes in both, control and LGMD2A samples (**Figure 23 a**). At protein level, myosin heavy chain (all isoforms) also was significantly downregulated (**Figure 23 b**).

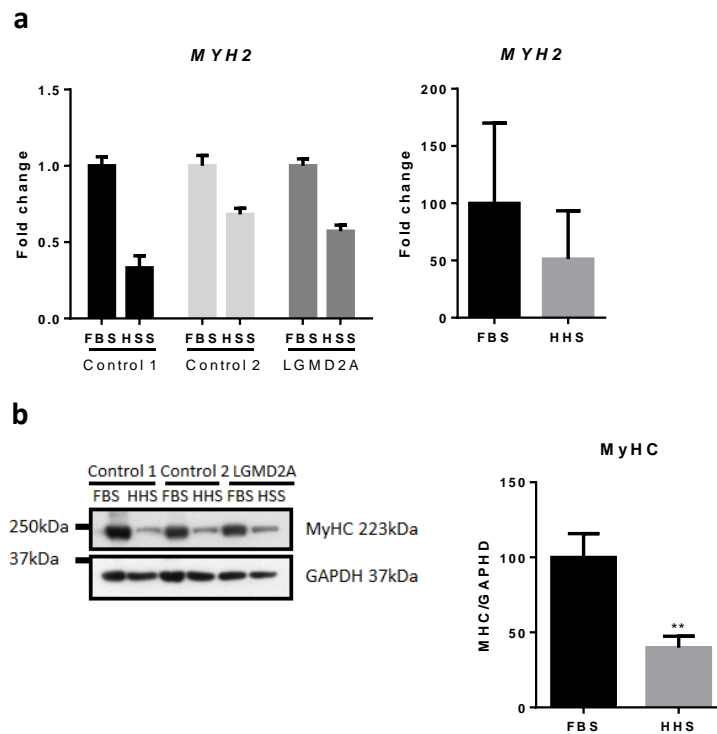


Figure 23. (a) Gene expression analysis of *MYH2* in 2 controls and one LGMD2A patient myotubes grown with FBS and HHS. *GAPDH* was used as endogenous control. Data are represented as mean fold change \pm standard deviation. (b) Western blot and densitometry analyses of MyHC protein expression (all isoforms) in 2 controls and one LGMD2A patient myotubes grown with FBS and HHS. Data are represented as mean band density normalized relative to *GAPDH* \pm standard deviation. **= $p < 0.001$.

1.4 Skeletal muscle specific genes and proteins expression analyses

Structural proteins which are required for costamere formation, namely melusin and $\beta 1$ integrin were significantly downregulated at protein level and also at RNA level in the case of melusin (*ITGB1BP2*) (Figure 24 a and b). Similarly, the analysis of myogenic marker myogenin, showed a significant downregulation at protein level (Figure 24 b). Finally, desmin (*DES*), which is essential for sarcomere maintenance, was downregulated at RNA level (Figure 24 a).

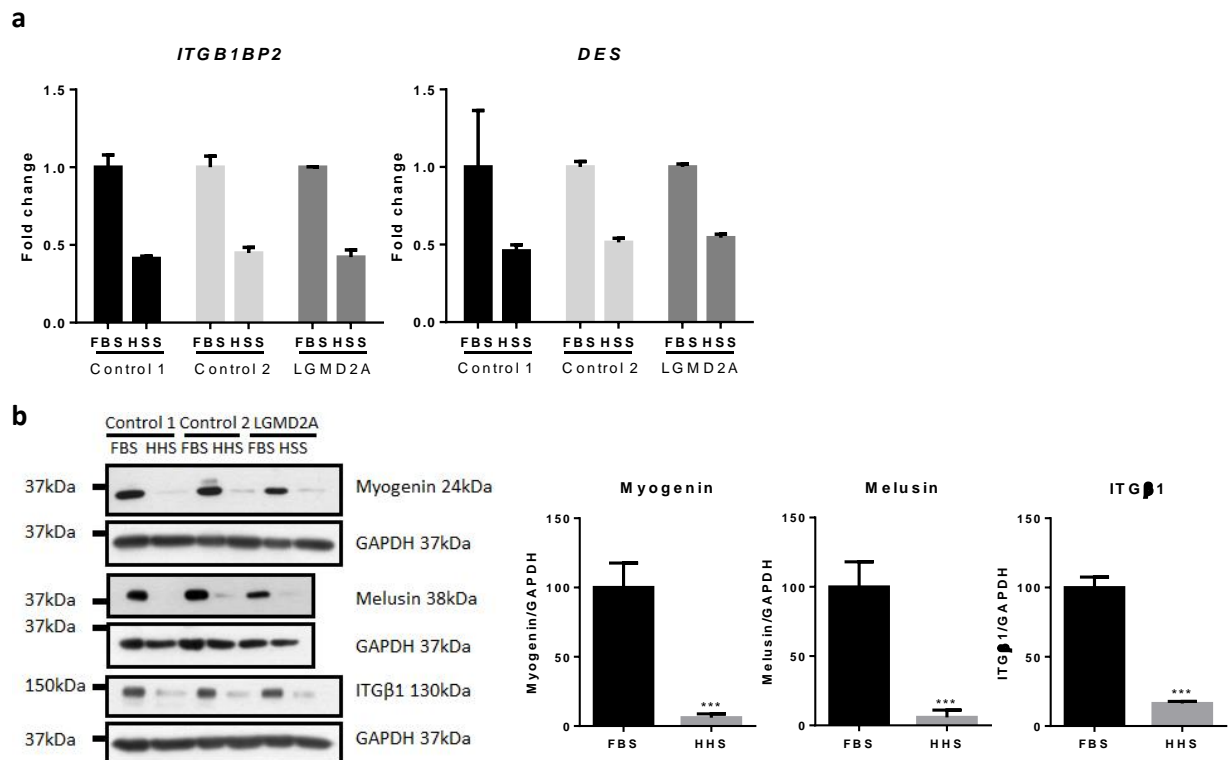


Figure 24. (a) Gene expression analysis of *ITGB1BP2* and *DES* in 2 controls and one LGMD2A patient myotubes at 16 days of differentiation grown with FBS and HHS. *GAPDH* was used as endogenous control. Data are represented as mean fold change \pm standard deviation. (b) Western blot and densitometry analyses of myogenin, melusin and ITG β 1 protein expression in 2 controls and one LGMD2A patient myotubes at 16 days of differentiation grown with FBS and HHS. Data are represented as mean band density normalized relative to GAPDH \pm standard deviation. ***= $p < 0.0001$.

2. RNA SILENCING TO REGULATE OVEREXPRESSED GENES IN LGMD2A

Given the results obtained in the present thesis are part of a previous published work (Jaka et al., 2017), below is detailed a brief introduction of the section from which this work is part of.

Studies carried out in cells obtained from proximal muscles showed that myotubes of LGMD2A patients presented different morphology. Patients' myotubes showed clustered nuclei with altered distribution. Oversized myotubes containing more than 50 nuclei were found in LGMD2A cultures, while such myotubes were absent in control cultures. The fusion index was significantly higher in myotubes from LGMD2A patients and an abnormal process of fusion of myoblast was detected (Jaka et al., 2017).

As integrins are transmembrane glycoproteins receptors that are essential for myoblast fusion (Schwander et al., 2003), we focused our studies on their analysis. Under normal physiological conditions, the β 1A isoform is replaced by the β 1D isoform in muscle fibre maturation (Belkin et al., 1996) and this replacement has been shown to be altered in myotubes of calpain 3 knockout (C3KO) mice, which show a similar anomalous distribution of myonuclei as LGMD2A myotubes (Kramerova et al., 2006).

Moreover, in order to direct the study to the analysis of genes/proteins that may have relevance in the pathophysiology of LGMD2A, overexpressed proteins in LGMD2A patients' muscles (Sáenz et al., 2008) that interact with integrins, such as melusin and CD9 (Schwander et al., 2003; Przewoźniak et al., 2013), were studied. In addition to these two proteins, FRZB also was studied because it was the only gene that showed common pattern of deregulation in muscle and in myotubes and presented one of the highest Fold-change value in expression profiling analysis in LGMD2A muscles (Sáenz et al., 2008).

Silencing experiments were carried out in patients' myotubes and it was found that *CD9* and *FRZB* are positive regulators of *ITGB1BP2* gene expression and *ITGB1BP2* is a negative regulator of *FRZB* gene expression (Jaka et al., 2017).

2.1 Confirmation of gene silencing effect in distal skeletal muscle

As previous silencing experiments were carried out in proximal muscles, to confirm this common regulation mechanism, additionally, *CD9*, *FRZB* and *ITGB1BP2* silencing experiments were carried out in myotubes obtained from non-affected distal muscles (*Tibialis anterior*). This common regulation was ascertained in distal origin myotubes. After 48h of treatment with *CD9*, *FRZB* or *ITGB1BP2* siRNA, all cultures showed less expression of these genes, being *ITGB1BP2* the most silenced

followed by *CD9* and *FRZB* respectively. *ITB1BP2* gene silencing produced an upregulation in *FRZB* expression. In the case of *FRZB* gene silencing, a reduction in *ITGB1BP2* gene expression was observed. Lastly, *CD9* gene silencing induced a parallel reduction of *ITGB1BP2* gene expression. In addition, an upregulation of *FRZB* was observed in three out of four samples, not observed in proximal muscle silencing (**Figure 25**).

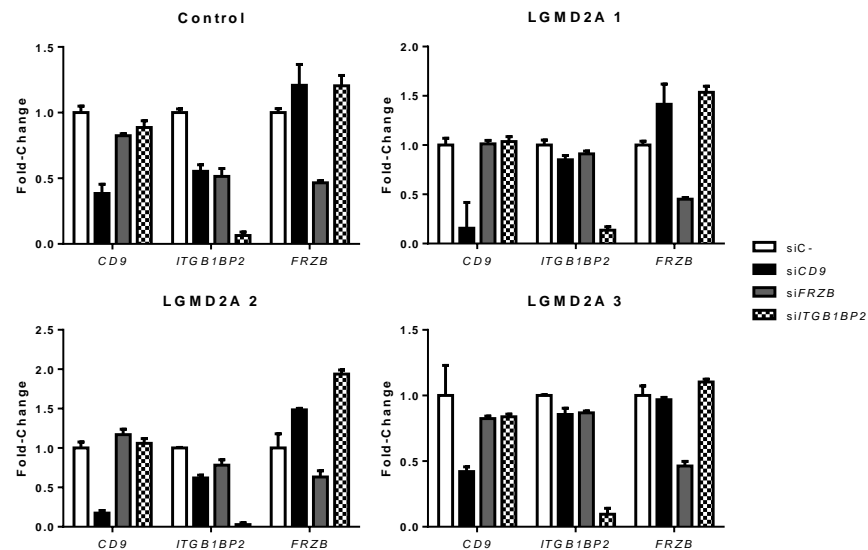


Figure 25. *CD9*, *ITGB1BP2* and *FRZB* genes expression analysis after gene silencing (si*CD9*, si*FRZB* and si*ITGB1BP2*) in one control and three patients' myotubes obtained from distal muscle (*Tibialis anterior*). siC-: control siRNA, scramble RNA. *GAPDH* was used as the endogenous control. Data are represented as relative mean expression \pm standard deviation.

2.2 Integrin β 1A and β 1D isoform replacement analysis in LGMD2A patients' myotubes

The presence of integrins in myoblasts and myotubes at different stages (days) of differentiation was analysed. Regarding expression of the β 1A isoform (ITG β 1A), no differences were observed in the differentiation process between patients and controls. Moreover, in the case of β 1D isoform (ITG β 1D), less amount of protein was observed in myotubes of patients, and the level of this isoform progressively increased in controls as the differentiation process advanced (**Figure 26**).

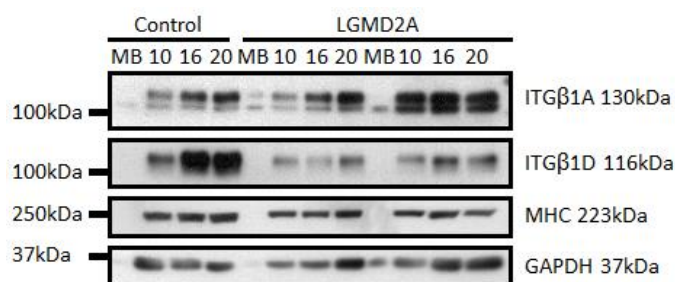


Figure 26. Western blot analysis of integrin β 1A and β 1D isoforms in myoblasts and myotubes at days 10, 16 and 20 of differentiation (1 control and one patient). Data are represented as mean band density normalized relative to GAPDH \pm standard deviation.

Since β 1A- β 1D isoform replacement is defective in LGMD2A myotubes and melusin (overexpressed in LGMD2A patients) binds directly to β 1 integrins, melusin gene silencing effect on β 1 integrin expression level in myotubes was studied. Melusin gene silencing produced an increase in the β 1A isoform, while a trend toward a decrease in the β 1D isoform in the myotubes of both patients and controls was observed (**Figure 27 a**).

As silencing of the melusin gene affected *FRZB* gene expression and *vice versa*, the effect of *FRZB* gene silencing on β 1 integrins also was analysed. This silencing led to a decrease in levels of the β 1A isoform only in LGMD2A patients, while this decrease was less clear in controls. In the case of β 1D isoform, *FRZB* gene silencing induced an increase in its protein amount in the myotubes of both, controls and patients. In LGMD2A patients, after *FRZB* gene silencing, the level of integrin β 1D was similar to that in controls without any treatment (**Figure 27 b**).

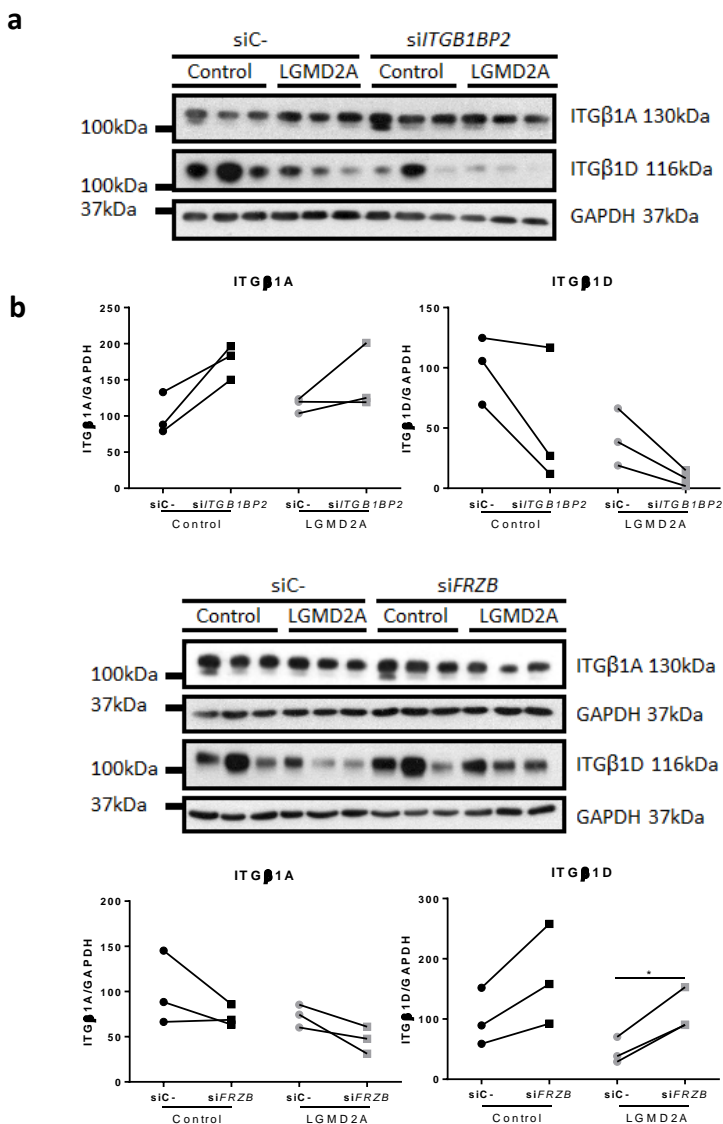


Figure 27. (a) Western blot and densitometry analyses of β 1A and β 1D integrin isoforms after silencing *ITGB1BP2* gene (*siITGB1BP2*). (b) Western blot and densitometry analyses of β 1A and β 1D integrin isoforms after silencing *FRZB* gene (*siFRZB*). Data are represented as mean band density normalized relative to GAPDH \pm standard deviation. siC-: control siRNA, scramble RNA. Three controls and 3 patients. ITG β 1D after *siFRZB* in LGMD2A patients statistical significance $p= 0.019$ (paired t test).

According to the obtained results, decrease in β 1D integrin levels due to melusin gene silencing and parallel increase of *FRZB* gene after *CD9* gene silencing in distal muscles, further studies were focused on *FRZB* gene silencing experiments.

2.3 Analysis of *FRZB* involvement in the canonical Wnt/ β -catenin pathway

Since *FRZB* is an antagonist of some Wnt proteins involved in Wnt/ β -catenin pathway, such as Wnt-1, Wnt-8, Wnt-5a and Wnt-9 (Leyns et al., 1997; Wang et al., 1997; Person et al., 2005; Qian et al., 2007), how *FRZB* silencing was affecting canonical Wnt/ β -catenin pathway was evaluated in myotubes. A nuclear translocation of β -catenin in human myotubes was observed after *FRZB* gene silencing (Figure 28).

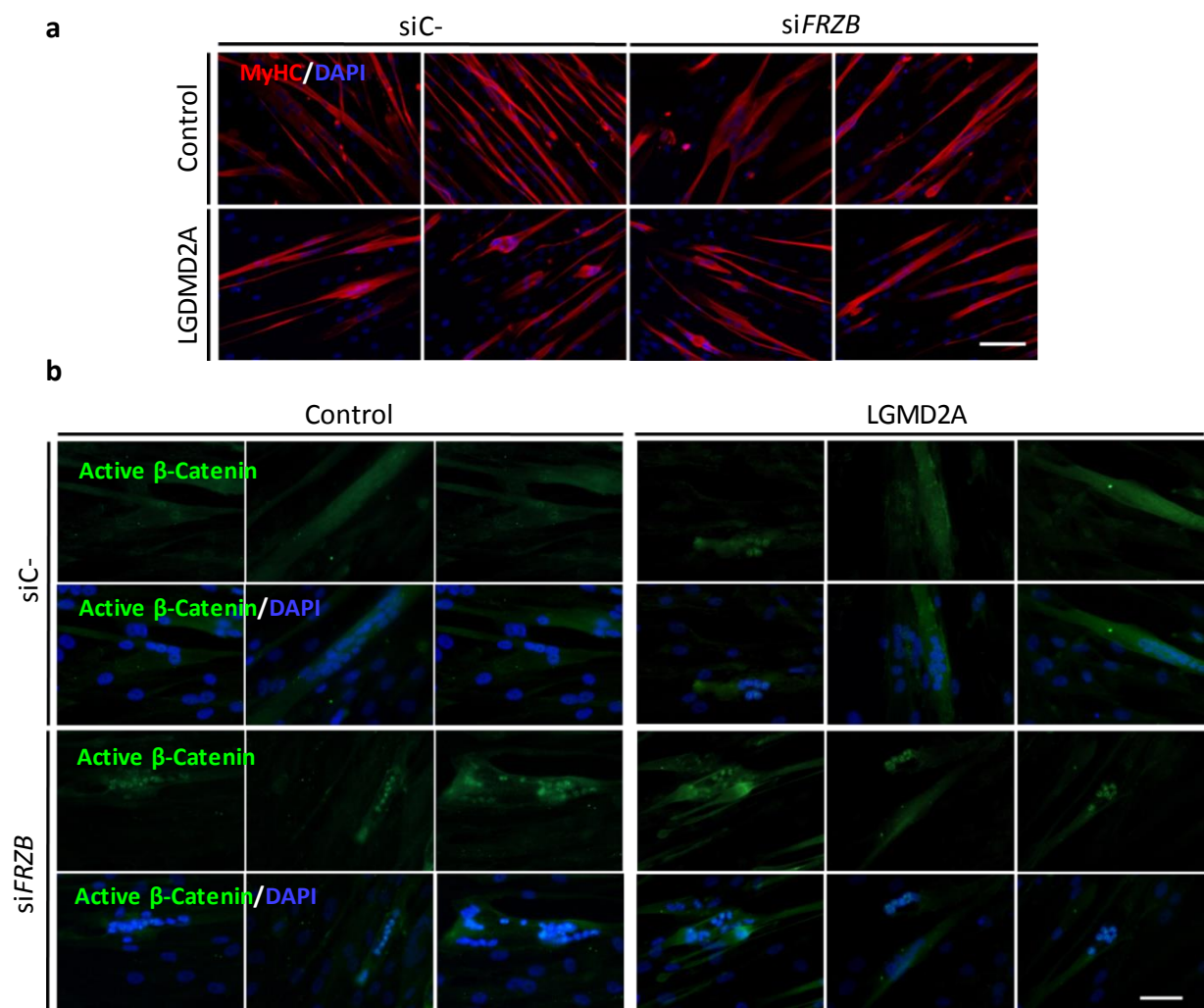


Figure 28. (a) Immunofluorescence analysis of myosin heavy chain (all isoforms), MyHC (red) after *FRZB* gene silencing (siFRZB) in control and LGMD2A patients' myotubes. Scale bar 100 μ m. (b) Immunofluorescence analysis of β -catenin nuclear translocation after siFRZB. Control and patients' myotubes are stained for active β -catenin (green). Scale bar 50 μ m. In both cases nuclei are visualized with DAPI (blue).

2.4 Gene expression analysis after activation of Wnt/ β -catenin pathway

The expression of some genes deregulated in the muscles of LGMD2A patients (Sáenz et al., 2008) were analysed to establish whether *FRZB* expression was involved in their regulation. Firstly, some of the extracellular matrix (ECM) coding genes, involved in fibrosis, such as *COL1A1*, *COL5A1* and *FN1* showed a trend to upregulation after *FRZB* gene silencing, although great variability was observed between the samples. Additionally, genes coding for a transcriptional factor (*FOS*) and for genes coding for proteins interacting with integrin or Wnt signaling pathway (*KAL1*, which codes for anosmin-1 and *VLDLR*, very low density lipoprotein receptor respectively) (Choy et al., 2013; García-González et al., 2016) all deregulated in LGMD2A patients (Sáenz et al., 2008), showed a trend to upregulation once *FRZB* gene was silenced (Figure 29).

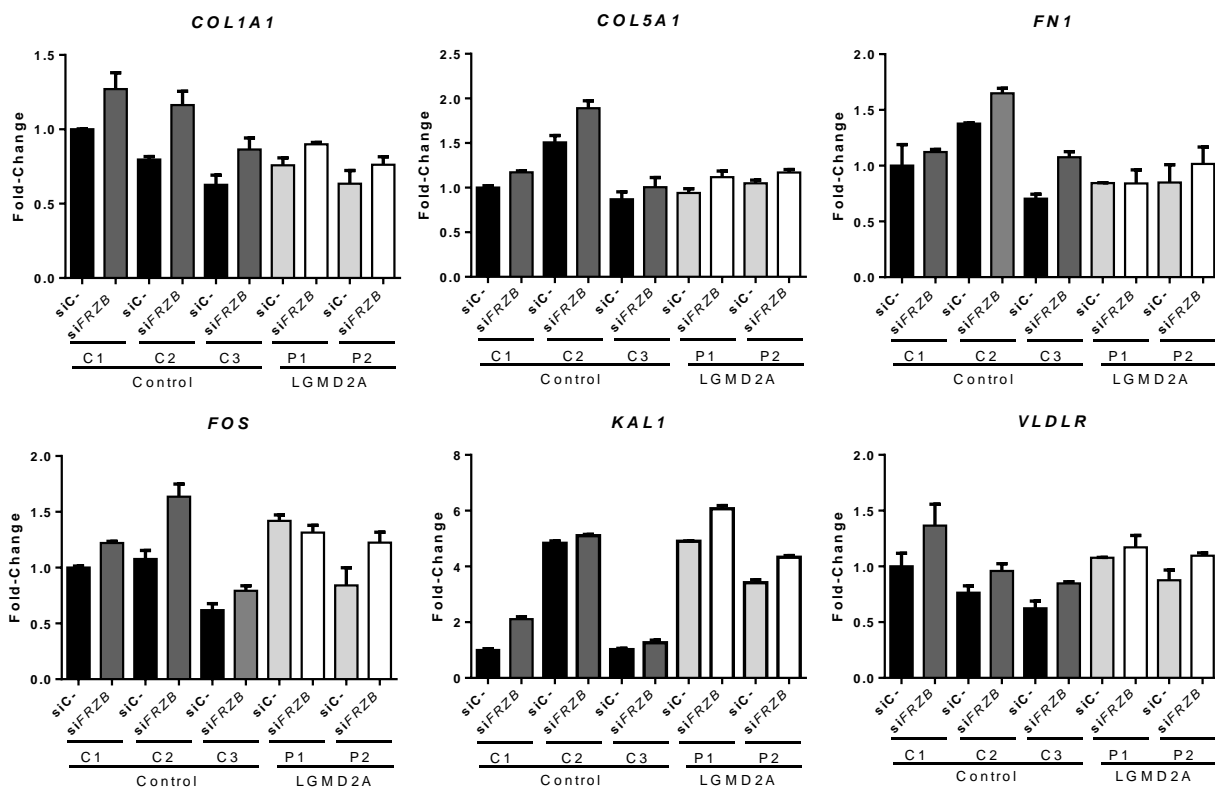


Figure 29. Gene expression analysis of *COL1A1*, *COL5A1*, *FN1*, *FOS*, *KAL1* and *VLDLR* genes in human myotubes after *FRZB* silencing (*siFRZB*). Three controls and two patients. Data are represented as relative mean expression \pm standard deviation. *GAPDH* was used as the endogenous control. siC-: control siRNA, scramble RNA.

If paired comparison was performed to analyse the effect of silencing considering all the samples together (control and patients), genes upregulation were statistically significant in all cases except for *FOS* gene expression (**Figure 30**).

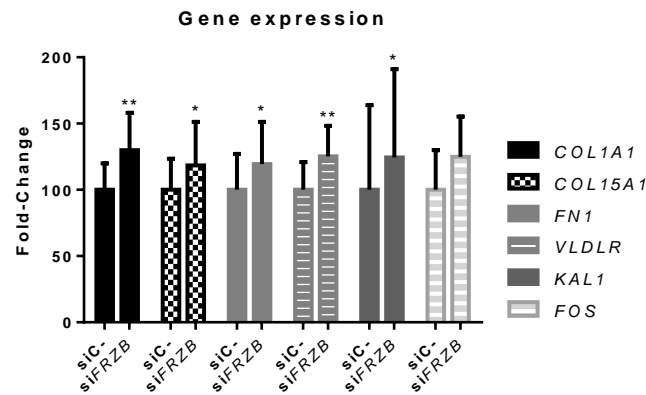


Figure 30. Gene expression analysis of *COL1A1*, *COL5A1*, *FN1*, *VLDLR*, *KAL1* and *FOS* genes where silencing effect is shown. Data are represented as relative mean expression \pm standard deviation. N= 5 for each condition. Statistical value for siC- versus siFRZB for *COL1A1*; p= 0.0066, *COL5A1*; p= 0.0142, *FN1*; p= 0.043, *VLDLR*; p= 0.072 and *KAL1*; p= 0.0213 (paired t test). *GAPDH* was used as the endogenous control. siC-: control siRNA, scramble RNA.

In silico analysis (AliBaba v2.1) of the promoter of these genes indicated the presence of various binding sequences for transcription factors such as c-Fos (upregulated after *FRZB* silencing), c-Jun and AP-1 (a heterodimer of the oncogenes Fos and Jun, members of the bZIP family of transcription factors) which are regulated by β -catenin (He et al., 1998; Mann et al., 1999) (**Table 20**).

Gene	Promotor sequence	TF	Nucleotide position	TF nucleotide sequence
<i>COL1A1</i>	c t g c c t c a g c	AP-1	211 -220	s T G m s T C A G C
<i>COL5A1</i>	t g a c t c t g g g	AP-1	1900-1909	T G A C T m w k k G
	g c t t g c t g a c t	c-Jun	3171-3180	G s T k k s T G A C
		AP-1	3172-3181	s T k n C T G A C T
	t g t g t c a g c a	AP-1	3291-3300	T G y G T C A G y w
<i>FN1</i>	g a a t g a a t c a	c-Jun	1555-1564	r n A T G A r T C A
	c c g t g a c g t c	c-Jun	4814-4823	C y n T G A y G T C
<i>VLDLR</i>	t c t g a c t a a t	c-Jun	947 -956	n y T G A C T m A T
		c-Fos	947- 956	k C T G A m T m A y
		AP-1	947-956	n m T G A C T m A T
		AP-1	947 -956	k m T G A C T m A y
<i>KAL1</i>	g c c t g a g t c a a g a	AP-1	4198-4207	s y n T G A G T C A
		AP-1	4200-4209	n T G A s T C A w r
		c-Jun	4198-4207	s s m T G A G T C A
		c-Jun	4201-4210	T G A s T C A w G m
		c-Fos	4198-4207	s s m T G A G T C A
		c-Fos	4201-4210	T G A s T C A w G m
		AP-1	4200-4209	m T G A G T C A n G

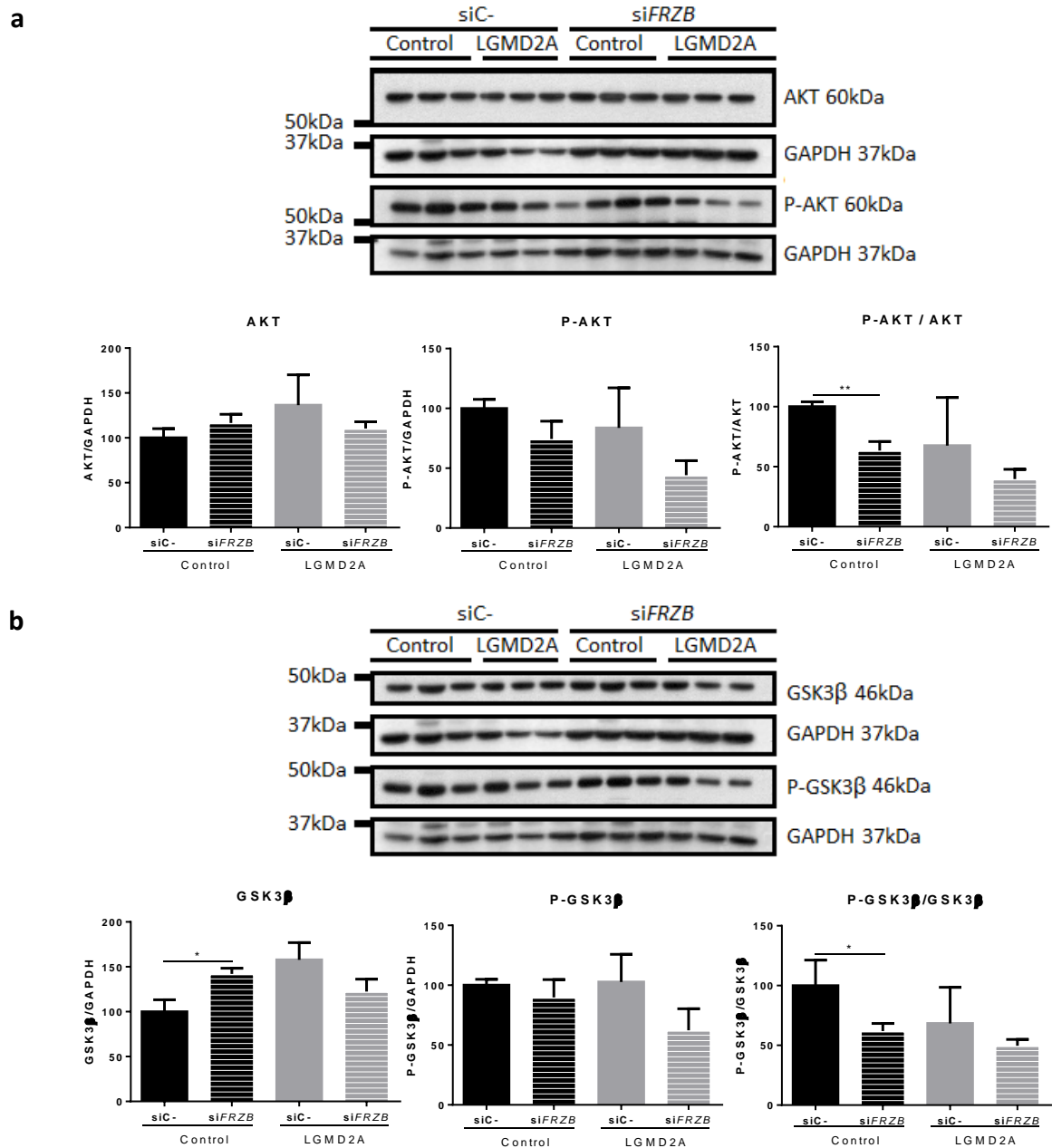
Table 20. A summary of c-Fos, c-Jun and AP-1 transcription factors (TF) binding site prediction for *COL1A1*, *COL5A1*, *FN1*, *VLDLR* and *KAL1* genes. Being k= G/T, m= A/C, n =T/C/A, s= C/G, w= T/A and y= C/T.

2.5 Analyses of the phosphorylation of several signaling pathways after *FRZB* gene silencing

P-AKT/AKT are proteins that act downstream of the integrin signaling pathway (King et al., 1997; Ivaska et al., 2002; Pankov et al., 2003) thus, the potential effect of the reduction in β 1D integrin in *LGMD2A* patients, as well as its upregulation after *FRZB* gene silencing was studied. Moreover, the phosphorylation status of other kinases such ERK1/2 and GSK3 β was studied since melusin could phosphorylate ERK1/2 and AKT kinase (Brancaccio et al., 1999) (which in turn phosphorylates the GSK3 β) (Cross et al., 1995).

The total amount of AKT did not differ after *FRZB* gene silencing, but the signal corresponding to phosphorylated AKT was lower. In addition, the P-AKT/AKT ratio was significantly lower after si*FRZB* treatment, indicating a reduction in AKT activity. In the case of GSK3 β , a lower level of phosphorylation and a lower P-GSK3 β /GSK3 β ratio was observed, which suggested an increase in the

activity of this kinase. Finally, the ERK1/2 phosphorylation levels also decreased after *siFRZB* treatment, showing a significantly lower P-ERK1/2/ERK1/2 ratio than in non-silenced myotubes and therefore a reduction in the activity of the protein (**Figure 31**).



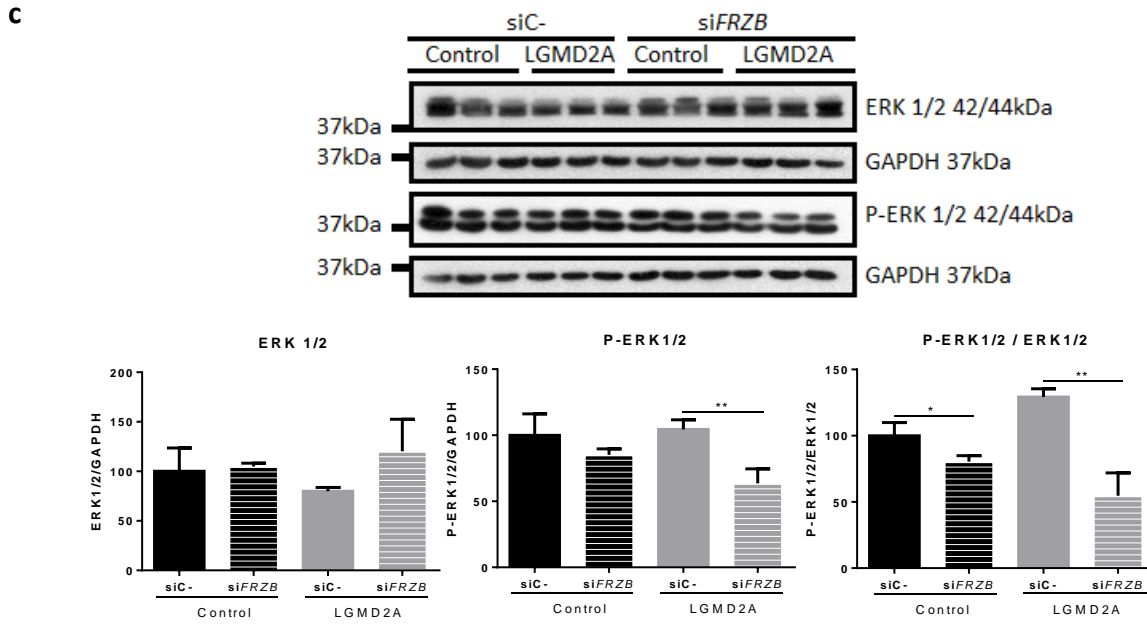


Figure 31. Western blot and densitometry analyses of (a) P-AKT (Ser473)/AKT, (b) P-GSK3 β (Ser9)/GSK3 β and (c) P-ERK1/2 (Thr202/Tyr204)/ERK1/2 after *FRZB* gene silencing (*siFRZB*) in control and LGMD2A myotubes. Data are represented as mean band density normalized relative to GAPDH \pm standard deviation (3 controls and 3 patients). Statistical significance values; P-AKT/AKT in controls, $p = 0.0018$; GSK3 β in controls, $p = 0.0466$; P-GSK3 β /GSK3 β in controls, $p = 0.0414$; P-ERK1/2 in LGMD2A, $p = 0.0058$; PERK1/2 /ERK1/2 in controls, $p = 0.0359$ and in LGMD2A, $p = 0.0021$. siC-: control siRNA, scramble RNA.

To corroborate if all the observed effects were due to Wnt/ β -catenin pathway activation, lithium chloride (LiCl) was used as a positive control. LiCl is a well-known Wnt/ β -catenin pathway activator as it inhibits GSK3 β mediated β -catenin phosphorylation, preventing its subsequent degradation by ubiquitin proteasome system (Klein and Melton, 1996) and also increases Wnt1 expression (Hiyama et al., 2011).

The treatment with LiCl produced similar results to those obtained in the treatment with *siFRZB*. On the one hand, higher level of expression of the *FOS*, *KAL1* and *VLDLR* genes were observed, although variability between different samples was observed. On the other hand, melusin gene expression did not show conclusive result after LiCl treatment even if most of the samples did not show any variation in its expression. Finally, a downregulation of *FRZB* and an upregulation of *MYH2* genes expressions were observed (Figure 32 a). Furthermore, β 1D integrin protein expression was evaluated and LiCl treatment also increased it (Figure 32 b).

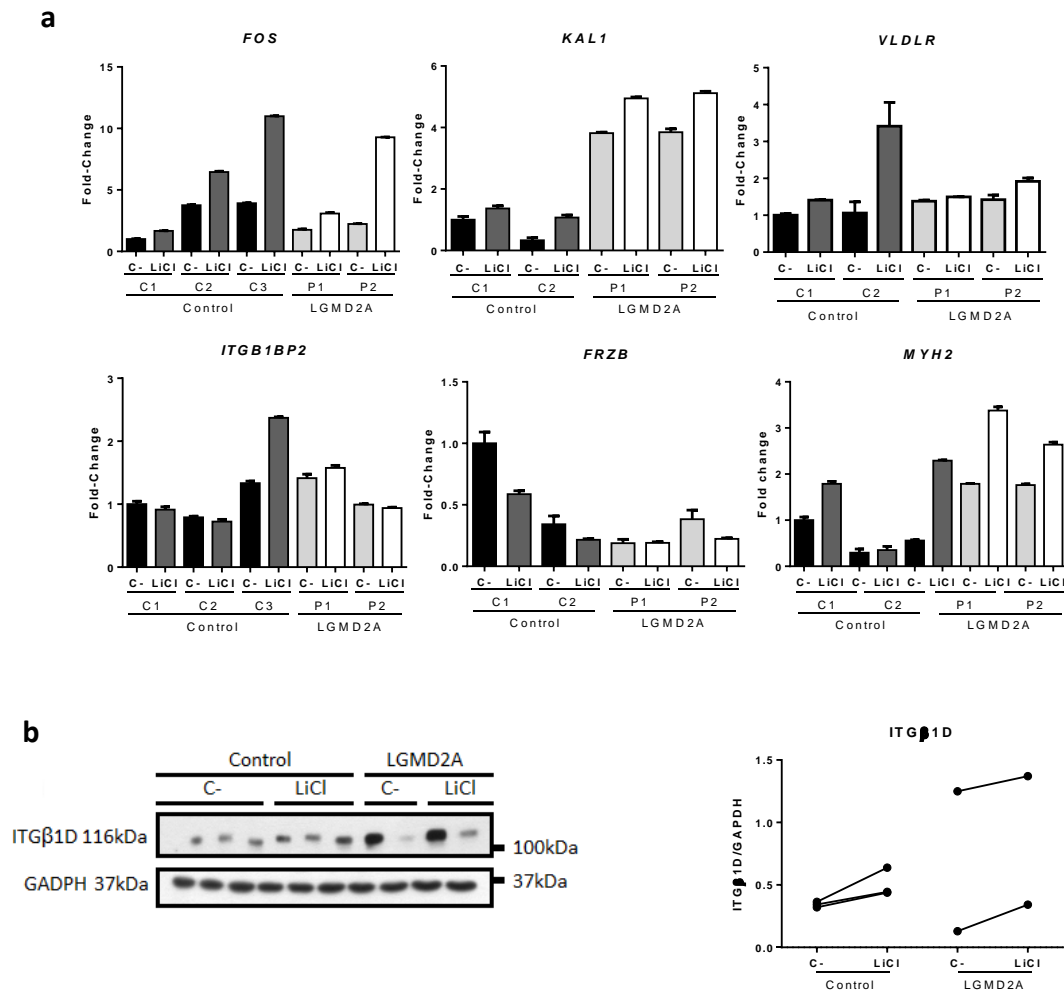


Figure 32. (a) Gene expression analysis of *FOS*, *KAL1*, *VLDLR*, *ITGB1BP2*, *FRZB* and *MYH2* genes in human myoblasts after LiCl 10 mM administration. Data are represented as relative mean expression \pm standard deviation. *GAPDH* was used as endogenous control. (b) Western blot and densitometry analyses of ITG β 1D after LiCl 10 mM administration. Data are represented as mean band density normalized relative to GAPDH \pm standard deviation (3 controls and 2 patients). C-: not-treated control samples.

Given that the administration of LiCl also increases the expression of β 1D integrin, downstream phosphorylations were also studied. LiCl administration slightly decreased AKT phosphorylation without affecting AKT protein expression, but great variability between samples was observed. An increased P-GSK3 β which caused a significant upregulation of P-GS3 β /GSK3 β ratio was observed, and in turn, an inhibitory effect on GSK3 β . Finally, less ERK1/2 phosphorylation was achieved upon LiCl treatment that led to significantly reduced of P-ERK1/2/ERK1/2 ratio in control samples (Figure 33).

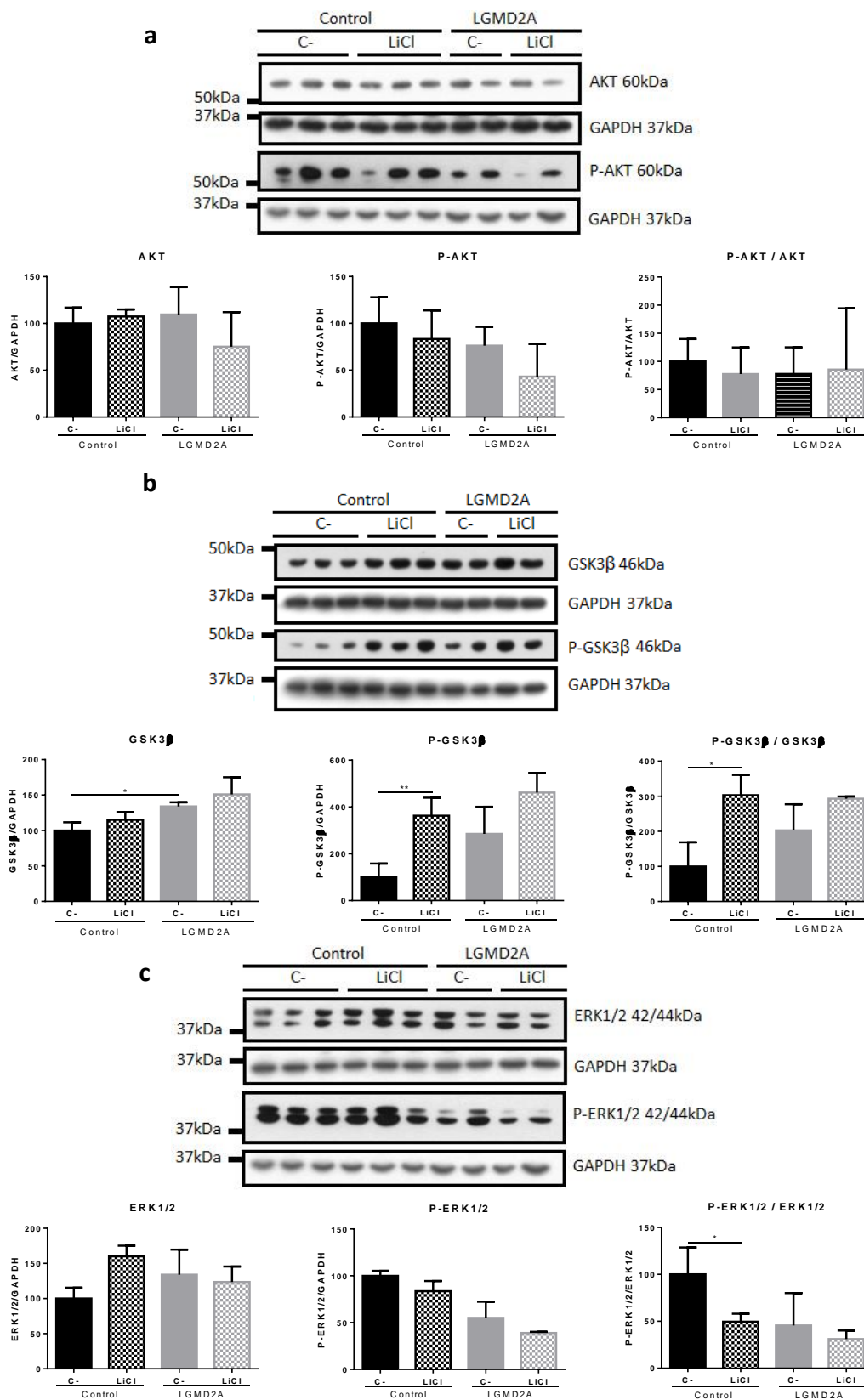


Figure 33. Western blot and densitometry analyses of (a) P-AKT (Ser473)/AKT, (b) P-GSK3 β (Ser9)/GSK3 β and (c) P-ERK1/2 (Thr202/Tyr204)/ERK1/2 after LiCl 10mM treatment in control and LGMD2A myotubes. Data are represented as mean band density normalized relative to GAPDH \pm standard deviation (3 controls and 3 patients). Statistical significance values; GSK3 β , control versus LGMD2A without treatment, $p=0.00377$; P-GSK3 β in controls, $p=0.0093$; P-GSK3 β /GSK3 β in controls, $p=0.0173$; P-ERK1/2/ERK1/2 in controls, $p=0.0432$. C-: not-treated control samples.

2.6 Treatment effect in early and late stage treated human myotubes

Given the known influence of Wnt signaling pathway on myogenesis, the effect of LiCl and *siFRZB* administration in myotubes at early (at first day of differentiation) and later (at day 8 of differentiation) stages were studied. Moreover, to avoid transitory effect of the treatments, every 3 days *siFRZB* and LiCl were administered and myotubes were finally analysed at 11 days of differentiation. On the one hand, when treatments were administered early, at day 1 of differentiation, myotube formation decreased in both treatments. Both, nuclei number and myotubes fusion index were significantly lower than in non-treated samples. On the other hand, no statistical differences were observed in total nuclei number or fusion index when myotubes were treated at 8 day post-differentiation (**Figure 34**).

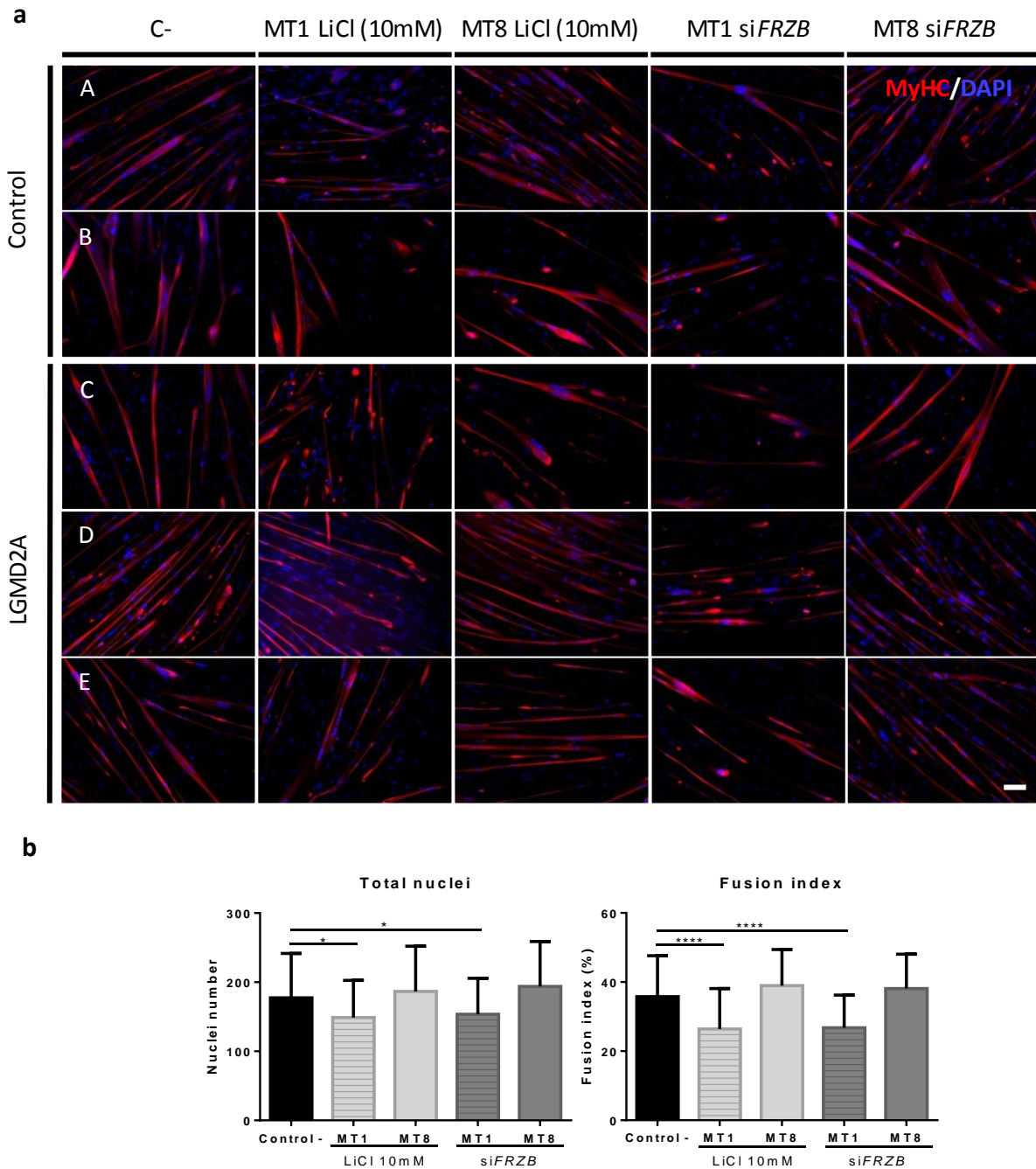


Figure 34. (a) Immunofluorescence analysis of myotubes at day 11 of differentiation after LiCl administration and *FRZB* gene silencing (*siFRZB*) at one day or 8 days of differentiation. Two controls (A and B) and 3 LGMD2A patients (C-E). Myotubes are visualized with myosin heavy chain (all isoforms), MyHC (red) and nuclei are visualized with DAPI (blue). Scale bar 100 μ m. (b) Total nuclei and fusion index (%) analyses of myotubes after two different treatments. Data are represented as mean \pm standard deviation. N= 5 (2 controls and 3 LGMD2A patients). Statistical value for total nuclei control versus LiCl MT1 sample; $p = 0.0154$, control versus *siFRZB* MT1 sample; $p = 0.0354$, fusion index control versus LiCl MT1 and *siFRZB* MT samples; $p < 0.0001$. C-: non-treated control samples and *siFRZB*: *FRZB* gene silencing. MT1= myotubes treated at 1 day of differentiation and MT8= myotubes treated at 8 days of differentiation.

2.7 *Frzb* gene silencing on C2C12 myotubes

In order to confirm some obtained data in human myotubes, murine C2C12 myoblast cell line was used. *Frzb* gene silencing was studied in myotubes at early (at day 1 of differentiation) and later (at day 3 of differentiation) stages. In early treated myotubes, treatment was maintained until day 7 of differentiation while in late treated myotubes, treatment was maintained until day 9 of differentiation. At both stages nuclear translocation of β -catenin was observed (**Figure 35 a and Figure 36 a**).

Early treated myotubes had increased fusion index without myonuclei amount variation (**Figure 35 b**). Conversely, in late treated myotubes no fusion index or nuclei amount variation was observed (**Figure 36 b**).

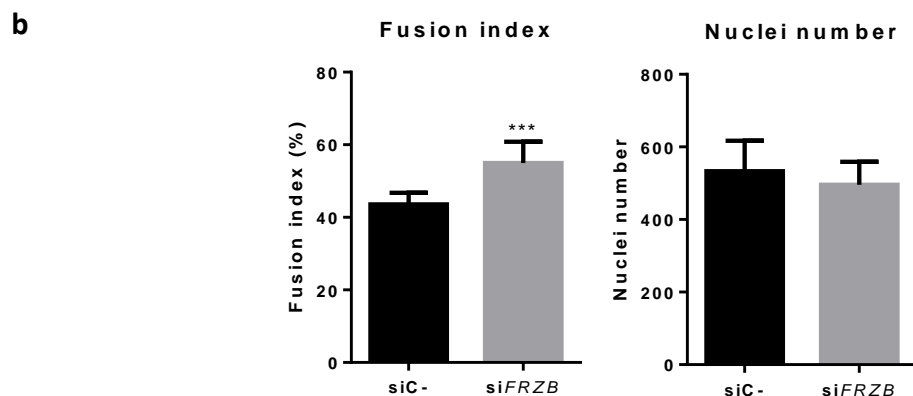
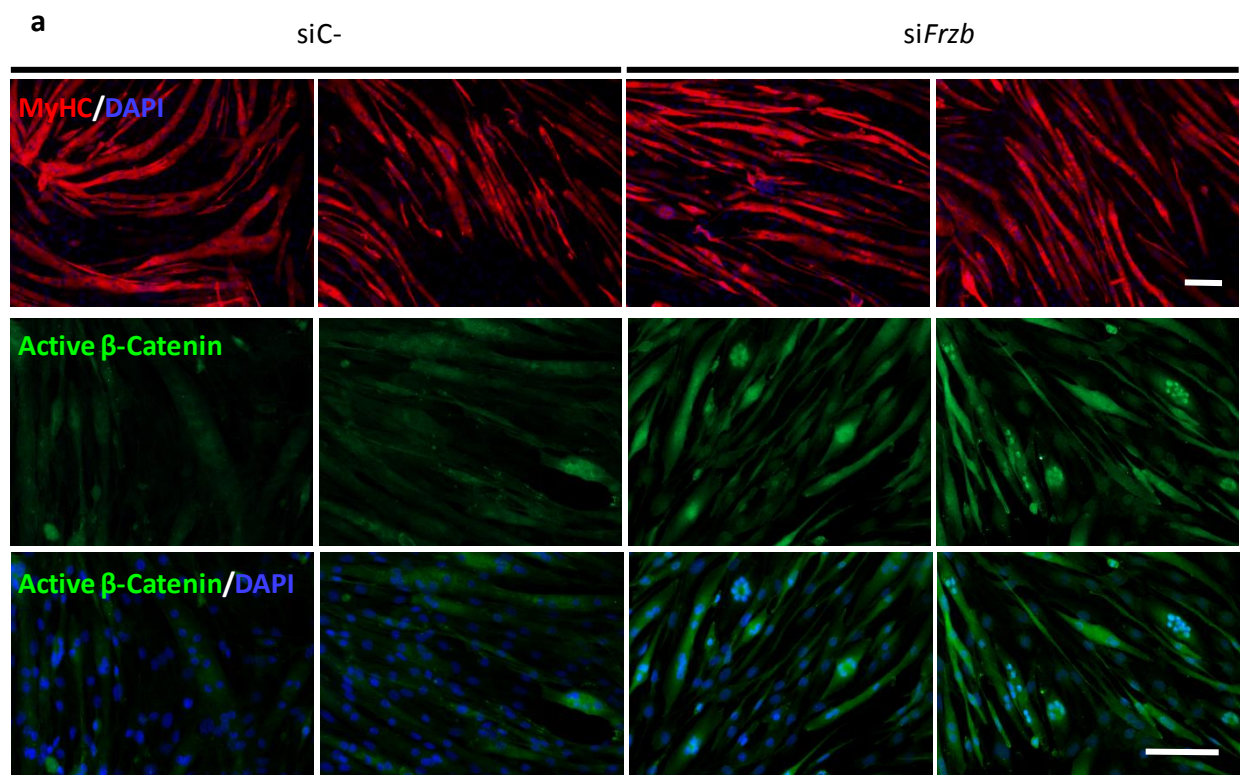


Figure 35. (a) Immunofluorescence analysis of myotubes formation and β -catenin nuclear translocation after *Frzb* gene silencing (siFrzb) in myotubes at 1 day of differentiation and fixed at day 7 post differentiation. Upper images are stained for myosin heavy chain, MyHC all isoforms (red) and lower images for active β -catenin (green). In all cases nuclei are visualized with DAPI (blue). Scale bar 100 μm . (b) Fusion index (%) and total nuclei analyses after *Frzb* gene silencing. Data are represented as mean \pm standard deviation. Statistical value for fusion index is $p= 0.003$.

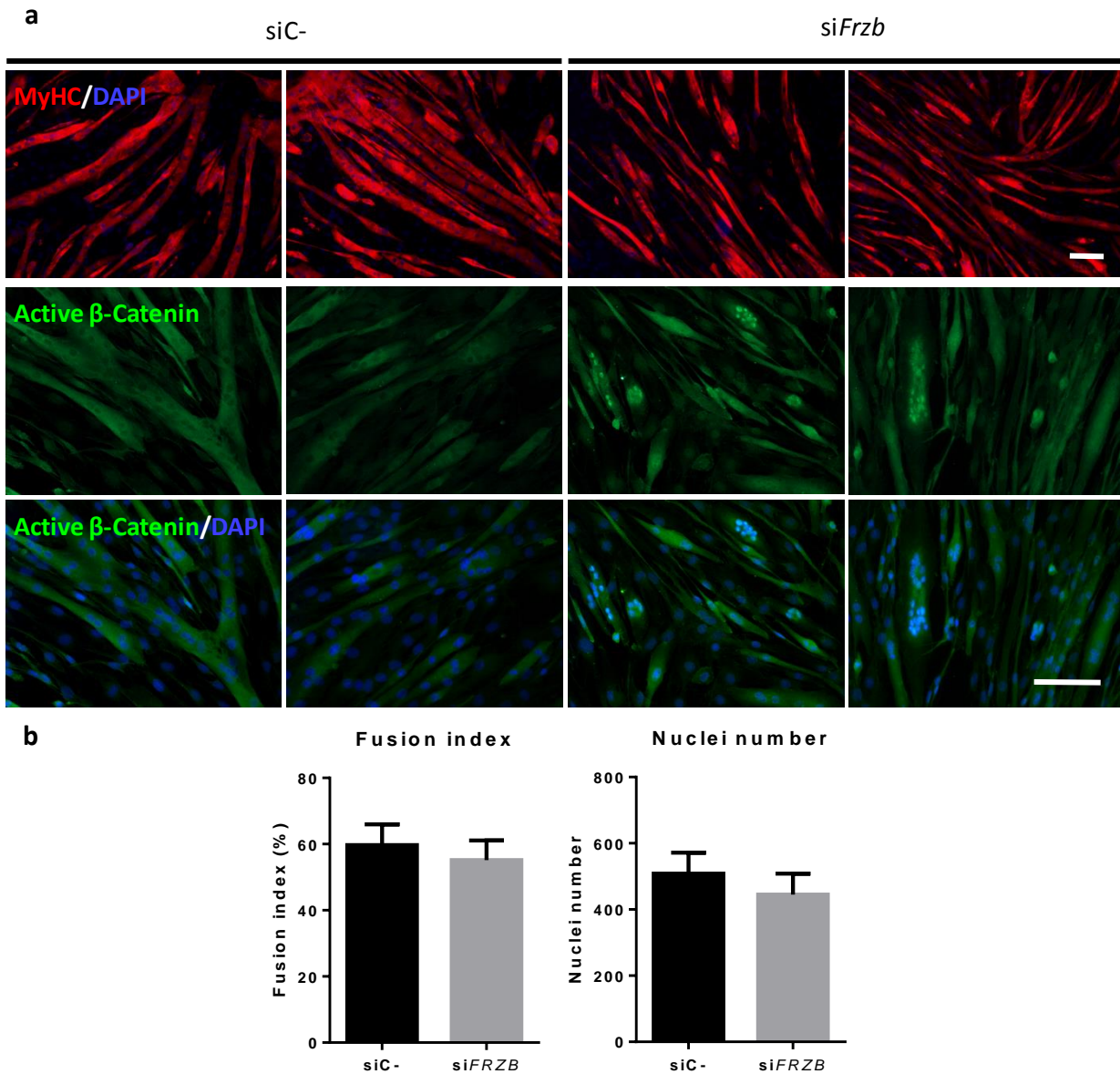


Figure 36. (a) Immunofluorescence analysis of myotubes formation and β -catenin nuclear translocation after *Frzb* gene silencing (siFrzb) in myotubes at 3 day of differentiation and fixed at day 9 post differentiation. Upper images are stained for myosin heavy chain, MyHC all isoforms (red) and lower images for active β -catenin (green). In all cases nuclei are visualized with DAPI (blue). Scale bar 100 μm . (b) Fusion index (%) and total nuclei analyses after *Frzb* gene silencing. Data are represented as mean \pm standard deviation.

For expression analysis three different approaches were used to study *Frzb* gene silencing in C2C12 myotubes. **a)** Myotubes treated at early stage (at day 1) of differentiation, **b)** myotubes treated at late stage (at day 3) of differentiation (both treatments were maintained for 4 and 5 days, for gene and protein expression analysis respectively) and **c)** Myotubes treated at day 3 of differentiation which were analysed after 2 days for gene expression and 3 days for protein.

a) Gene expression analysis

First, *Frzb* downregulation was corroborated at every analysed time points. The three different approaches used for *Frzb* gene silencing gave rise to the same regulation pattern in all the analysed genes: *Pax7*, *Myog*, *Myh2*, *Murf1* and *Fbx32*. The most noticeable change was the downregulation of *MyH2* gene. *Pax7* gene expression was more affected in later stage silencing and myogenin gene expression was almost unchanged. In the case of both atrogenes, it was observed that they showed an opposite trend, while *Murf1* was downregulated, *Fbx32* gene expression was slightly upregulated (Figure 37 a and b).

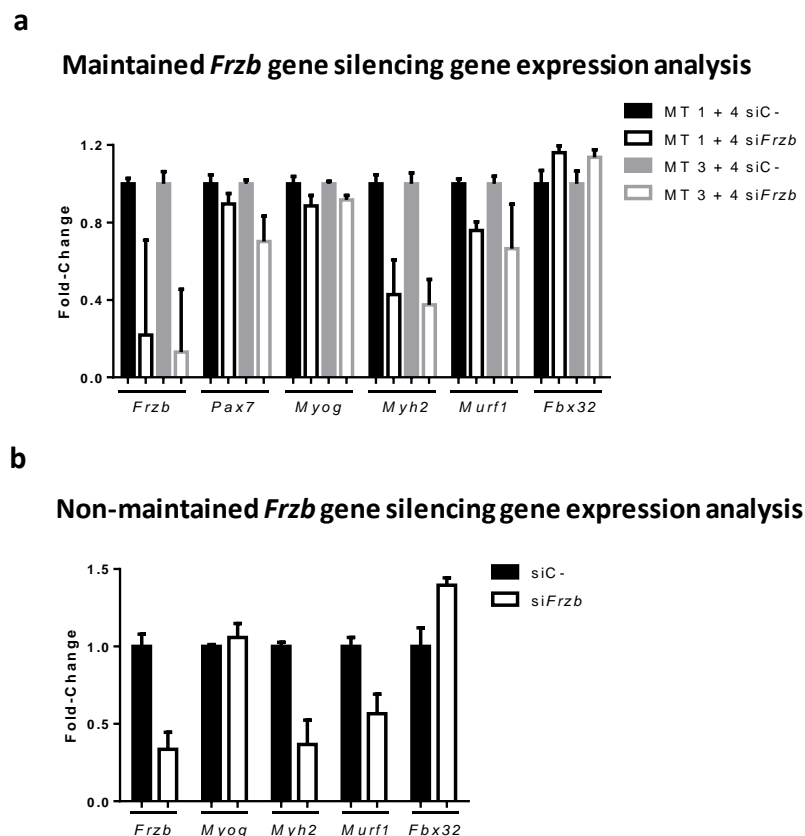


Figure 37. Gene expression analysis of C2C12 myotubes after *Frzb* gene silencing (siFrzb). **(a)** *Frzb*, *Pax7*, *Myog*, *Myh2*, *Murf1* and *Fbx32* genes analysis after *Frzb* silencing at early and late stages. **(b)** *Frzb*, *Myog*, *Myh2*, *Murf1* and *Fbx32* genes analysis after *Frzb* gene silencing (non-maintained). Data are represented as mean \pm standard deviation. siC-; control siRNA, scramble RNA. MT1= myotubes treated at 1 day of differentiation and MT3= myotubes treated at 3 days of differentiation.

b) β 1A and β 1D integrin isoform analysis

β 1A to β 1D integrin isoforms were studied at protein level. Long term *Frzb* silencing in both, early and late stage, showed an increased ITG β 1D protein after silencing. ITG β 1A downregulation was only observed in myotubes silenced the first day of differentiation. On the other hand, when *Frzb* silencing was performed in mature myotubes, ITG β 1A and ITG β 1D proteins amount were diminished after treatment (**Figure 38**).

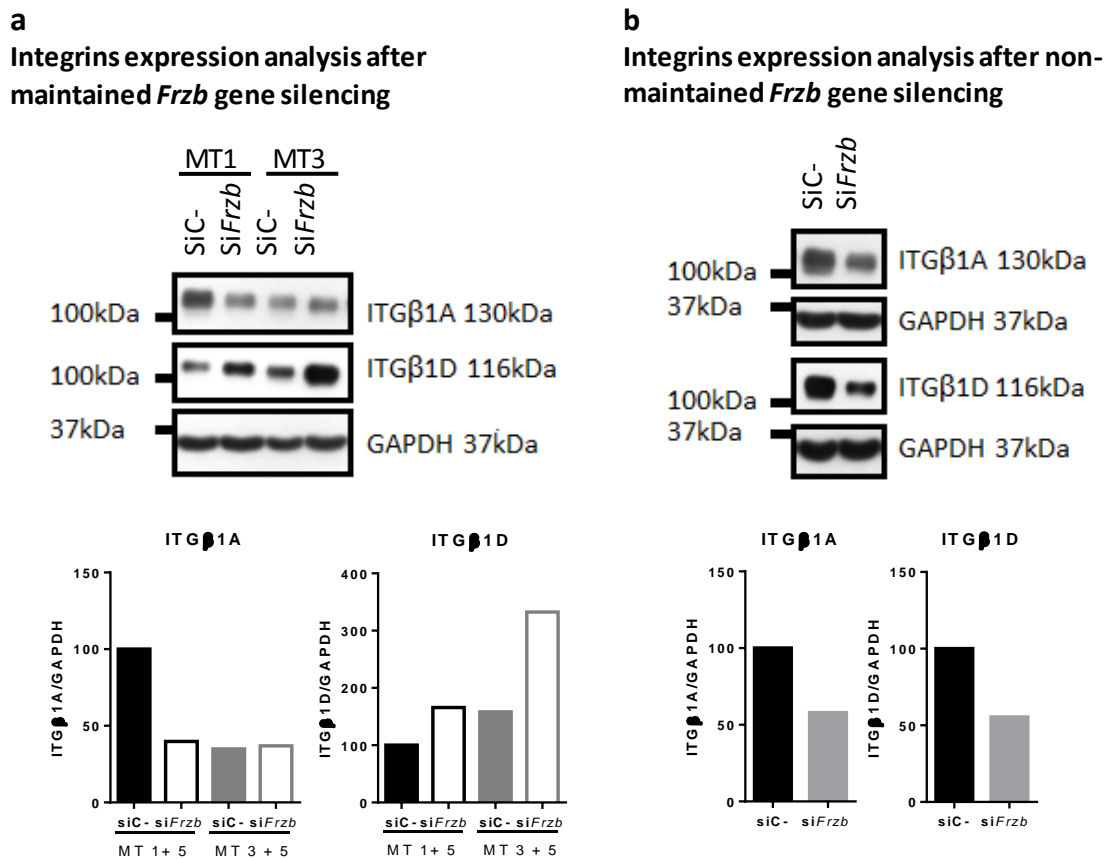


Figure 38. Western blot and densitometry analyses of integrin isoforms β 1D and β 1A in C2C12 myotubes after *Frzb* gene silencing (*siFrzb*). **(a)** ITG β 1D and ITG β 1A protein analyses after *Frzb* silencing that was performed at 1 day as well as 3 days post-differentiation maintained for 5 days more. **(b)** ITG β 1D and ITG β 1A protein analyses after *Frzb* silencing at 3 days of differentiation until 6 days of differentiation. Data are represented as mean band density normalized relative to GAPDH. siC-; control siRNA, scramble RNA.

3. PERTURBATIONS IN SIGNALING PATHWAYS IN LGMD2A

AKT/mTOR and mitogen-activated protein kinase (MAPK) signaling pathways are altered in LGMD2A patients, P-AKT/AKT and P-GSK3 β /GSK3 β ratios were increased and a reduction in the ratio of P-ERK1/2/ERK1/2 was observed in the patients (Jaka, 2014). Consequently, downstream effectors and modulating cell response were studied.

3.1 AKT/mTOR signaling pathway analysis

As a downstream effector of AKT/mTOR pathway, S6 kinase 1 was studied (S6K1). S6K1 exists in two distinct isoforms, cytosolic 70-kDa isoform (p70S6 kinase) and 85-kDa nuclear isoform (p85S6 kinase). Different phosphorylations of p70S6 kinase were studied. Due to the first obtained results (great differences between patients' samples, strong signal and complete absence of band) and in order to confirm there was no any problem with the antibody, western blot analysis was repeated including new LGMD2A samples and keeping the most divergent LGMD2A cases. It was confirmed that, Thr-421 and Ser-424 residues phosphorylation levels of 05 and 09 cases (asymptomatic patients) were similar to those of controls, however, 36, 114, 168 and 169 cases (severely affected patients) showed a great decrease in the phosphorylations (**Figure 39 a**). Nevertheless, the phosphorylation on Thr-389 residue showed high variability to obtain any conclusion (**Figure 39 b**).

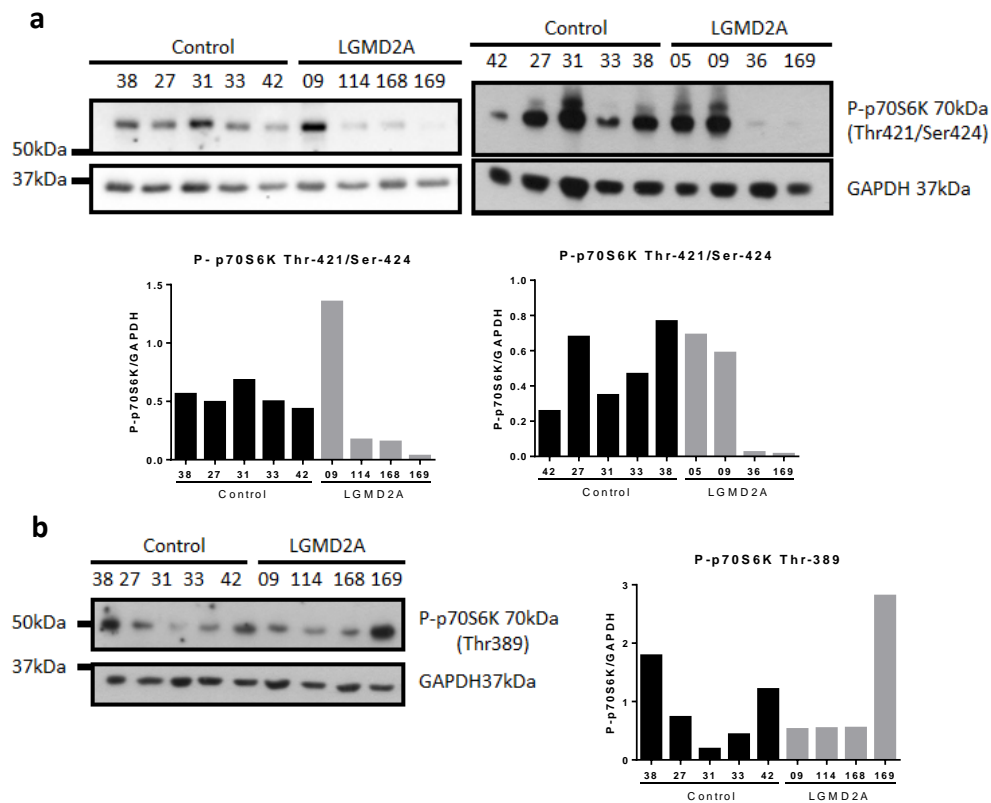


Figure 39. (a) Western blot and densitometry analyses of P-p70S6K (Thr-421/Ser-424) in control and LGMD2A patients' skeletal muscles. (b) Western blot and densitometry analyses of P-p70S6K (Thr-389) in skeletal muscle of control and LGMD2A patients. Control samples: 27, 31, 33, 38 and 42. LGMD2A samples: 05, 09, 36, 114, 168 and 169 (05 and 09 asymptomatic patients). Data are represented as mean band density normalized relative to GAPDH.

Ribosomal protein S6 (RPS6) phosphorylations were studied as a downstream effector of S6K1 (Gressner and Wool, 1974). LGMD2A patients showed significantly less phosphorylation in Ser-235 and Ser-236 residues of RPS6. While most severely affected LGMD2A patients showed almost no phosphorylation, the 09 case, the asymptomatic patient, showed similar levels to control samples (Figure 40).

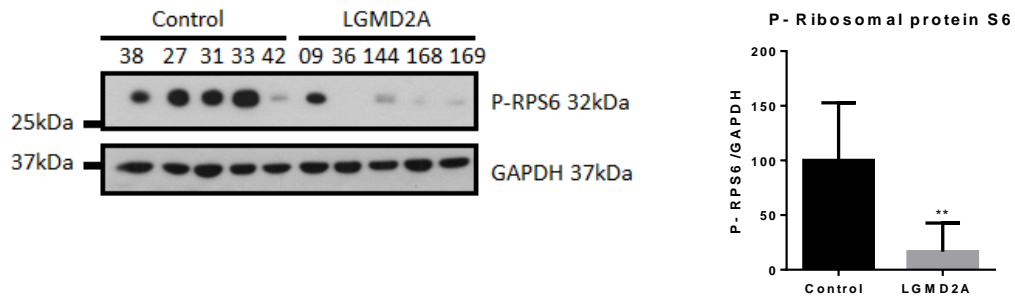


Figure 40. Western blot and densitometry analyses of P-RPS6 (Ser-235/Ser-236) in control and LGMD2A patients' skeletal muscles. Statistical significance of control versus LGMD2A patients is $p= 0.0075$. Control samples: 27, 31, 33, 38 and 42. LGMD2A samples: 09, 39, 114, 168 and 169 (09 asymptomatic patient). Data are represented as mean band density normalized relative to GAPDH \pm standard deviation.

3.2 FoxO signaling pathway analysis

Forkhead box class O family member proteins (FoxOs) are transcription factors involved in several functions which could be phosphorylated and inhibited by P-AKT, among others (Brunet et al., 1999; Kops et al., 1999; Takaishi et al., 1999; Stitt et al., 2004). In human skeletal muscle four members of FoxO transcription factors are expressed namely FoxO1, FoxO3 (or FoxO3a), FoxO4 and FoxO6. Total FoxO1, FoxO3 and FoxO4 and their phosphorylations were analysed since they are the most widely studied in skeletal muscle (Furuyama et al., 2000; Chung et al., 2013; Sanchez et al., 2014).

Despite the variability observed in FoxO1 as well as phosphorylated FoxO1, no differences were observed between control and LGMD2A patients samples, thus P-FoxO1/FoxO1 rate did not show either differences (**Figure 41**).

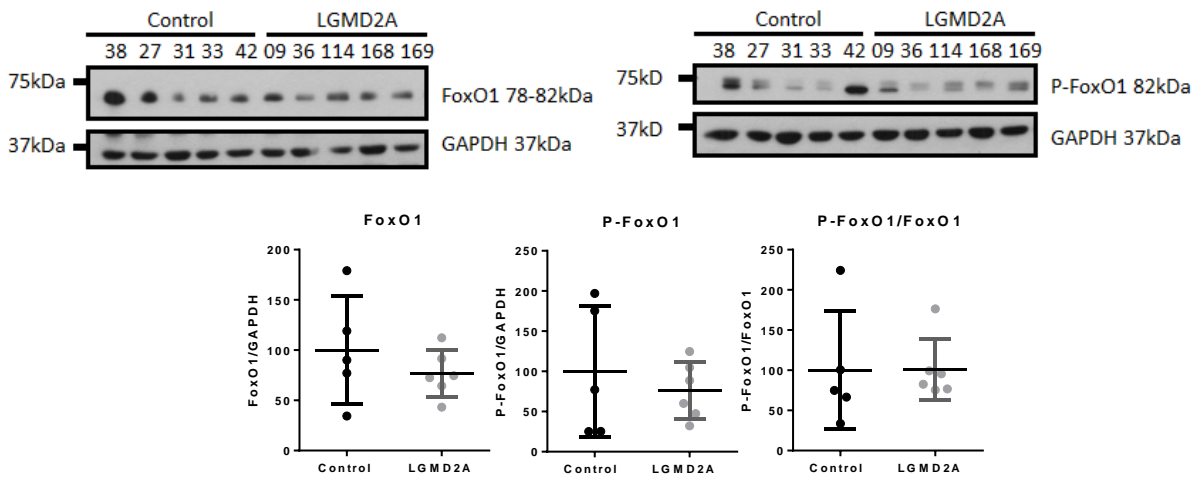


Figure 41. Western blot and densitometry analyses of total FoxO1 and phosphorylated FoxO1 (Ser-256) proteins in control and LGMD2A patients' skeletal muscles. Control samples: 27, 31, 33, 38 and 42. LGMD2A samples: 09, 36, 114, 168 and 169. Data are represented as mean band density normalized relative to GAPDH \pm standard deviation.

The analysis of FoxO3 phosphorylation in skeletal muscles showed a trend to increase in LGMD2A patients. However, due to the great variability no statistical significance was achieved (**Figure 42**).

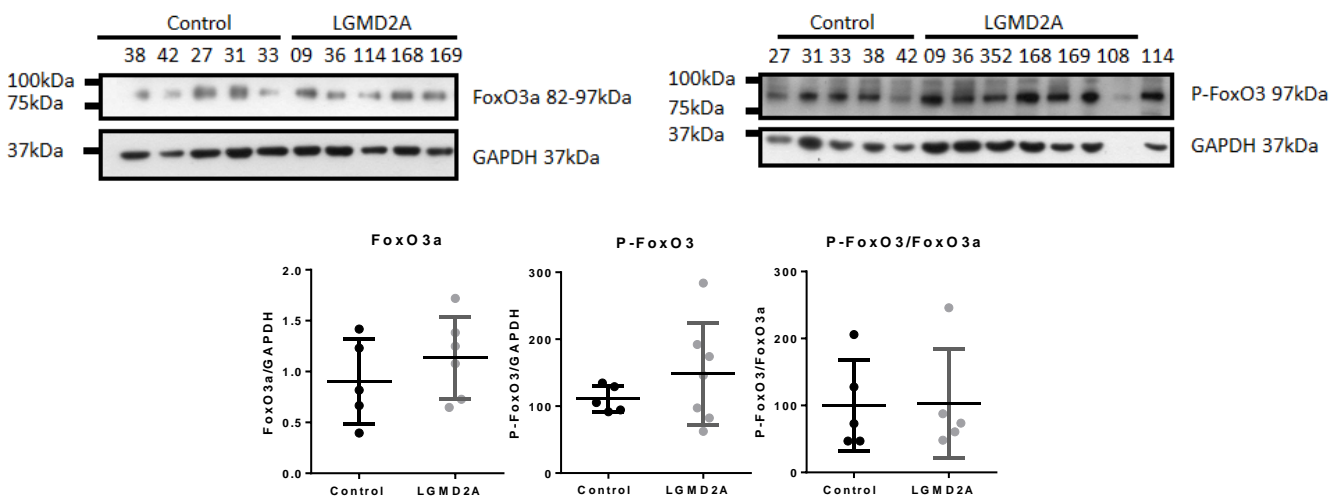


Figure 42. Western blot and densitometry analyses of total FoxO3a and phosphorylated FoxO3 (Ser-253) proteins in control and LGMD2A patients' skeletal muscles. Control samples: 27, 31, 33, 38 and 42. LGMD2A samples: 09, 36, 114, 168 and 169. Data are represented as mean band density normalized relative to GAPDH \pm standard deviation.

Finally, phosphorylated FoxO4 was evaluated in these muscles and a statistically significant increase was shown in LGMD2A patients (**Figure 43**).

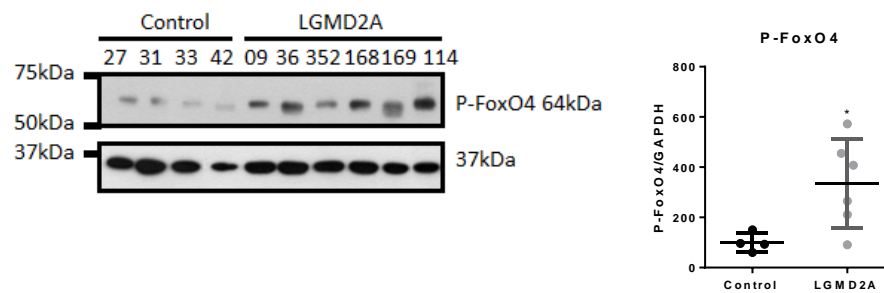


Figure 43. Western blot and densitometry analyses of phosphorylated FoxO4 (Thr-28) proteins in control and LGMD2A patients' skeletal muscles. Control samples: 27, 31, 33 and 42. LGMD2A samples: 09, 36, 114, 168, 169 and 352. Data are represented as mean band density normalized relative to GAPDH \pm standard deviation. Statistical significance is $p = 0.00337$.

FoxO transcription factors regulates atrogen-1 (coded by *FBX32* gene) and MuRF1 (coded by *MURF1* gene) muscle-specific E3 ubiquitin ligases, which are responsible of the protein breakdown in the skeletal muscle (Kamei et al., 2004; Sandri et al., 2004; Nakashima and Yakabe, 2007). Thus, in order to test whether observed FoxO transcription factors deregulations were affecting these downstream effectors, MuRF1 and atrogen-1 protein levels were measured in controls and LGMD2A patients' skeletal muscles. MuRF1 showed a statistically significant increase in LGMD2A patients (**Figure 44 a**) while atrogen-1 did not vary (**Figure 44 b**).

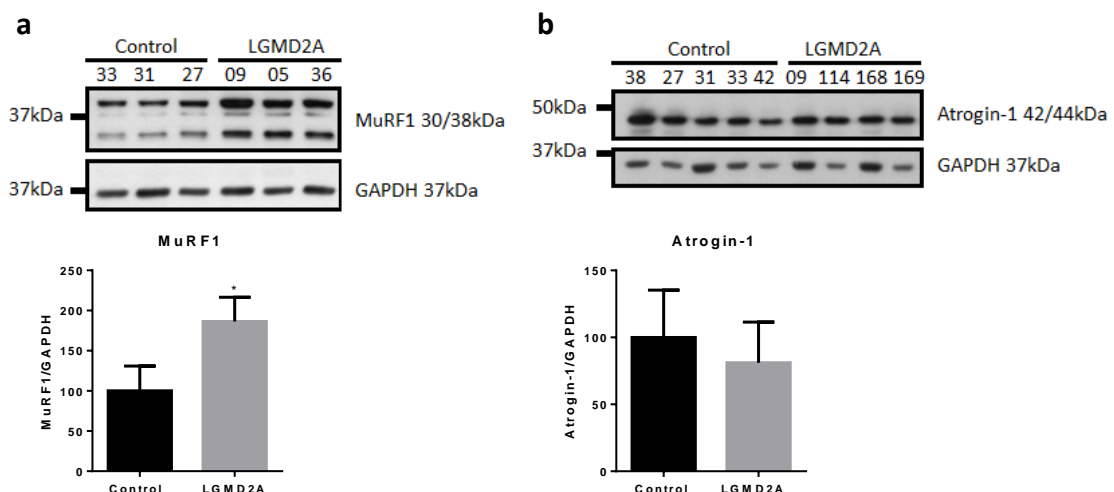


Figure 44. (a) Western blot and densitometry analyses of MuRF1 protein in control and LGMD2A patients' skeletal muscles. Statistical significance is $p = 0.00256$. (b) Western blot and densitometry analyses of atrogen-1 protein in control and LGMD2A patients' skeletal muscles. Control samples: 27, 31, 33, 38 and 42. LGMD2A samples: 05, 09, 36, 114, 168 and 169. Data are represented as mean band density normalized relative to GAPDH \pm standard deviation.

Besides atrogenes, FoxO3 regulates the expression of several proteins related to autophagy-lysosomal pathway (Yamazaki et al., 2010). Hence, Bcl2 interacting protein 3 (BNIP3) and beclin-1 protein were analysed in both, control and LGMD2A patient's muscles, but no differences were observed (**Figure 45**).

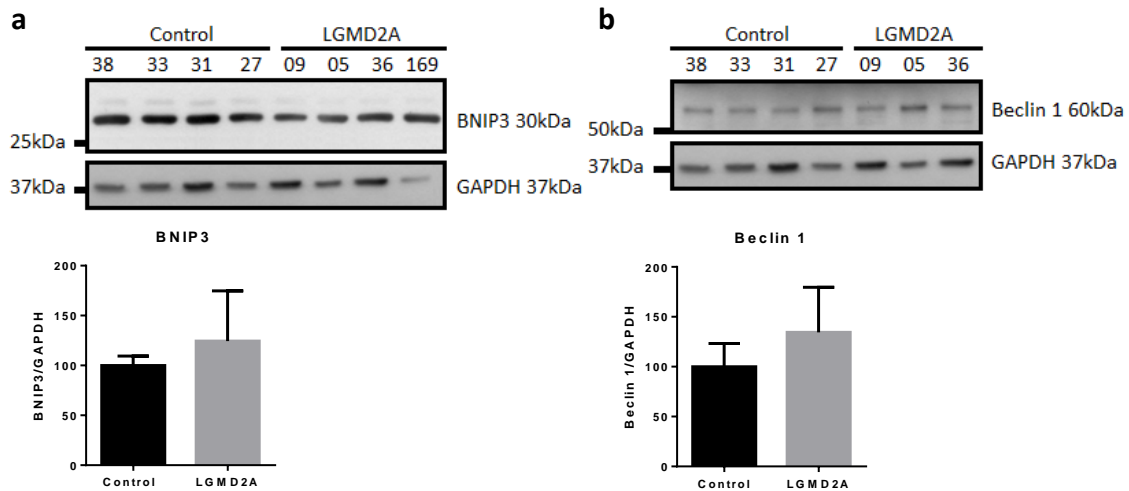


Figure 45. (a) Western blot and densitometry analyses of BNIP3 protein in control and LGMD2A patients' skeletal muscles. (b) Western blot and densitometry analyses of beclin-1 protein in control and LGMD2A patients' skeletal muscles. Control samples: 27, 31, 33 and 38. LGMD2A samples: 05, 09, 36 and 169. Data are represented as mean band density normalized relative to GAPDH \pm standard deviation.

CHAPTER 1: DISCUSSION

1. APPROACH TO THE OPTIMIZATION OF CELL CULTURE FOR THE INVESTIGATION OF MECHANISM UNDERLYING MUSCULAR DYSTROPHIES

The lack of correlation between cells and their tissue of origin has already been described (Smith et al., 1994; Cornelison and Wold, 1997; Hawke and Garry, 2001; LaFramboise et al., 2003). Previous data from our group are in line with these findings since skeletal muscle cellular model (myotubes) did not recapitulate observed muscle gene expression profile (Jaka, 2014). In a study where expression profiling was compared in human cultured myotubes and skeletal muscle tissue, downregulation of the *CAPN3* gene was detected (Raymond et al., 2010). This relevant finding might be one of the factors influencing the cellular models, resembling the control profile to the patient behaviour. For our studies neural cell adhesion molecule (N-CAM or C56), a widely used cell surface marker for satellite and myoblast (Illa et al., 1992), was used for myoblast isolation from human biopsies. It is known that is not cell-specific marker, since it is also expressed in different cell types such as natural killers, neural and hematopoietic cells (Abo and Balch, 1981; Lanier et al., 1983; Edelman, 1986; Cashman et al., 1987; Lanier et al., 1989; Figarella-Branger et al., 1990).

On the other hand, FBS is a widely used supplement for cell culture growth that contains a huge variety of growth factors, hormones, vitamins, amino acids, fatty acids and trace elements. Even if it is extensively used worldwide, there is, however, a fundamental problem underlying its use; batch to batch variations. This could provoke a great variability in cell cultures. In fact, depending on the FBS origin, alterations in engineered C2C12 mice skeletal muscle cell line as well as in molecular and biochemical markers associated with myoblast fate and myotube protein synthesis have been reported (Khodabukus and Baar, 2014; Saini et al., 2018).

Due to all these reasons, the present study has been conducted with the aim to recapitulate the events observed in muscle. For that purpose, sera obtained from healthy as well as LGMD2A patients has been used to growth, control and LGMD2A myoblasts respectively *in vitro*.

As an alternative to animal serum, the use of human serum has been widely studied and its use was first described by Chang and colleagues (1954). Most of these studies were focused on clinical transplantation. However, the use of human serum, as well as different origin serum effectiveness for cell growth has been a subject of debate for many years, resulting in contradictory results. While Kuznetsov and colleagues (2000) reported that for *ex vivo* expansion of human bone marrow stromal cells (BMSCs), medium with FBS was the most effective, Yamamoto and colleagues (2003) concluded that human serum is more efficient to expand the same cell type. Nevertheless the observed

discrepancy could be attributed to the used different human serum, given that one was a commercial allogous serum while the other was an autologous serum.

In this study heterologous human serum has been used because serum from the patients of the available biopsy specimens it was not possible to obtain. Even if the age of serum donors was not perfectly matched, it is noteworthy that the age of the serum donors has no effect on proliferation and differentiation nor in the expression of proliferation and myogenic markers on myotubes (George et al., 2010).

The first observation in this study was the highest proliferation rate in myoblast grown with human serum. This result is in agreement with studies carried out in different cell types such as monocyte-derived hepatocyte-like cells, fibroblast or chondrocytes (Tallheden et al., 2005; Chua et al., 2007; Munirah et al., 2008; Isaac et al., 2011; Ehnert et al., 2011). However, contradictory results have been observed regarding this issue. Some studies showed no differences in proliferation rates in human BMSCs, conjunctival epithelial cells or chondrocytes (Yamamoto et al., 2003; Ang, 2005; Chua et al., 2007). But, other study showed greater effectiveness with FBS stimulating BMSC proliferation (Kuznetsov et al., 2000). These differences could be due to experimental procedure variability, cell type as well as human origin serum diversity (heterologous, autologous, pulled or externally purchased).

The second observation was the downregulation of several skeletal muscle specific genes, such as *MYH2*, *ITGB1BP2* and *DES* and proteins; myosin heavy chain, melusin, β 1 integrin and myogenin (**Figure 23 and 24**) which confirms the reduced myotubes formation and the deleterious effect of the use of HHS.

Several studies have been carried out to determine serum influence in myogenesis. On the one hand, there are studies that compare the effects of different non-human serum in human myoblasts. The influence of different origin sera such as foetal calf serum (FCS), hormone and growth factors depleted FCS and horse serum (HS) on primary myogenic cells was studied. It was concluded that the variable composition of mitogenic and anabolic factors of the sera was the responsible of the observed alterations in myoblasts proliferation and myotube protein synthesis as well as of the myogenic markers variation (Saini et al., 2018). Moreover, a study focused on extracellular vesicles of FBS, suggested that extracellular vesicles' content could reduce myoblast proliferation correlated with upregulation of differentiation genes in an *in vitro* model of skeletal muscle cells (Aswad et al., 2016).

On the other hand, human serum influence in human myoblasts culture has also been studied in different works. One study analysed human burnt victims' serum. In myoblasts grown with this serum, reduced anabolic signaling and impaired protein synthesis which led to loss of total protein content and reduced cell size was observed (Corrick et al., 2015). Another study reported the used of

serum from differently exercised subjects in myogenesis. The serum from exercise subjects increased myogenic differentiation and these differences were attributed to IGF-1 content (Vitucci et al., 2018) since it plays a crucial role in this process (Frost et al., 1997; Jacquemin et al., 2004; Cen et al., 2008).

Although apparently unexpected, serum from the same cell species does not always show the optimal conditions for culture, primary equine bronchial fibroblasts grew better with FBS than with horse serum (Franke et al., 2014).

Based on previously described works, the observed altered proliferation and differentiation of skeletal muscle cells *in vitro* could be attributed to the different composition of both sera. The variable composition of human serum and FBS could affect differentially the gene expression pattern of myotubes leading to diverse responses. It could be suggested that cells cultured in HHS may show a gene expression imbalance that maintains cells in a non-differentiated stage blocking differentiation. This idea would be in line with the fact that a higher multiplication rate was observed in HHS grown myotubes and with previous findings reported by Aswad and colleagues (2016).

In conclusion, although initially it was proposed that human serum could improve the growth and differentiation conditions of myoblast and myotubes *in vitro*, allowing a greater resemblance between tissue and cell culture, this aim was not achieved. The results showed that the use of human serum has a negative impact on myotube differentiation. In view of these findings, it was concluded that FBS, the widely used serum, despite mentioned limitations, is the most appropriate for myoblasts and myotubes culture. Hence, FBS was used in all the *in vitro* posterior studies carried out for the pathophysiology study of LGMD2A disease.

2. RNA SILENCING TO REGULATE OVEREXPRESSED GENES IN LGMD2A

Myotubes obtained from biopsies of LGMD2A patients have more clustered nuclei that lead to a higher fusion index compared with control myotubes (Jaka et al., 2017). The same feature was also observed in C3KO mice myotubes (Kramerova et al., 2006). Due to the observed incorrect myotube fusion, integrins were studied since they are transmembrane glycoproteins receptors that are essential for myoblast fusion (Schwander et al., 2003) which under normal physiological conditions, the $\beta 1A$ isoform is replaced by the $\beta 1D$ isoform in muscle fibre maturation (Belkin et al., 1996). This substitution was altered in C3KO mice myotubes (Kramerova et al., 2006) and in our study, absence of replacement was also reported in LGMD2A myotubes (**Figure 26**). Integrins play an important role in myoblast fusion for a correct muscle regeneration that is impaired in LGMD2A patients.

Even if $\beta 1D$ integrin protein expression was studied in LGMD2A muscles, no conclusive results, due to a great variability, were obtained (data not shown). This could be due to the different origin of the analysed muscle samples. The localization of different integrin isoforms at neuromuscular and myotendinous junctions and non-junctional sites vary and their expression is also influenced by exercise since it has been shown they have a protective effect against mechanical damage (Boppart et al., 2006). These features made it difficult to compare integrins in muscles samples of different cases as the available muscles were very limited.

Regarding integrins involvement in muscular dystrophies, in Duchenne patients as well as in *mdx* mice, elevated levels of $\alpha 7\beta 1$ integrin have been detected (with altered ratio of $\beta 1A/\beta 1D$ isoforms that suggests a reversion to a less differentiated state where $\beta 1A$ chain predominates) while by contrast, reduced levels were found in laminin $\alpha 2$ chain congenital dystrophy muscular dystrophy and in *dy/dy* mice (Hodges et al., 1997). The analysis of the effect of integrins demonstrated that their enhanced expression could alleviate muscular dystrophy in transgenic mice lacking dystrophin and utrophin (Burkin et al., 2001, 2005). Moreover, studies carried out by Liu and colleagues (2001) have proven that the specific increase of $\beta 1D$ isoform enhances transcription of $\alpha 7$ a $\alpha 2$ laminin genes and protects against sarcolemmal damage in *mdx* mice.

Due to the altered expression of integrins in muscular dystrophies and the impaired integrin isoforms replacement in LGMD2A disease, proteins that interact with integrins were also studied. Thus, the analysis were focused on melusin and CD9 specifically, since both proteins interact with integrins (specifically melusin with $\beta 1A$, $\beta 1B$ and $\beta 1D$) (Brancaccio et al., 1999; Armulik, 2002; Schwander et al., 2003; Przewoźniak et al., 2013) and both were overexpressed in patients' muscle (Sáenz et al., 2008). In addition to these two proteins FRZB protein was analysed because its expression was the only one that was concordantly upregulated in muscle and in culture (Jaka, 2014).

Previous studies showed that these three genes coding for melusin, *CD9* and *FRZB* are upregulated in the muscles of LGMD2A patients (Sáenz et al., 2008). Further research made possible to verify this upregulation at protein level (Jaka et al., 2017).

Given that normal muscle regeneration requires a tight control of myoblast fusion by tetraspanins CD9 and CD81 (Charrin et al., 2013) the surface CD9 protein upregulation could explain the morphology of the LGMD2A patients' myotubes.

Additionally, although a direct interaction of melusin, CD9 and FRZB has not previously been described, at least *in vitro*, their relationship at gene expression level was reported (Jaka et al., 2017). Related to the silencing experiments, as *CD9* and *FRZB* genes silencing produced a parallel downregulation of melusin, it has been suggested that *CD9* and *FRZB* act upstream on the regulation of the *ITGB1BP2* gene. Similarly, the fact that *ITGB1BP2* gene silencing upregulates *FRZB* expression suggests that these proteins are involved in a common regulatory pathway that is impaired in LGMD2A dystrophy (**Figure 46**). Further studies are required to determine the mechanism that controls this apparent contradictory regulation, but it could be suggested that there is a negative feedback mechanism for the activation or control both pathways. The fact that this regulation control has been confirmed in distal muscles reinforces the idea that these genes are closely related at expression level.

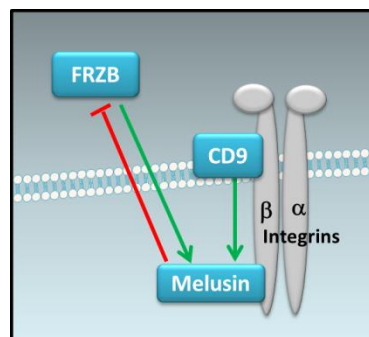


Figure 46. Schematic representation of a potential model of the regulation of FRZB, CD9 and melusin in the skeletal muscle. Green arrows indicate positive expression signal while red stripe indicates a negative expression signal.

Since on the one hand, integrins replacement seemed to be defective in LGMD2A myotubes and melusin binds directly to $\beta 1$ isoforms, whether silencing of melusin could affect $\beta 1$ integrin levels in myotubes was studied. On the other hand, as silencing of the melusin gene affected *FRZB* expression and *vice versa*, the effect of *FRZB* silencing on $\beta 1$ integrins was also studied. Studies carried out in *FRZB* and melusin gene silencing have provided evidence of the importance of their expression regulation for a proper muscle fibre growth and/or maturation.

FRZB overexpression apparently showed a negative impact on the cell as silencing this gene caused the β 1D integrin isoform to return to normal levels in myotubes from LGMD2A patients. Nevertheless, melusin upregulation and its silencing are both associated with a decrease in the integrin β 1D isoform. Based on these results, it could be proposed that this decrease occurs both when too much melusin is present (potentially because of steric problems) but also when there is too little melusin (because of lack of an anchoring protein). These data therefore would indicate that the quantity of melusin needs to be finely tuned for proper formation of the protein complex. There are similar biological systems responsible for reverse effects in the cell, such as the one reported by Bernick and colleagues (2010), in which loss or overexpression of *unc-45b* leads to defective myofibril organisation; that is, *unc-45b* expression must be precisely regulated to ensure normal myofibril organisation. There are also other examples, for instance, abnormally high or low levels of IQGAP1 and SRPK1 expression reduce activation of MEK and ERK or promote cancer respectively (Roy et al., 2005; Wang et al., 2014). This is the reason why further studies were focused on *FRZB* gene silencing experiments since melusin gene silencing would be negatively affecting myotubes differentiation. Moreover, since *CD9* gene silencing upregulates melusin gene expression in distal muscles, this approach also was discarded for further analysis.

Hence, when the connection between integrins and *FRZB* was sought, it was found that *Frzb*^{-/-} mice cartilage showed an overrepresentation of upregulated genes related to this pathway (Lodewyckx et al., 2012). Further studies confirmed that Wnt/ β -catenin pathway and integrins were also related (Renner et al., 2016; Sorcini et al., 2017). *FRZB* gene silencing increased β -catenin nuclear translocation in primary human myotubes (**Figure 28b**) as observed in a gastric cancer cell line model (Qin et al., 2014). This observation suggests that *FRZB* may play a role in the crosstalk between integrin and Wnt signaling pathways. The link between these pathways may involve the nuclear translocation of β -catenin that would activate transcription factors such as *FOS* (target gene of Wnt/ β -catenin signaling pathway) which in turn could bind to the promoter of *KAL1* gene, which codes for anosmin-1, a protein that also interacts with β 1D integrins (Choy et al., 2013) (**Figure 29**). *KAL1* gene was underexpressed in the muscle of LGMD2A patients with eosinophilic infiltrates (significantly lower) and the level of expression was also notably lower in other LGMD2A patients (two-fold lower, though the difference did not reach statistical significance (Sáenz et al., 2008) and unpublished data respectively). Expression of this protein is elevated after *siFRZB*, and this could facilitate an increase in the β 1D isoform of the integrin. These findings suggest that there is a relationship between the regulation of the two pathways and that anosmin-1 may be involved in the organisation of the integrin complex, to ensure its correct replacement in the maturation process of muscle fibres.

The nuclear translocation of β -catenin may also act as a regulator of the Wnt/ β -catenin pathway itself, given that the observed elevated expression of the *VLDLR* after *siFRZB* treatment.

Moreover, since *in silico* analysis indicated the presence of various binding sequences for transcription factors such as c-Fos (upregulated after *FRZB* silencing). VLDLR is a negative regulator of the Wnt signaling pathway through heterodimerization with lipoprotein receptor-related protein (LRP6; a transmembrane protein that binds to Frizzled and that is involved in the canonical Wnt pathway) that accelerate the turnover of LRP6 (Lee et al., 2014). This represents a potential new mechanism for the regulation of the Wnt/ β -catenin pathway which could limit the duration or intensity of a Wnt-initiated signal (**Figure 47**).

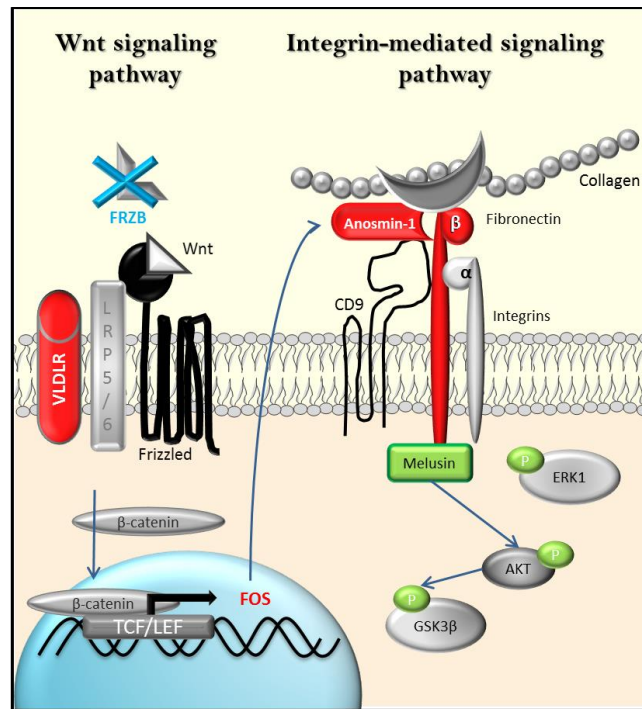


Figure 47. Schematic representation of a potential model of the regulation of the genes of interest. Upregulated genes and increased proteins are shown in red while downregulated genes and decreased proteins are shown in green.

On the other hand, several studies have related Wnt/ β -catenin signaling pathway to fibrosis in different tissues (Brack et al., 2007; Guo et al., 2012). Accordingly, experiments carried out in *Frzb*^{-/-} cartilage showed upregulation of fibrosis markers such as *Col1a1* as well as *Col5a1* (Lodewyckx et al., 2012).

In parallel, an enhancer of the Wnt signaling pathway, LiCl was administered to myotubes as a positive control of the Wnt signaling pathway activation. It has long been known that LiCl inhibits GSK3 β (Klein and Melton, 1996) activating Wnt pathway and thereby stabilizing free cytosolic β -catenin effectively (Hedgepeth et al., 1997).

Gene expression analysis showed *FOS*, *KAL1* and *VLDLR* genes upregulation after LiCl administration, as observed after si*FRZB*. Even if LiCl reduced *FRZB* gene expression, no alterations in

melusin gene expression was observed. Since the specific effects of LiCl have not been fully elucidated and they are not very specific for just activating the Wnt pathway (Cohen and Goedert, 2004), the lack of melusin gene expression downregulation could be attributed to additional unknown effects of the LiCl.

The observed upregulation of *MYH2* gene after LiCl treatment could be expected since it has been demonstrated that Wnt and LiCl play an important role in regulating myotube hypertrophy and myogenic differentiation (Rochat et al., 2004).

Both approaches produced an increase in β 1D integrin level probably due to an activation of the Wnt/ β -catenin pathway. To better understand how these treatments were affecting myotubes, several signaling pathways were analysed.

It would be expected that by increasing levels of β 1D integrin, P-AKT would increase (Pfister et al., 2007). However, *FRZB* gene silencing seemed to be more closely associated with a reduction in the phosphorylation of all the kinases analysed, and this may be mainly because of a reduction in the expression of melusin, given that melusin is known to phosphorylate ERK1/2 and AKT (Brancaccio et al., 2006).

Given that GSK3 β regulation in Wnt and AKT signaling is not regulated by the same mechanisms (Ding et al., 2000), the reduction of phosphorylated GSK3 β in silenced myotubes could be due to the reduction of phosphorylated-AKT (Cross et al., 1995) which in turn could be due to the parallel downregulation of melusin (Brancaccio et al., 2006). Even some cross talk between Wnt and insulin pathways have been reported (Fukumoto et al., 2001) other authors suggest that Wnt signaling does not affect insulin signaling pathway (Yuan et al., 1999; Taelman et al., 2010).

In the case of LiCl, despite no reduction in melusin, a trend to decrease in the phosphorylation of kinases AKT and ERK was observed, suggesting that the phosphorylation of these kinases is not regulated by melusin in these circumstances. Even though LiCl is widely used experimentally, the molecular mechanisms by which LiCl treatment regulates ERK phosphorylation have not yet been elucidated. Various different responses have been obtained depending on the type of cell studied (Zassadowski et al., 2015). Finally, the well-documented increase of GSK3 β phosphorylation of Ser9 after LiCl treatment was also observed in LiCl myotubes (Klein and Melton, 1996; Du et al., 2009).

Summarizing, it can be concluded that both approaches, even if with different mechanism of action, activates Wnt/ β -catenin pathway that lead to the upregulation of target genes that could modulate integrin expression. In addition, the obtained results proved the importance of an appropriate coordination in the expression of proteins that interact with, or are components of the costamere. So far, mechanisms underlying common expression of different genes are not well known.

However, it is likely that genes whose products function together are under a common regulatory system such that they are expressed in a coordinated manner (Farina et al., 2007; Ewen et al., 2011).

Although LGDM2A patients show reduced β 1D integrin, there is no evidence of a direct interaction between calpain 3 and integrin. It could be suggested that there is an intermolecular interaction, as reported for titin, but at present there is no evidence of that. In addition, the possibility of integrin being a direct calpain 3 substrate has already been ruled out by Kramerova and colleagues (2006), who showed that neither β 1A nor β 1D integrin are digested by calpain 3, suggesting that the changes in integrin isoform levels are because of an indirect effect.

With regard to a potential direct interaction between calpain 3 and integrin regulating transcription factors, it could be supposed that a decrease in FOS (as observed in LGMD2A patients) (Sáenz et al., 2008) would control the expression of integrin because integrin has c-Fos and AP-1 binding sequences in its promoter. However, we did not observe a reduction in integrin RNA levels in patients muscle biopsies (Sáenz et al., 2008). Since the *ITGB1* gene encodes both integrin isoforms, β 1D and β 1A, it could be suspected that the alteration in the amount of integrin β 1D is because of post-translational events and the substitution of the isoform might be mediated by the increase in anosmin-1. In LGMD2A patients, myogenesis is impaired, because of the lack of replacement of the integrin isoforms required for appropriate costamere assembly, as well as for the fusion of myotubes.

Treatment effect in early and late stage treated myotubes

Related to Wnt signaling, its involvement in embryonic and postnatal myogenesis has already been proven (Borello et al., 1999; Brack et al., 2008; Otto et al., 2008). Specifically, in cell culture, Suzuki and colleagues (2015) established that Wnt/ β -catenin signaling can regulate myogenesis at different steps including, cell proliferation, myoblast fusion and homeostasis of muscle cells by targeting step-specific molecules. Brack and colleagues (2008) inhibited Wnt signaling with intramuscular Frzb injection after injury during proliferative (early) and differentiating (late) stages. Less differentiated phenotype was observed in late treated mice with no effects in early treated mice. Moreover premature induction of progenitor cell differentiation was observed when Wnt3a was added after injury at early stage. Thus, authors suggested that Wnt signaling acts directly on myogenic progenitors to promote the progression from early proliferating progenitors to more differentiated progenitors. Based on these results, it could be suggested that FRZB is one of the possible responsible of the impaired myotube formation observed in LGMD2A patients (Jaka et al., 2017). Thus, due to Wnt signaling knowledge together with previous findings where the genetic or pharmacological inhibition of GSK3 β was reported to promote myogenic differentiation and reverse muscle atrophy (Evenson et

al., 2005; van der Velden et al., 2008; Pansters et al., 2011) myogenic differentiation was studied in control and LGMD2A patients' myotubes after Wnt signaling activation.

Wnt signaling activation was carried out by *FRZB* gene silencing and LiCl administration at early (at day 1 of differentiation) and late stage (at day 8 of differentiation) maintained until day 11 of differentiation. Both treatments displayed similar results, in late treated myotubes fusion index did not show major changes even if a higher fusion index could be observed in some samples possibly because the myotubes were already formed. Conversely when treated at early stage, a deleterious effect was shown, reported by statistical significant decreased fusion index and with a parallel significant reduction on total nuclei (**Figure 34**). Since the treatment was maintained until the day 11 of differentiation, it was not possible to observe if a premature differentiation occurs, as happened when Wnt3a was added in early (Brack et al., 2008).

Nuclei number decrease at early stage treated myotubes could suggest that treatments had a negative impact in cell survival. Wnt signaling pathway is known to promote cell growth and survival since its activation enhanced gene expression of several proteins that support cell survival (Polakis, 1999). Even if it has been reported that suppression of GSK3 β protects against mitochondria-associated apoptosis during myogenic differentiation (Wang et al., 2011) many studies showed that GSK3 promotes intrinsic apoptotic signaling cascade (Beurel and Jope, 2006). Furthermore, LiCl has been found to increase TNF-mediated cytotoxicity in several cell types (Beyaert et al., 1989). Thus, further studies would be necessary to clarify if apoptosis pathway activation was the responsible of the decline in nuclei amount.

In conclusion, it could be suggested that excessive Wnt signaling activation from early stages was deleterious for myogenesis. It is noteworthy that excessive Wnt signaling activation has been linked with altered stem cell fate and increased fibrosis in mice (Brack et al., 2007). Thus, continuous Wnt signaling activation, could be the reason why myotubes formation was impaired in our study.

Moreover, murine C2C12 cell line was analysed to confirm the previous findings. *Frzb* gene was silenced at early and late stages of differentiation. Regarding nuclei amount, in none of the cases alterations were observed. This result suggested that, contrary to what was observed in human myotubes treated in early stages, C2C12 viability is not influenced by Wnt signaling. The increase in fusion index was observed when *Frzb* gene was silenced at early stages. This is in agreement with previously findings where premature induction of progenitor cell differentiation was observed when Wnt3a was injected after injury (Brack et al., 2008). However, fusion index was not altered when silencing was carried out at later stages, as happened with human samples.

Pax7 downregulation was previously observed after canonical Wnt signaling activation (Jones et al., 2015) as happened in the present study. Together with *Pax7* downregulation a parallel

upregulation of *Myog* could be expected as was the case in Wnt3a treated mice myoblasts (Jones et al., 2015). However, no major differences in *Myog* levels were shown. This difference could be due to the different Wnt effectors, since FRZB is a specific antagonist of Wnt1, Wnt5, Wnt8 and Wnt9.

On the other hand, *Myh2* gene downregulation was also reported in dilated cardiomyopathy mice model where increased Wnt signaling activation was observed. This enhanced Wnt/ β -catenin signaling also contributes to the fibre type shift toward fatigable fibre (type IIb), mediated by FoxO transcription factors (Okada et al., 2015). However, β -catenin has also been described to promote fibre type shift toward type I fatigue-resistant fibres (Kuroda et al., 2013). Since it has been proposed that TCF/LEF sequence and FoxO transcription factors compete for the pool of active β -catenin (Almeida et al., 2007) it seems that the effect of activated Wnt signaling may depend on other factors such as FoxO transcription factors accessibility.

Furthermore, since atrophy is a common hallmark of LGMD2A disease (Urtasun et al., 1998; Fanin and Angelini, 2015), the effect of *Frzb* gene silencing was evaluated in atrogenes expression. A different trend was observed in both atrogenes, while *Murf1* gene was downregulated, *Fbx32* gene was upregulated. Little is known about direct interaction between Wnt signaling pathway and atrogenes so far. β -catenin could bind to FoxO transcription factors to activate its effectors genes (Okada et al., 2015) and since FoxO transcription factors are necessary for atrogenin-1 and MuRF1 expression (Kamei et al., 2004; Sandri et al., 2004; Nakashima and Yakabe, 2007), it could be expected an atrogenin-1 and MuRF1 increase after Wnt signaling activation. However the downregulation of *Murf1* gene expression could be explained since it has been reported that FOXO3a activates these two genes through different mechanisms (McLoughlin et al., 2009; Senf et al., 2010).

Since *MURF1* gene is the only atrogene upregulated in LGMD2A patient's muscles (Fanin and Angelini, 2015) a downregulation after *FRZB* gene silencing to avoid the excessive protein breakdown, could be beneficial for patients. By contrast, the upregulation of atrogenin-1 gene deserves special attention since atrogenin-1 seems to act as protein synthesis inhibitor and it has been described as MyoD protein degrader (Tintignac et al., 2005; Attaix and Baracos, 2010).

Finally, after *siFrzb* treatment, β 1D integrin expression differences were observed depending on the used procedure (**Figure 38**). In human samples an upregulation of β 1D integrin was observed while in C2C12 myotubes, only when *Frzb* gene silencing was maintained for a longer period, an upregulation of integrin protein level was observed. It is known that differences regarding gene and protein expression are present in human and mouse models (Kho et al., 2006). Even if the same procedure was carried out, different results could be obtained, suggesting a methodological issue. Several factors could regulate differently the same pathway and a specific siRNA could present different performance in human and mice. Thus, the required conditions, such as the dose, its

transitory effect, etc. should be finely tuned in each species given that the obtained results might mask the real consequences of the experiment. This underlines the requirement of a thorough analysis when result obtained from mouse and human are compared.

Further studies are required to assess whether FRZB expression is altered in other types of muscular dystrophy, to establish whether it is also involved in their pathophysiology. Similarly, further research should investigate the mechanisms of action of FRZB, since controlling an inhibitor of the Wnt signaling pathway may be useful for the treatment of other conditions, as already described for osteoarthritis (Lories et al., 2007, 2009) and it might also be applicable to ischemic cardiopathy, in which low levels of β 1D integrin are observed (Pfister et al., 2007).

Collectively, with the obtained results, the regulation of FRZB expression could be proposed as a potential therapeutic target for LGMD2A disease, given that *in vitro* studies support the idea that it may be possible to bring expression back towards appropriate levels in LGMD2A patients.

3. PERTURBATIONS IN SIGNALING PATHWAYS IN LGMD2A

The impairment of different signaling pathways in the implication and progression of several muscular dystrophies have already been described. In *mdx* mice disease progression correlated with activation of p70S6K activity and decreased phosphorylation of p38 was observed (Lang et al., 2004). Moreover, perturbed AKT/mTORC1 signaling pathway was reported in regenerating muscles of LGMD2A mice model (Yalvac et al., 2017).

AKT/mTOR signaling pathway stimulates fibre growth through activating protein synthesis and inhibiting protein degradation (Kubica et al., 2005; Léger et al., 2006; Mammucari et al., 2007). Moreover, mTOR kinase dependency for myotubes/myofibres maturation has also been reported (Park and Chen, 2005).

A downstream effector of AKT/mTOR pathway is S6K1 and for its activation, this protein is sequentially phosphorylated, first in residues located on the pseudosubstrate domain; Ser-411, Ser-418, Thr-421 and Ser-424, followed by residues implicated in the catalytic activity; Thr-229 in the catalytic domain and Thr-389 and Ser-404 in the linker region (Price et al., 1991; Han et al., 1995; Mahalingam and Templeton, 1996; Pullen and Thomas, 1997).

In LGMD2A muscles, phosphorylation levels of Thr-421 and Ser-424 residues were decreased, while two asymptomatic patients showed normal phosphorylation levels. However, Thr-389 phosphorylation levels remained unchanged. Thr-421 and Ser-424 residues could be phosphorylated by MAPKs (Mukhopadhyay et al., 1992) thus, the reduced ERK1/2 phosphorylation reported in LGMD2A patients could be responsible of these phosphorylations decreases. The phosphorylation at Thr-389 did not show alterations even if P-AKT/AKT ratio was increased in LGMD2A patients (Jaka, 2014) however, it is worthy to mention that not only mTOR kinase can phosphorylate this residue *in vivo*, but also NIMA-related kinase (NEK6/7) can (Belham et al., 2001; Templeton, 2001).

The fact that other kinases as well as other residues participate in the activation of S6K1 (Pearson et al., 1995; Pullen et al., 1998) made difficult to obtain clear conclusions.

To date several S6K1 substrates have been described (Ruvinsky, 2005), however RPS6 was the first identified member of the family of S6K substrates (Gressner and Wool, 1974). It is part of the 40S (small) subunit of ribosome and it could be phosphorylated in several sites (Martin-Pérez and Thomas, 1983; Wettenhall et al., 1992). Related to the phosphorylation patterns, different groups reported contrary results, although Ser-235 and Ser-236 are directly phosphorylated by S6K1 (Ruvinsky and Meyuhas, 2006), later studies suggested that Ser-240 and Ser-244, but not Ser-235 and Ser-236 phosphorylations are mediated by S6K1 (Roux et al., 2007). It was reported that Ser-235 and Ser-236

are phosphorylated in an mTOR independent way through the MERK/ERK and RSK (p90 ribosomal S6K kinases) pathways (Pende et al., 2004; Roux et al., 2007).

The effects of RPS6 phosphorylation have remained obscure. EF2 kinase, eIF4B and RPS6 are S6K1 dependent downstream effectors of protein synthesis, however while the phosphorylation of EF2 kinase and eIF4B increase protein synthesis, the phosphorylation of RPS6, also mediated by S6K1, reduce it (Wang, 2001; Raught et al., 2004; Ruvinsky, 2005). In addition, studies carried out in a knockin mouse in which all five phosphorylatable serine residues of RPS6 were substituted by alanines (RPS6^{P-/-}) have demonstrated that cell proliferation and cell size determination are influenced by RPS6 phosphorylation. These mice have decreased total muscle mass due to smaller size of fibres which leads to compromised muscle strength (Ruvinsky, 2005; Ruvinsky et al., 2009).

In this study a significant reduction in Ser-235 and Ser-236 residues phosphorylation was observed in LGMD2A patients. In this case again, the asymptomatic patient showed normal phosphorylation levels. The correlation between the reduced phosphorylations on the Thr-421 and Ser-424 residues in S6K1 and Ser-235 and Ser-236 residues in RPS6, could suggest pseudosubstrate phosphorylations in S6K1, have influence in its enzymatic activity. Even so, the lack of phosphorylation at Ser-235 and Ser-236 could also be the result of the lower levels of P-ERK1/2 previously observed in the LGMD2A muscles.

The fact that asymptomatic patient, which have nearly non affected muscles, maintain these phosphorylations, has led to the idea that the maintenance of these phosphorylations are necessary for the normal homeostasis of the muscle.

These findings together with studies carried out in RPS6^{P-/-} mice where reduced fibre CSA was reported (Ruvinsky et al., 2009), could suggest that the observed downregulation of RPS6 phosphorylation, could be the reason why smaller and medium size lobulated fibres are present in LGMD2A patients' muscles (Fardeau et al., 1996a; Rosales et al., 2013; Fanin and Angelini, 2015). Moreover, a recent study where disrupted AKT/mTORC1 pathway was described in the *Capn3*-deficient mice (Yalvac et al., 2017), could also explain the observed reduced skeletal muscle mass with smaller fibre CSA in C3KO mice (Kramerova et al., 2004).

Although several different pathways could be responsible of this perturbed AKT/mTOR signaling pathway, the implication of 5' AMP-activated protein kinase (AMPK) would require further analysis since an increase of its activity which in turn inhibits mTORC1 activity has been reported in *Capn3*-deficient mice (Yalvac et al., 2017).

Since AKT could affect different signaling pathways, AKT-dependent FoxO transcription factors were analysed. IGF-1/AKT pathway phosphorylates FoxOs preventing its nuclear translocation, thus its

activation (Stitt et al., 2004). FoxOs are transcription factors involved in the regulation of genes related with cell cycle, DNA damage repair, oxidative stress resistance, energy metabolism, atrophy, autophagy and apoptosis (Ogg et al., 1997; Dijkers et al., 2000; Medema et al., 2000; Kops et al., 2002; Nemoto and Finkel, 2002; Tran, 2002; Furukawa-Hibi et al., 2002).

Among their functions it has been postulated that FoxO1 and FoxO3 are central regulators of protein breakdown since their activation regulates the expression of atrogen-1 and MuRF1, muscle-specific E3 ubiquitin ligases, whose expression leads to myofibrillar proteolysis (Kamei et al., 2004; Sandri et al., 2004; Nakashima and Yakabe, 2007). Together with ubiquitin-proteasome system, FoxO also regulates autophagy-lysosomal pathway. More precisely, FoxO3 has been linked to the regulation of several autophagy related proteins (Atgs), including LC3B, BNIP3, beclin 1, GABARAPL1, PI3KIII, Atg4B, Atg12 I and Ulk2 (Mammucari et al., 2007; Zhao et al., 2007) while FoxO1 to cathepsin L expression (Yamazaki et al., 2010).

LGMD2A patients' muscles showed increased phosphorylation of FoxO4 and to a less extent of FoxO3 (**Figures 42 and 43**). These increased phosphorylations could be due to the increased P-AKT/AKT ratio in these muscles. Conversely, the fact that an increased phosphorylation of FoxO1 was not clearly observed, suggests that this phosphorylation is not AKT dependent as previously observed in hibernating squirrels. In disuse atrophy AKT/mTOR pathway activity reduction together with FoxO1 phosphorylation increase was observed (Dang et al., 2016). On the other hand, ERK1/2 could also phosphorylate FoxO transcription factors (Yamaguchi et al., 2012; Sun et al., 2018) however, this interaction could be discarded due to the observed P-ERK1/2 reduction in LGMD2A patients.

Ubiquitin-proteasome system together with autophagy-lysosomal degradation system are the two main effectors of muscle atrophy, thus, several studies have been carried out to establish how they are regulated in LGMD2A patients. Even if some studies reported no upregulation of *MURF1* or *FBX32* gene expression (Keira et al., 2007; Sáenz et al., 2008), at protein level upregulation of MuRF1 without atrogen-1 deregulation was observed in our LGMD2A patients, also reported by Fanin and colleagues (2015).

Overall, the obtained results suggested that FoxO3 and FoxO4 transcription factors are not the responsible of MuRF1 increase in LGMD2A patients. Thus, other mechanisms would be responsible of this, for instance, MuRF1 upregulation could be mediated by IKK β /NF- κ B activation which in turn causes muscle wasting that resembles clinical cachexia (Cai et al., 2004).

In addition to the atrogenes, FoxO transcription factors also regulate other genes expression. The increased FoxO activation found in *Lmna*^{-/-} mice (laminopathies mice model) and in LLC and C26 tumour-bearing cachectic mice, allowed to identify specific FoxO target genes (Reed et al., 2012; Judge et al., 2014; Auguste et al., 2018). As in LGMD2A patients FoxOs are mainly phosphorylated, the

regulation of some of these genes in *Lmna*^{-/-} mice as well as in C26 tumour-bearing cachectic mice, showed an opposite trend to the observed deregulation in LGMD2A patients (Sáenz et al., 2008) (**Table 21**). Unlike what was observed in LGMD2A muscle genes, some genes were upregulated; *Egr1*, *Fos* and *Junb* (in both mice models), *Cited2* and *Myc* (only in *Lmna*^{-/-}) while *Col1a1*, *Col1a2* and *Itg1bp2* genes (in C26 tumor-bearing cachectic mice) and *Dok5* gene (in *Lmna*^{-/-}) were downregulated (Sáenz et al., 2008; Judge et al., 2014; Auguste et al., 2018). These findings, together with our results, confirm the implication of FoxOs in the regulation of these genes in LGMD2A (**Table 21**).

LGMD2A	<i>Lmna</i> ^{-/-}	C26 tumour-bearing cachectic mice
<i>EGR1</i>	<i>Egr1</i>	<i>Egr1</i>
<i>FOS</i>	<i>Fos</i>	<i>Fos</i>
<i>JUNB</i>	<i>Junb</i>	<i>Junb</i>
<i>CITED2</i>	<i>Cited2</i>	
<i>MYC</i>	<i>Myc</i>	
<i>DOK5</i>	<i>Dok5</i>	
<i>COL1A1</i>		<i>Col1a1</i>
<i>COL1A2</i>		<i>Col1a2</i>
<i>ITGB1BP2</i>		<i>Itgb1bp2</i>

Table 21. Gene expression representation in LGMD2A patients (increased FoxO phosphorylation) and in FoxO activated models (*Lmna*^{-/-} and C26 tumour-bearing cachectic mice) (Sáenz et al., 2008; Judge et al., 2014; Auguste et al., 2018). Downregulated genes= green and upregulated genes= red.

On the other hand, type I fibre predominance as disease progress has been reported in LGMD2A disease (Fardeau et al., 1996a; Rosales et al., 2013). Since FoxOs regulate skeletal muscle fibre type specification and fibre type shift from type I to type II fibre (Sandri et al., 2004; Keira et al., 2007; Yuan et al., 2011) the lack of FoxO activation could be suggested as responsible of the increased type I fibres that are present in more affected LGMD2A patients.

Altogether it could be concluded that although FoxO activity could be also regulated by different mechanisms (Eijkelenboom and Burgering, 2013) the increased phosphorylated AKT present in LGMD2A patients could be the responsible of the increased phosphorylation of FoxO3 and FoxO4 which lead to the lack of FoxO nuclear translocation. This lack, could lead to the increase of type I fibres observed in LGMD2A patients, as well as the deregulation of several genes in LGMD2A patients. Furthermore, it could be suggested that the increased FRZB protein expression shown in LGMD2A patients (Jaka et al., 2017) would be inhibiting Wnt signaling thus, β -catenin nuclear translocation would be avoided due to its degradation. Since β -catenin binds to FoxO transcription factors to induce the expression of FoxO target genes (Essers et al., 2005) it could be suggested that an increased blockage of FoxO transcription factors may be occurring.

The obtained results, together with previously results of our group, allowed establishing the possible scenario of the pathophysiology of the LGMD2A muscle.

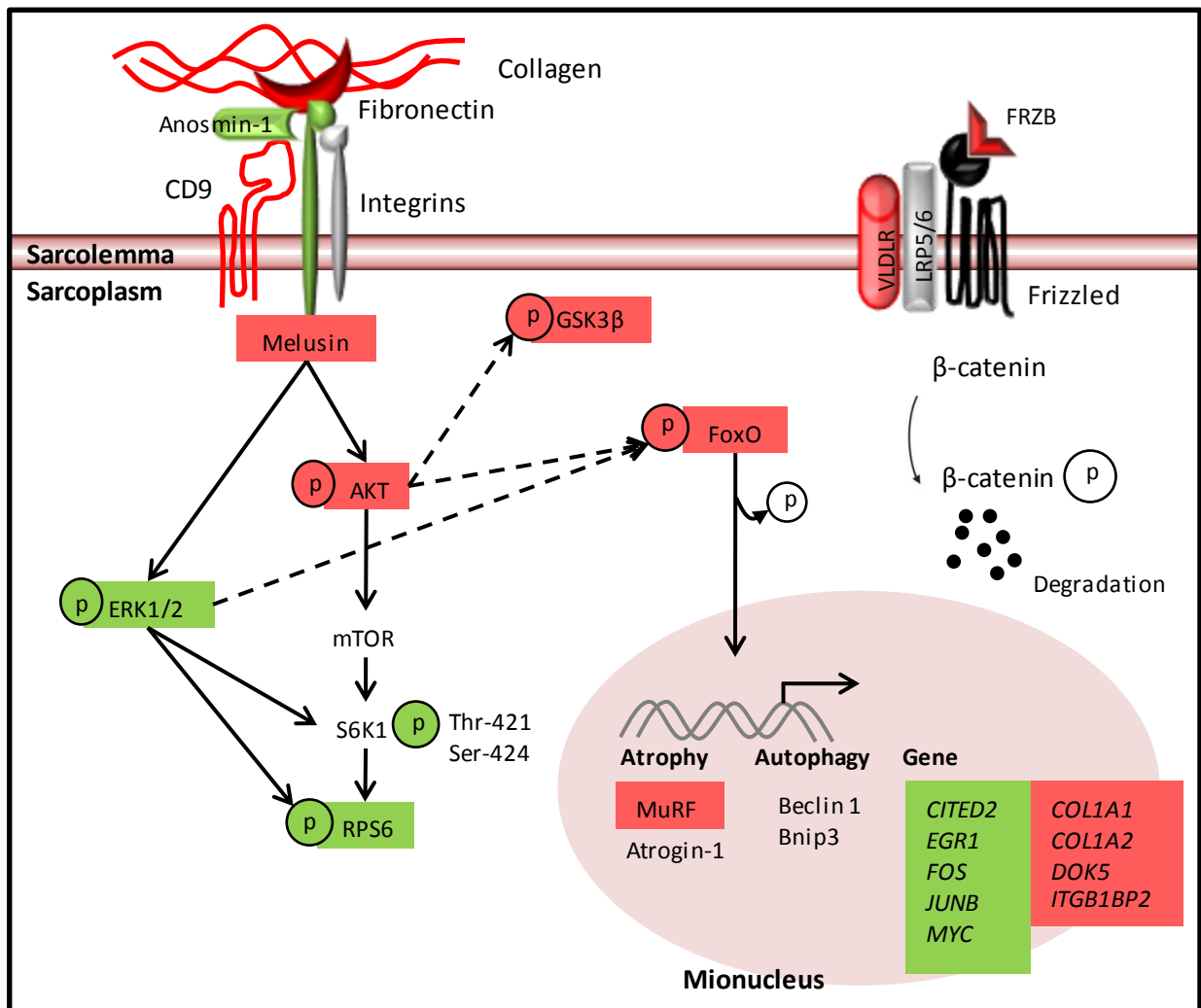


Figure 48. Schematic representation of LGMD2A patients' pathophysiological scenario in the skeletal muscle. Black arrows indicate activation signal of the protein while striped arrows indicate inhibition signal of the protein. Increased proteins and upregulated genes are shown in red and decreased proteins and downregulated genes are shown in green.

CHAPTER 2:

Study of Frzb absence effects in the muscle of a murine model (*Frzb^{-/-}*) *in vitro* and *in vivo*

CHAPTER 2: RESULTS

In this study in order to establish *Frzb* relevance in mice muscles, *Frzb*^{-/-} mice was used to characterize at different levels what happens when *Frzb* is absent.

4. MUSCLE STRENGTH ANALYSIS

Five to six week-old mice muscle strength was measured with four limb hanging test. First of all, body weigh was measured and was observed that *Frzb*^{-/-} mice were significantly smaller than WT mice (**Figure 49 a**). Great variability was observed in hanging time, and was greater in WT group. None of the *Frzb*^{-/-} mice resisted beyond 14 minutes, one mouse did not reached 1 minute and 8 mice remained hanging around 1 minute while 4 mice reached 5-13 minutes. Within WT group, 4 mice spent similar time than *Frzb*^{-/-} mice while 5 mice remained hanging more than 20 minutes (**Figure 49 b**).

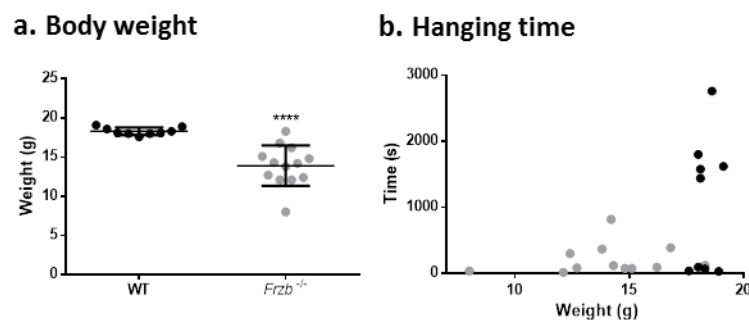


Figure 49. (a) WT and *Frzb*^{-/-} mice body weight (g) represented as mean \pm standard deviation where each dot represents one mouse. WT (N= 9; 18.36 \pm 0.1599 g), *Frzb*^{-/-} (N= 13; 13.91 \pm 0.7186 g), significance of the differences is represented as $p < 0.0001$. (b) Correlation graph of the hanging time (s) according to mice weight (g). Each dot represents a mouse. WT= black and *Frzb*^{-/-}= grey.

5. MICE GAIT ANALYSIS

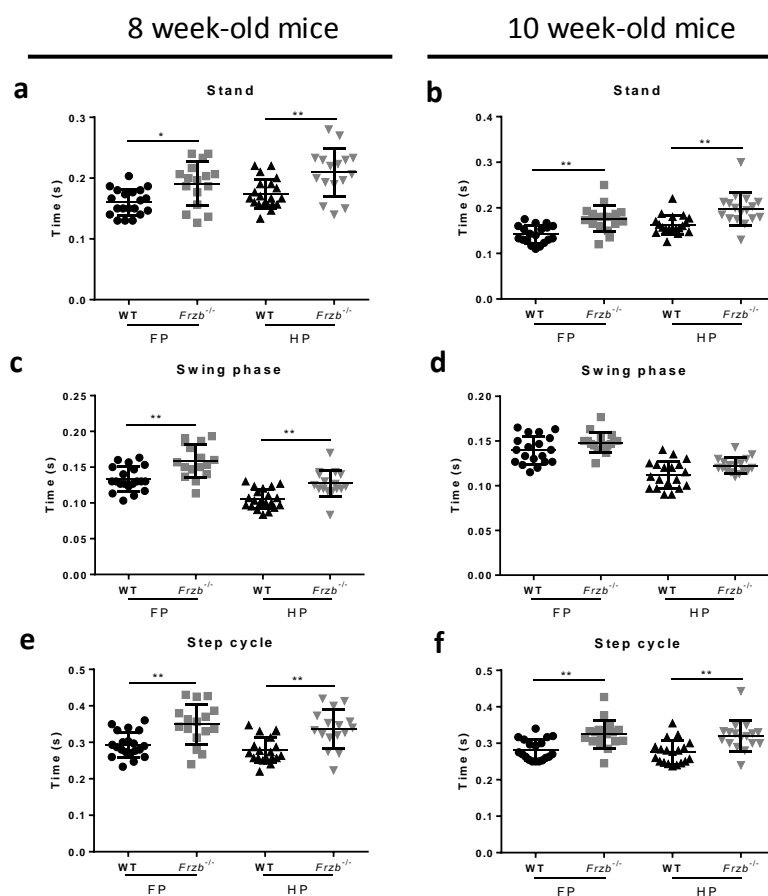
Prior to gait analysis, mice body weight was measured. Even though mice gait analysis was performed in thirty-six 8 and 10 week-old mice, not all the weights were available. The body weight of thirty-one 8 week-old and twenty-seven 10 week-old mice are shown in **Table 22**. Significant difference between WT and *Frzb*^{-/-} body weight was observed in 10 week-old mice.

	8 week-old		10 week-old	
	Weight (g)	N	Weight (g)	N
WT	20.20 ± 0.2865	20	21.91 ± 0.3834	19
<i>Frzb</i> ^{-/-}	20.27 ± 0.6618	11	19.99 ± 0.8450	8
Total		31		27

Table 22. WT and *Frzb*^{-/-} mice body weight (g) in 8 and 10 week-old mice, represented as mean ± standard deviation. Significance of the differences between WT and *Frzb*^{-/-} mice in 10 week-old is $p < 0.05$.

5.1 Paw statistics

The influence of genotype in paw statistics was studied by two-way ANOVA comparison (**Table 23**). *Frzb*^{-/-} mice paws spent significantly more time in contact with the glass plate and in the air as showed by **stand** and **swing phase**. In consequence **step cycle** was longer in *Frzb*^{-/-} mice. **Swing speed** was significantly lower in *Frzb*^{-/-}. Moreover, although *Frzb*^{-/-} mice moved more slowly (increased stand and swing phase), the distance covered by their paws, **stride length**, did not differ between WT and *Frzb*^{-/-} mice (in both study groups) (**Figure 50**).



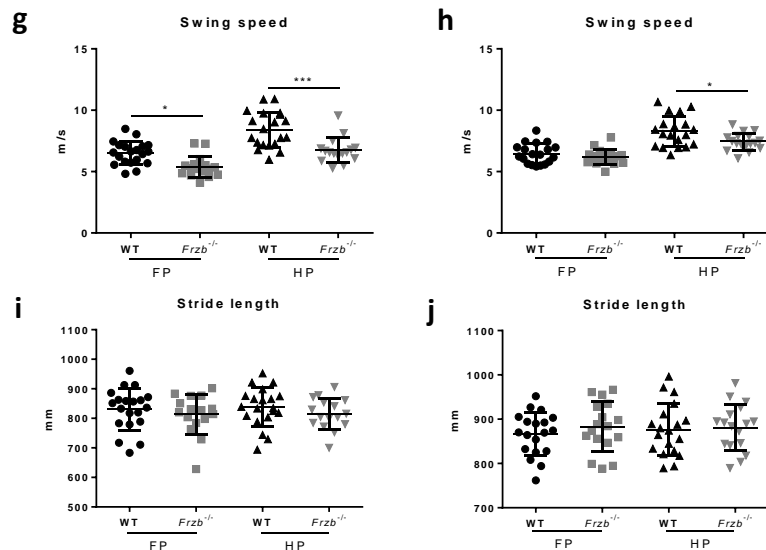


Figure 50. Paw statistics in (a, c, e, g and i) 8 week-old and (b, d, f, h and j) 10 week-old mice. (a-b) Stand, (c-d) swing time, (e-f) step cycle, (g-h) swing speed and (i-j) stride length. Each dot represents the mean of three consecutive runs of one mouse. Data are represented as mean \pm standard deviation. Significance of the differences are represented as the result of Tukey's multiple comparisons test being * = $p < 0.05$, ** = $p < 0.01$ and *** = $p < 0.001$.

	8 week-old	10 week-old
Stand	F (1, 68), $p < 0.0001$	F (1, 68), $p < 0.0001$
Swing phase	F (1, 68), $p < 0.0001$	F (1, 68), $p = 0.0031$
Step cycle	F (1, 68), $p < 0.0001$	F (1, 68), $p < 0.0001$
Swing speed	F (1, 68), $p < 0.0001$	F (1, 68), $p = 0.0130$
Stride length	F (1, 68), $p = ns$	F (1, 68), $p = ns$

Table 23. Genotype influence in stand, swing phase, step cycle, swing speed and stride length calculated by two-way ANOVA analysis. ns= not significant.

5.2 Step sequence

The **base of support** is smaller in *Frzb*^{-/-} mice F (1, 68), $p < 0.01$ in 8 and 10 week-old mice, as reported by two-way ANOVA comparison. Post hoc analyses using the Sidak's criterion for significance indicated that *Frzb*^{-/-} mice HP BOS is significantly smaller in 10 week-old mice ($p < 0.01$) (Figure 51 a and b). It was also observed that *Frzb*^{-/-} mice used significantly more **step patterns** than WT mice at 10 weeks (Figure 51 c) while at 8 weeks no differences were seen (Figure 51 f). **Step regularity index** value was similar within groups over time (Figure 51 d and g). **Step sequence** at 8 weeks was the same in both genotypes (Figure 51 h) however, older *Frzb*^{-/-} mice used less AA step sequence whereas AB step sequence was more frequently used (Figure 51 e). *Frzb*^{-/-} mice used more different step patterns over time (Figure 51j) whereas, WT mice step patterns did not change (Figure 51 i). WT mice step

sequence change over time; older mice used more AA step sequence and less AB sequence (**Figure 51 k**) while *Frzb*^{-/-} mice step sequence remains unaltered (**Figure 51 l**).

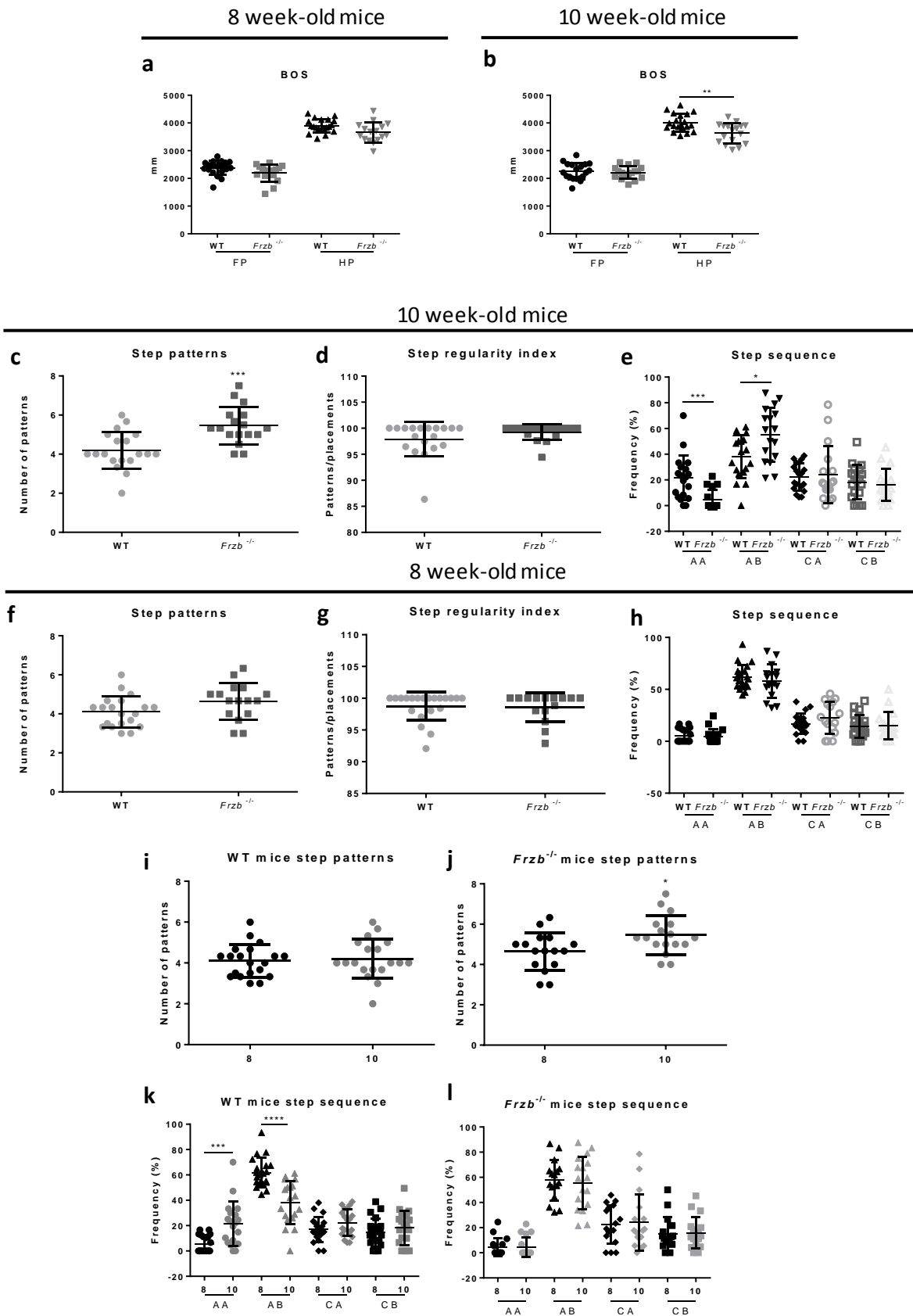


Figure 51. (a-b) Base of support in (a) 8 week-old and (b) 10 week-old mice. (c) Step pattern, (d) step regularity index and (e) step sequence in 10 week-old mice. (f) Step pattern, (g) step regularity index and (h) step sequence in 8 week-old mice. (i and j) WT and *Frzb*^{-/-} mice step patterns over time respectively. (k and l) WT and *Frzb*^{-/-} mice step sequence over time respectively. Each dot represents the mean of three consecutive runs of one mouse. Data are represented as mean ± standard deviation. FP= front paw, HP= hind paw; 8= 8 week-old mice and 10= 10 week-old mice. Significance of the differences are represented as *= p < 0.05, **= p < 0.01, ***= p < 0.001 and ****= p < 0.0001.

Related to the **paw support**, the overall preference is the two paw support, more specifically, the diagonal one, in all the genotypes, followed by three paws support in 10 week-old mice. Focusing on genotype, *Frzb*^{-/-} mice spent significantly less time on one paw and girdle support and more time in three and four paw support (Figure 52 a and b). WT mice paw support was shifted over time, they decreased the use of three paw support and they increased the use of two paw support. However *Frzb*^{-/-} genotype mice paw support remains unaltered (data not shown) (Figure 52 c and d).

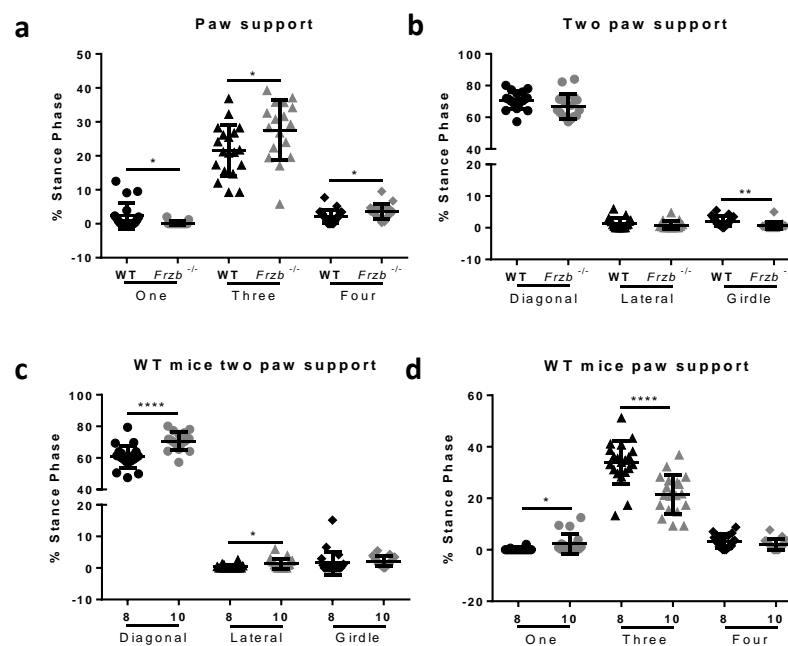


Figure 52. (a) Different paw support and (b) two paw support in 10 week-old mice. (c) Different paw supports and (d) two paw support in 8 and 10 week-old WT mice. Each dot represents the mean of three consecutive runs of one mouse. Data are represented as mean ± standard deviation. 8= 8 week-old mice and 10= 10 week-old mice. Significance of the differences are represented as *= p < 0.05 and ***= p < 0.001.

6. SKELETAL MUSCLE ANALYSIS

A two-way analysis of variance of muscles weight yielded a significant effect for the genotype in muscle weight, $F(1, 108)$, $p < 0.0001$, being *Frzb*^{-/-} muscles significantly smaller. The difference of muscle type was significant $F(3, 108)$, $p < 0.0001$. The interaction effect also was significant $F(3, 108)$, $p < 0.05$, indicating that the genotype effect was different in all analysed muscles.

Post hoc analyses using the Sidak's criterion for significance indicated that *Gastrocnemius* and *Quadriceps* weights were significantly smaller in *Frzb*^{-/-} mice, $p < 0.0001$ (**Figure 53**).

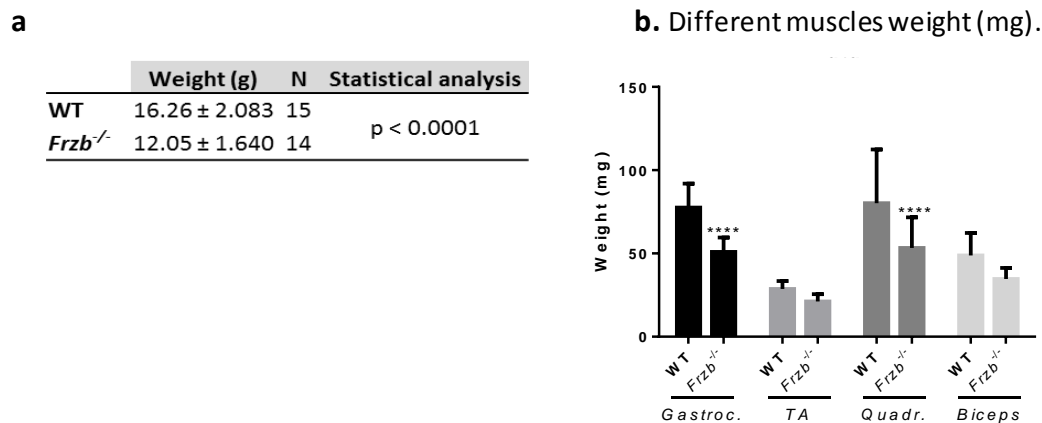


Figure 53. (a) 4 week-old WT (N= 15) and *Frzb*^{-/-} (N= 14) mice body weight (g). (b) WT and *Frzb*^{-/-} mice muscles weight (mg). Data are represented as mean ± standard deviation. *Gastroc.*= *Gastrocnemius*, *TA*= *Tibialis anterior* and *Quadr.*= *Quadriceps*. Significance of the differences are represented as ****= $p < 0.0001$.

6.1 Muscle cross-sectional area and fibre composition analyses

Ten and 14 week-old mice *Soleus* fibre CSA was measured in WT and *Frzb*^{-/-} mice. *Frzb*^{-/-} mice were smaller at both ages but this difference was not statistically significant.

Ten week-old and 14 week-old mice *Soleus* fibre CSA was measured and compared by two-way ANOVA. It was found that genotype was significantly influencing fibres CSA, $F(1, 10)$, $p < 0.0054$. It was shown that *Frzb*^{-/-} muscles fibres were smaller. However, no influence of mice age or of the interaction between both factors was observed. A posterior Sidak's multiple comparison analysis showed that only CSA in 10 week-old mice was significantly smaller in *Frzb*^{-/-} mice, $p < 0.05$ (**Figure 54**).

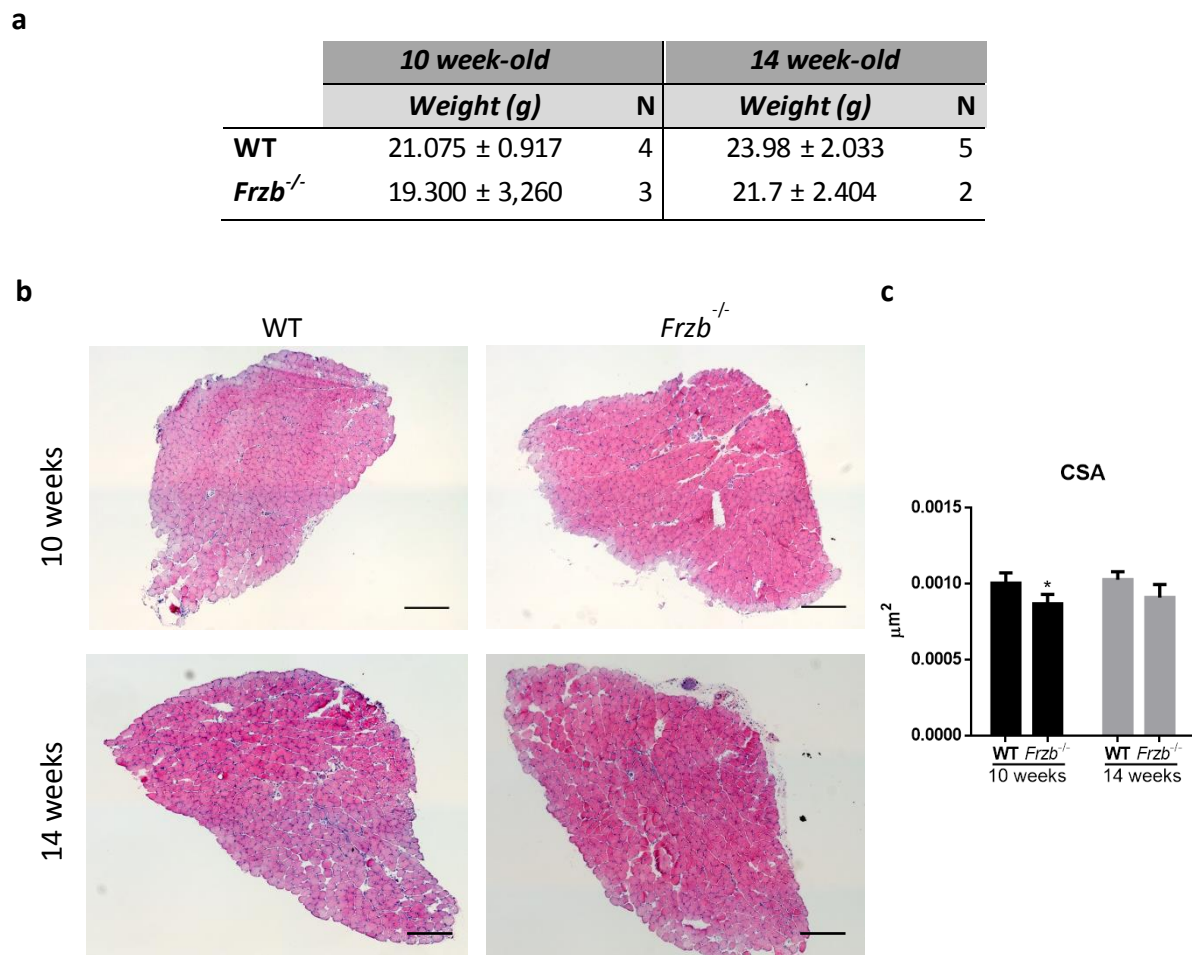


Figure 54. (a) WT and *Frzb*^{-/-} mice body weight (g). (b) Hematoxylin and eosin stained *Soleus* in 10 and 14 week-old WT and *Frzb*^{-/-} mice. Scale bar 250 μm. (c) Ten and 14 week-old mice *Soleus* fibre cross-sectional area in μm². Data are represented as mean ± standard deviation. Ten week-old mice; WT N= 4 and *Frzb*^{-/-} N= 3, and 14 week-old mice; WT N= 5 and *Frzb*^{-/-} N= 2. Significance of the differences is represented as *= p < 0.05.

Fibre composition is based on different myosin heavy chain isoforms (*Myh1*, *Myh2* and *Myh4*), their expression were analysed in 10 week-old mice. *Tibialis anterior* expressed predominantly *Myh4* (myosin present in 2B fibre type) followed by *Myh1* (myosin present in 2X fibre type) while *Myh2* showed a minimum expression (myosin present in 2A fibre type). *Soleus* showed similar expression of *Myh1* and *Myh2* while *Myh4* was minimally expressed. Different genotypes did not show significant differences in myosin's expression although myosin composition in *Soleus* is more variable (Figure 55).

Myosin heavy chain isoforms expression

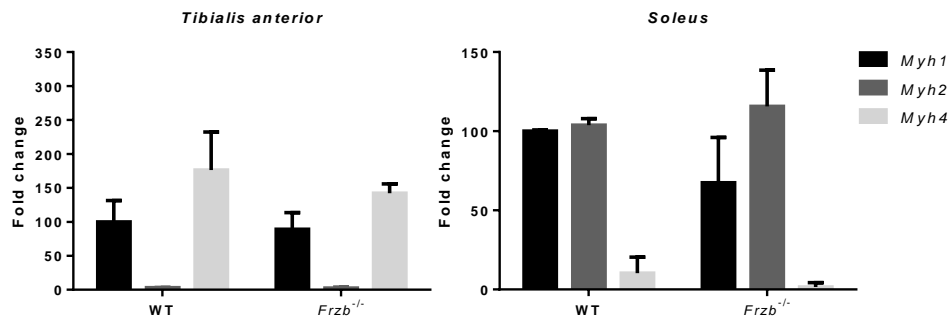
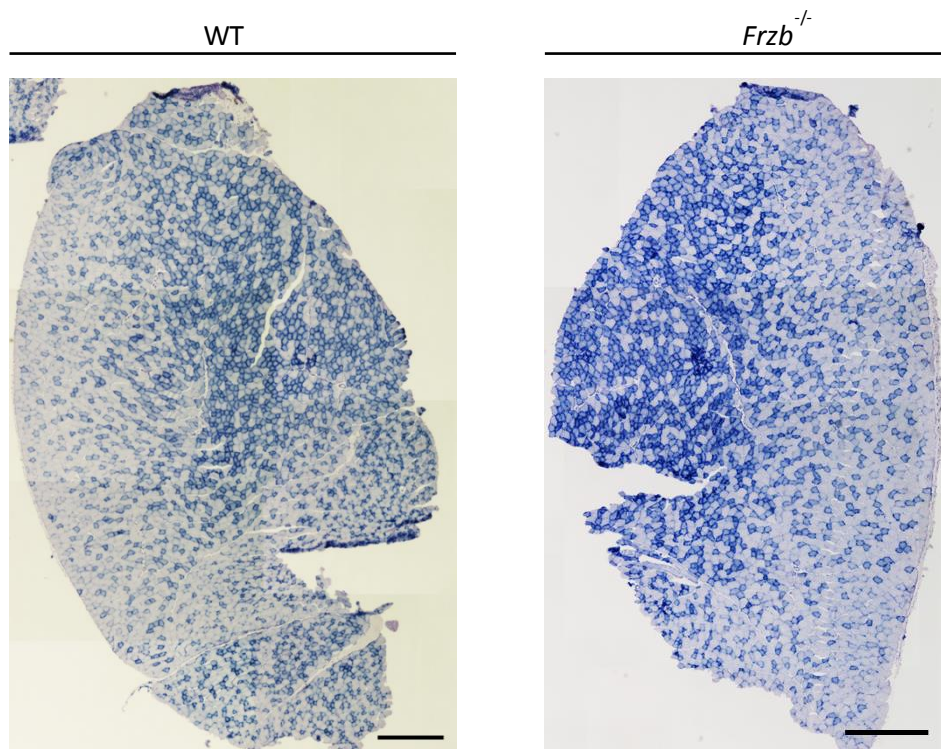


Figure 55. Myosin heavy chains isoforms (*Myh1*, *Myh2* and *Myh4*) gene expression in *Tibialis anterior* (3 WT and 3 *Frzb*^{-/-}) and *Soleus* (2 WT and 5 *Frzb*^{-/-}). *GAPDH* was used as endogenous control. Data are represented as mean fold-change \pm standard deviation.

NADH transferase staining was used to visualize different fibre types in 11 week-old *Soleus* of WT and *Frzb*^{-/-} mice. No differences were observed in any of the fibre types. The most abundant were barely stained fibres, around 41%, followed by strongly stained fibres, around 22%. Fibres stained in-between colour were around 36%, more precisely, medium-strong fibres were a bit more abundant than medium-weak fibres in WT and in *Frzb*^{-/-} muscles (**Figure 56**).

a. NADH-t staining of *Tibialis anterior*



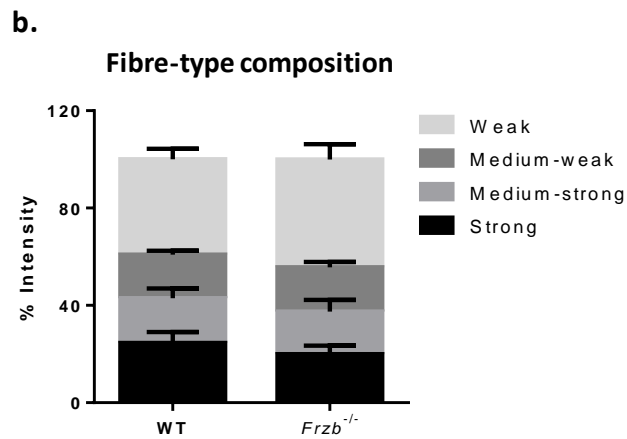


Figure 56. (a) NADH transferase staining of transverse sections of WT (N= 3) and *Frzb*^{-/-} (N= 3) *Tibialis anterior*. Scale bar 500 μ m. (b) NADH transferase staining based fibre-type composition of *Tibialis anterior* (3 WT and 3 *Frzb*^{-/-} mice) where fibre-type intensity was measured. Data are represented as mean \pm standard deviation. Colour intensity was divided as weak (39.11 \pm 4.3 % in WT and 44.38 \pm 6.22 % in *Frzb*^{-/-} mice), medium-weak (17.99 \pm 1.57 in WT and 18.12 \pm 2.27 in *Frzb*^{-/-} mice), medium-strong (18.39 \pm 4.05 in WT and 17.55 \pm 4.79 in *Frzb*^{-/-} mice) and strong (24.51 \pm 4.55 % in WT and 19.94 \pm 3.52 % in *Frzb*^{-/-} mice) .

7. CHRONIC EXERCISE INDUCED MUSCLE ALTERATIONS

To analyse the effect of the chronic exercise the treadmill was used. All the trained animals were able to perform selected chronic exercise protocol. No abnormal behaviour or signs of exhaustion were observed.

First, mice body weights were measured and no differences between trained and not-trained groups were seen. The differences between WT and *Frzb*^{-/-} mice body weight were gradually diminishing over the weeks (**Figure 57**).

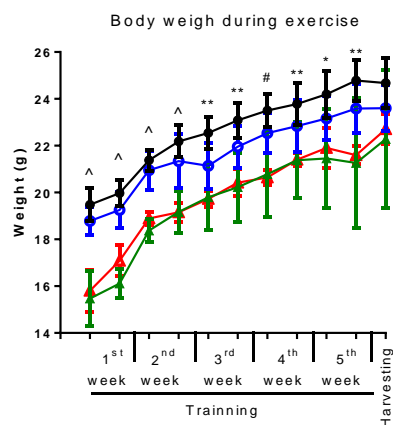


Figure 57. WT and *Frzb*^{-/-} mice body weight (g) while training period. Data are represented as mean \pm standard deviation where each dot represents the mean weight of each group. Black; not-trained WT group (N= 4). Blue; trained WT group (N= 5). Red; not-trained *Frzb*^{-/-} group (N= 2). Green; trained *Frzb*^{-/-} group (N= 4). Significance of the differences are represented as \wedge = p < 0.0001, #= p < 0.001, **= p < 0.01 and *= p < 0.005.

Later, muscle weights were studied and no effect of exercise was found after two-way ANOVA analysis. However genotype effect in *Tibialis anterior* was observed, being *Frzb*^{-/-} muscles smaller, $F(1, 11)$, $p < 0.0023$. Post hoc analysis using the Sidak's criterion for significance indicated that trained *Frzb*^{-/-} mice *Tibialis anterior* were significantly smaller than trained WT mice *Tibialis anterior* (**Figure 58**).

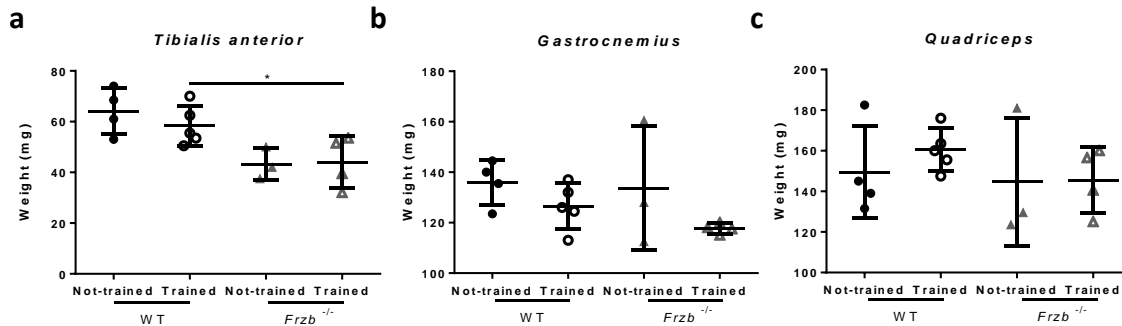


Figure 58. (a) *Tibialis anterior*, (b) *Gastrocnemius* and (c) *Quadriceps* weight (mg). Data are represented as mean \pm standard deviation where each dot represents the mean weight of left and right muscles of one mouse. Significance of the differences is represented as $p < 0.05$ for not-trained WT (N= 4) versus *Frzb*^{-/-} (N= 3) and trained WT (N= 5) versus *Frzb*^{-/-} (N= 4).

Fibre CSA area of *Soleus* was measured and a two-way ANOVA analysis of variance showed no influence of exercise. However *Frzb*^{-/-} muscle fibres were smaller, as was reported by the influence of genotype in CSA $F(1, 11)$, $p < 0.0066$. Further Sidak's multiple comparisons test showed that the difference between WT and *Frzb*^{-/-} fibres CSA in not-trained mice was statistically significant, $p < 0.05$ (**Figure 59**). No exercise induced damage was observed in any of transverse sections of *Soleus* or *Tibialis anterior*.

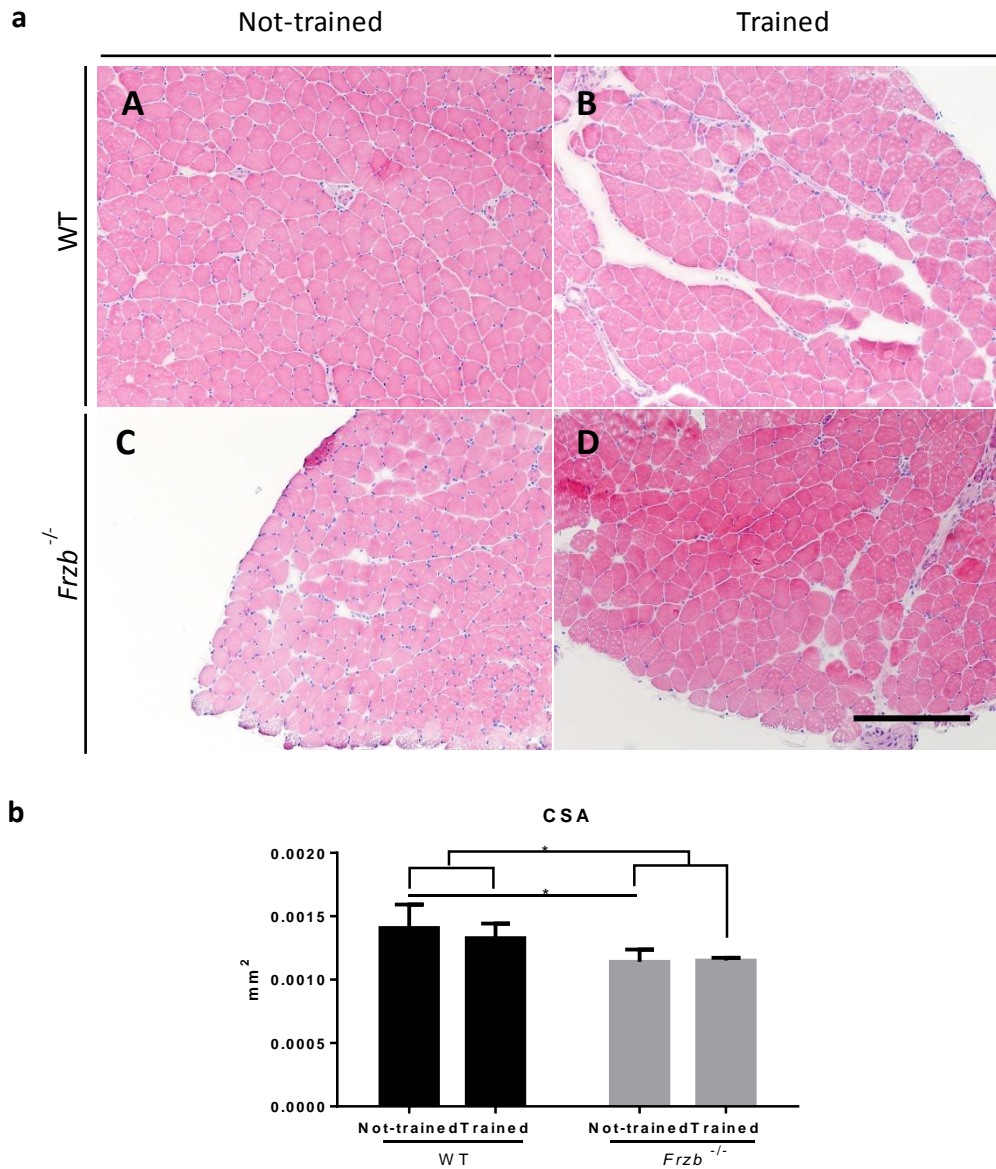
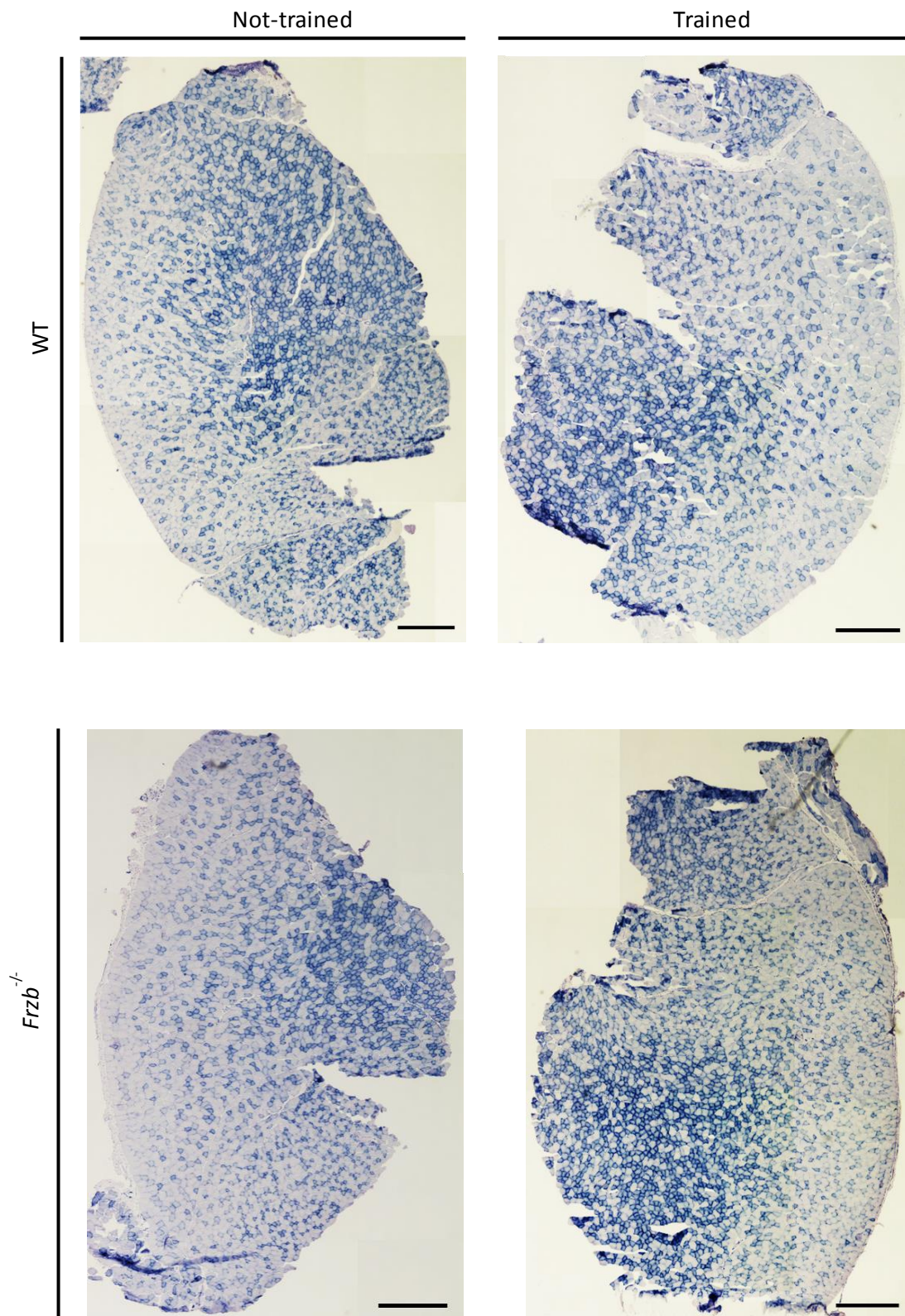


Figure 59. (a) Hematoxylin and eosin stained *Soleus* from (A and B) WT and (C and D) *Frzb*^{-/-} mice. Left images correspond to not-trained samples while right images correspond to trained samples. Scale bar 250 μ m. (b) *Soleus* fibres cross-sectional area (mm²) represented as mean \pm standard deviation. Not-trained WT group N= 4, trained WT group N= 5, not-trained *Frzb*^{-/-} group N= 3 and trained *Frzb*^{-/-} group N= 3. Significance of the difference is represented as $p > 0.05$.

Muscle fibre type composition was analysed in both study groups in *Tibialis anterior* (Figure 60).

a. NADH-t satining of *Tibialis anterior*.



b

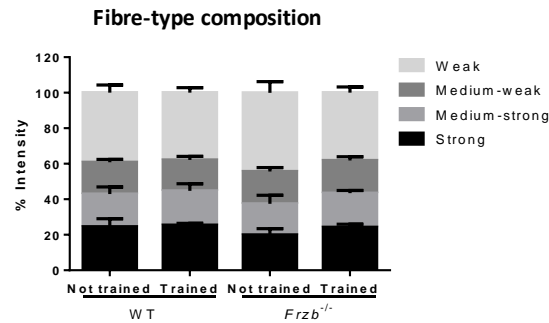


Figure 60. (a) NADH transferase staining distribution of transverse sections of WT and *Frzb*^{-/-} *Soleus* of not-trained and trained mice. Scale bar 500 μ m. (b) NADH transferase staining based fibre-type composition of *Soleus* (3 WT and 3 *Frzb*^{-/-} mice for not-trained and trained groups) where fibre-type intensity was measured. Data are represented as mean \pm standard deviation. Colour intensity was assigned as weak, medium-weak, medium-strong and strong.

In order to analyse the effect of exercise in gene and protein expression, myogenic genes as well as genes implicated in atrophy were studied. In myogenic genes (*Pax7*, *Myod*, *Myog* and *Myh3*) no differences were observed after exercise as reported by two-way ANOVA analysis (Figure 61). However, genotype influence was observed in *Myod* gene expression. *Frzb*^{-/-} mice have upregulated *Myod* gene expression F (1, 8), $p < 0.0144$. Further post hoc analysis did not report any specific means differences (Figure 61 b).

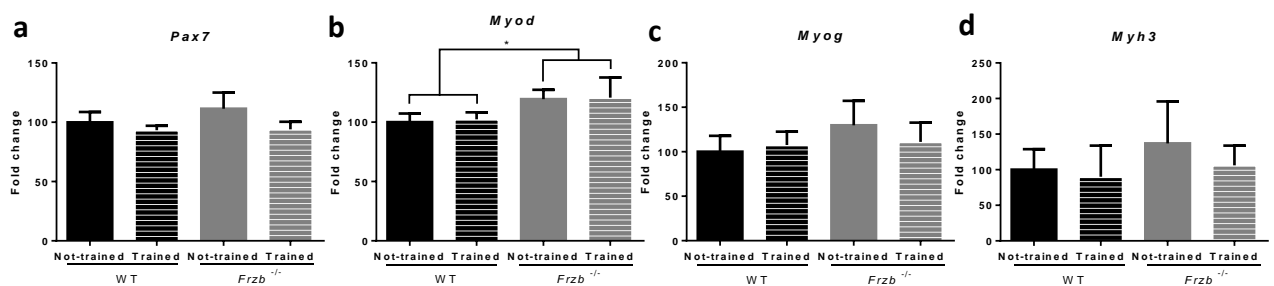
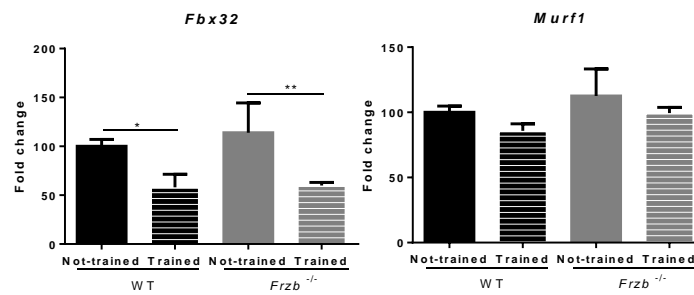


Figure 61. (a) *Pax7*, (b) *Myod*, (c) *Myog* and (d) *Myh3* gene expression in *Gastrocnemius* in trained and not-trained WT and *Frzb*^{-/-} mice. *GAPDH* was used as endogenous control. Data are represented as mean fold-change \pm standard deviation. Significance of the differences is represented as * = $p < 0.05$.

Atrophy related *Fbx32* and *Murf1* genes expression were analysed by two-way ANOVA. *Fbx32* gene expression showed exercise influence F (1, 8), $p < 0.0013$ being its expression lower in trained mice. Further Sidak's multiple comparisons test showed that the trained muscles expression was significantly lower, $p < 0.05$ and $p < 0.01$ for WT and for *Frzb*^{-/-} mice respectively. However, although a trend to downregulation of *Murf1* gene expression was observed in trained mice, no differences were observed after two-way ANOVA analysis (Figure 62 a). The proteins coded by these genes also were analysed. Neither of them showed any exercise or genotype induced alterations (Figure 62 b).

a. Atrogenes gene expression.



b. Atrogenes protein expression.

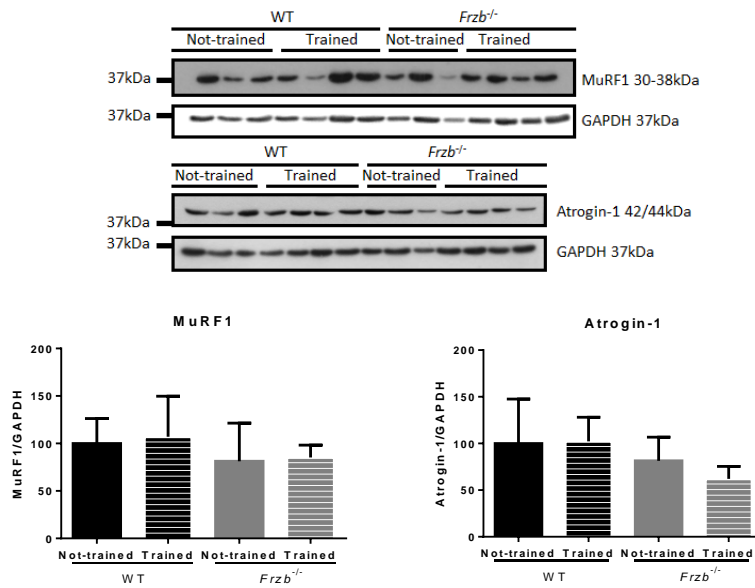


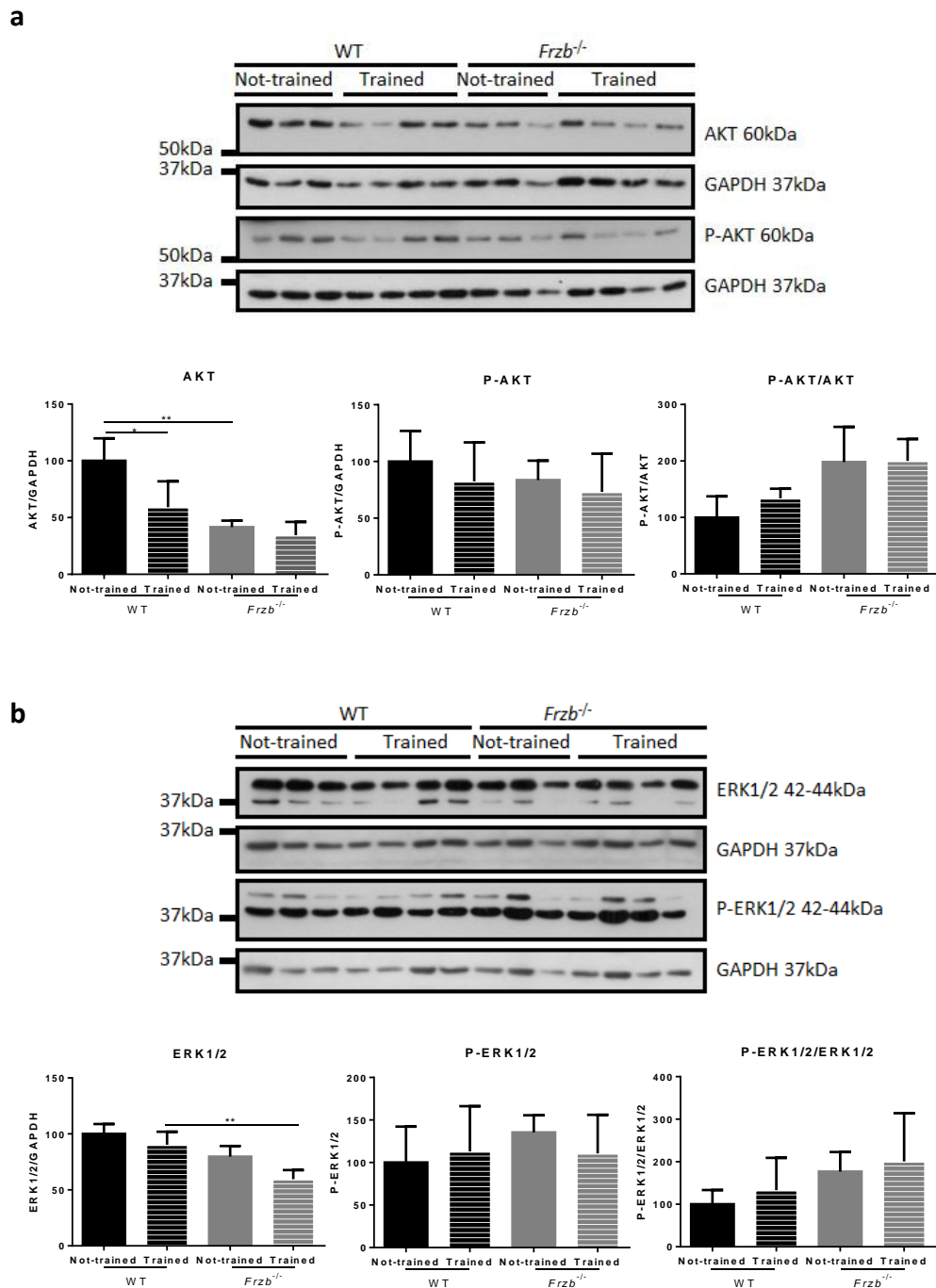
Figure 62. (a) Gene expression analysis of *Fbx32* and *Murf1* in *Gastrocnemius*. *GAPDH* was used as endogenous control. Data are represented as mean fold-change \pm standard deviation. $N=3$ in all groups (b) Western blot and densitometry analyses of MuRF1 and Atrogin-1 in *Gastrocnemius*. Data are represented as mean band density normalized relative to GAPDH \pm standard deviation. Not-trained; $N=3$ and trained; $N=4$. Significance of the differences are represented as * = $p < 0.05$ and ** = $p < 0.01$.

As activation of different signaling pathways after exercise have been described, PI3K/AKT/mTOR, MAPK/ERK signaling pathway and GSK3 β kinase activity were analysed. First of all, the effect of genotype was analysed. Two-way ANOVA study showed statistically significant reduced expression in total AKT, ERK1/2 and GSK3 β F (1, 10), $p=0.001$, $p=0.0007$ and $p=0.002$ respectively in *Frzb*^{-/-} mice. Further, Tukey's multiple comparisons test showed that AKT was significantly reduced in not-trained *Frzb*^{-/-} mice in comparison with not-trained WT mice ($p < 0.001$) and trained *Frzb*^{-/-} mice have less ERK1/2 than trained WT mice ($p < 0.001$). Moreover Sidak's multiple comparisons test showed reduced GSK3 β in not-trained *Frzb*^{-/-} mice in comparison with not-trained WT mice.

On the other hand, phosphorylation was only shown influenced by genotype in GSK3 β protein F (1, 10), $p=0.0109$, *Frzb*^{-/-} mice had higher phosphophorylation ratios.

After that, exercise influence was studied. It was found a negative effect of exercise in AKT and ERK1/2 total proteins. Exercise induced a decrease of these proteins F (1, 10), $p=0.0245$ and $p=0.0177$ respectively. Next, Tukey's multiple comparisons test showed significant lower levels of total AKT after training in WT mice ($p<0.05$).

Finally, only genotype influence was found between phosphorylated and non-phosphorylated AKT and GSK3 β proteins. *Frzb*^{-/-} mice had higher phosphorylated proteins ratio of AKT and GSK3 β F (1, 10), $p=0.0034$ and $p=0.0063$ respectively (**Figure 63**).



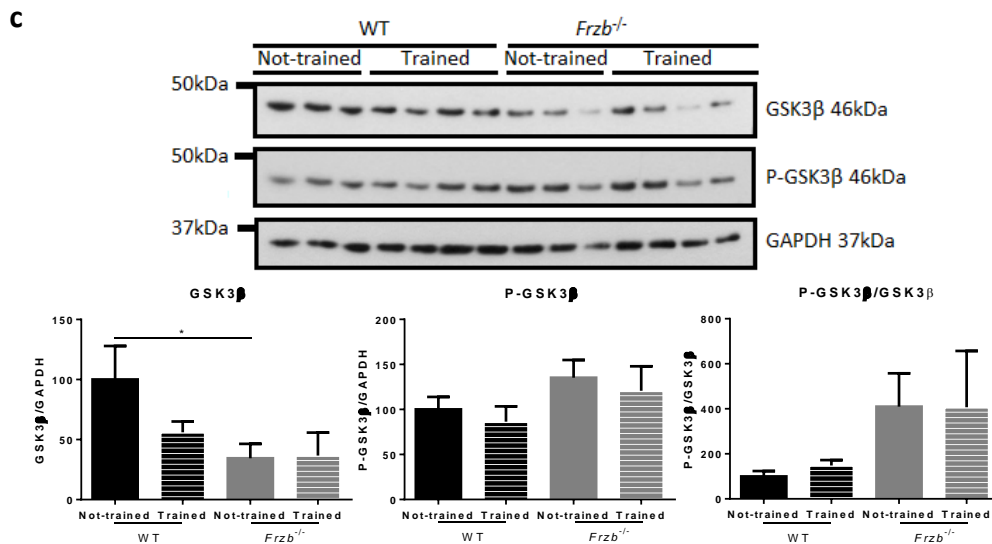


Figure 63. Western blot and densitometry analyses of (a) AKT and P-AKT (Ser473), (b) ERK1/2 and P-ERK1/2 (Thr202/Tyr204) and (c) GSK3 β and P-GSK3 β (Ser9). Data are represented as mean band density normalized relative to GAPDH \pm standard deviation. Not-trained; N= 3 and trained; N= 4. Significance of the differences are represented as * = $p < 0.5$, ** = $p < 0.01$.

8. MUSCLE REGENERATION CAPACITY AFTER INTRAMUSCULAR CARDIOTOXIN-INDUCED MUSCLE INJURY

Induction of acute skeletal muscle regeneration by Cardiotoxin Injection in WT and *Frzb*^{-/-} *Soleus* and *Tibialis anterior* was analysed in hematoxylin and eosin stained muscles sections.

Non-injured skeletal muscle showed polygonal myofibres with peripheral nuclei (**Figure 64 a-d** and **Figure 65 a-b**). At day 3 post injection, muscles showed degenerative myofibres and inflammatory cellular infiltration. In the *Soleus*, most of the fibres were damaged, while in the case of *Tibialis anterior*, just the area where the cardiotoxin had been injected appeared affected (**Figure 64 e-h** and **Figure 65 c-d**). One week after injury, small regenerating myotubes with centrally located nuclei were observed (**Figure 64 i-l** and **Figure 65 e-f**). Some inflammatory cellular infiltrations were still present (more evident in *Soleus*). Regenerating fibress with centrally located nuclei increased their diameter by two weeks (**Figure 64 m-n** and **Figure 65 g-h**). At 4 weeks, centrally located nuclei were still present but fibre diameters were more homogeneous. In the *Soleus* (**Figure 65 i-j**), newly formed fibre size were more variable than in the *Tibialis anterior* fibres (**Figure 64 o-p**). Neither adipocytes nor collagen infiltrations in WT or *Frzb*^{-/-} muscles were observed.

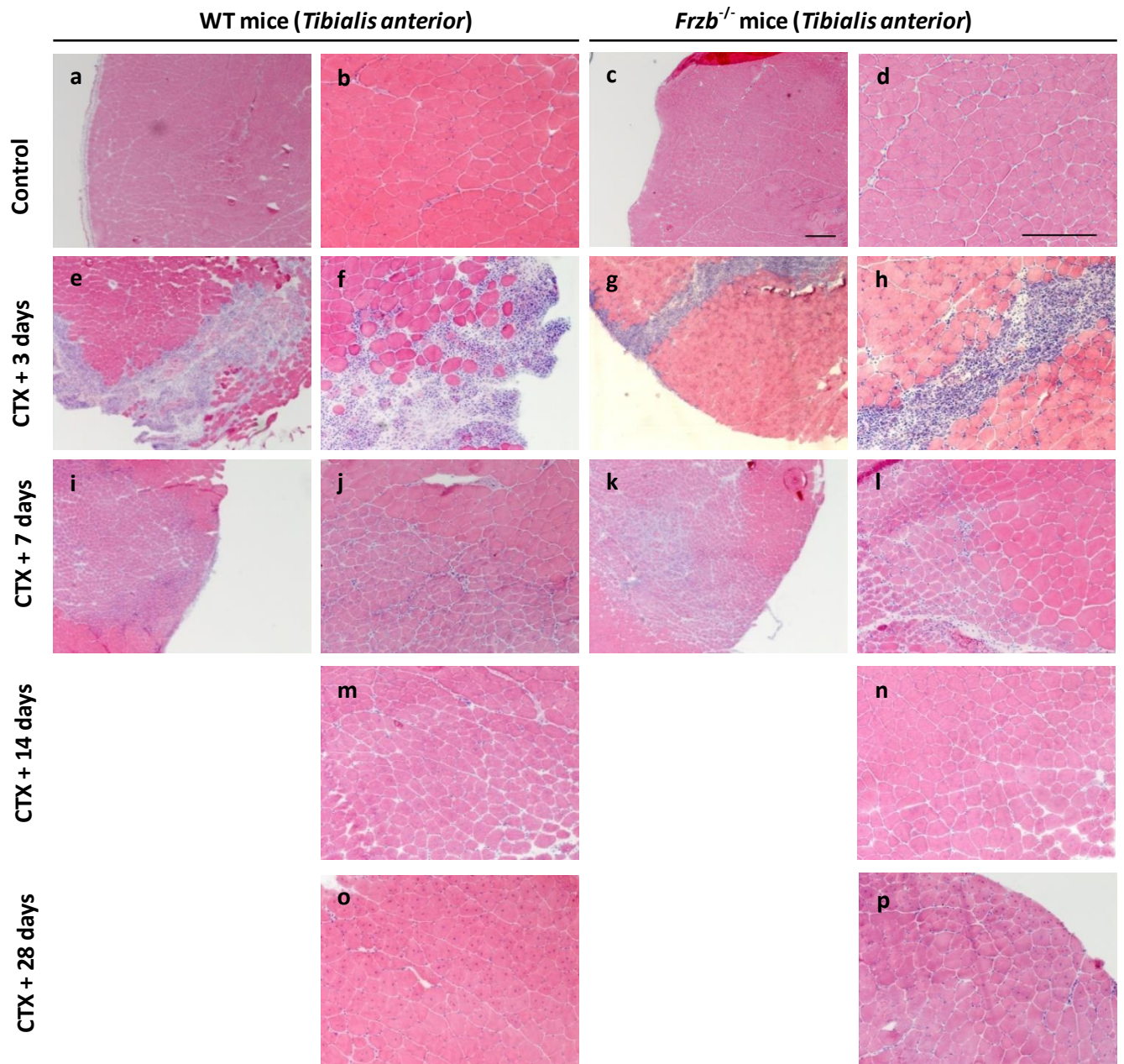


Figure 64. Hematoxylin and eosin stained *Tibialis anterior* sections of (a, b, e, f, i, j, m and o) WT and (c, d, g, h, k, l, n and p) *Frzb*^{-/-} mice. (a-d) Control, not-damaged muscles, (e-h) 3 days after CTX injection, (i-l) 7 days after CTX injection, (m and n) 14 days after CTX injection and (o and p) 28 days after CTX injection. Scale bar 250 μ m.

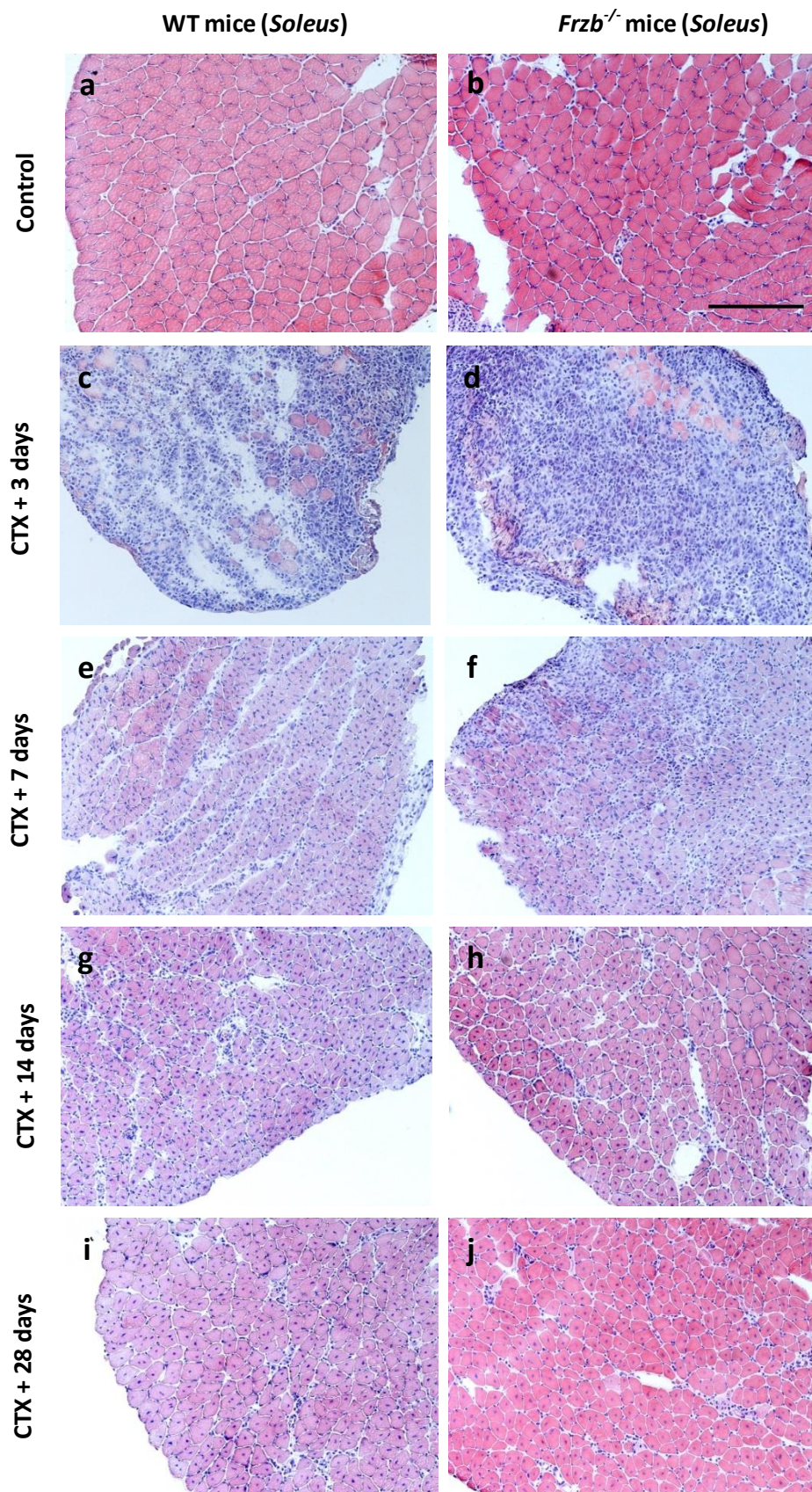


Figure 65. Hematoxylin and eosin stained *Soleus* sections of (a, c, e, g and i) WT and (b, d, f, h and j) *Frzb*^{-/-} mice. (a and b) Control not-damaged muscles, (c and d) 3 days after CTX injection, (e and f) 7 days after CTX injection, (g and h) 14 days after CTX injection and (i and j) 28 days after CTX injection. Scale bar 50 μ m.

9. MICE CELL MODEL

9.1 Satellite cells

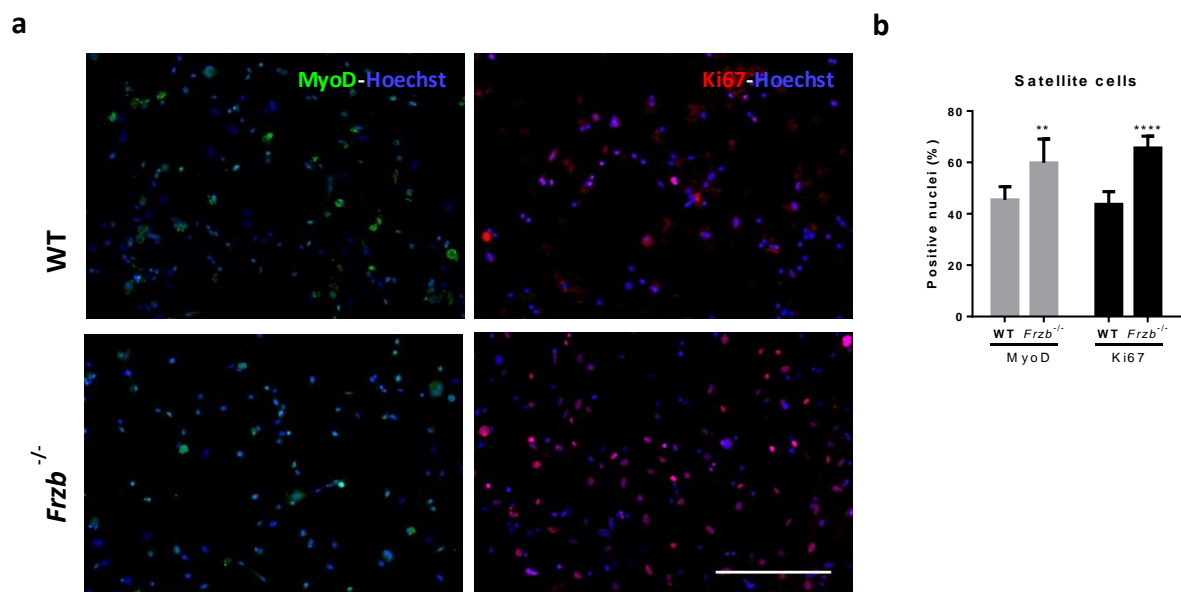
Satellite cells were extracted from 4 week-old WT and *Frzb*^{-/-} mice *Biceps*, *Gastrocnemius*, *Tibialis anterior* and *Quadriceps*.

As previously mentioned *Frzb*^{-/-} mice were significantly smaller and had less total muscles mass, nevertheless the obtained cell amount after enzymatic muscle disruption did not show differences (**Table 24**).

	N	Body weight (g)	Statistic value	Total muscle weight (mg)	Statistic value	Cell amount	Statistic value
WT	7	14.71 ± 0.570	p < 0.01	441.28 ± 48.517	p < 0.01	209264.286 ± 80206.913	p = 0,632
<i>Frzb</i> ^{-/-}	6	11.48 ± 0.502		332.73 ± 45.423		189500.000 ± 61173.426	

Table 24. WT and *Frzb*^{-/-} mice body weight (g), total muscle weight (mg) and obtained cell amount after muscle digestion, data are represented as mean ± standard deviation. Statistic value column represents pairwise comparison (t test) between different genotypes. Not sig.= not significant.

The immunofluorescence analysis showed first more MyoD positive cells in *Frzb*^{-/-} mice muscles after enzymatic digestion and second, more abundant proliferation marker protein; Ki67 (**Figure 66 a and b**). At myotube stage comparable fusion index with similar myogenin and MyoD positive nuclei were observed (**Figure 65 c-e**).



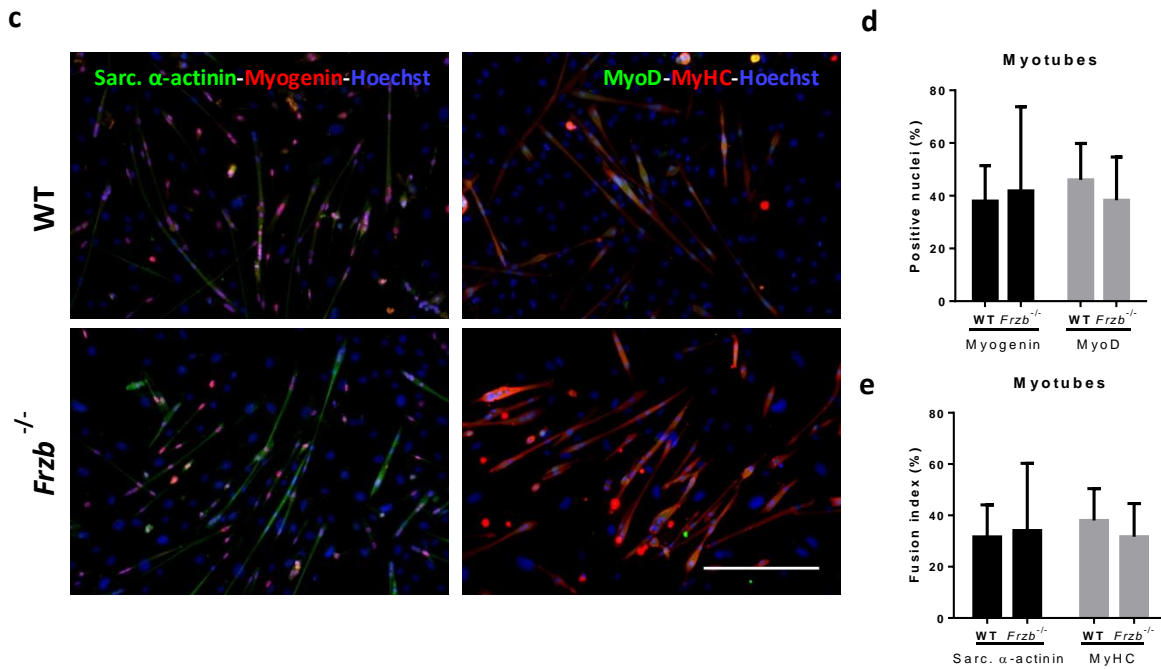


Figure 66. (a) Immunofluorescence analysis of WT and *Frzb*^{-/-} satellite cells. Left were stained for MyoD (green) and right images for Ki67 (red). (b) Percentage of Ki67 and MyoD positive nuclei are represented as mean \pm standard deviation. (c) Immunofluorescence analysis of WT and *Frzb*^{-/-} myotubes at day 3 of differentiation. Left showed nuclear staining for myogenin (red) and cytoplasmic staining for sarcomeric α -actinin (green). Right showed nuclear staining for MyoD (green) and cytoplasmic MyHC staining (red). In all cases nuclei were visualized with Hoechst (blue). (d) Percentage of MyoD and myogenin positive nuclei are represented as mean \pm standard deviation. (e) Myotubes fusion index, calculated as the percentage of nuclei inside myotubes represented as mean \pm standard deviation. Scale bar 250 μ m. For each mouse 5-6 fields were counted. WT N= 7 and *Frzb*^{-/-} N= 6. Significance of the differences are represented as **= $p < 0.01$ and ****= $p < 0.0001$.

9.2 Mesoangioblasts

Five week-old *Biceps*, *Gastrocnemius*, *Tibialis anterior* and *Quadriceps* from WT and *Frzb*^{-/-} mice were used for mesoangioblasts collection. Cells were sorted for alkaline phosphatase cell surface marker.

The obtained ALP+ cell distribution was different in WT and *Frzb*^{-/-} mice since significant effect of genotype as well as ALP cell surface marker was observed in the amount of obtained cells after sorting as reported by two-way ANOVA analysis, F (1, 22), $p = 0.004$ and F (1, 22), $p = 0.005$ respectively. The interaction effect also was significant F (1, 22), $p < 0.0001$, indicating that the ALP cell surface marker presence is influenced by genotype. Further, Tukey's multiple comparisons test showed that ALP+ cells amount was higher in *Frzb*^{-/-} mice than in WT mice and *Frzb*^{-/-} mice have significantly higher amount of positive cells than negative (**Figure 67**).

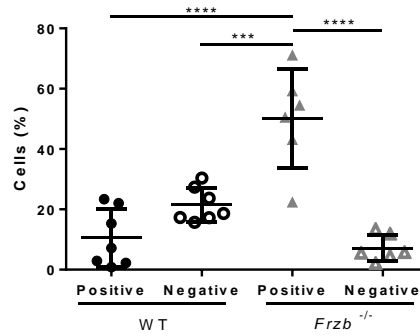


Figure 67. Percentage of alkaline phosphatase positive and negative cells in WT (N= 7) and *Frzb*^{-/-} (N= 6) mice. In WT mice ALP+ cells were $10.54 \pm 3.63\%$ and negative were $21.47 \pm 2.166\%$. In *Frzb*^{-/-} mice ALP+ cells were $50.13 \pm 6.732\%$ and negative were $7.183 \pm 1.803\%$. Data are represented as mean \pm standard deviation where each dot represents one mouse. Significance of the differences are represented as ***= $p < 0.001$ and ****= $p < 0.0001$.

ALP+ cells were negative for endothelial cell marker CD31 and hematopoietic cell marker CD45. Nevertheless, while WT ALP+ cells were around 81% positive for platelet derived growth factor receptor alpha (CD140A or PDGFR α), *Frzb*^{-/-} ALP+ cells were only around 43% positive for this marker (Figure 68).

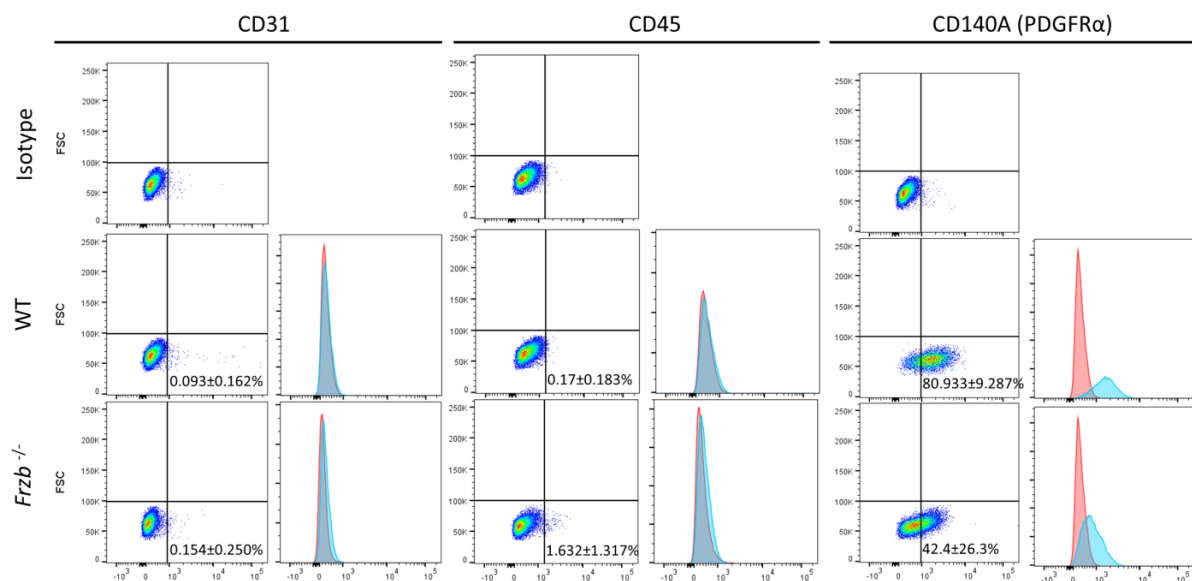


Figure 68. FACS data showing CD31, CD45 and CD140A expression in WT N= 3 and *Frzb*^{-/-} N= 7 samples. Mean \pm standard deviation of each protein value is also present.

In order to establish whether PDGFR α levels were also differentially expressed in skeletal muscles, *Cd140a (Pdgfra)* and *Cd140b (Pdgfrb)* genes expression were measured. No differences in gene expression were observed in *Tibialis anterior* or in *Soleus* regarding mice genotype, as reported by two-way ANOVA study. While it is true that significant lower *Pdgfra* gene expression was observed in *Soleus* than in *Tibialis anterior*, $F(1, 14)$, $p=0.0149$ (**Figure 69**).

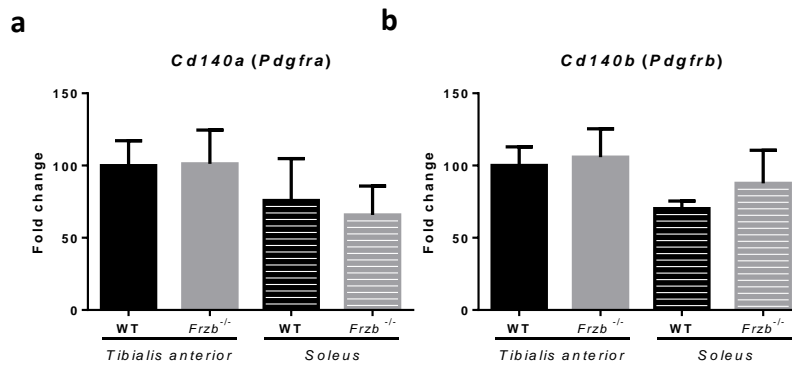
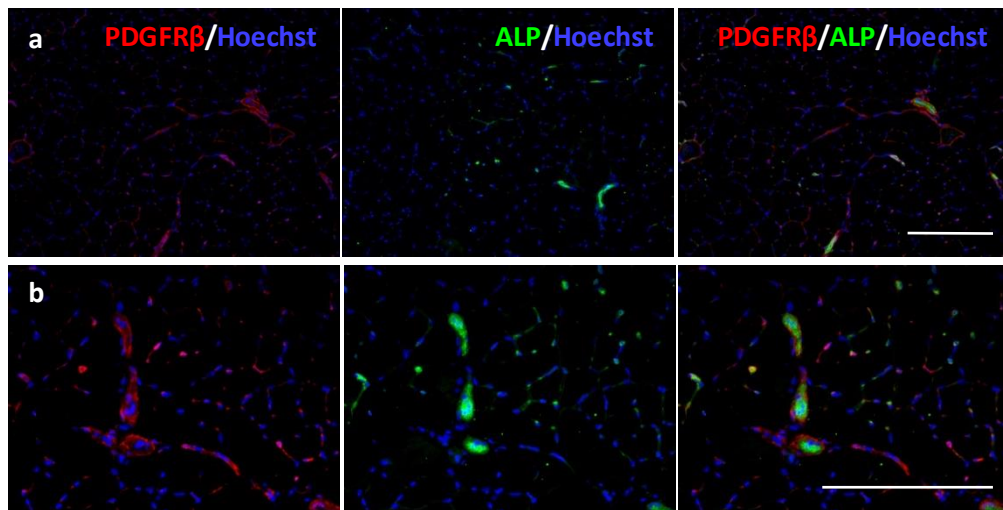
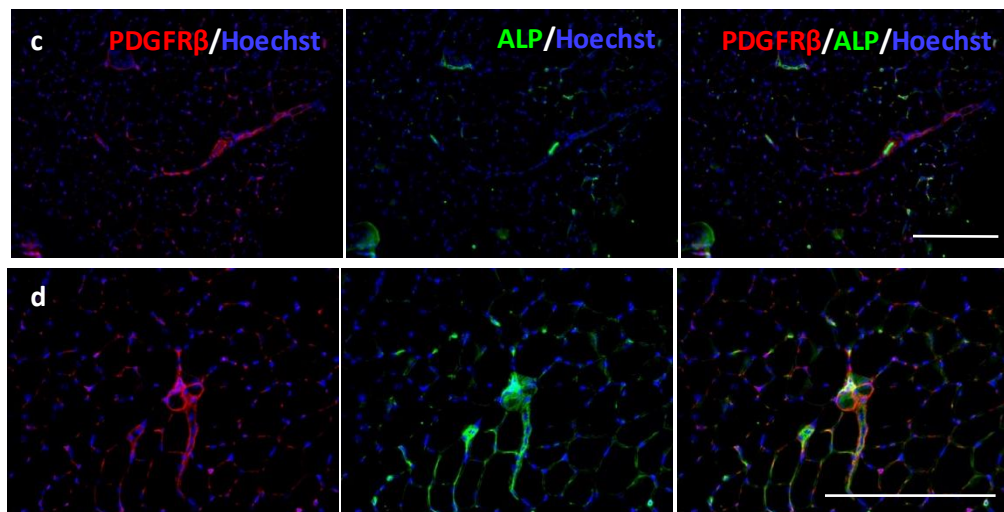


Figure 69. (a) *Cd140a (Pdgfra)* and (b) *Cd140b (Pdgfrb)* gene expression in *Tibialis anterior* and *Soleus* of 10 week-old WT and *Frzb*^{-/-} mice. *GAPDH* was used as endogenous control. Data are represented as mean fold-change \pm standard deviation. WT; N= 4 and *Frzb*^{-/-}; N= 5 for both muscles.

ALP expressing mesenchymal cells are a heterogeneous cell group. In order to establish different population distribution, several mesenchymal cells markers were analysed in skeletal muscles with two different approaches.

First, immunofluorescence studies were carried out in *Tibialis anterior* sections. No differences between *Frzb*^{-/-} and WT were noticed in immunofluorescence analysis (**Figure 70**).

WT

*Frzb*^{-/-}

WT

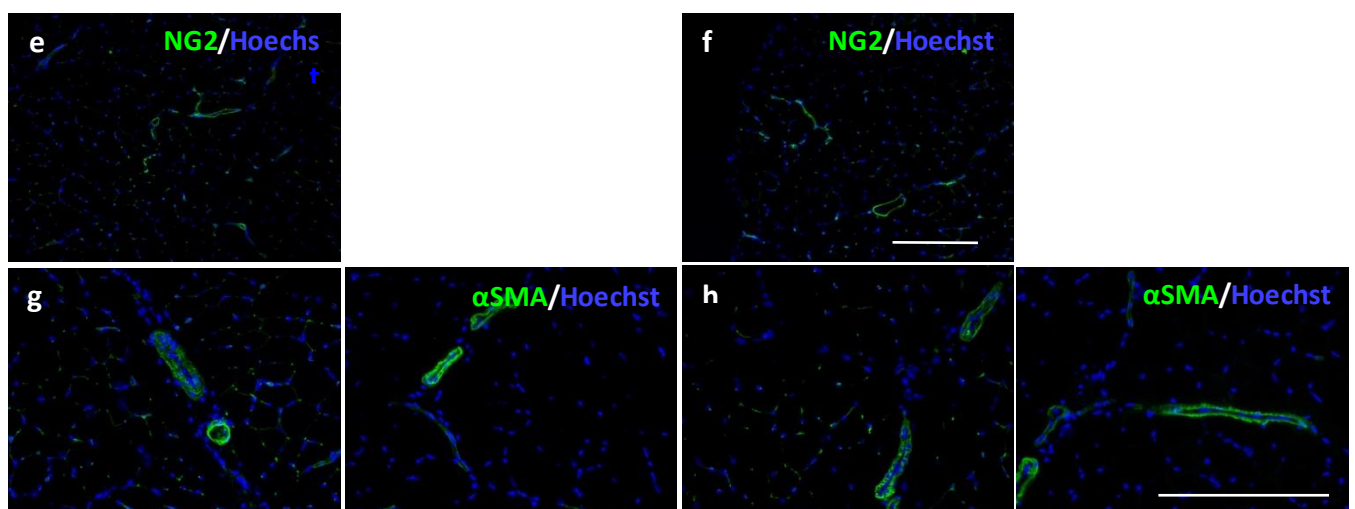
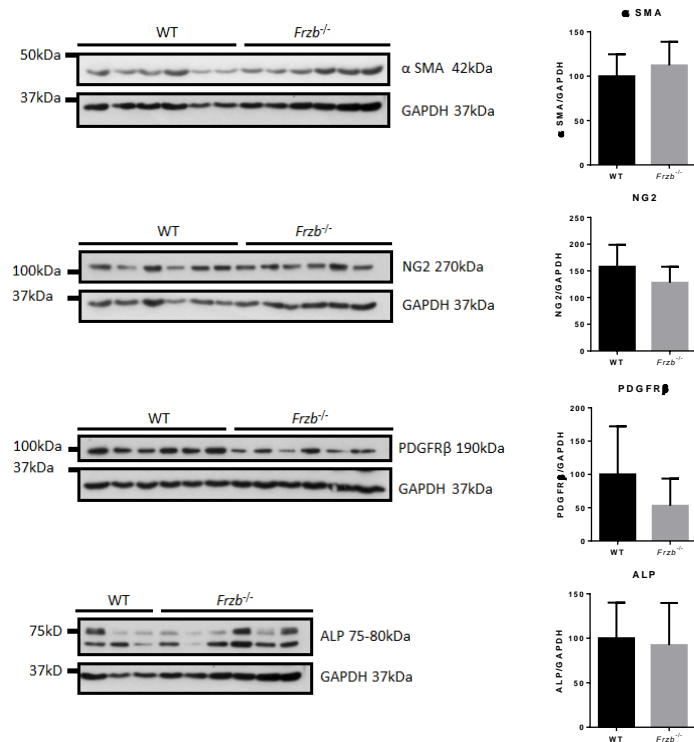
Frzb^{-/-}

Figure 70. Immunofluorescence staining of *Tibialis anterior* WT and *Frzb*^{-/-} muscle sections using (a-d) PDGFRβ (red), alkaline phosphatase (green), (e and f) NG2 (green) and (g and h) αSMA (green) antibodies. Nuclei were visualized with Hoechst (blue). Scale bar 250 μm.

Second, several western blot analyses in *Tibialis anterior* and *Soleus* were made. No major differences were observed (**Figure 71**).

a. Protein expression in *Tibialis anterior*.



b. Protein expression in *Soleus*.

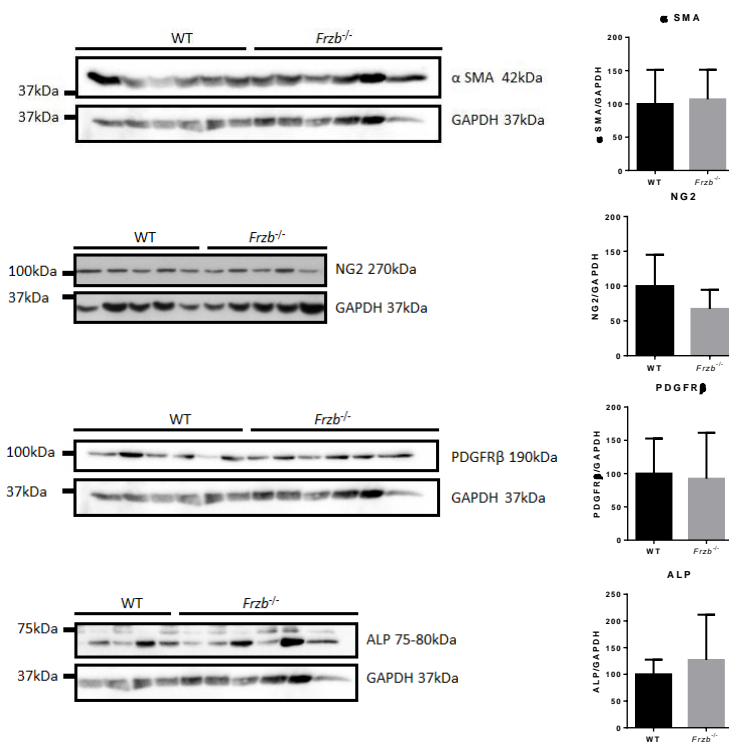


Figure 71. Western blot and densitometry analyses in (a) *Tibialis anterior* and (b) *Soleus* of WT and *Frzb*^{-/-} mice where α SMA, NG2, PDGFR β and ALP proteins were analysed. Data are represented as mean band density normalized relative to GAPDH \pm standard deviation.

Due to the capacity of WT and *Frzb*^{-/-} ALP⁺ cells to differentiate towards adipogenic lineage, adipogenic differentiation capacity was studied. Adipocytes were visualized with Oil red O dye and lipid droplet-associated protein perilipin A/B which mark lipid droplets that are inside the cells (**Figure 72**).

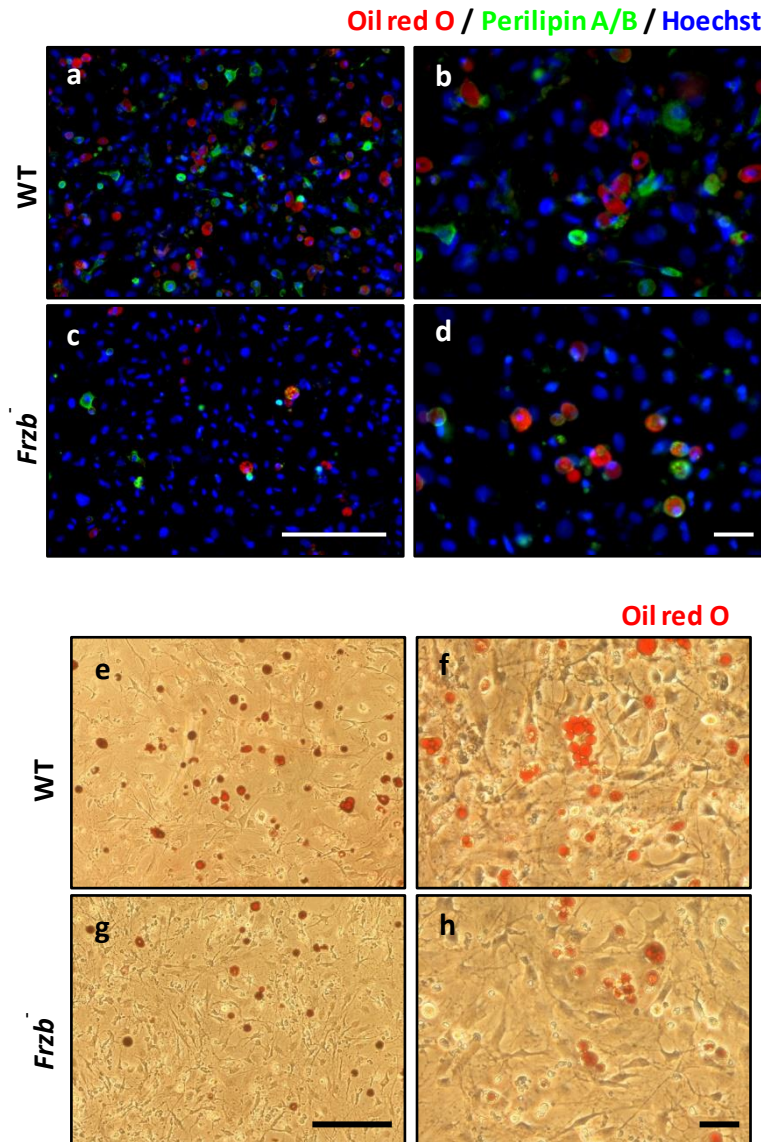


Figure 72. Representative images of ALP⁺ cells differentiated into adipocytes, WT (N= 3) and *Frzb*^{-/-} (N= 3). (a-d) Immunofluorescence images where lipid droplets are visible with Oil red O (red) and perilipin A/B staining (green). Nuclei are stained with Hoechst (blue). (e-h) Bright field images where lipid droplets are visible with Oil red O (red). Scale bars 250 μ m (a and c), 200 μ m (e and g) and 50 μ m (b, c, f and h).

Oil red O quantification showed that the 66% of WT samples produced more adipocytes than the 66% of *Frzb*^{-/-} samples (Figure 73).

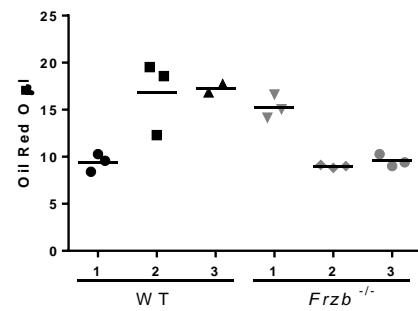


Figure 73. Oil red O quantification in three WT and 3 *Frzb*^{-/-} mice samples. Each sample was assayed as triplicate.

10. MUSCLE EXPRESSION ANALYSIS

The successful genetic deletion of *Frzb* gene in muscles was confirmed by the absence of *Frzb* messenger RNA (data not shown) as previously confirmed in mouse articular cartilage (Lories et al., 2007). Among all the analysed genes, *Cthrc1*, *Mest*, *Wnt8a* and *Wnt8b* genes expression was not detectable in these samples.

The analysis of the genes was subjected to a two-way ANOVA analysis of variance in order to test the relationship between genotype and gene expression. They are listed as previously mentioned:

a) Muscle specific genes: *Myod* gene expression showed statistically significant influence of genotype F (1, 17), $p < 0.0051$ being *Frzb*^{-/-} mice muscles expression higher. Post hoc analysis using the Sidak's criterion for significance indicated that *Myod* gene expression in *Tibialis anterior* was the only one statistically significantly upregulated, $p < 0.05$. Regarding myogenin gene expression, genotype influence was also observed F (1, 17), $p < 0.0397$ without any statistically significant differences when post hoc analysis was carried out. Finally, *Pax7* and *Ryr1* genes expression were not influenced by genotype (Figure 74 a).

b) Skeletal muscle atrophy markers: Atrophy-related ubiquitin ligases *Fbx32* and *Murf1* did not show differences between WT and *Frzb*^{-/-} mice (Figure 74 b).

c) Deregulated genes in C3KO mice: *Park2* gene expression was influenced by genotype, *Frzb*^{-/-} mice have higher expression F (1, 17), $p = 0.0386$. Further post hoc analysis did not report any specific means differences. *Ky* gene was significantly downregulated in *Frzb*^{-/-} mice F (1, 17) $p = 0.0009$. This difference was only significantly downregulated in *Tibialis anterior* ($p < 0.001$) as reported by Tukeys' multiple comparison test (Figure 74 c).

d) Adipose tissue markers: none of the analysed genes *Pparg*, *Adipo* and *Fasn* showed expression differences (Figure 74 d).

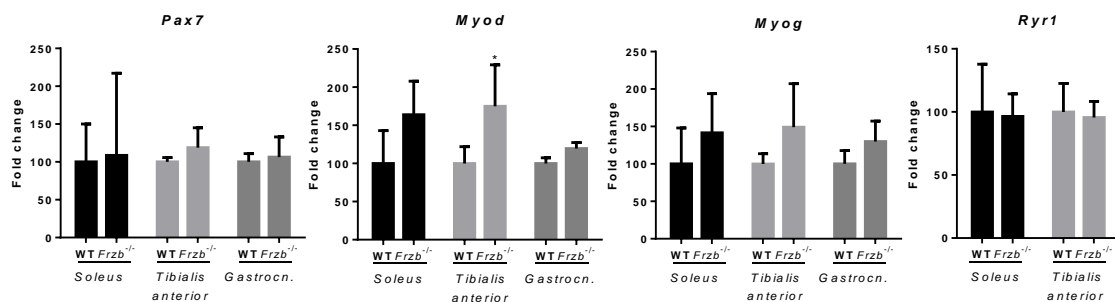
e) Deregulated genes in LGMD2A patients: The only two genes that showed genotype influence were *Capn3* and *Fn1*. On the one hand, *Capn3* gene was significantly upregulated in *Frzb*^{-/-} mice F (1, 12), $p = 0.0019$. The difference in *Soleus* was significant ($p < 0.01$) as reported by Tukey's multiple comparison test. On the other, *Fn1* gene was significantly downregulated in *Frzb*^{-/-} mice F (1, 8), $p = 0.0472$ (Figure 74 e).

f) Deregulated genes in *Frzb*^{-/-} mice articular cartilage and LGMD2A patients' muscles: The influence of the genotype was found significant in *Rora* (F (1, 8) $p = 0.0315$), *Slc16a1* (F (1, 8), $p = 0.0008$) and *Tfrc* (F (1, 8), $p = 0.0102$) genes expression. Further Tukey's multiple comparisons test showed that *Slc16a* gene expression was statically downregulated in *Frzb*^{-/-} *Soleus* ($p < 0.01$) and *Tfrc* gene expression was statistically downregulated in *Soleus* ($p < 0.05$). However *Rora* gene expression upregulation in *Frzb*^{-/-} mice did not show specific pairwise differences. *Igf1* gene expression was downregulated in *Frzb*^{-/-} *Soleus* while the trend in *Tibialis anterior* was contrary. The rest of the genes did not show genotype influence in their expression (Figure 74 f).

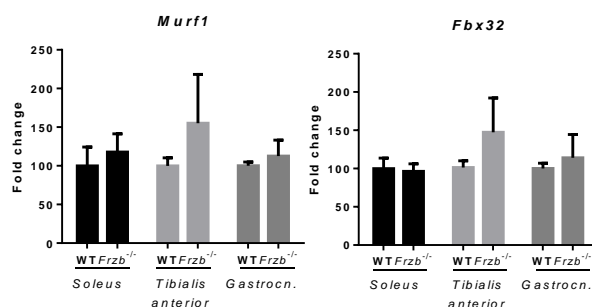
g) Collagens: no alterations were reported regarding genotype in any of the analysed collagens coding genes (Figure 74 g).

h) Genes coding for proteins participating in Wnt signaling pathway: Wnt signaling co-receptors *Lrp5* and *Lrp6* as well as β -catenin coding gene (*Cttnb1*) did not show different expression in *Frzb*^{-/-} mice (Figure 74 h).

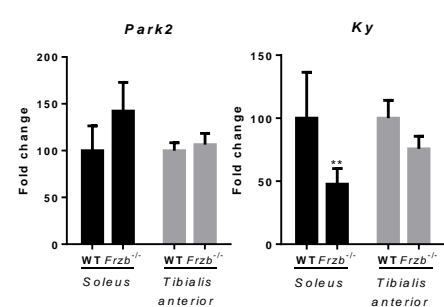
a. Muscle specific genes



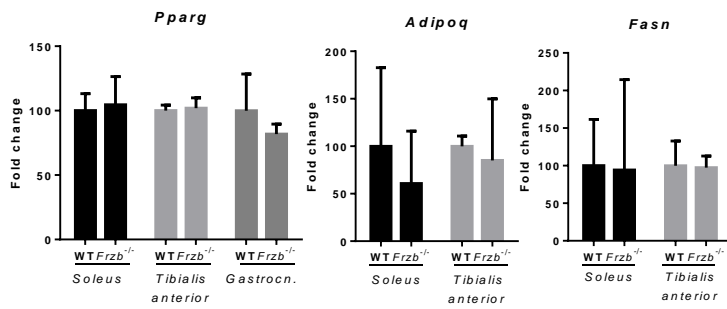
b. Skeletal muscle atrophy markers



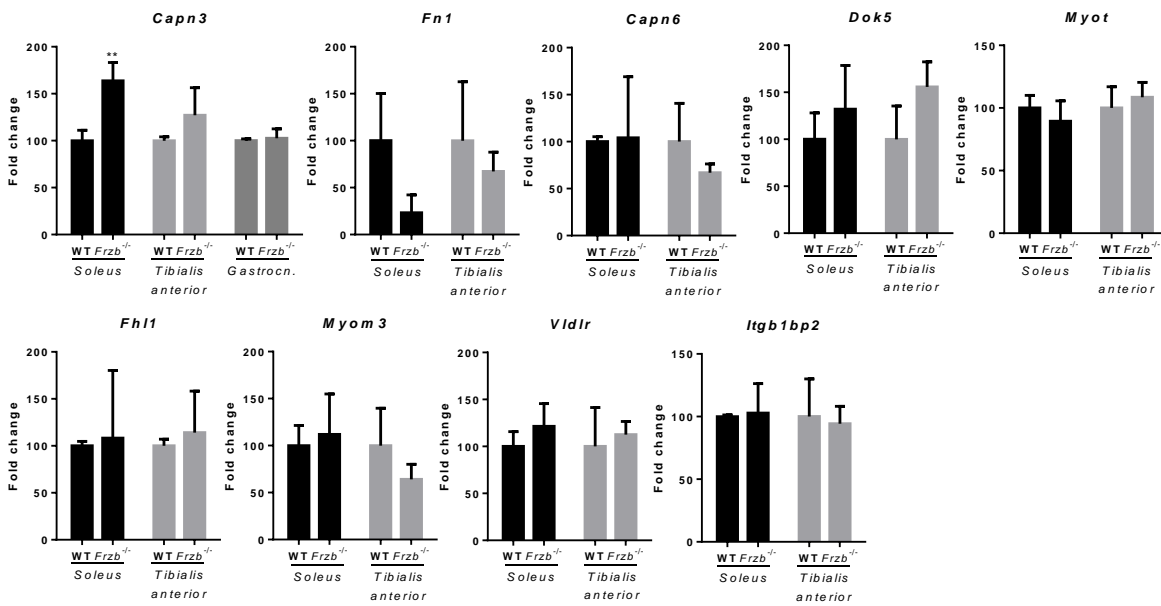
c. Deregulated genes in C3KO mice



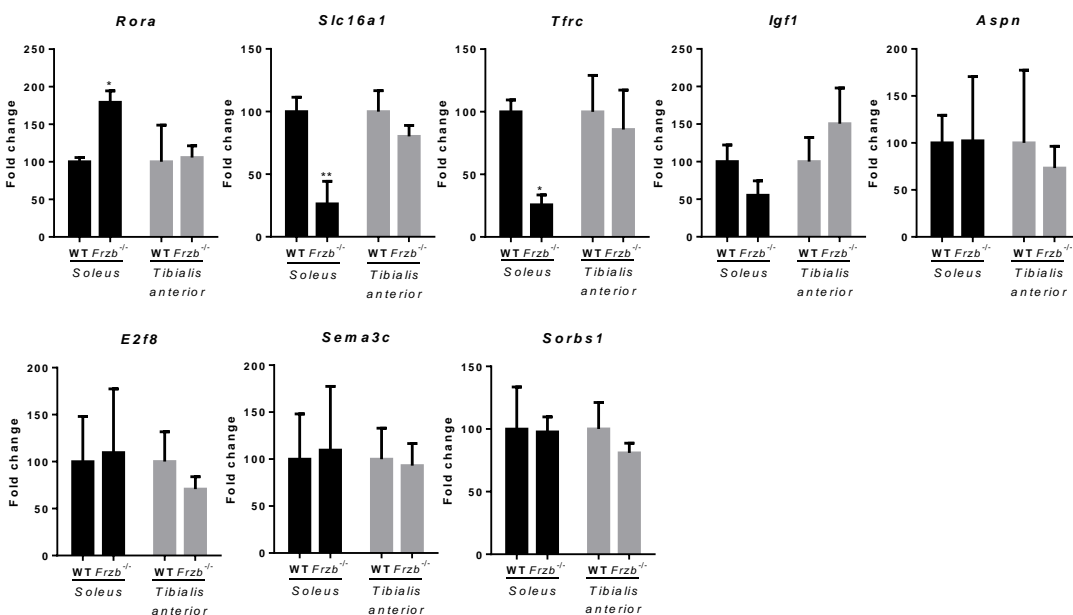
d. Adipose tissue



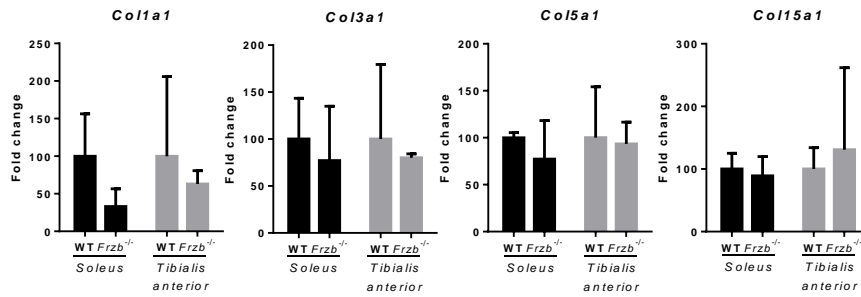
e. Deregulated genes in LGMD2A patients



f. Deregulated genes in *Frzb*^{-/-} mice articular cartilage as well as LGMD2A patients' muscles



g. Collagens



h. Genes coding for proteins participating in Wnt signaling pathway

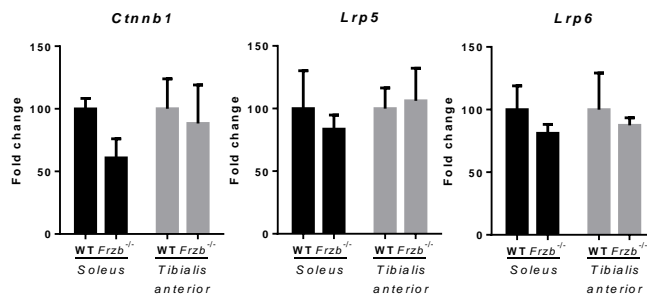


Figure 74. Gene expression analysis of (a) muscle specific genes, (b) skeletal muscle atrophy markers, (c) deregulated genes in C3KO mice, (d) adipose tissue markers, (e) deregulated genes in LGMD2A patients, (f) deregulated genes in *Frzb*^{-/-} mice articular cartilage as well as LGMD2A patients' muscles, (g) collagens and (h) genes coding for proteins participating in Wnt signaling pathway in *Soleus*, *Tibialis anterior* and *Gastrocnemius (Gastrocn.)*. *GAPDH* was used as endogenous control. Data are represented as mean fold-change \pm standard deviation. Significance of the differences are represented as * = $p < 0.05$ and ** = $p < 0.01$.

10.1 *FRZB* gene expression silencing in human

Some of the deregulated genes in *Frzb*^{-/-} mice were validated in human myotubes by *FRZB* gene silencing (*siFRZB*).

FRZB gene was silenced in both control and LGMD2A patient myotubes. Myogenic markers *MYOD* and *MYOG* were analysed and while no change in *MYOG* was observed *MYOD* gene showed upregulation trend after *FRZB* silencing even this differences were not significant. *CAPN3* gene was significantly upregulated in control samples when paired t test was applied. However, although in patients this upregulation did not reach significance a trend to upregulation was observed (**Figure 75**).

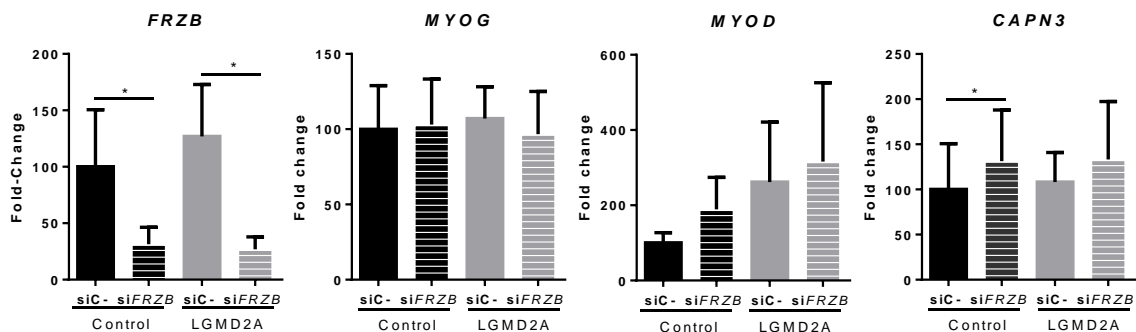


Figure 75. Gene expression analysis of *FRZB* (6 controls and 6 LGMD2A), *CAPN3* (6 controls and 4 LGMD2A), *MYOD* (3 controls and 2 LGMD2A) and *MYOG* (3 controls and 3 LGMD2A) genes in *FRZB* silencing experiments (*siFRZB*) in human control and LGMD2A patients myotubes at day 10 of differentiation. Data are represented as relative mean expression \pm standard deviation. Significance of the differences are represented as *= $p < 0.05$, **= $p < 0.01$. For *CAPN3* siC- versus *siFRZB* in control, paired t test was used.

As on previous studies, LiCl was used for mimic *FRZB* gene silencing in human myotubes. LiCl treatment downregulated *CAPN3* gene expression in both, control and LGMD2A patients' myotubes. This difference reached significance in control samples when paired t test was applied (**Figure 76**).

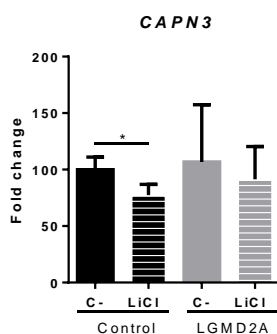


Figure 76. Gene expression analysis of *CAPN3* in 3 controls and two LGMD2A patients' myotubes treated with LiCl 10 mM. *GAPDH* was used as endogenous control. Data are represented as mean fold-change \pm standard deviation.

In silico analysis (AliBaba v.2.1) of the promotor of *CAPN3* gene indicated the presence of various binding sequences for transcription factors such as c-Fos, c-Jun and AP-1, which are regulated by β -Catenin (Figure 25).

<i>Promotor sequence</i>	<i>Transcription factor</i>	<i>Nucleotide position</i>	<i>Transcription factor nucleotide sequence</i>
g t g a c t c c c c	AP-1	499-508	r T G A C T s m s C
t g c t g a g t a a	c-Jun AP-1	1657-1666	y G C T G A s T m A y G C T G A s k m A
c t t a g t c a c a	AP-1	1758-1767	s T k A G T C A m w
a a t t a a t c a g	c-Jun	2456-2465	A A T k A r T C A k
g c t g a c t a a t	c-Jun AP-1 AP-1	2587-2596	k C T G A s T m A y n m T G A C T m A T n m T G A C T A A y
c t a c t a a t g	c-Fos AP-1	2588-2597	C T G A C k m A K K m T G A s T m w T G
a g g a g t c a t g	AP-1	3259-3268	n k G A G T C A k G
t g a g a c a a g c	AP-1	3988-3997	T G A s w C r A r C
t c t t g a g t c a	c-Jun c-Fos AP-1	4247-4256	k s w T G A G T C A k s w T G A G T C A k s w k G A G T C A
a g t c a t c t g t	AP-1	4522-4531	r G T C A T C w s A
c t g a a t c a t t	AP-1	5243-5252	C T G A r T C A y n
c t g c c t c a g c	AP-1	7560-7569	n T G m s T C A G C
g t g t c t c a g c	AP-1	7879-7888	r T G w C T s w G C

Table 25. A summary of c-Fos, c-Jun and AP-1 transcription factors binding site prediction for *CAPN3* gene. Being k= G/T, m= A/C, n= T/C/A, s= C/G, w= T/A and y= C/T.

10.2 Protein expression analysis

No differences in MyoD or calpain 3 protein levels were observed in *Tibialis anterior* neither in *Soleus* (Figure 77).

a. *Tibialis anterior*.



b. *Soleus*.

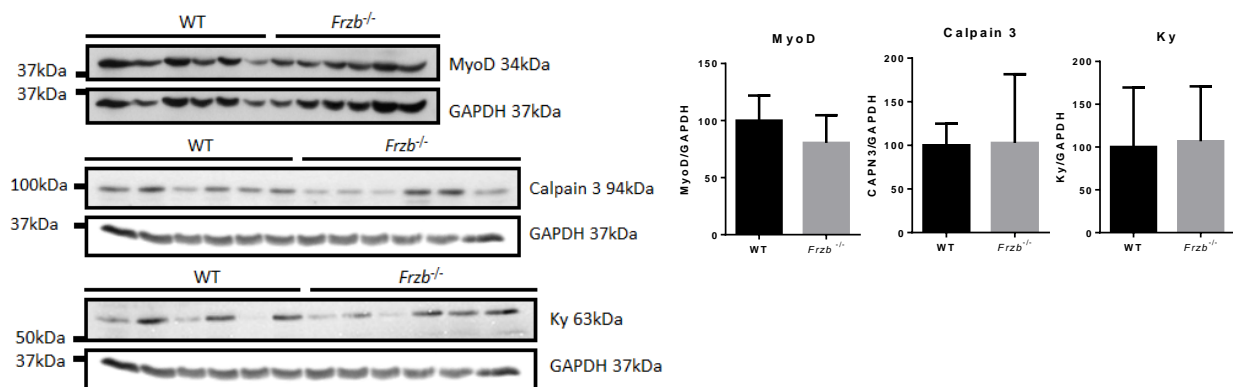


Figure 77. (a) Western blot and densitometry analyses of MyoD and calpain 3 in *Tibialis anterior* of WT and *Frzb*^{-/-} mice. (b) Western blot and densitometry analyses of MyoD, calpain 3 and Ky in *Soleus* of WT and *Frzb*^{-/-} mice. Data are shown as mean band density normalized relative to GAPDH ± standard deviation. WT; N= 6 and *Frzb*^{-/-}; N= 6.

CHAPTER 2: DISCUSSION

LGMD2A patients have high levels of FRZB expression. In myotubes of LGMD2A patients, correct costamere assembly appears to be disturbed and has been linked with the absence of the required integrin isoform replacement from $\beta 1A$ to $\beta 1D$. Remarkably *FRZB* silencing in myotubes leads to a costamere proteins rescue. We therefore suggested that FRZB may be a potential therapeutic target for LGMD2A patients. To better understand the function of FRZB in muscles, different aspects of muscle biology in the *Frzb*^{-/-} murine model were studied at the functional, cellular and molecular level.

1. MUSCLE STRENGTH ANALYSIS

Given that muscular dystrophies show muscle weakness as the main hallmark, mice's strength analysis was analysed. It is known that high standardization is needed to reduce variability in muscle strength analysis. To standardized analysis, requirements regarding room conditions (type of room, room temperature, room occupancy, time of the day, etc.) as well as gender, age and body weight of control and test animals should be similar (Carlson et al., 2010). Even though in this study room conditions were homogenous, used mice characteristic were different. *Frzb*^{-/-} were grown in the animal facility of the university while WT mice were externally purchased. Thus, given the difference body weight between WT and *Frzb*^{-/-} mice, it might be concluded that the different hanging time could be more due to mice body weight than to muscle strength differences.

2. MICE GAIT ANALYSIS

LGMD2A patients show gait alterations that are accentuated as the disease progresses due to muscle weakness (Fardeau et al., 1996a). We therefore performed gait analysis of *Frzb*^{-/-} mice to gain insights into the effect of *Frzb* deficiency on muscle function. In animal models, gait pattern analyses are commonly used to study the impact of nerve lesions or brain injuries (Maricelli et al., 2016). However, a well-established gait pattern in animal models could provide a tool to assess disease progression as well as a recovery pattern after treatment. In this study, *Frzb*^{-/-} mice showed a longer step cycle, spending more time with the paw in contact with the walkway (stand time) as well as airborne (swing time). Thus, their limb movement was slower, however, with no effect on the covered distance. In a previous research of our group, we showed that *Frzb*^{-/-} mice ran daily significantly lower distance in a voluntary running wheel setup (Lories et al., 2009). This reduced voluntary running exercise performance could be attributed to the lower speed rather than to the fact that they spend

less time running. Thus, *Frzb*^{-/-} mice appear to have some detectable issues in their gait and mobility compared to wild-type controls.

Since Jackson and collaborators (2015) showed that depletion of Pax7 expressing satellite cells in muscles resulted in reduced voluntary wheel running performance, *Pax7* expression was also analysed in the study. No reduction of its expression in all the tested muscles was reported thus, reduced speed is likely not caused by the lack of satellite cells in the muscles of *Frzb*^{-/-} mice.

To better understand the reasons why this reduced speed was observed, several other factors were analysed. Previously, physical activity has been related to maternal diet or body composition (Hiramatsu et al., 2017; Liu et al., 2018). It is also known that increased adipose tissue infiltration of muscles is a common hallmark in neuromuscular disorders (Lamminen et al., 1990; McDaniel et al., 1999; Marden et al., 2005). *Frzb*^{-/-} mice have lower body and muscle mass. Nevertheless *Frzb*^{-/-} mice did not show fatty infiltration in the analysed muscle sections. The regulators of adipocyte differentiation, peroxisome proliferator activated receptor gamma or adiponectin coded by *Pparg* and *Adipoq* respectively, that are expressed exclusively in adipose tissue were not altered. In addition to fat infiltration, atrophy can also cause muscle weakness, by upregulation of atrogenes (MAFbx/Atrogin-1 and MuRF1) that lead to loss of muscle mass and atrophy (Fleckenstein et al., 1993; Bodine et al., 2001; Sandri et al., 2004). None of the atrogenes were upregulated in *Frzb*^{-/-} muscles at RNA or protein level. Therefore, we have no evidence that fat or atrophy could be the reason why mice spent more time to complete a step cycle.

Related to the paw support, the extended paws in contact with the floor seemed to be the consequence of the increased stand and swing phase. The switch in the support pattern observed in WT group by 10 weeks did not occur in *Frzb*^{-/-} group. A wider base of support might be considered a way to compensate a weakness or balance impairment (Hamers et al., 2001; Kloos et al., 2005), but results observed in this study showed the contrary as narrower BOS was observed.

Gait might not only be altered by impairment in muscles; but also by changes in the nervous system or bones. So far, there is no evidence of nervous system alterations in *Frzb*^{-/-} mice. Nevertheless, it is known they have thicker cortical bone, with increased stiffness and higher cortical appositional bone formation after loading of the long bones (Lories et al., 2007). These differences with WT animals cannot be excluded as factors contributing to the slight changes observed in *Frzb*^{-/-} mice gait.

In summary, altogether *Frzb*^{-/-} mice do not appear to show major functional impairment as the observed gait difference would not be considered as pathological.

3. EXERCISE INDUCED MUSCLE ALTERATIONS

Exercise has direct effects, triggering changes in cross-sectional area of the fibres, fibre type distribution, weight change and potentially muscle injury (Wernig et al., 1990). Although physical training induces beneficial adaptive changes in skeletal muscle of healthy individuals, its effects in patients with muscular dystrophy remain controversial. While some studies attributed a beneficial effect without reporting muscle injury, other studies reported training-induced muscle damage and creatine kinase elevations in high-intensity training programs in patients, or even an earlier onset of symptoms associated with exercise in LGMD2B patients (Vignos and Watkins, 1966; McCartney et al., 1988; Ansved, 2003; Sveen et al., 2013; Sczesny-Kaiser et al., 2017; Moore et al., 2018). Since distinct muscular dystrophies show different progression of muscle degeneration and strength loss, leading to diverse exercise tolerance, endurance treadmill training tolerance and muscle changes were studied in *Frzb*^{-/-} mice model.

Exercise-induced muscle adaptations were examined at different levels, from a structural point of view and at molecular level.

Endurance training leads to fibre-type switching, mostly a transition towards slow-twitch muscle fibres, but without consensus of its effects on fibres CSA (Andersen and Henriksson, 1977; Green et al., 1979; Kraemer et al., 1995; McCarthy et al., 1995; Sipilä et al., 1997; Carter et al., 2001). Even that, two studies reported that exercise effects were only apparent in genetically modified mice or in cisplatin treated mice while their WT or control mice did not display any apparent changes (Sakakima et al., 2004; Sakai et al., 2017). Thus, the lack of structural changes in *Frzb*^{-/-} mice after exercise, suggests the absence of a severe phenotype. Another important aspect was reported by Warhol and colleagues (1985) where exercise induced ultrastructural changes followed by a regenerative response characterized by centrally located nuclei in newly formed fibres were shown. None of these features were detected in trained animals, suggesting that exercise does not have a harmful nor clear beneficial effect in *Frzb*^{-/-} mice.

With regards to the influence of exercise on myogenic markers, there is controversy, since upregulation as well as unchanged MyoD and myogenin expression have been reported after the same experimental trials (Liu et al., 2008; Drummond et al., 2010). Therefore the lack of myogenic markers alteration after exercise is something that could be expected, suggesting that other type of exercise or higher intensity is needed to provoke these modifications.

Finally, in agreement with our findings, *Fbx32* and *Murf1* downregulation after exercise, at low or moderate intensity, with no changes in body or *Tibialis anterior* weight nor in CSA have been already described (Durigan et al., 2009).

We considered the activation of different signaling cascades. AKT activation has been described as responsible of protein synthesis and muscle fibre hypertrophy (Pallafacchina et al., 2002; Yang et al., 2008; Rasmussen and Richter, 2009), MAPK also promotes biochemical responses and gene expression after exercise (Goodyear et al., 1996; Aronson et al., 1997, 1998) and GSK3 β activity also appears to be regulated by exercise (mediated by AKT) (Lawrence et al., 1997; Markuns et al., 1999). Nevertheless, no major alterations in the phosphorylation of these kinases were observed after exercise. Thus, the result obtained from the ratio between phosphorylated and total-protein did not give conclusive results.

However, it has been observed that after exercise, the levels of total ERK1/2, AKT and GSK3 β decreased. The same trend was observed in non-exercised *Frzb*^{-/-} mice, which suggested that the lack of *Frzb* and exercise may have some similar effects in muscles.

The downregulation of these proteins in *Frzb*^{-/-} mice suggests that they are regulated at gene expression level. However, little is known about AKT, ERK1/2 and GSK3 β genes transcriptional regulation in skeletal muscle since most of the studies are performed in cancer (Goto et al., 2002; Park and Chen, 2005; Zhang et al., 2013; Agarwal et al., 2013). Nevertheless, Wnt signaling pathway may regulate the expression of these kinases. In support of this idea Dihlmann and colleagues (2005) found out TCF/LEF-binding elements upstream of the *AKT1* gene, suggesting its expression might be regulated by Wnt/ β -catenin signaling. However, gene expression analysis of these proteins would be necessary to confirm this regulation.

To sum up, since no exercise induced differences and no altered expression of different kinases were observed, altogether, it could be concluded that exercise does not appear to be deleterious for *Frzb*^{-/-} mice.

4. MUSCLE REGENERATION ANALYSIS

The CSA of muscle fibres in *Frzb*^{-/-} mice was smaller. Consequently, fibre type composition was studied. *Tibialis anterior* and *Soleus* fibre type distribution were within normal range values as has been described for C57BL/6 mice (Augusto et al., 2004; Kammoun et al., 2014). Previous studies in *Soleus* and *Extensor digitorum longus* analysed by immunofluorescence, showed similar fibre composition in WT and *Frzb*^{-/-} mice (Lories et al., 2009). Additionally, myosin gene expression as well as NADH-t staining were analysed obtaining the same result, fibre composition in *Soleus* and *Tibialis anterior* mice did not vary.

Although several muscular dystrophy models, such as syntrophin α 1 null mice and murine models for LGMD2L and LGMD2A, showed aberrant muscle regeneration with longstanding necrosis

and impaired exercise and contractile properties with aberrant neuromuscular junctions (Hosaka et al., 2002; Griffin et al., 2016; Yalvac et al., 2017) in *Frzb*^{-/-} mice, after cardiotoxin injection, no aberrant or impaired regeneration capacity or fibrosis was noticed.

In summary, *Frzb*^{-/-} mice muscles showed normal fibre composition and they do not display altered regeneration capacity.

5. SKELETAL MUSCLE RESIDENT PROGENITOR CELLS

5.1 Satellite cells

Murine primary cell cultures have been widely used for myogenesis and muscular dystrophies studies such as LGMD2A, LGMD2I or DMD (Robert et al., 2001; Kramerova et al., 2004; Grefte et al., 2012; White et al., 2014; Smolina et al., 2015; Manabe et al., 2016; Jaka et al., 2017; Vannoy et al., 2017). In this work when satellite cells were isolated, a smaller amount of cells was expected after muscle digestion because smaller *Frzb*^{-/-} muscles were observed. Nevertheless, the same amount of cells was obtained. Furthermore, *Frzb*^{-/-} mice cells showed enrichment for MyoD and Ki67 nuclear proteins.

Frzb inhibits MyoD expression at RNA and protein level (Wang et al., 1997, 1997; Borello et al., 1999). We here show that, in the absence of Frzb, MyoD was upregulated in our cells. As myotube formation was not altered, myogenesis may not be strongly impaired, but further studies will be required to identify the consequences of MyoD increase could cause in myogenesis in the absence of FRZB.

On the other hand, the increased Ki67 expression, which is a proliferation marker, suggested an increased proliferation capacity in *Frzb*^{-/-} muscles. However, there is controversy about the way in which the presence or absence of Frzb could affect proliferation. Some studies described that Frzb inhibits the growth of mesoangioblasts and suppressed cell proliferation in gastric cancer (Tagliafico, 2004; Qu et al., 2008). However, other authors suggested that Frzb suppression reduce proliferation in alveolar rhabdomyosarcoma (Kephart et al., 2015). Moreover, tissue dependent differences have been observed in the same model, since *Frzb*^{-/-} mice chondrocytes proliferated less than those obtained from WT mice, contrary to the observation in satellite cells in the same mice. This would suggest that result must be thoroughly analysed since different tissues express different gene expression.

5.2 Mesoangioblasts

Considering that some muscle resident cell population are able to generate muscle, both *in vitro* and *in vivo* (De Angelis et al., 1999; Minasi et al., 2002; Sampaolesi, 2003) pericyte-derived adult mesoangioblasts were studied. Pericyte –derived adult mesoangioblasts originate from embryonic MABs and they maintain the same characteristics (Morosetti et al., 2006; Dellavalle et al., 2007; Crisan et al., 2008; Pierantozzi et al., 2016).

Since more APL+ cells were obtained from *Frzb*^{-/-} muscle explants, *Frzb*^{-/-} muscles may have more resident MSCs. However, no differences were observed between WT and *Frzb*^{-/-} mice regarding MSCs markers. As described before, *Frzb* inhibits the growth of MABs (Tagliafico, 2004) and therefore lack of *Frzb* may be acting in MABs proliferation rather than in proliferation of the rest of the cells. In addition to these findings, Kuroda and colleagues (2013) have reported that canonical Wnt signaling induces ALP expression in C2C12 cells, suggesting the same could be happening to these cells obtained from muscle explants.

A more detailed analysis of the ALP+ cells showed significantly less PDGFR α expression. So far, two types of pericytes have been described type-1 and type-2. Both of them differ in their cell surface markers as well as in their differentiation capacity. Type-1 are Nestin-/PDGFR α + and are characterized by their ability to differentiate into adipocytes while type-2 are Nestin+/PDGFR α - and do not differentiate into adipocytes but form myotubes in culture (Birbrair et al., 2013a, 2013b). Given that, the lower PDGFR α expression could lead us to suppose that *Frzb*^{-/-} mice have more type-2 pericytes. However, this could not be fully confirmed since at RNA level no alteration in *PDGFRA* gene expression was observed in *Frzb*^{-/-} mice muscles. Even if PDGFR α should be analysed at protein level in muscle, its lower expression suggests *Frzb* is implicated in its control although no direct regulation has been described so far.

On the other hand, since PDGFR α expressing cells are the responsible of fat formation in skeletal muscle (Olson and Soriano, 2009; Joe et al., 2010; Uezumi et al., 2010; Birbrair et al., 2013a), whether ALP+ cells could differentiate into adipocyte lineage was studied. The reduced amount of PDGFR α cells suggested that adipogenic differentiation was attenuated in *Frzb*^{-/-} samples. This idea is also supported by the fact that overexpression of Wnt-1 inhibits adipogenesis (Ross et al., 2000). Since *Frzb* is Wnt-1 antagonist, it would be tempting to speculate that FRZB (upregulated in LGMD2A patients) would be the reason why muscle replacement with adipose tissue is occurring in these patients, due to an increase in pre-adipocyte differentiation.

6. GENE EXPRESSION ANALYSIS

In previous studies, differentially expressed genes have been analysed in articular cartilage-subchondral bone biomechanical unit of *Frzb*^{-/-} mice (Lories et al., 2007; Lodewyckx et al., 2012). However, gene expression analysis in muscle has not been carried out. Thus, one aim of this study was to establish whether *Frzb* deficiency impairs muscle gene expression in *Frzb*^{-/-} mice. The analysis was focused mainly in *Soleus*, as *Soleus* showed the greatest molecular similarities to human skeletal muscles (Kho et al., 2006) and since together with diaphragm these are the most affected muscles in C3KO mice (Kramerova et al., 2004).

Myogenesis, a process that takes place during growth and regeneration in adult, depends on satellite cell activation by Pax7 and it is regulated by muscle-specific transcription factors such as MyoD and Myogenin (Buckingham and Rigby, 2014; Comai and Tajbakhsh, 2014). In the studied samples Pax7 was not upregulated, but *MyoD* and myogenin were upregulated in *Frzb*^{-/-} mice. However, in the *FRZB* silenced human samples; *MYOD* expression was upregulated but not *MYOG* expression. This showed a direct relation between *Frzb* and MyoD. Moreover, in *Xenopus*, *Frzb* inhibits axis duplication induced by *Xwnt8* and also muscle development by blocking MyoD induction (Hoppler et al., 1996; Leyns et al., 1997; Wang et al., 1997). In mammals, myogenesis inhibition by *Frzb* accompanied by reduction in *Myf5* and *MyoD* expression was reported, suggesting a direct effect on gene activation (Borello et al., 1999). So far, a direct mechanism between *Frzb* and MyoD has not been established. Although most of the works were carried out in embryonic stage, the possibility that *Frzb* has a role in adult myogenesis or muscle maintenance, regulating MyoD levels, should be considered. Although *Myod* gene expression was upregulated in *Frzb*^{-/-} mice muscles, increased myogenesis was not observed (centrally located nuclei were absent and different size fibres were not observed). Given that myogenesis is a tightly regulated process that keeps the muscle in a post-mitotic stage in the absence of any external stimuli such as injury or disease (Andrés and Walsh, 1996; Chargé and Rudnicki, 2004) could be the reason why detectable upregulation of the MyoD protein did not happen. However, *MYOD* gene expression upregulation after si*FRZB* in LGMD2A patients could be considered as a beneficial consequence given that muscle degeneration stimuli is occurring and consequently new myofibres formation would be necessary. Nevertheless, further studies will be required to analyse if this increase improves cell physiology.

Between the selected genes deregulated in C3KO mice (Jaka et al., 2012) the *Ky* gene showed expression changes in *Frzb*^{-/-} mice. Its protease activity targets different proteins and its absence could disrupt muscle cytoskeleton homeostasis (Beatham et al., 2004). Natural *ky* mutant mice have smaller muscles with slower contraction time and are weaker than controls (Marechal et al., 1995; Blanco et

al., 2001). In *Frzb*^{-/-} mice, unlike in C3KO mice, there is no measured downregulation of Ky protein which maintains the knowledge of its effects elusive.

β-catenin is the main effector of canonical Wnt signaling and its gene expression (*Cttnb1*) downregulation has been previously reported (Lories et al., 2007). The same trend was observed in the *Soleus* of *Frzb*^{-/-} mice, however no statistical significance was achieved. The lack of *Frzb* would result in Wnt signaling pathway activation accompanied with cytosolic β-catenin accumulation. The observed downregulation could be a compensatory mechanism to avoid the continuous activation of this pathway. However, given that β-catenin is not only involved in Wnt/β-catenin pathway, makes it difficult to elucidate a consequence.

When focusing on common deregulated genes in *Frzb*^{-/-} mice and LGMD2A patients (Sáenz et al., 2008; Lodewyckx et al., 2012) *Aspn*, *E2F8*, *Sema3c* and *Sorbs1* genes were not deregulated in *Frzb*^{-/-} mice muscles as showed in mice cartilage (Lodewyckx et al., 2012). Thus since LGMD2A patients have upregulated these genes (Sáenz et al., 2008) could be suggested that these genes are not under the control of FRZB as its absence did not change their expression in muscles.

However, it is noteworthy to mention that *Rora*, *Slc16a* and *Tfrc* genes showed the same regulation pattern in cartilage and muscle of *Frzb*^{-/-} mice. Their regulations are opposite to what was observed in LGMD2A patients (FRZB upregulated), reinforcing the involvement downstream of the Wnt pathway in their regulation.

Tfrc it has been reported that it is implicated in several muscular functions; consequently its strict control is needed to maintain muscle homeostasis. On one hand, it participates in iron acquisition in skeletal muscle (Hofer et al., 2008). On the other hand, *Tfrc* has been already described as a Wnt target gene where Wnt-1 treated C57MG cells downregulated its expression (Prieve and Moon, 2003), in agreement with our findings. Moreover, it has been shown that Wnt/Frizzled receptors colocalizes in vesicles containing transferrin (Blitzer and Nusse, 2006; Chen et al., 2009). Finally, regarding *Tfrc* implication in muscular dystrophies, it has been described that *Tfrc* is elevated in regenerating fibres in patients with Duchenne muscular dystrophy as well as in facioscapulohumeral muscular dystrophy (FSHD) (Feero et al., 1997; Winokur, 2003). In line with these observations, Demonbreun and collaborator (2011) described dysferlin null myoblasts accumulate transferrin containing vesicles suggesting that they have a defect in endocytic recycling of the transferrin receptor. However, the effects of *TFRC* upregulation in LGMD2A patients have so far no been studied. But, as *TFRC* upregulation has been observed in different dystrophies, this could have deleterious effect in muscle fibre. Thus, the reduction of its expression by Wnt pathway activation could be a beneficial mechanism.

In skeletal muscle, retinoic acid receptor-related orphan receptor α (ROR α) has been described as positive regulator of myogenesis by its interaction with MyoD and p300 cofactor which lead to activate muscle-specific genes transcription (Lau et al., 1999). Furthermore ROR α is involved in the regulation of glucose and lipid metabolism in skeletal muscle (Lau et al., 2004, 2011). On the other hand, its implication in Wnt signaling has been described since Wnt5a/PKC α -dependent as well as PGE2/PKC α -dependent ROR α phosphorylation exerts inhibitory function of the expression of Wnt/ β -catenin target genes (Lee et al., 2010; Shin et al., 2014). Altogether, the rescue of *Rora* expression by Wnt signaling pathway, could be beneficial for LGMD2A patients due to its importance in muscle homeostasis.

Slc16a1 a proton-linked monocarboxylate transporter, is highly expressed in oxidative fibres (type I fibres) consistent with the role of Slc16a1 in mediating lactate uptake for oxidative metabolism (Hashimoto et al., 2005). Due to this, its deregulation may be responsible of the metabolic impairment in LGMD2A patients. No previous relation between *Slc16a1* and Wnt pathway was reported so far, but its downregulation in mice *Soleus* and in cartilages as well as its upregulation in LGMD2A patients, where FRZB is overexpressed, suggests a direct interaction in its regulation.

Igf1 downregulation in *Frzb*^{-/-} muscles is opposite to previously described regulation in cartilage (Lodewyckx et al., 2012). This difference suggested tissue dependent regulation. This downregulation in muscles could be beneficial as *IGF1* is upregulated in LGMD2A.

The fact that these genes (*Tfrc*, *Rora*, *Slc16a1* and *Igf1*) showed an inverse expression regulation in presence or absence of *Frzb*, confirms that the regulation of them depends on Wnt signaling pathway. The expression regulations of these genes have not been thoroughly analysed so far. However, these findings, highlights their considerable potential in the correct muscle fibre homeostasis maintenance. Further studies would be necessary to shed some light on LGMD2A physiopathology.

The extracellular matrix components, collagens (*Col3a1*, *Col5a1*, and *Col15a1*) even if they were upregulate in *Frzb*^{-/-} cartilage and in LGMD2A patients, they were not deregulated in *Frzb*^{-/-} muscles. This is not in agreement with what was observed when *FRZB* was silenced. In human myotubes *FRZB* silencing led to upregulation of *COL1A1* and *COL5A1* genes. Along with collagens, another extra-cellular matrix component, fibronectin, did not show the same expression deregulation as observed after *FRZB* gene silencing in human myotubes (Jaka et al., 2017). Moreover, *FN1* was downregulated in *Frzb*^{-/-} *Soleus*. Given that extra-cellular components regulation is crucial in the fibrosis process in muscular dystrophies (Kanagawa and Toda, 2006) fibronectin and collagens expression regulation by *Frzb*, in skeletal muscle would need special attention.

Finally, focusing on genes altered not only in LGMD2A (Sáenz et al., 2008), also altered by *FRZB* gene silencing, it is interesting how *Vldlr* and *Itgb1bp2* did not recapitulate their trend in human myotubes after *FRZB* gene silencing (Jaka et al., 2017). This phenomenon has been already described in several studies where phenotypic differences between knockouts (i.e., mutants) and knockdowns (e.g., antisense-treated animals) have been observed in mice or human origin cell lines (De Souza et al., 2006; Karakas et al., 2007; McJunkin et al., 2011; Daude et al., 2012; Morgens et al., 2016). These differences have been attributed to reasons including off-target effects of the antisense reagents (Robu et al., 2007; Olejniczak et al., 2010; Baek et al., 2014; Olejniczak et al., 2016). Other alternative explanation has been genetic compensation (upregulation of related genes) in mutant that does not happened in knockdown animals (Rossi et al., 2015). Functional redundancy of genes where the loss of one could be compensated by another with overlapping functions has been reported for several mutants (Wang et al., 1996). Therefore si*FRZB* and *Frzb* knockout should be thoroughly compared. For example, *Vldlr* suppressed Wnt signaling by internalization and degradation of Wnt signaling receptors (Lee et al., 2014). The differences observed between the *Frzb*^{-/-} mice and the silenced cell model, could be explained because in the silencing model, *VLDLR* is upregulated as a feedback control mechanism to regulate excessive Wnt activity. On the contrary in *Frzb*^{-/-} mice, this excessive Wnt activity could not be occurring, consequently *Vldlr* gene upregulation would not be required.

No alterations in *Capn6*, *Dok5*, *Myl6b*, *Myom3* (upregulated in LGMD2A muscles (Sáenz et al., 2008)), *Myot* and *Fhl1* genes (upregulated at protein level in LGMD2A muscles (De la Torre et al., 2009)) were observed, suggesting that their upregulation is not due to Wnt pathway alterations in LGMD2A patients.

One of the most important finding was *Capn3* gene upregulation in *Frzb*^{-/-} mice *Soleus* and its upregulation after *FRZB* gene silencing in human myotubes since no genetic regulatory mechanism of *Capn3* expression have been described so far. The fact that *Capn3* gene downregulation was observed after LiCl treatment in human myotubes showed that two different mechanisms are regulating its expression. Even if LiCl activates Wnt/ β -catenin pathway, it has different and unknown molecular targets which could be the responsible of *Capn3* gene downregulation.

FRZB gene upregulation in *CAPN3* deficient LGMD2A patients was already described (Sáenz et al., 2008), however the reciprocal regulation has never been reported. It should be noted that *Frzb* increase has been discarded as a beneficial compensatory mechanism since its silencing rescued several proteins level reaching normal levels in patients (Jaka et al., 2017). Calpain 3 functions are poorly understood and few proteins degraded by its protease activity have been described. *Frzb* could be considered as a target of calpain 3 because in calpain 3 absence in LGMD2A patients, *FRZB* is upregulated. But, the regulation is more likely occurring at RNA level, since the lack of *Frzb*, upregulated *Capn3* expression. Regulatory mechanisms that control calpain 3 expression are also

unknown. *In silico* analysis has shown c-Fos, c-Jun and AP-1 binding sequences in its promoter. This finding suggested that calpain 3 expression could be modulated by these transcription factors. Since no protein upregulation was observed in *Frzb*^{-/-} mice, it could be suggested that there is a tight regulatory mechanism for this protease. The fact that a common mechanism has been observed in two different species reinforces a possible regulatory mechanism underlying CAPN3-FRZB.

In summary, the result presented here confirm the direct involvement of *Frzb* in the regulation of *Rora*, *Slc16a1*, *Tfrc*, and *Capn3* genes, making further studies necessary to clarify their implication in muscle homeostasis and/or in LGMD2A disease. Furthermore, *Frzb* involvement in myogenesis was confirmed, since it regulates MyoD gene expression, however, the lack of *Frzb* did not alter skeletal muscle regeneration capacity and neither induced modifications after exercise. In addition it has been suggested that, *Frzb* modulation could modify muscle resident pericytes cell fate to a myogenic lineage more than to an adipose lineage. Further studies are required to analyse the fact that *Frzb* modulation, might avoid the muscle replacement with adipose tissue observed in LGMD2A patients. Consequently FRZB could be proposed as a pharmacological target in order to improve muscle function in LGMD2A patients.

CONCLUSIONS

- I. The use of human serum, not only does not improve the growth and differentiation of human myotubes but it also has a negative impact on myotube differentiation.
- II. It has been confirmed the common gene expression regulation between *CD9*, *FRZB* and *ITGB1BP2* in distal muscles. *CD9* and *FRZB* are positive regulators acting upstream of the *ITGB1BP2* gene and, *ITGB1BP2* gene is a negative regulator of *FRZB* gene expression.
- III. It has been demonstrated that *ITGB1BP2* and *CD9* genes silencing have detrimental effect in myotubes, since *ITGB1BP2* gene silencing produced a parallel downregulation of β 1D integrin (already reduced in LGMD2A patients) and on the other hand, *CD9* gene silencing produced a parallel increase of *FRZB* (already increased in LGMD2A patients).
- IV. *FRZB* plays a role in the crosstalk between Wnt signaling and integrin pathways. The link between these pathways may involve the activation of transcription factors, such as FOS (by means of Wnt/ β -catenin pathway) which in turn could regulate the expression of several genes implicated in integrin pathway.
- V. Two different ways of activation of Wnt/ β -catenin signaling pathway, a pharmacological treatment (LiCl administration) and a gene expression regulation (si*FRZB*) showed similar effects, in cultured skeletal muscle cells. Both lead to the regulation of target genes that rescue protein expression implicated in costamere formation such as β 1D integrin and anosmin-1.
- VI. Early induction of the Wnt signaling pathway is detrimental for myotubes differentiation, its expression is required to be tightly controlled at this stage in order to obtain an appropriate differentiation. However, it was confirmed that its later increase is also required for a functional muscle fibre formation.
- VII. AKT/mTOR signaling pathway is perturbed in LGMD2A patients' muscles. AKT shows an increased phosphorylation, however it is not responsible of the downstream effector's phosphorylation given that S6K1 and RPS6 show reduced phosphorylation in their Thr-421/Ser-424 and Ser-235/Ser-236 residues respectively.
- VIII. The elevated phosphorylated levels of AKT give rise to the phosphorylation of FoxO transcription factors, FoxO3 (showing an increasing tendency) and FoxO4 (significantly increased), preventing their nuclear translocation, thus their activation.
- IX. The obtained result together with previous knowledge of FoxO regulation have confirmed the implication of FoxO transcription factors in the regulation of *EGR1*, *FOS*, *JUNB*, *CITED2*, *MYC*, *DOK5*, *COL1A1*, *COL1A2* and *ITGB1BP2* genes in LGMD2A disease.
- X. Lack of *Frzb* gene in *Frzb*^{-/-} mice and its increased expression in LGMD2A patients, showed opposite regulation of *Rora*, *Slc16a1*, *Tfrc* and *Capn3* genes. Therefore, the direct involvement of *Frzb* in the regulation of these genes was established.
- XI. *Frzb* plays a role in myogenesis since it regulates MyoD gene and protein expression.

- XII. Lack of *Frzb* gene does not alter skeletal muscle regeneration capacity after CTX-induced muscle injury.
- XIII. Exercise induces downregulation of atrogenes in WT and *Frzb*^{-/-} mice, with no differences between the two genetic backgrounds.
- XIV. *Frzb*^{-/-} mice muscles show more ALP+ cells albeit lower PDGFR α expression that might lead to a lower adipocyte differentiation capacity.

APPENDIX

APPENDIX I. Product references.

PRODUCT	MANUFACTURER	REFERENCE
2.5% Trypsin (10X), no phenol red	Life technologies	15090-046
2-Mercaptoethanol	Thermo Fisher Scientific	31350-010
2-Mercaptoethanol	Sigma Aldrich	M3148
2-Methylbutane for HPLC, chromasolv, = 99.5%	Thermo Fisher Scientific	270342-1L
Absolute ethanol	VWR Chemicals	20821.296
Acrylamide/Bis solution 30% , 29:1	Bio Rad	1610156
Alkaline phosphatase/ALPL antibody (B4-78) [Phycoerythrin]	R&D Systems a biotechnie brand	FAB1448P
Amersham hyperfilm ECL (18 × 24 cm)	GE Healthcare	28906836
Amersham™ Protran™ 0,45 µm nitrocellulose blotting membranes	GE Health Care Life Science	10600002
Ammonium persulfate, (NH ₄) ₂ S ₂ O ₈	Sigma-Aldrich	A3678
APC Rat IgG2a, κ Isotype control clone R35-95	BD Bioscience	551139
AutoMACS Running Buffer – MACS separation buffer	MACS Milteny Biotec	130-091-221
bisBenzimide H33258 (Hoechst)	Sigma-Aldrich	B2883
Bovine serum albumin lyophilised pH ~7	Biowest	P6154
Bromophenol blue	Panreac Applichem ITW Reagents	131165.1606
C2C12 cell line	ATCC	ATCC® CRL- 1772™
Cardiotoxin	Latoxan	L8102
CD140a (PDGFRA) monoclonal antibody (APA5), APC, eBioscience™	Thermo Fisher Scientific	17-1401-81
CD140b (PDGFRB) monoclonal antibody (APB5), PE, eBioscience™	Thermo Fisher Scientific	12-1402-81
CD31 (PECAM-1) monoclonal antibody (390), APC, eBioscience™	Thermo Fisher Scientific	17-0311-82
CD31 (PECAM-1) monoclonal antibody (390), APC, eBioscience™	Thermo Fisher Scientific	17-0311-82
CD45 monoclonal antibody (30-F11), FITC, eBioscience™	Thermo Fisher Scientific	11-0451-82
CD45 monoclonal antibody (30-F11), FITC, eBioscience™	Thermo Fisher Scientific	11-0451-82
CD56 MicroBeads, human	MACS Milteny Biotec	130-050-401
Chicken embryo extract	Bio-connect BV	CE-650-JL
Chloroform	Merck KGaA	102445
Collagenase D from <i>Clostridium histolyticum</i>	Roche	11088858001
cOmplete mini, EDTA free protease inhibitor cocktail tablets	Roche	11836170001
Dimethyl sulfoxide, Fisher BioReagents™	Fisher Scientific	10103483
DMEM, high glucose, GlutaMAX™ supplement	Thermo Fisher Scientific	61965-026
Donkey serum	VWR	BWSTS2170- 100
Dulbecco's phosphate buffered saline (1X)	Gibco	14190-094
Dulbecco's modified Eagle's medium with 4.5 g/l glucose with L-Glutamine	Lonza	BE12-604F
Dulbecco's phosphate buffered saline	Thermo Fisher Scientific	14190-004

E-64	Sigma Aldrich	E3132
Eosin yellowish hydroalcoholic solution 1% for clinical diagnosis	PanReac AppliChem ITW Reagents	251301.1611
Ethanol absolute	VWR Chemicals	20821.296
Falcon® 5 ml round bottom high clarity PP test tube, with snap cap, sterile	Corning	#352063
Falcon® 5 ml round bottom polystyrene test tube, with cell strainer snap cap	Corning	#352235
Falcon® 5 ml round bottom polystyrene test tube, with snap cap, sterile	Corning	#352054
Foetal Bovine Serum, qualified, E.U.-approved, South America origin	Thermo Fisher Scientific	10270-106
Filter-tips, 1000 µl (1024)	QUIAGEN	990352
FITC Mouse IgG2a, κ Isotype Control antibody clone G155-178	BD Bioscience	553456
Fluoro-gel (with tris buffer)	Electron Microscopy Sciences	17985-10
Fungizone® antimycotic 20ml	Life technologies	15290-018
Gelatine from porcine skin	Sigma Aldrich	G1890
Gentamicin solution	Sigma Aldrich	G1272
Gerhard menzel cover glasses round pure white 12 mm	Thermo Fisher Scientific	CB00120ra1
Glycerol technical grade	Panreac AppliChem ITW Reagents	211339.1211
Glycine	Sigma Aldrich	G8898-1KG
Glycine	Bio Rad	161-0718
Hank's Balanced Salt Solution with Ca ²⁺ and Mg ²⁺	Thermo Fisher Scientific	24020-083
Hank's Balanced Salt Solution without Ca ²⁺ and Mg ²⁺	Thermo Fisher Scientific	14170-088
Harrison hematoxylin solution for clinical diagnosis	PanReac AppliChem ITW Reagents	253949.1610
Hepes	Sigma Aldrich	H3375
High-capacity cDNA reverse transcription kit	Thermo Fisher Scientific	4368814
Hoechst 33342 solution (20 mM)	Thermo Fisher Scientific	62249
Horse Serum, heat inactivated, New Zealand origin	Thermo Fisher Scientific	26050-070
Human EGF	Peprotech	AF-100-15
Human FGF	Peprotech	100-18-B
Hydrochloric acid 37% for analysis, ACS, ISO	Panreac AppliChem ITW Reagents	1.310.201.211
IgG1, K Mouse, PE, Clone: P3.6.2.8.1, isotype control, eBioscience™	Affymetrix eBioscience, Thermo Fisher Scientific	12-4714-81
Insulin Human 25 mg	Sigma Aldrich	I2643
iTaq™ Universal SYBR® Green Supermix, 500x 20 µl rxns	Bio Rad	1725121

L-Glutamine 100X 20ml (200mM)	Life technologies	25030032
Macs LS Columns	Milteny Biotec	130-042-401
MEDIUM 199 with Earle's balanced salt solution with L-Glutamine and Hepes	Lonza	BE12-117F
MEM Non-essential amino acids solution (100X)	Thermo Fisher Scientific	11140-035
Methanol (Reag. Ph. Eur.) for UHPLC supergradient, ACS	Panreac Applichem ITW Reagents	221091.1612
miRNeasy Mini Kit	QUIAGEN	217004
MX35 ultra microtome blade 34°/80 mm	Thermo Fisher Scientific	3053835
N,N,N',N'-Tetramethylethylenediamine, BioReagent, for molecular biology, ≥ 99%	Sigma Aldrich	T7024
Na·Deoxycholate	Sigma Aldrich	D6750
NADH Grade I, disodium salt	Sigma Aldrich	10107735001
Nimatek 100 mg/ml	Eurovet animal health	804132
Nitrotetrazolium Blue chloride	Sigma Aldrich	N6876-100MG
Nunc* cell scrapers handle length 23 cm	Thermo Fisher Scientific	179693
Oil red O	Sigma Aldrich	O0625
Pancreatin from porcine pancreas	Sigma Aldrich	P3292
Paraformaldehyde 4% aqueous solution, em grade	Electron Microscopy Sciences	157-4-100
PE Rat IgG2a, κ Isotype control clone R35-95 (RUO)	BD Bioscience	553930
Penicillin-Streptomycin (10,000 U/mL)	Thermo Fisher Scientific	15140-122
Petroleum ether 30-40 pure	Panreac Applichem ITW Reagents	A0760
Phenylmethanesulfonyl fluoride (PMSF)	Sigma Aldrich	P7626
Ponceau S Solution	Sigma Aldrich	P7170
Precision plus protein™ kaleidoscope™ prestained protein standars	Bio Rad	1610375
Propan-2-ol, isopropyl alcohol	PanReac AppliChem ITW Reagents	131090.1611
QIAzol® lysis reagent	QIAgen	79306
Quick start™ bovine serum albumin standard	Bio Rad	500-0206
Quick start™ bradford 1x dye reagent	Bio Rad	500-0205
Quick Start™ bradford protein assay Kit 1	Bio Rad	#500-0201
RiboCellin siRNA delivery reagent, 1.0 ml	Buldog Bio	RC1000
RNase Inhibitor	Life technologies	N8080119
Rotor adapters (10 x 24)	QUIAGEN	990394
SDS for molecular biology	Panreac Applichem ITW Reagents	A2263.0100
Shandon™ Consul-Mount™	Thermo Fisher Scientific	9990441
siCD9	Thermo Fisher Scientific	s2598
siFRZB	Thermo Fisher Scientific	s5369
SignalFire™ Plus ECL Reagent	Cell Signaling Technologies	12630S
siITGB1BP2	Thermo Fisher Scientific	s25536
Silencer® Negative Control No. 1 siRNA (50 µM)	Life technologies	AM4611

Skim milk powder	Sigma Aldrich	70166
Sodium azide, NaN ₃	Sigma Aldrich	769320
Sodium chloride for analysis ACS, ISO, NaCl	Panreac Applichem ITW Reagents	131659.122
Sodium fluoride, NaF	Sigma Aldrich	S6776
Sodium orthovanadate, Na ₃ O ₄ V	Sigma Aldrich	S6508
Sodium pyrophosphate tetra basic decahydrate	Sigma Aldrich	S6422
Sodium pyruvate (100 mM)	Thermo Fisher Scientific	11360-039
StemPro [®] adipogenesis differentiation kit	Thermo Fisher Scientific	A10070-01
Superfrost [™] Plus microscope slides	Thermo Fisher Scientific	J1800AMNZ
TaqMan [™] Gene expression master mix	Thermo Fisher Scientific	4369514
Tissue-Tek Cryomold biopsy 10 mm x 10 mm x 5 mm	Sakura Finetek USA INC	4565
Tissue-Tek [®] O.C.T. Compound, Sakura [®] Finetek	Sakura Finetek USA INC	4583
Tris (USP,BP,Ph,Eur) pure pharma grade	Panreac Applichem ITW Reagents	141940.1211
Trlton [™] X-100	Sigma Aldrich	T8787
Trypan Blue Solution 0.4%, liquid, sterile-filtered, suitable for cell culture	Sigma Aldrich	T8154
Trypsin (10X) 2.5%, no phenol red	Thermo Fisher Scientific	15090-046
Tween [®] 20	Merck Millipore	8.22184.0500
UltraPure [™] distilled water DNase/RNase free	Invitrogen	10977-035
Urea	Panreac Applichem ITW Reagents	141754
Vacutainer [®] K2E (EDTA) 18.0 mg plus blood collection Tubes	BD Bioscience	367525
Vacutainer [®] SST II advance plus Blood collection tubes	BD Bioscience	367953
Vetergesic multidosis 0,3mg/ml	Ecuphar	
Whatman [™] 3mm CHR	GE Health Care Life Science	3030-917
Xylene	Oppac s.a	1330-20-7
XYL-M 2% (Xylazine hydrochloride)	VMD	
β-Glycerophosphate disodium salt hydrate	Sigma Aldrich	G9422

APPENDIX II: Material and methods supplementary material.

Table 1. Mice information.

Number	Mother	Father	Code	Sex	Mice strain	Backcross	Birth day	Use	Used on	Age	Genotype
47440	F-KO-3/2166	F-KO-3/2195	F-KO-3/2200	f	C57BL/6	19b	03/08/2016	Muscle isolation	20/10/2016	11 weeks + 1 day	KO
47443	F-KO-3/2166	F-KO-3/2195	F-KO-3/2202	f	C57 BL/6	19b	03/08/2016	Muscle isolation	20/10/2016	11 weeks + 1 day	KO
47444	F-KO-3/2166	F-KO-3/2195	F-KO-3/2204	f	C57BL/6	19b	03/08/2016	Muscle isolation	20/10/2016	11 weeks + 1 day	KO
47448	F-KO-3/2166	F-KO-3/2195	F-KO-3/2206	f	C57BL/6	19b	03/08/2016	Muscle isolation	20/10/2016	11 weeks + 1 day	KO
47439	F-KO-3/2166	F-KO-3/2195	F-KO-3/2237	m	C57BL/6	19b	03/08/2016	Muscle isolation	20/10/2016	11 weeks + 1 day	KO
47441	F-KO-3/2166	F-KO-3/2195	F-KO-3/2239	m	C57BL/6	19b	03/08/2016	Muscle isolation	20/10/2016	11 weeks + 1 day	KO
47442	F-KO-3/2166	F-KO-3/2195	F-KO-3/2241	m	C57BL/6	19b	03/08/2016	Muscle isolation	20/10/2016	11 weeks + 1 day	KO
47445	F-KO-3/2166	F-KO-3/2195	F-KO-3/2243	m	C57BL/6	19b	03/08/2016	Muscle isolation	20/10/2016	11 weeks + 1 day	KO
47446	F-KO-3/2166	F-KO-3/2195	F-KO-3/2245	m	C57BL/6	19b	03/08/2016	Muscle isolation	20/10/2016	11 weeks + 1 day	KO
47447	F-KO-3/2166	F-KO-3/2195	F-KO-3/2247	m	C57BL/6	19b	03/08/2016	Muscle isolation	20/10/2016	11 weeks + 1 day	KO
47449	F-KO-3/2166	F-KO-3/2195	F-KO-3/2249	m	C57BL/6	19b	03/08/2016	Muscle isolation	20/10/2016	11 weeks + 1 day	KO
48868	F-KO-3/2178	F-KO-3/2225	F-KO-3/2361	m	C57BL/6	20b	12/12/2016	Muscle isolation	24/02/2017	10 weeks + 4 days	KO
48872	F-KO-3/2178	F-KO-3/2225	F-KO-3/2365	m	C57BL/6	20b	12/12/2016	Muscle isolation	24/02/2017	10 weeks + 4 days	KO
49245	F-KO-3/2210	F-KO-3/2231	F-KO-3/2328	f	C57BL/6	19b	06/01/2016	Muscle isolation	17/03/2017	10 weeks	KO
								Wire test	17/02/2017	6 weeks	
49317	F-KO-3/2180	F-KO-3/2225	F-KO-3/2413	m	C57BL/6	20b	13/01/2017	Muscle isolation	24/03/2017	10 weeks	KO
								Wire test	17/02/2017	5 weeks	
48545				f	C57BL/6	100%	22/09/2016	Muscle isolation	02/12/2016	10 weeks	WT
48546				f	C57BL/6	100%	22/09/2016	Muscle isolation	02/12/2016	10 weeks	WT
48547				f	C57BL/6	100%	22/09/2016	Muscle isolation	02/12/2016	10 weeks	WT
48548				f	C57BL/6	100%	22/09/2016	Muscle isolation	02/12/2016	10 weeks	WT
48549				f	C57BL/6	100%	22/09/2016	Muscle isolation	02/12/2016	10 weeks	WT
48550				m	C57BL/6	100%	22/09/2016	Muscle isolation	02/12/2016	10 weeks	WT
48551				m	C57BL/6	100%	22/09/2016	Muscle isolation	02/12/2016	10 weeks	WT
48552				m	C57BL/6	100%	22/09/2016	Muscle isolation	02/12/2016	10 weeks	WT
48553				m	C57BL/6	100%	22/09/2016	Muscle isolation	02/12/2016	10 weeks	WT
48554				m	C57BL/6	100%	22/09/2016	Muscle isolation	02/12/2016	10 weeks	WT
48555				m	C57BL/6	100%	22/09/2016	Muscle isolation	02/12/2016	10 weeks	WT
48556				m	C57BL/6	100%	22/09/2016	Muscle isolation	02/12/2016	10 weeks	WT
48557				m	C57BL/6	100%	22/09/2016	Muscle isolation	02/12/2016	10 weeks	WT
48558				m	C57BL/6	100%	22/09/2016	Muscle isolation	02/12/2016	10 weeks	WT
48559				m	C57BL/6	100%	22/09/2016	Muscle isolation	02/12/2016	10 weeks	WT
48133	F-KO-3/2170	F-KO-3/2195	F-KO-3/2262	f	C57BL/6	19b	07/10/2016	Muscle cell extraction	08/11/2016	4 weeks + 4 days	KO
48134	F-KO-3/2170	F-KO-3/2195	F-KO-3/2291	m	C57BL/6	19b	07/10/2016	Muscle cell extraction	08/11/2016	4 weeks + 4 days	KO

48135	F-KO-3/2170	F-KO-3/2195	F-KO-3/2293	m	C57BL/6	19b	07/10/2016	Muscle cell extraction	08/11/2016	4 weeks + 4 days	KO
48136	F-KO-3/2170	F-KO-3/2195	F-KO-3/2264	f	C57BL/6	19b	07/10/2016	Muscle cell extraction	08/11/2016	4 weeks + 4 days	KO
48137	F-KO-3/2170	F-KO-3/2195	F-KO-3/2295	m	C57BL/6	19b	07/10/2016	Muscle cell extraction	08/11/2016	4 weeks + 4 days	KO
48138	F-KO-3/2170	F-KO-3/2195	F-KO-3/2266	f	C57BL/6	19b	07/10/2016	Muscle cell extraction	08/11/2016	4 weeks + 4 days	KO
48139	F-KO-3/2170	F-KO-3/2195	F-KO-3/2297	m	C57BL/6	19b	07/10/2016	Muscle cell extraction	08/11/2016	4 weeks + 4 days	KO
48140	F-KO-3/2170	F-KO-3/2195	F-KO-3/2299	m	C57BL/6	19b	07/10/2016	Muscle cell extraction	08/11/2016	4 weeks + 4 days	KO
48216				f	C57BL/6	100%	13/10/2016	Muscle cell extraction	08/11/2016	3 weeks + 3 days	WT
48217				f	C57BL/6	100%	13/10/2016	Muscle cell extraction	08/11/2016	3 weeks + 3 days	WT
48218				f	C57BL/6	100%	13/10/2016	Muscle cell extraction	08/11/2016	3 weeks + 3 days	WT
48219				f	C57BL/6	100%	13/10/2016	Muscle cell extraction	08/11/2016	3 weeks + 3 days	WT
48220				m	C57BL/6	100%	13/10/2016	Muscle cell extraction	08/11/2016	3 weeks + 3 days	WT
48221				m	C57BL/6	100%	13/10/2016	Muscle cell extraction	08/11/2016	3 weeks + 3 days	WT
48222				m	C57BL/6	100%	13/10/2016	Muscle cell extraction	08/11/2016	3 weeks + 3 days	WT
48223				m	C57BL/6	100%	13/10/2016	Muscle cell extraction	08/11/2016	3 weeks + 3 days	WT
48370	F-KO-3/2160	F-KO-3/2231	F-KO-3/2268	f	C57BL/6	19b	31/10/2016	Muscle cell extraction	01/12/2016	4 weeks + 3 days	KO
48371	F-KO-3/2160	F-KO-3/2231	F-KO-3/2305	m	C57BL/6	19b	31/10/2016	Muscle cell extraction	01/12/2016	4 weeks + 3 days	KO
48372	F-KO-3/2160	F-KO-3/2231	F-KO-3/2307	m	C57BL/6	19b	31/10/2016	Muscle cell extraction	01/12/2016	4 weeks + 3 days	KO
48373	F-KO-3/2160	F-KO-3/2231	F-KO-3/2270	f	C57BL/6	19b	31/10/2016	Muscle cell extraction	01/12/2016	4 weeks + 3 days	KO
48374	F-KO-3/2160	F-KO-3/2231	F-KO-3/2272	f	C57BL/6	19b	31/10/2016	Muscle cell extraction	01/12/2016	4 weeks + 3 days	KO
48375	F-KO-3/2160	F-KO-3/2231	dead	f	C57BL/6	19b	31/10/2016	Muscle cell extraction	01/12/2016	4 weeks + 3 days	KO
48376	F-KO-3/2160	F-KO-3/2231	F-KO-3/2309	m	C57BL/6	19b	31/10/2016	Muscle cell extraction	01/12/2016	4 weeks + 3 days	KO
48479				f	C57BL/6	100%	03/11/2016	Muscle cell extraction	01/12/2016	4 weeks	WT
48480				f	C57BL/6	100%	03/11/2016	Muscle cell extraction	01/12/2016	4 weeks	WT
48481				f	C57BL/6	100%	03/11/2016	Muscle cell extraction	01/12/2016	4 weeks	WT
48482				f	C57BL/6	100%	03/11/2016	Muscle cell extraction	01/12/2016	4 weeks	WT
48483				m	C57BL/6	100%	03/11/2016	Muscle cell extraction	01/12/2016	4 weeks	WT
48484				m	C57BL/6	100%	03/11/2016	Muscle cell extraction	01/12/2016	4 weeks	WT
48485				m	C57BL/6	100%	03/11/2016	Muscle cell extraction	01/12/2016	4 weeks	WT
47659	F-KO-3/2170	F-KO-3/2195	F-KO-3/2224	f	C57BL/6	19b	29/08/2016	Catwalk 8weeks	24/10/2016	8 weeks	KO
								Catwalk 10weeks	07/11/2016	10weeks	
								CTX injection	09/11/2016	10 weeks + 2 days	
								Muscles freezing	07/12/2016	CTX + 4 weeks	
47660			F-KO-3/2226	f	C57BL/6	19b	29/08/2016	Catwalk 8weeks	24/10/2016	8 weeks	KO
								Catwalk 10weeks	07/11/2016	10 weeks	
								CTX injection	09/11/2016	10 weeks + 2 days	
								Muscles freezing	07/12/2016	CTX + 4 weeks	

47661			F-KO-3/2228	f	C57BL/6	19b	29/08/2016	Catwalk 8weeks	24/10/2016	8 weeks	KO
								Catwalk 10weeks	07/11/2016	10 weeks	
								CTX injection	09/11/2016	10 weeks + 2 days	
								Muscles freezing	07/12/2016	CTX + 4 weeks	
47662			F-KO-3/2253	m	C57BL/6	19b	29/08/2016	Catwalk 8weeks	24/10/2016	8 weeks	KO
								Catwalk 10weeks	07/11/2016	10 weeks	
								CTX injection	09/11/2016	10 weeks + 2 days	
								Muscles freezing	07/12/2016	CTX + 4 weeks	
47663			F-KO-3/2230	f	C57BL/6	19b	29/08/2016	Catwalk 8weeks	24/10/2016	8 weeks	KO
								Catwalk 10weeks	07/11/2016	10 weeks	
								CTX injection	09/11/2016	10 weeks + 2 days	
								Muscles freezing	23/11/2016	CTX + 2 weeks	
47664			F-KO-3/2232	f	C57BL/6	19b	29/08/2016	Catwalk 8weeks	24/10/2016	8 weeks	KO
								Catwalk 10weeks	07/11/2016	10 weeks	
								CTX injection	09/11/2016	10 weeks + 2 days	
								Muscles freezing	23/11/2016	CTX + 2 weeks	
47665			F-KO-3/2255	m	C57BL/6	19b	29/08/2016	Catwalk 8weeks	24/10/2016	8 weeks	KO
								Catwalk 10weeks	07/11/2016	10 weeks	
								CTX injection	09/11/2016	10weeks+2 days	
								Muscles freezing	23/11/2016	CTX + 2 weeks	
48570	F-KO-3/2170	F-KO-3/2195	F-KO-3/2300	f	C57BL/6	19b	14/11/2016	Catwalk 8weeks	09/01/2017	8 weeks	KO
								Catwalk 10weeks	23/01/2017	10 weeks	
								CTX injection	24/01/2017	10 weeks + 1day	
								Muscles freezing	27/01/2017	CTX+ 3 days	
48571	F-KO-3/2170	F-KO-3/2195	F-KO-3/2302	f	C57BL/6	19b	14/11/2016	Catwalk 8weeks	09/01/2017	8 weeks	KO
								Catwalk 10weeks	23/01/2017	10 weeks	
								CTX injection	24/01/2017	10 weeks + 1day	
								Muscles freezing	31/01/201	CTX + 1 week	
48572	F-KO-3/2170	F-KO-3/2195	F-KO-3/2304	f	3	19b	14/11/2016	DEAD			KO
48573	F-KO-3/2170	F-KO-3/2195	F-KO-3/2306	f	C57BL/6	19b	14/11/2016	Catwalk 8weeks	09/01/2017	8 weeks	KO
								Catwalk 10weeks	23/01/2017	10 weeks	
								CTX injection	24/01/2017	10 weeks + 1 day	
								Muscles freezing	07/02/2017	CTX + 2weeks	

48576	F-KO-3/2170	F-KO-3/2195	F-KO-3/2308	f	C57BL/6	19b	14/11/2016	Catwalk 8weeks	09/01/2017	8 weeks	KO
								Catwalk 10weeks	23/01/2017	10 weeks	
								CTX injection	24/01/2017	10 weeks + 1day	
								Muscles freezing	27/01/2017	CTX+ 3 days	
48569	F-KO-3/2170	F-KO-3/2195	F-KO-3/2337	m	C57BL/6	19b	14/11/2016	Catwalk 8weeks	09/01/2017	8 weeks	KO
								Catwalk 10weeks	23/01/2017	10 weeks	
								CTX injection	24/01/2017	10 weeks+ 1day	
								Muscles freezing	27/01/2017	CTX+ 3 days	
48574	F-KO-3/2170	F-KO-3/2195	F-KO-3/2339	m	C57BL/6	19b	14/11/2016	Catwalk 8weeks	09/01/2017	8 weeks	KO
								Catwalk 10weeks	23/01/2017	10 weeks	
								CTX injection	24/01/2017	10 weeks+ 1day	
								Muscles freezing	31/01/2017	CTX + 1 week	
48575	F-KO-3/2170	F-KO-3/2195	F-KO-3/2341	m	C57BL/6	19b	14/11/2016	Catwalk 8weeks	09/01/2017	8 weeks	KO
								Catwalk 10weeks	23/01/2017	10 weeks	
								CTX injection	24/01/2017	10 weeks+ 1 day	
								Muscles freezing	31/01/2017	CTX + 1 week	
48577	F-KO-3/2170	F-KO-3/2195	F-KO-3/2343	m	C57BL/6	19b	14/11/2016	Catwalk 8weeks	09/01/2017	8 weeks	KO
								Catwalk 10weeks	23/01/2017	10 weeks	
								CTX injection	24/01/2017	10 weeks+ 1day	
								Muscles freezing	21/02/2017	CTX + 4 weeks	
48720	F-KO-3/2160	F-KO-3/2219	F-KO-3/2347	m	C57BL/6	19b	30/11/2016	Catwalk 8 weeks	23/01/2017	7 weeks + 5 days	KO
								CTX injection	09/02/2017	10 weeks + 1 day	
								Muscle freezin	24/02/2017	CTX + 2 weeks	
48721	F-KO-3/2160	F-KO-3/2219	F-KO-3/2349	m	C57BL/6	19b	30/11/2016	Catwalk 8 weeks	23/01/2017	7 weeks + 5 days	KO
								CTX injection	09/02/2017	10 weeks + 1 day	
								Muscle freezin	09/03/2017	CTX + 4 weeks	
48722	F-KO-3/2160	F-KO-3/2219	F-KO-3/2351	m	C57BL/6	19b	30/11/2016	Catwalk 8 weeks	23/01/2017	7 weeks + 5 days	KO
								CTX injection	09/02/2017	10 weeks + 1 day	
								Muscle freezin	09/03/2017	CTX + 4 weeks	
49475	F-KO-3/2254	F-KO-3/2273		f	C57BL/6	20b	23/01/2017	Catwalk 8 weeks	20/03/2017	8 weeks	KO
								Wire test	01/03/2017	5 weeks + 2 days	
49476	F-KO-3/2254	F-KO-3/2273		f	C57BL/6	20b	23/01/2017	Catwalk 8 weeks	20/03/2017	8 weeks	KO
								Wire test	01/03/2017	5 weeks + 2 days	

49477	F-KO-3/2254	F-KO-3/2273		m	C57BL/6	20b	23/01/2017	Catwalk 8 weeks	20/03/2017	8 weeks	KO
								Wire test	01/03/2017	5 weeks + 2 days	
49478	F-KO-3/2254	F-KO-3/2273		f	C57BL/6	20b	23/01/2017	Catwalk 8 weeks	20/03/2017	8 weeks	KO
								Wire test	01/03/2017	5 weeks + 2 days	
49479	F-KO-3/2254	F-KO-3/2273		f	C57BL/6	20b	23/01/2017	Catwalk 8 weeks	20/03/2017	8 weeks	KO
								Wire test	01/03/2017	5 weeks + 2 days	
49576	F-KO-3/2288	F-KO-3/2219	F-KO-3/2364	f	C57BL/6	20b	06/02/2017	catwalk 10 weeks	18/04/2017	10 weeks + 1 day	KO
49577	F-KO-3/2288	F-KO-3/2219	F-KO-3/2435	m	C57BL/6	20b	06/02/2017	catwalk 10 weeks	18/04/2017	10 weeks + 1 day	KO
49578	F-KO-3/2288	F-KO-3/2219	dead	m	C57BL/6	20b	06/02/2017	catwalk 10 weeks	18/04/2017	10 weeks + 1 day	KO
49579	F-KO-3/2288	F-KO-3/2219	F-KO-3/2439	m	C57BL/6	20b	06/02/2017	catwalk 10 weeks	18/04/2017	10 weeks + 1 day	KO
49580	F-KO-3/2288	F-KO-3/2219	F-KO-3/2366	f	C57BL/6	20b	06/02/2017	catwalk 10 weeks	18/04/2017	10 weeks + 1 day	KO
49581	F-KO-3/2166	F-KO-3/2195	F-KO-3/2368	f	C57BL/6	19b	06/02/2017	catwalk 10 weeks	18/04/2017	10 weeks + 1 day	KO
49582	F-KO-3/2166	F-KO-3/2195	F-KO-3/2441	m	C57BL/6	19b	06/02/2017	catwalk 10 weeks	18/04/2017	10 weeks + 1 day	KO
49583	F-KO-3/2166	F-KO-3/2195	F-KO-3/2370	f	C57BL/6	19b	06/02/2017	catwalk 10 weeks	18/04/2017	10 weeks + 1 day	KO
49584	F-KO-3/2166	F-KO-3/2195	F-KO-3/2443	m	C57BL/6	19b	06/02/2017	catwalk 10 weeks	18/04/2017	10 weeks + 1 day	KO
49585	F-KO-3/2166	F-KO-3/2195	F-KO-3/2372	f	C57BL/6	19b	06/02/2017	catwalk 10 weeks	18/04/2017	10 weeks + 1 day	KO
48951				f	C57BL/6	100%	17/11/2016	Catwalk 8weeks	12/01/2017	8 weeks	WT
								Catwalk 10weeks	26/01/2017	10 weeks	WT
								CTX injection	27/01/2017	10 weeks + 1day	WT
								Muscles freezing	03/02/2017	CTX + 1 week	WT
48952				f	C57BL/6	100%	17/11/2016	Catwalk 8weeks	12/01/2017	8 weeks	WT
								Catwalk 10weeks	26/01/2017	10 weeks	WT
								CTX injection	27/01/2017	10 weeks + 1 day	WT
								Muscles freezing	03/02/2017	CTX + 1 week	WT
48953				f	C57BL/6	100%	17/11/2016	Catwalk 8weeks	12/01/2017	8 weeks	WT
								Catwalk 10weeks	26/01/2017	10 weeks	WT
								CTX injection	27/01/2017	10 weeks + 1 day	WT
								Muscles freezing	10/02/2017	CTX + 2 weeks	WT
48954				f	C57BL/6	100%	17/11/2016	Catwalk 8weeks	12/01/2017	8 weeks	WT
								Catwalk 10weeks	26/01/2017	10 weeks	WT
								CTX injection	27/01/2017	10 weeks + 1 day	WT
								Muscles freezing	30/01/2017	CTX + 3 days	WT

48955				f	C57BL/6	100%	17/11/2016	Catwalk 8weeks	12/01/2017	8 weeks	WT
								Catwalk 10weeks	26/01/2017	10 weeks	WT
								CTX injection	27/01/2017	10 weeks + 1 day	WT
								Muscles freezing	30/01/2017	CTX + 3 days	WT
48956				f	C57BL/6	100%	17/11/2016	Catwalk 8weeks	12/01/2017	8 weeks	WT
								Catwalk 10weeks	26/01/2017	10 weeks	WT
								CTX injection	27/01/2017	10 weeks + 1 day	WT
								Muscles freezing	24/02/2017	CTX + 4 weeks	WT
48957				f	C57BL/6	100%	17/11/2016	Catwalk 8weeks	12/01/2017	8 weeks	WT
								Catwalk 10weeks	26/01/2017	10 weeks	WT
								CTX injection	27/01/2017	10 weeks + 1 day	WT
								Muscles freezing	24/02/2017	CTX + 4 weeks	WT
48958				f	C57BL/6	100%	17/11/2016	Catwalk 8weeks	12/01/2017	8 weeks	WT
								Catwalk 10weeks	26/01/2017	10 weeks	WT
								CTX injection	27/01/2017	10 weeks + 1 day	WT
								Muscles freezing	24/02/2017	CTX+ 4 weeks	WT
48959				f	C57BL/6	100%	17/11/2016	Catwalk 8weeks	12/01/2017	8 weeks	WT
								Catwalk 10weeks	26/01/2017	10 weeks	WT
								CTX injection	27/01/2017	10 weeks + 1 day	WT
								Muscles freezing	10/02/2017	CTX+ 2 weeks	WT
48960				f	C57BL/6	100%	17/11/2016	Catwalk 8weeks	12/01/2017	8 weeks	WT
								Catwalk 10weeks	26/01/2017	10 weeks	WT
								CTX injection	27/01/2017	10 weeks+ 1day	WT
								Muscles freezing	24/02/2017	CTX + 4 weeks	WT
48961				m	C57BL/6	100%	17/11/2016	Catwalk 8weeks	12/01/2017	8 weeks	WT
								Catwalk 10weeks	26/01/2017	10 weeks	WT
								CTX injection	27/01/2017	10 weeks+ 1 day	WT
								Muscles freezing	30/01/2017	CTX + 3 days	WT
48962				m	C57BL/6	100%	17/11/2016	Catwalk 8weeks	12/01/2017	8 weeks	WT
								Catwalk 10weeks	26/01/2017	10 weeks	WT
								CTX injection	27/01/2017	10 weeks + 1day	WT
								Muscles freezing	30/01/2017	CTX+ 3 days	WT

48963				m	C57BL/6	100%	17/11/2016	Catwalk 8weeks	12/01/2017	8 weeks	WT
								Catwalk 10weeks	26/01/2017	10 weeks	WT
								CTX injection	27/01/2017	10 weeks + 1day	WT
								Muscles freezing	10/02/2017	CTX + 2 weeks	WT
48964				m	C57BL/6	100%	17/11/2016	Catwalk 8weeks	12/01/2017	8 weeks	WT
								Catwalk 10weeks	26/01/2017	10 weeks	WT
								CTX injection	27/01/2017	10 weeks+ 1 day	WT
								Muscles freezing	03/02/2017	CTX + 1 week	WT
48965				m	C57BL/6	100%	17/11/2016	Catwalk 8weeks	12/01/2017	8 weeks	WT
								Catwalk 10weeks	26/01/2017	10 weeks	WT
								CTX injection	27/01/2017	10 weeks+ 1 day	WT
								Muscles freezing	03/02/2017	CTX + 1 week	WT
48966				m	C57BL/6	100%	17/11/2016	Catwalk 8weeks	12/01/2017	8 weeks	WT
								Catwalk 10weeks	26/01/2017	10 weeks	WT
								CTX injection	27/01/2017	10 weeks+ 1 day	WT
								DEAD			WT
48967				m	C57BL/6	100%	17/11/2016	Catwalk 8weeks	12/01/2017	8 weeks	WT
								Catwalk 10weeks	26/01/2017	10 weeks	WT
								CTX injection	27/01/2017	10 weeks + 1 day	WT
								Muscles freezing	24/02/2017	CTX+ 4 weeks	WT
48968				m	C57BL/6	100%	17/11/2016	Catwalk 8weeks	12/01/2017	8 weeks	WT
								Catwalk 10weeks	26/01/2017	10 weeks	WT
								CTX injection	27/01/2017	10 weeks+ 1 day	WT
								Muscles freezing	24/02/2017	CTX+ 4 weeks	WT
48969				m	C57BL/6	100%	17/11/2016	Catwalk 8weeks	12/01/2017	8 weeks	WT
								Catwalk 10weeks	26/01/2017	10 weeks	WT
								CTX injection	27/01/2017	10 weeks + 1 day	WT
								Muscles freezing	10/02/2017	CTX + 2 weeks	WT
48970				m	C57BL/6	100%	17/11/2016	Catwalk 8weeks	12/01/2017	8 weeks	WT
								Catwalk 10weeks	26/01/2017	10 weeks	WT
								CTX injection	27/01/2017	10 weeks + 1 day	WT
								Muscles freezing	24/02/2017	CTX + 4 weeks	WT
48940	F-KO-3/2184	F-KO-3/2223	F-KO-3/2367	m	C57BL/6	20b	16/12/2017	Treadmill no run	06/02/2017	7 weeks + 3 days	KO
48947	F-KO-3/2184	F-KO-3/2223	F-KO-3/2375	m	C57BL/7	20b	16/12/2017	Treadmill no run	06/02/2017	7 weeks + 3 days	KO
48949	F-KO-3/2184	F-KO-3/2223	F-KO-3/2320	f	C57BL/8	20b	16/12/2017	Treadmill no run	06/02/2017	7 weeks + 3 days	KO

48950	F-KO-3/2184	F-KO-3/2223	F-KO-3/2377	m	C57BL/9	20b	16/12/2017	Treadmill run	06/02/2017	7 weeks + 3 days	KO
49121	F-KO-3/2166	F-KO-3/2195	F-KO-3/2326	f	C57BL/6	19b	26/12/2016	Treadmill no run	06/02/2017	6 weeks	KO
								Wire test	03/02/2017	5 weeks + 4 days	
49122	F-KO-3/2166	F-KO-3/2195	F-KO-3/2401	m	C57BL/6	19b	26/12/2016	Treadmill no run	06/02/2017	6 weeks	KO
								Wire test	03/02/2017	5 weeks + 4 days	
49123	F-KO-3/2166	F-KO-3/2195	F-KO-3/2403	m	C57BL/6	19b	26/12/2016	Treadmill run	06/02/2017	6 weeks	KO
								Wire test	03/02/2017	5 weeks + 4 days	
49124	F-KO-3/2166	F-KO-3/2195	F-KO-3/2405	m	C57BL/6	19b	26/12/2016	Treadmill run	06/02/2017	6 weeks	KO
								Wire test	03/02/2017	5 weeks + 4 days	
49125	F-KO-3/2166	F-KO-3/2195	F-KO-3/2407	m	C57BL/6	19b	26/12/2016	Treadmill run	06/02/2017	6 weeks	KO
								Wire test	03/02/2017	5 weeks + 4 days	
49126	F-KO-3/2166	F-KO-3/2195	F-KO-3/2409	m	C57BL/6	19b	26/12/2016	Treadmill run	06/02/2017	6 weeks	KO
								Wire test	03/02/2017	5 weeks + 4 days	
49326				m	C57BL/6	100%	28/12/2016	Treadmill no run	06/02/2017	5 weeks + 5 days	WT
								Wire test	03/02/2017	5 weeks + 2 days	
49327				m	C57BL/6	100%	28/12/2016	Treadmill no run	06/02/2017	5 weeks + 5 days	WT
								Wire test	03/02/2017	5 weeks + 2 days	
49328				m	C57BL/6	100%	28/12/2016	Treadmill no run	06/02/2017	5 weeks + 5 days	WT
								Wire test	03/02/2017	5 weeks + 2 days	
49329				m	C57BL/6	100%	28/12/2016	Treadmill no run	06/02/2017	5 weeks + 5 days	WT
								Wire test	03/02/2017	5 weeks + 2 days	
49330				m	C57BL/6	100%	28/12/2016	Treadmill no run	06/02/2017	5 weeks + 5 days	WT
								Wire test	03/02/2017	5 weeks + 2 days	
49331				m	C57BL/6	100%	28/12/2016	Treadmill no run	06/02/2017	5 weeks + 5 days	WT
								Wire test	03/02/2017	5 weeks + 2 days	
49332				m	C57BL/6	100%	28/12/2016	Treadmill no run	06/02/2017	5 weeks + 5 days	WT
								Wire test	03/02/2017	5 weeks + 2 days	
49333				m	C57BL/6	100%	28/12/2016	Treadmill no run	06/02/2017	5 weeks + 5 days	WT
								Wire test	03/02/2017	5 weeks + 2 days	
49334				m	C57BL/6	100%	28/12/2016	Treadmill no run	06/02/2017	5 weeks + 5 days	WT
								Wire test	03/02/2017	5 weeks + 2 days	

Table 2. Custom-designed SYBR Green panel gene list.

Gene name	Gene symbol	Amplicon sequence	Amplicon length (bp)
Muscle specific genes			
Myosin, heavy polypeptide 1, skeletal muscle, adult	<i>Myh1</i>	CAAGTGAGTGAGCTGAAGACCAAGGAGGAGGAACA GCAGCGGCTGATCAATGAGCTGACTGCGCAGAGGG GGCGTCTGCAGACGGAGTCAGGTGAATACTCACGCC AGCTAGA	113
Myosin, heavy polypeptide 2, skeletal muscle, adult	<i>Myh2</i>	AACACGAGAGACGAGTGAAGGAGCTTACTTACCAGA CAGAAGAAGACCGAAAAAATATTCTCAGGCTTCAGG ATTTGGTGGATAAACTCCAGGCAAAAGTAAAATCTTA CAAGAGACAAGCTGAGGAGGCTGAGGAACAATCCA ACACAAATCTATCCAAGTTCCG	166
Myosin, heavy polypeptide 4, skeletal muscle	<i>Myh4</i>	CAGAAATCCGGGTTGAAGACTCTGGCTTTCCTATTTT CTGGGGGACAAGCTGCGGAAGCAGAGGGCGGCGGT GGAAAGAAAGGTGGCAAGAAGAAGGTTCTTCTTTC CAGACCGTGTGAGCTCTTTCAGGGAGAATTTAAATA AGCTGATGACCAACTTGAAGAGCACCCACCCCACTT TGTCAGATGCCTCATTCC	200
Paired box gene 7	<i>Pax7</i>	ACTCGGGTTGCTAAGGATGCTCATGACCTGAGGAGA CAGGCCATTGCTGACAGGGTTCAT	60
Deregulated genes in LGMD2A patients' muscles (Sáenz et al., 2008; De la Torre et al., 2009)			
Calpain 3	<i>Capn3</i>	ATTCATCCTCCGAGTCTTCTCCGAAAAGAGGAATCTC TCTGAGGAAGCTGAAAATACAATCTCTGTGGATCGG	73
Calpain 6	<i>Capn6</i>	GTCCTTCTGTTGCAGTGACATGATGACTTTATGGCCA TCCTCGGGCACAGTAAAATGTAAGGATTCTGCA AGAAGGTATCACGGTTGTTATAGCAACCTCCTGATCG GTTTCAT	117
Collagen, type I, alpha 1	<i>Col1a1</i>	GCATGGCCAAGAAGACATCCCTGAAGTCAGCTGCAT ACACAATGGCCTAAGGGTCCCAATGGTGAGACGTG GAAACCGAGGTATGCTTGATCTGTATCTGCC	104
Docking protein 5	<i>Dok5</i>	AACTTTCACTCCCTCAGTCTGTCTGACCCTCCTCC CCACATCCCTCCTCGAAGCCACTCAGGGTGCCGAGCG CACGCTGGGGGACAGAGGCTACTGTCTGTCTGGGA TGGCTTCCAATTTAATGACATAGTGAAGCAGGGGTA CGTGAGGATCCGGAGCAGACGCCTAGGGATTTATCA ACGATGCTGGTTAGTG	200
Four and a half LIM domains 1	<i>Fhl1</i>	GTGCTTTGACAAGTTCTGCGCCAACACCTGCGTGGAC TGCCGCAAGCCATAAGCGCTGATGCCAAGGAGGTG CATTATAAGAATCGCTACTGGCACGACAACCTGCTTCC GCTGTGCCAAGTGCCTTACCCTTGGCCAGTGAGAC CTTTGTGTTCAAGGATGGCAAGATCCTGTGCAACAAG TG	186
Integrin beta 1 binding protein 2	<i>Itgb1bp2</i>	AAGTTCACTTCAGGAGCAAAAACCTCTAAATACAATT CCAAAGTCAGCAGAGACCTTGTTCCGAGAAAGGCCT AAGTCTGAGATGCCTCCCAAAGTCTACCACTTCTT	109
Myosin, light polypeptide 6B	<i>Myf6b</i>	TCTACACGTCGGGACTTCAGCTCCTCGTTTTTGGGGT TCCCAGGACCTTGAGCACCTCGGCGTTGGTAGGGTT CTGGCCAGGGCCCTCATCAGGTCCCACACTGGCTG TACAGGATCTTGCCATCACCTACTCGGTCAAAC	144

Myomesin family, member 3	<i>Myom3</i>	GGTGTCTGAATGTGCATAGAGACTGCCTGACCCTGAC CTGGGTCCCAGCGACACCCGGGCGAGCACCAT CACTGGCTATTCCATTGAGATGTGCCAGGGTGATTCC GAGGAGTGGA	120
Myotilin	<i>Myot</i>	CTCAGTTCTATATTACCGTCTCAACCCGATTACTGTAA CAGTAAAATCCCATCCACTGTGGACTCCAATATCAA CAATCCTCAGTTAACCAACCTG	97
Very low density lipoprotein receptor	<i>Vldlr</i>	GCTTCTGTAGGACACATACCCAGCAATATCAGTTG TAAGCACAGATGATGATCTGGCTTGAGTTCTGAAC	72
<i>Deregulated genes in Frzb^{-/-} mice articular cartilage and in LGMD2A patients' muscles (Sáenz et al., 2008; Lories et al., 2009; Lodewyckx et al., 2012)</i>			
Asporin	<i>Aspn</i>	GTTGTTCACTGCTCTGATCTAGGTCTGACATCGGTTCC AAACAACATTCCATTTGATACTCGAATGGTTGACCTTC GTGGAACCTGGTTTCTTCCACCTTCTTCATCCCCT CTTATTTTGGCACAGCAGTCCAACGTAGATGAATTGG GATGCAGCCACCTTGGTCAGTCTATGAGTCTAGAGA TGCTGGAAGCCAGAACCATGTCAAATATGTGTCTGT GACTCAGGA	76
Collagen, type III, alpha 1	<i>Col3a1</i>	GTTGCCTACCGAGTCTCTAAAGATGCACAGCTCAGCA TGCCACCAAGCAGCTGTACCCTGAGTCTGGTTTTCC CGAGGACTTCTCCATCCTGACAAC	158
Collagen, type V, alpha 1	<i>Col5a1</i>	GTTGCCTACCGAGTCTCTAAAGATGCACAGCTCAGCA TGCCACCAAGCAGCTGTACCCTGAGTCTGGTTTTCC CGAGGACTTCTCCATCCTGACAAC	98
Collagen, type XV, alpha 1	<i>Col15a1</i>	GTCCCTCTGGAAATGATGAAGGGGAGAAAGGGTGA ACCTGGAATCCATGGTGCACCGGGACCCATGGGACC CAAAGGACCACAGGACACAAAGGAGAGTTTGGC CCATCGAAGCCATCATCTATCTGGACCAAGGAAGCCC TGAGTTAAATTCAACTATTAATTCATCGTACTTCTCT CTGTGGAAGGACTCTGTGAAGGGATTGGTGTCTGGAT TGGTAG	105
Collagen triple helix repeat containing 1	<i>Cthrc1</i>	ACAGTCCCCTGACAGAGTTACTCCACTCCAGGAATG AAGCGTGGCAACATAC GCAGCTGCTGTCTATTCCGAATGTCTGAGGACAAGC CACAGGATTACAAGAAG CGGCTTTCAGTCGAGCTGACCAGTTCCTTTCAGGA CAGAGCCAATGGCTTGG AATGAGACTGCAGATCTTGGACTGGACATTGGTGCC CAGGGAGAAGCC	117
Catenin (cadherin associated protein), beta 1	<i>Ctnnb1</i>	CAATGTCATACAGCCTCCTAATTTTTGTTTTATACTTG CTTTTATCCAGATCTTCCACGTGGTCTTCCCAATTA AATCTTGGCAGCAATTTCCAGGCTCACTATCTGAGGC GTCGAC	180
E2F transcription factor 8	<i>E2f8</i>	AGACGCCAGTGTTTCGTTCTCGGAGTGAGGCTGGGT TGATACCTCCATCCACAATTGCTTCATAGCTGACTTCC AACAG	119
Fatty acid synthase	<i>Fasn</i>	CAGAGTCGCACTGGTAGAAGTTCCAGGAACCTGGAA CTGTAAGGGCTCTTCGTCGGTGCCAACTGGTTGGCAT GAAATGATGTAAGTCTCAGAACTCTCCTGGAACG	79
Fibronectin 1	<i fn1<="" i=""></i>	GCGGTCACATCATGACATTTTCATCTTTACCTCTTTAAC TTTAGCCCGGATGACATAGTTGTAATTGTTCCGGAAA TAGGTCTTCTGTGTAGCTCTGACA	104
Frizzled-related protein	<i>Frzb</i>	GTTGGATGCTCTTCAGTTCGTGTGTGGACCGAGGGG CTTTTACTTCAACAAGCCACAGGCTATGGCTCCAGC ATTCGGAGGGCACCTCAGACAGGCATTGTGGATGAG TGTTGCTT	99
Insulin-like growth factor 1	<i>Igf1</i>	GTTGGATGCTCTTCAGTTCGTGTGTGGACCGAGGGG CTTTTACTTCAACAAGCCACAGGCTATGGCTCCAGC ATTCGGAGGGCACCTCAGACAGGCATTGTGGATGAG TGTTGCTT	117

Mesoderm specific transcript	<i>Mest</i>	CTCTGCACTCATGGAAGACTTCTGGCAAGTTTTTCACC TACAAAGGCTACGCATCTTCTACCAAGTTAGATTTT GGTGTGTCGCAAGGCTGCCTTGCATGCAGTTTGCCTCA TTTCTCATTTCCTCCTAGATTCTGTCTGG	141
Myelocytomatosis oncogene	<i>Myc</i>	CTAGTGCTGCATGAGGAGACACCGCCACCACCAGC AGCGACTCTGAAGAAGAGCAAGAAGATGAGGAAGA AATTGATGTGGTGTCTGT	89
RAR-related orphan receptor alpha	<i>Rora</i>	TACAGAAGAACCACCGAGAAGATGGAATTCTAACCA AGCTAATATGCAAGGTGTCTACGTTAAGAGC	67
Sema domain, immunoglobulin domain (Ig), short basic domain, secreted, (semaphorin) 3C	<i>Sema3c</i>	CTCCACAGGCATCTATCAAGTGGTTGCTGCAGAAAGA CAAAGACAGGAGGAAGGAGGTTAACTGAACGAGC GCATTATAGCTACTTCCAAGGACTACTGATTCGCTCT GTTCAAGA	118
Solute carrier family 16 (monocarboxylic acid transporters), member 1	<i>Slc16a1</i>	CTGTAACACAGTACAGGAACCTTACTTGTGCATTGGT GTTATTGGAGGTCTTGGGCTTGCTTCAACTTGAACC CAGCTCTGACTATGATTGGCAAGTAT	100
Sorbin and SH3 domain containing 1	<i>Sorbs1</i>	AATGTCTTGGTACTCTGAATCTTTAGTGAAGCTGA GCTGGAAGGTCGCTTGAAGCCACTGAGGCCCTGAAG AGGGATGTCGCCACCTTCCAAGACTCTTATAGATC TGCCTCT	117
Transferrin receptor	<i>Tfrc</i>	AGCCAGATCAGCATTCTCTAACTTGTGGTGGGGAA CCATTGTCATACACCGGTTTAGCCTTGCTCGGCAAG TAGATGGAGATAACAGTCATGTGGAGATGA	104
Genes coding for proteins participating in Wnt signaling pathway			
Low density lipoprotein receptor-related protein 5	<i>Lrp5</i>	TAGTCACTGTCACACACATCTGTGCTGCACGGTGTG TTGGGGGTGCCATACCTCGAATGACGTAGGGCCTGT ATGGTCTAGCGGTGG	88
Low density lipoprotein receptor-related protein 6	<i>Lrp6</i>	TAGGAGCATAGTCACTGTCACAGACATCAGTGTGCA GGGTGTGGTGGGCGGTGCAAAGTGCCGGTAGCTGT ACGGCCTATAGCTGTAGGACCTATGTGTGGAAGGAC TGTTG	113
Wingless-related MMTV integration site 8A	<i>Wnt8a</i>	CGAAGAGTGTAAGTTCCAGTTTGCCTGGGAACGGTG GAATTGTCCTGAGCATGCTTTTCAGTTTTCAACCACA ACAGGCTGCGAGCTGCCACGAGAGACATCCTTCA TTCATGCC	118
Wingless related MMTV integration site 8b	<i>Wnt8b</i>	GTGCGTTCTTCTAGTCACTTGTGTCTTACCAGCC ACGCCTGGTCACTGAACAATTTTCTGATGACCGGTCC AA	77
Endogenous controls			
Glyceraldehyde-3-phosphate dehydrogenase	<i>Gapdh</i>	AACCTGGTCTCAGTGTAGCCCAAGATGCCCTTCAGT GGGCCCTCAGATGCCTGCTTACCACCTTCTTGATGT C	75
TATA box binding protein	<i>Tbp</i>	GGAGAATCATGGACCAGAACAACAGCCTTCCACCTTA TGCTCAGGGCTTGGCCTCCACAGGGCGCCATGACT CCTGGAATCCCATCTTTAGTCCAATGA	102

Table 3. Human and murine origin TaqMan™ probes.

Gene name	Gene symbol	Assay ID	Amplicon length (bp)
Human			
CD9	<i>CD9</i>	Hs00233521_m1	72
Calpain 3	<i>CAPN3</i>	Hs00181057_m1	77
Collagen, Type I, Alpha 1	<i>COL1A1</i>	Hs00164004_m1	66
Desmin	<i>DES</i>	Hs00157258_m1	83
Fibronectin 1	<i>FN1</i>	Hs00365052_m1	82
C-FOS, Fos Proto-Oncogene, AP-1 Transcription Factor Subunit	<i>FOS</i>	Hs99999140_m1	77
Frizzled-related protein	<i>FRZB</i>	Hs00173503_m1	108
Glyceraldehyde-3-Phosphate Dehydrogenase	<i>GAPDH</i>	Hs99999905_m1	122
Melusin, Integrin Subunit Beta 1 Binding Protein 2	<i>ITGB1BP2</i>	Hs00183746_m1	72
Anosmin 1	<i>KAL1</i>	Hs01085107_m1	61
Myosin Heavy Chain 2	<i>MYH2</i>	Hs00430042_m1	76
Myogenic Differentiation 1	<i>MYOD</i>	Hs00159528_m1	67
Myogenin	<i>MYOG</i>	Hs01072232_m1	76
TATA box binding protein	<i>TBP</i>	Hs00427620_m1	91
Very Low Density Lipoprotein Receptor	<i>VLDLR</i>	Hs01045922_m1	98
Murine			
Adiponectin	<i>Adipoq</i>	Mm00456425_m1	75
Calpain 3	<i>Capn3</i>	Mm00482985_m1	53
Dystrophin	<i>Dmd</i>	Mm01216954_m1	92
Atrogin 1	<i>Fbx32</i>	Mm00499523_m1	73
Glyceraldehyde-3-Phosphate Dehydrogenase	<i>Gapdh</i>	Mm99999915_g1	109
Kyphoscoliosis peptidase	<i>Ky</i>	Mm01224823_m1	
Muscle-specific RING finger protein 1	<i>Murf1</i>	Mm01185221_m1	57
Myosin heavy chain 2	<i>MyH2</i>	Mm01332564_m1	105
Myosin heavy chain 3	<i>MyH3</i>	Mm01332463_m1	96
Myogenic Differentiation 1	<i>Myod1</i>	Mm00440387_m1	86
Myogenin	<i>Myog</i>	Mm00446194_m1	68
Parkin	<i>Park2</i>	Mm00450186_m1	115
Paired box 7	<i>Pax7</i>	Mm01354484_m1	68
Peroxisome Proliferator Activated Receptor Gamma	<i>Pparg</i>	Mm01184322_m1	101
Ryanodine receptor 1	<i>Ryr1</i>	Mm01175211_m1	93
Ryanodine receptor 2	<i>Ryr2</i>	Mm00465877_m1	63
TATA-box binding protein	<i>Tbp</i>	Mm00446973_m1	73

Table 4. Table X. TLDA custom-designed human TaqMan™ probes.

Gene name	Gene symbol	Assay ID	Amplicon length (bp)
RNA, 18S Ribosomal 5	18S5	Hs99999901_s1	187
Acetyl-CoA Carboxylase Beta	ACACB	Hs00153715_m1	88
Actin Beta	ACTB	Hs99999903_m1	171
Actin, Alpha, Cardiac Muscle 1	ACTC1	Hs01109515_m1	70
Actinin Alpha 2	ACTN2	Hs00153809_m1	94
Aldehyde Dehydrogenase 2 Family (Mitochondrial)	ALDH2	Hs00355914_m1	78
Anaphase Promoting Complex Subunit 1	ANAPC1	Hs00224096_m1	69
Carbonic Anhydrase 2	CA2	Hs00163869_m1	85
Calpain 6	CAPN6	Hs00560073_m1	69
CD44 antigen, Chondroitin Sulfate Proteoglycan 8	CD44	Hs00153310_m1	82
CD9	CD9	Hs00233521_m1	72
CCAAT/Enhancer Binding Protein Delta	CEBPD	Hs00270931_s1	107
Cbp/P300 Interacting Transactivator With Glu/Asp Rich Carboxy-Terminal Domain 2	CITED2	Hs00366696_m1	80
Collagen, Type I, Alpha 1	COL1A1	Hs00164004_m1	66
Collagen Type III Alpha 1 Chain	COL3A1	Hs00164103_m1	66
Collagen Type V Alpha 1 Chain	COL5A1	Hs00609088_m1	87
Desmin	DES	Hs00157258_m1	83
DnaJ (Hsp40) homolog, subfamily A, member 4	DNAJA4	Hs00388055_m1	99
Docking Protein 5	DOK5	Hs00218324_m1	80
E2F Transcription Factor 8	E2F8	Hs00226635_m1	68
Early Growth Response 1	EGR1	Hs00152928_m1	72
EYA Transcriptional Coactivator And Phosphatase 1	EYA1	Hs00166804_m1	64
Fatty Acid Binding Protein 3	FABP3	Hs00269758_m1	92
Fatty Acid Binding Protein 7	FABP7	Hs00361426_m1	96
Family With Sequence Similarity 129 Member A	FAM129A	Hs00223000_m1	94
Four And A Half LIM Domains 1	FHL1	Hs00740811_m1	139
Fibronectin 1	FN1	Hs00365052_m1	82
C-FOS, Fos Proto-Oncogene, AP-1 Transcription Factor Subunit	FOS	Hs99999140_m1	77
Frizzled-related protein	FRZB	Hs00173503_m1	108
Glyceraldehyde-3-Phosphate Dehydrogenase	GAPDH	Hs99999905_m1	122
HECT And RLD Domain Containing E3 Ubiquitin Protein Ligase Family Member 1	HERC1	Hs00187497_m1	83
Histone Cluster 1 H1 Family Member C	HIST1H1C	Hs00271185_s1	97
Insulin Like Growth Factor 1	IGF1	Hs00153126_m1	70
Immunoglobulin Heavy Constant Gamma 1	IGHG1	Hs00378340_m1	98
Interleukin 32	IL32	Hs00170403_m1	54
Melusin, Integrin Subunit Beta 1 Binding Protein 2	ITGB1BP2	Hs00183746_m1	72
Jun Proto-Oncogene, AP-1 Transcription Factor Subunit	JUN	Hs99999141_s1	64
Anosmin 1	KAL1	Hs00608006_m1	90
Kruppel Like Factor 10	KLF10	Hs00194622_m1	71
Large Tumor Suppressor Kinase 2	LATS2	Hs00324396_m1	65
Leucine Rich Repeat Containing G Protein-Coupled Receptor 5	LGR5	Hs00173664_m1	112
Lysyl Oxidase Like 2	LOXL2	Hs00158757_m1	62

Myoglobin	MB	Hs00193520_m1	105
MYC Proto-Oncogene, BHLH Transcription Factor	MYC	Hs00153408_m1	107
Myosin Heavy Chain 3	MYH3	Hs00159463_m1	65
Myosin Light Chain 5	MYL5	Hs00267323_m1	59
Myosin Light Chain 6B	MYL6B	Hs00365997_g1	90
Myomesin 3	MYOM3	Hs00537054_m1	65
Myotilin	MYOT	Hs00199016_m1	57
Pyruvate Dehydrogenase Phosphatase Catalytic Subunit 1	PDP1	Hs00372607_m1	70
6-Phosphofructo-2-Kinase/Fructose-2,6-Biphosphatase 3	PFKFB3	Hs00190079_m1	77
3-Hydroxyacyl-CoA Dehydratase 1	PTPLA	Hs00171965_m1	74
S100 Calcium Binding Protein A6	S100A6	Hs00170953_m1	94
S100 Calcium Binding Protein A8	S100A8	Hs00374263_m1	70
Sodium Voltage-Gated Channel Alpha Subunit 7	SCN7A	Hs00161546_m1	109
Semaphorin 3C	SEMA3C	Hs00170762_m1	78
Solute Carrier Family 2 Member 5	SLC2A5	Hs00161720_m1	57
SMG1, Nonsense Mediated MRNA Decay Associated PI3K Related Kinase	SMG1	Hs00247891_m1	77
Secreted Protein Acidic And Cysteine Rich	SPARC	Hs00234160_m1	76
TATA box binding protein	TBP	Hs00427620_m1	91
Transferrin Receptor	TFRC	Hs00174609_m1	79
Troponin I1, Slow Skeletal Type	TNNI1	Hs00268531_m1	71
Thioredoxin Interacting Protein	TXNIP	Hs00197750_m1	81
Very Low Density Lipoprotein Receptor	VLDLR	Hs01045922_m1	98

bp= base pair.

Table 5. Antibodies.

Western blot analysis						
Protein	Reference	Brand	Polyclonal/ monoclonal	Specie	1st Ab dilution	2nd Ab dilution
Primary antibodies						
AKT	#9272	CST	Polyclonal	Rabbit	1:1000	1:5000
Active β -catenin	#05-665	Millipore	Monoclonal	Mouse	1:1000	1:5000
Alkaline phosphatase, ALP	AF2910	R&D Systems	Polyclonal	Goat	1:200	1:3000
Alpha smooth muscle actin, α SMA	ab5694	Abcam	Polyclonal	Rabbit	1:400	1:3000
Atrogin-1/Fbx32	ab92281	Abcam	Polyclonal	Goat	1:1666	1:5000
Calpain 3	COP-080049	Cosmobio	Polyclonal	Goat	1:1000	1:3000
Beclin 1	#4122	CST	Monoclonal	Mouse	1:1000	1:5000
BNIP3	ab10433	Abcam	Monoclonal	Mouse	1:1000	1:5000
ERK	sc-93	Sant cruz	Polyclonal	Rabbit	1:1000	1:5000
FoxO1	#2880	CST	Monoclonal	Rabbit	1:1000	1:5000
FoxO3a	#12829	CST	Monoclonal	Rabbit	1:1000	1:5000
GAPDH (14C10)	#2118	CST	Monoclonal	Rabbit	1:1000	1:5000
GSK3B β	#9315	CST	Monoclonal	Rabbit	1:1000	1:5000
ITG β 1	MAB2251	Millipore	Monoclonal	Mouse	1:1000	1:5000
ITG β 1A	AB1952	Millipore	Polyclonal	Rabbit	1:1000	1:5000
ITG β 1D	MAB1900	Millipore	Monoclonal	Mouse	1:300	1:3000
Ky	ab108011	Abcam	Polyclonal	Rabbit	1:500	1:5000
Melusin	ab62300	Abcam	Polyclonal	Rabbit	1:400	1:5000
MuRF1	MP3401	ECM Bioscience	Polyclonal	Rabbit	1:1000	1:5000
MyHC	A4-1025	DSHB	Monoclonal	Mouse	1:10000	1:20000
MyoD	M351201	DAKO	Monoclonal	Mouse	1:1000	1:5000
Myogenin	ab124800	Abcam	Monoclonal	Rabbit	1:1000	1:5000
NG2	AB5320	Millipore	Polyclonal	Rabbit	1:1000	1:3000
P-AKT (Ser473)	#4060	CST	Polyclonal	Rabbit	1:1000	1:3000
PDGFR β	#3169	CST	Monoclonal	Rabbit	1:1000	1:3000
P-ERK1/2 (Thr202/Tyr204)	#9101	CST	Polyclonal	Rabbit	1:1000	1:5000
P-FoxO1 (Ser256)	#9461	CST	Polyclonal	Rabbit	1:1000	1:5000
P-FoxO1 (Thr24)/P-FoxO3a (Thr32)/P-FoxO4 (Thr28)	#2599	CST	Monoclonal	Rabbit	1:1000	1:5000
P-FoxO3 (Ser253)	#13129	CST	Monoclonal	Rabbit	1:1000	1:5000
P-GSK3 β (Ser9)	#9323	CST	Monoclonal	Rabbit	1:1000	1:5000
P-p70 S6 kinase (Thr389)	#9205	CST	Polyclonal	Rabbit	1:1000	1:5000
P-p70 S6 kinase (Thr421/Ser424)	#9204	CST	Polyclonal	Rabbit	1:1000	1:5000

Secondary antibodies

Anti-rabbit IgG, HRP-linked antibody	#7074	CST
Donkey α Goat, HRP-linked antibody	SC-2020	Santa cruz
Goat α Rabbit, HRP-linked antibody	SC-2004	Santa cruz
Rabbit α Goat, HRP-linked antibody	P0449	DAKO
Rabbit α Mouse, HRP-linked antibody	P0260	DAKO

Immunofluorescence analysis

Protein	Reference	Brand	Polyclonal/ monoclonal	Specie	1st Ab dilution	2nd Ab dilution
----------------	------------------	--------------	-----------------------------------	---------------	---------------------------------------	---------------------------------------

Primary antibodies

Alkaline phosphatase, ALP	AF2910	R&D Systems	Polyclonal	Goat	1:20	1:500
Alpha smooth muscle actin, α SMA	ab5694	Abcam	Polyclonal	Rabbit	1:500	1:500
Ki67	556003	BD Bioscience	Monoclonal	Mouse	1:300	1:500
MyHC	A4-1025	DSHB	Monoclonal	Mouse	1:50	1:500
MyHC*		DSHB		Mouse	1:20	1:500
MyoD	SC-760	Santa cruz	Polyclonal	Rabbit	1:50	1:500
Myogenin*		DSHB		Mouse	1:10	1:500
NG2	AB5320	Millipore	Polyclonal	Rabbit	1:500	1:500
PDGFR β	#3169	CST	Monoclonal	Rabbit	1:50	1:500
Perilipin A/B	P1873	Sigma	Polyclonal	Rabbit	1:300	1:500
Sarcomeric alpha actinin	ab72592	Abcam	Polyclonal	Rabbit	1:500	1:500

Secondary antibodies

Donkey anti-Mouse IgG (H+L) Highly Cross-Adsorbed Secondary Antibody, Alexa Fluor 594	A-21203	Thermo Scientific
Donkey anti-Rabbit IgG (H+L) Highly Cross-Adsorbed Secondary Antibody, Alexa Fluor 488	A-21206	Thermo Scientific
Donkey anti-Goat IgG (H+L) Highly Cross-Adsorbed Secondary Antibody, Alexa Fluor 488	A-11055	Thermo Scientific
Goat anti-Mouse IgG (H+L), Highly Cross-Adsorbed Secondary Antibody, Alexa Fluor [®] 555 conjugate	A-21422	Thermo Scientific
Goat anti-Mouse IgG (H+L), Highly Cross-Adsorbed Secondary Antibody, Alexa Fluor [®] 488 conjugate	A-11001	Thermo Scientific
Goat anti-Rabbit IgG (H+L), Highly Cross-Adsorbed Secondary Antibody, Alexa Fluor [®] 555 conjugate	A-21428	Thermo Scientific
Goat anti-Rabbit IgG (H+L), Highly Cross-Adsorbed Secondary Antibody, Alexa Fluor [®] 488 conjugate	A-11034	Thermo Scientific

Ab= antibody, CST= Cell Signaling Technology and DSHB= Developmental Studies Hybridoma Bank. *= Antibodies produced at host lab.

Table 6. Mediums compositions for human primary cells cultures.

Conditioned medium		Freezing medium	
Component	Final concentration	Component	Final concentration
M-199		DMEM	
FBS	37.5%	FBS	10%
penicillin/streptomycin + Fungizone	1.25%	Penicillin/streptomycin + Fungizone	1%
		DMSO	8%

Proliferation medium		Differentiation medium	
Component	Volume (ml)	Component	Volume (ml)
D-MEM	64.8	D-MEM	71.25
M-199	21.6	M-199	23.75
FBS	10.0	FBS	2
Insulin 1 mg/ml	1	Insulin 1 mg/ml	1
Glutamine 200 mM	1	Glutamine 200 mM	1
Fibroblast growth factor 5 µg/ml	0.5	Penicillin/streptomycin + fungizone	1
Epidermal growth factor 10 µg/ml	0.1		
Penicillin/streptomycin + fungizone	1		

APPENDIX III: Publications.

Jaka, O., Azpitarte, M., Paisán-Ruiz, C., Zulaika, M., **Casas-Fraile, L.**, Sanz, R., Trevisiol, N., Levy, N., Bartoli, M., Krahn, M., et al. (2014). Entire CAPN3 gene deletion in a patient with limb-girdle muscular dystrophy type 2A. *Muscle Nerve* 50, 448–453.

Jaka, O., **Casas-Fraile, L.**, López de Munain, A., and Sáenz, A. (2015). Costamere proteins and their involvement in myopathic processes. *Expert Rev. Mol. Med.* 17, e12.

Jaka, O., **Casas-Fraile, L.**, Azpitarte, M., Aiastui, A., López de Munain, A., and Sáenz, A. (2017). FRZB and melusin, overexpressed in LGMD2A, regulate integrin β 1D isoform replacement altering myoblast fusion and the integrin-signalling pathway. *Expert Rev. Mol. Med.* 19.

BIBLIOGRAPHY

- Abo, T., and Balch, C.M. (1981). A differentiation antigen of human NK and K cells identified by a monoclonal antibody (HNK-1). *J. Immunol. Baltim. Md* 1950 127, 1024–1029.
- Agarwal, N.K., Qu, C., Kunkalla, K., Kunkulla, K., Liu, Y., and Vega, F. (2013). Transcriptional regulation of serine/threonine protein kinase (AKT) genes by glioma-associated oncogene homolog 1. *J. Biol. Chem.* 288, 15390–15401.
- Albuquerque, M.A.V. de, Abath Neto, O., Silva, F.M.A. da, Zanoteli, E., and Reed, U.C. (2015). Limb-girdle muscular dystrophy type 2A in Brazilian children. *Arq. Neuropsiquiatr.* 73, 993–997.
- Allen, D.L., Harrison, B.C., Sartorius, C., Byrnes, W.C., and Leinwand, L.A. (2001). Mutation of the IIB myosin heavy chain gene results in muscle fiber loss and compensatory hypertrophy. *Am. J. Physiol.-Cell Physiol.* 280, C637–C645.
- Almeida, M., Han, L., Martin-Millan, M., O'Brien, C.A., and Manolagas, S.C. (2007). Oxidative stress antagonizes Wnt signaling in osteoblast precursors by diverting β -catenin from T cell factor- to forkhead box O-mediated transcription. *J. Biol. Chem.* 282, 27298–27305.
- Amit, S. (2002). Axin-mediated CKI phosphorylation of beta -catenin at Ser 45: a molecular switch for the Wnt pathway. *Genes Dev.* 16, 1066–1076.
- Andersen, P., and Henriksson, J. (1977). Training induced changes in the subgroups of human type II skeletal muscle fibres. *Acta Physiol. Scand.* 99, 123–125.
- Anderson, L.V.B., and Davison, K. (1999). Multiplex western blotting system for the analysis of muscular dystrophy proteins. *Am. J. Pathol.* 154, 1017–1022.
- Anderson, L.V.B., Harrison, R.M., Pogue, R., Vafiadaki, E., Pollitt, C., Davison, K., Moss, J.A., Keers, S., Pyle, A., Shaw, P.J., et al. (2000). Secondary reduction in calpain 3 expression in patients with limb girdle muscular dystrophy type 2B and Miyoshi myopathy (primary dysferlinopathies). *Neuromuscul. Disord.* NMD 10, 553–559.
- Andrés, V., and Walsh, K. (1996). Myogenin expression, cell cycle withdrawal, and phenotypic differentiation are temporally separable events that precede cell fusion upon myogenesis. *J. Cell Biol.* 132, 657–666.
- Ang, L.P.K. (2005). The use of human serum in supporting the *in vitro* and *in vivo* proliferation of human conjunctival epithelial cells. *Br. J. Ophthalmol.* 89, 748–752.
- Ansved, T. (2003). Muscular dystrophies: influence of physical conditioning on the disease evolution: *Curr. Opin. Clin. Nutr. Metab. Care* 6, 435–439.
- Armulik, A. (2002). Splice variants of human beta 1 integrins: origin, biosynthesis and functions. *Front. Biosci. J. Virtual Libr.* 7, d219-227.
- Aronson, D., Violan, M.A., Dufresne, S.D., Zangen, D., Fielding, R.A., and Goodyear, L.J. (1997). Exercise stimulates the mitogen-activated protein kinase pathway in human skeletal muscle. *J. Clin. Invest.* 99, 1251–1257.

- Aronson, D., Boppart, M.D., Dufresne, S.D., Fielding, R.A., and Goodyear, L.J. (1998). Exercise stimulates c-Jun NH2 kinase activity and c-Jun transcriptional activity in human skeletal muscle. *Biochem. Biophys. Res. Commun.* 251, 106–110.
- Aswad, H., Jalabert, A., and Rome, S. (2016). Depleting extracellular vesicles from fetal bovine serum alters proliferation and differentiation of skeletal muscle cells *in vitro*. *BMC Biotechnol.* 16, 32.
- Attaix, D., and Baracos, V.E. (2010). MAFbx/Atrogin-1 expression is a poor index of muscle proteolysis: *Curr. Opin. Clin. Nutr. Metab. Care* 13, 223–224.
- Auguste, G., Gurha, P., Lombardi, R., Coarfa, C., Willerson, J.T., and Marian, A.J. (2018). Suppression of activated FOXO transcription factors in the heart prolongs survival in a mouse model of laminopathies. *Circ. Res.* 122, 678–692.
- Augusto, V., Padovani, C.R., and Rocha Campos, G.E. (2004). Skeletal muscle fiber types in C57BL6J mice. *J. Morphol. Sci.* 21.
- Azuma, M., Fukiage, C., Higashine, M., Nakajima, T., Ma, H., and Shearer, T.R. (2000). Identification and characterization of a retina-specific calpain (Rt88) from rat. *Curr. Eye Res.* 21, 710–720.
- Babai, F., Musevi-Aghdam, J., Schurch, W., Royal, A., and Gabbiani, G. (1990). Coexpression of alpha-sarcomeric actin, alpha-smooth muscle actin and desmin during myogenesis in rat and mouse embryos I. Skeletal muscle. *Differ. Res. Biol. Divers.* 44, 132–142.
- Baek, S.T., Kerjan, G., Bielas, S.L., Lee, J.E., Fenstermaker, A.G., Novarino, G., and Gleeson, J.G. (2014). Off-target effect of doublecortin family shRNA on neuronal migration associated with endogenous microRNA dysregulation. *Neuron* 82, 1255–1262.
- Baghdiguian, S., Martin, M., Richard, I., Pons, F., Astier, C., Bourg, N., Hay, R.T., Chemaly, R., Halaby, G., Loiselet, J., et al. (1999). Calpain 3 deficiency is associated with myonuclear apoptosis and profound perturbation of the I κ B α /NF- κ B pathway in limb-girdle muscular dystrophy type 2A. *Nat. Med.* 5, 503–511.
- Baghdiguian, S., Richard, I., Martin, M., Coopman, P., Beckmann, J.S., Mangeat, P., and Lefranc, G. (2001). Pathophysiology of limb girdle muscular dystrophy type 2A: hypothesis and new insights into the I κ B α /NF- κ B survival pathway in skeletal muscle. *J. Mol. Med.* 79, 254–261.
- Barberi, T., Bradbury, M., Dincer, Z., Panagiotakos, G., Socci, N.D., and Studer, L. (2007). Derivation of engraftable skeletal myoblasts from human embryonic stem cells. *Nat. Med.* 13, 642–648.
- Bartoli, M., Roudaut, C., Martin, S., Fougereuse, F., Suel, L., Poupiot, J., Gicquel, E., Noulet, F., Danos, O., and Richard, I. (2006). Safety and efficacy of AAV-mediated calpain 3 gene transfer in a mouse model of limb-girdle muscular dystrophy type 2A. *Mol. Ther.* 13, 250–259.
- Bassel-Duby, R., and Olson, E.N. (2006). Signaling pathways in skeletal muscle remodeling. *Annu. Rev. Biochem.* 75, 19–37.
- Baylor, S.M., and Hollingworth, S. (2012). Intracellular calcium movements during excitation-contraction coupling in mammalian slow-twitch and fast-twitch muscle fibers. *J. Gen. Physiol.* 139, 261–272.

- Beatham, J., Romero, R., Townsend, S.K.M., Hacker, T., van der Ven, P.F.M., and Blanco, G. (2004). Filamin C interacts with the muscular dystrophy KY protein and is abnormally distributed in mouse KY deficient muscle fibres. *Hum. Mol. Genet.* 13, 2863–2874.
- Belham, C., Comb, M.J., and Avruch, J. (2001). Identification of the NIMA family kinases NEK6/7 as regulators of the p70 ribosomal S6 kinase. *Curr. Biol.* CB 11, 1155–1167.
- Belkin, A.M., Zhidkova, N.I., Balzac, F., Altruda, F., Tomatis, D., Maier, A., Tarone, G., Koteliansky, V.E., and BurrIDGE, K. (1996). Beta 1D integrin displaces the beta 1A isoform in striated muscles: localization at junctional structures and signaling potential in nonmuscle cells. *J. Cell Biol.* 132, 211–226.
- Benayoun, B., Baghdiguian, S., Lajmanovich, A., Bartoli, M., Daniele, N., Gicquel, E., Bourg, N., Raynaud, F., Pasquier, M.-A., Suel, L., et al. (2008). NF- κ B-dependent expression of the antiapoptotic factor c-FLIP is regulated by calpain 3, the protein involved in limb-girdle muscular dystrophy type 2A. *FASEB J.* 22, 1521–1529.
- Bennett, H.S. (1955). Modern concepts of structure of striated muscle. *Am. J. Phys. Med.* 34, 46–67.
- Berg, J.S., Powell, B.C., and Cheney, R.E. (2001). A millennial myosin census. *Mol. Biol. Cell* 12, 780–794.
- Bernick, E.P., Zhang, P.-J., and Du, S. (2010). Knockdown and overexpression of Unc-45b result in defective myofibril organization in skeletal muscles of zebrafish embryos. *BMC Cell Biol.* 11, 70.
- Beurel, E., and Jope, R.S. (2006). The paradoxical pro- and anti-apoptotic actions of GSK3 in the intrinsic and extrinsic apoptosis signaling pathways. *Prog. Neurobiol.* 79, 173–189.
- Beyaert, R., Vanhaesebroeck, B., Suffys, P., Van Roy, F., and Fiers, W. (1989). Lithium chloride potentiates tumor necrosis factor-mediated cytotoxicity *in vitro* and *in vivo*. *Proc. Natl. Acad. Sci. U. S. A.* 86, 9494–9498.
- Bhanot, P., Brink, M., Samos, C.H., Hsieh, J.C., Wang, Y., Macke, J.P., Andrew, D., Nathans, J., and Nusse, R. (1996). A new member of the frizzled family from *Drosophila* functions as a Wingless receptor. *Nature* 382, 225–230.
- Birbrair, A., Zhang, T., Wang, Z.-M., Messi, M.L., Enikolopov, G.N., Mintz, A., and Delbono, O. (2013a). Skeletal muscle pericyte subtypes differ in their differentiation potential. *Stem Cell Res.* 10, 67–84.
- Birbrair, A., Zhang, T., Wang, Z.-M., Messi, M.L., Enikolopov, G.N., Mintz, A., and Delbono, O. (2013b). Role of pericytes in skeletal muscle regeneration and fat accumulation. *Stem Cells Dev.* 22, 2298–2314.
- Biressi, S., Bjornson, C.R.R., Carlig, P.M.M., Nishijo, K., Keller, C., and Rando, T.A. (2013). Myf5 expression during fetal myogenesis defines the developmental progenitors of adult satellite cells. *Dev. Biol.* 379, 195–207.
- Bissell, M.J., Hall, H.G., and Parry, G. (1982). How does the extracellular matrix direct gene expression? *J. Theor. Biol.* 99, 31–68.

- Bissell, M.J., and Aggeler, J. (1987). Dynamic reciprocity: how do extracellular matrix and hormones direct gene expression? *Prog. Clin. Biol. Res.* 249, 251–262.
- Black, B.L., and Olson, E.N. (1998). Transcriptional control of muscle development by myocyte enhancer factor-2 (MEF2) proteins. *Annu. Rev. Cell Dev. Biol.* 14, 167–196.
- Blake, D.J., Tinsley, J.M., Davies, K.E., Knight, A.E., Winder, S.J., and Kendrick-Jones, J. (1995). Coiled-coil regions in the carboxy-terminal domains of dystrophin and related proteins: potentials for protein-protein interactions. *Trends Biochem. Sci.* 20, 133–135.
- Blanco, G., Coulton, G.R., Biggin, A., Grainge, C., Moss, J., Barrett, M., Berquin, A., Maréchal, G., Skynner, M., van Mier, P., et al. (2001). The kyphoscoliosis (ky) mouse is deficient in hypertrophic responses and is caused by a mutation in a novel muscle-specific protein. *Hum. Mol. Genet.* 10, 9–16.
- Blau, H., Pavlath, G., Hardeman, E., Chiu, C., Silberstein, L., Webster, S., Miller, S., and Webster, C. (1985). Plasticity of the differentiated state. *Science* 230, 758–766.
- Blázquez, L., Azpitarte, M., Sáenz, A., Goicoechea, M., Otaegui, D., Ferrer, X., Illa, I., Gutierrez-Rivas, E., Vilchez, J.J., and López de Munain, A. (2008). Characterization of novel CAPN3 isoforms in white blood cells: an alternative approach for limb-girdle muscular dystrophy 2A diagnosis. *Neurogenetics* 9, 173–182.
- Blázquez, L., Aiastui, A., Goicoechea, M., Martins de Araujo, M., Avril, A., Beley, C., García, L., Valcárcel, J., Fortes, P., and López de Munain, A. (2013). *In vitro* correction of a pseudoexon-generating deep intronic mutation in LGMD2A by antisense oligonucleotides and modified small nuclear RNAs. *Hum. Mutat.* 34, 1387–1395.
- Blitzer, J.T., and Nusse, R. (2006). A critical role for endocytosis in Wnt signaling. *BMC Cell Biol.* 7, 28.
- Bloch, R.J., Capetanaki, Y., O'Neill, A., Reed, P., Williams, M.W., Resneck, W.G., Porter, N.C., and Ursitti, J.A. (2002). Costameres: repeating structures at the sarcolemma of skeletal muscle. *Clin. Orthop.* S203-210.
- Bloemberg, D., and Quadriatero, J. (2012). Rapid determination of myosin heavy chain expression in rat, mouse, and human skeletal muscle using multicolor immunofluorescence analysis. *PLoS ONE* 7, e35273.
- Bodine, S.C., Latres, E., Baumhueter, S., Lai, V.K., Nunez, L., Clarke, B.A., Poueymirou, W.T., Panaro, F.J., Na, E., Dharmarajan, K., et al. (2001). Identification of ubiquitin ligases required for skeletal muscle atrophy. *Science* 294, 1704–1708.
- Bonne, G., Rivier, F., and Hamroun, D. (2017). The 2018 version of the gene table of monogenic neuromuscular disorders (nuclear genome). *Neuromuscul. Disord.* 27, 1152–1183.
- Boppart, M.D., Burkin, D.J., and Kaufman, S.J. (2006). $\alpha 7\beta 1$ -Integrin regulates mechanotransduction and prevents skeletal muscle injury. *Am. J. Physiol.-Cell Physiol.* 290, C1660–C1665.
- Borello, U., Coletta, M., Tajbakhsh, S., Leyns, L., De Robertis, E.M., Buckingham, M., and Cossu, G. (1999). Transplacental delivery of the Wnt antagonist Frzb1 inhibits development of caudal

- paraxial mesoderm and skeletal myogenesis in mouse embryos. *Dev. Camb. Engl.* 126, 4247–4255.
- Borello, U. (2006). The Wnt/ -catenin pathway regulates Gli-mediated Myf5 expression during somitogenesis. *Development* 133, 3723–3732.
- Borycki, A.G., Mendham, L., and Emerson, C.P. (1998). Control of somite patterning by Sonic hedgehog and its downstream signal response genes. *Dev. Camb. Engl.* 125, 777–790.
- Boudreau, N., Myers, C., and Bissell, M.J. (1995). From laminin to lamin: regulation of tissue-specific gene expression by the ECM. *Trends Cell Biol.* 5, 1–4.
- Bour, B.A., O'Brien, M.A., Lockwood, W.L., Goldstein, E.S., Bodmer, R., Taghert, P.H., Abmayr, S.M., and Nguyen, H.T. (1995). *Drosophila* MEF2, a transcription factor that is essential for myogenesis. *Genes Dev.* 9, 730–741.
- Brack, A.S., Conboy, M.J., Roy, S., Lee, M., Kuo, C.J., Keller, C., and Rando, T.A. (2007). Increased Wnt signaling during aging alters muscle stem cell fate and increases fibrosis. *Science* 317, 807–810.
- Brack, A.S., Conboy, I.M., Conboy, M.J., Shen, J., and Rando, T.A. (2008). A temporal switch from Notch to Wnt signaling in muscle stem cells is necessary for normal adult myogenesis. *Cell Stem Cell* 2, 50–59.
- Brancaccio, M., Guazzone, S., Menini, N., Sibona, E., Hirsch, E., De Andrea, M., Rocchi, M., Altruda, F., Tarone, G., and Silengo, L. (1999). Melusin is a new muscle-specific interactor for beta(1) integrin cytoplasmic domain. *J. Biol. Chem.* 274, 29282–29288.
- Brancaccio, M., Hirsch, E., Notte, A., Selvetella, G., Lembo, G., and Tarone, G. (2006). Integrin signalling: The tug-of-war in heart hypertrophy. *Cardiovasc. Res.* 70, 422–433.
- Braun, T., Buschhausen-Denker, G., Bober, E., Tannich, E., and Arnold, H.H. (1989). A novel human muscle factor related to but distinct from MyoD1 induces myogenic conversion in 10T1/2 fibroblasts. *EMBO J.* 8, 701–709.
- Braun, T., Bober, E., Winter, B., Rosenthal, N., and Arnold, H.H. (1990). Myf-6, a new member of the human gene family of myogenic determination factors: evidence for a gene cluster on chromosome 12. *EMBO J.* 9, 821–831.
- Bross, P., Frederiksen, J.B., Bie, A.S., Hansen, J., Palmfeldt, J., Nielsen, M.N., Duno, M., Lund, A.M., and Christensen, E. (2012). Heterozygosity for an in-frame deletion causes glutaryl-CoA dehydrogenase deficiency in a patient detected by newborn screening: investigation of the effect of the mutant allele. *J. Inherit. Metab. Dis.* 35, 787–796.
- Brunelli, S., Relaix, F., Baesso, S., Buckingham, M., and Cossu, G. (2007). Beta catenin-independent activation of MyoD in presomitic mesoderm requires PKC and depends on Pax3 transcriptional activity. *Dev. Biol.* 304, 604–614.
- Brunet, A., Bonni, A., Zigmond, M.J., Lin, M.Z., Juo, P., Hu, L.S., Anderson, M.J., Arden, K.C., Blenis, J., and Greenberg, M.E. (1999). Akt promotes cell survival by phosphorylating and inhibiting a Forkhead transcription factor. *Cell* 96, 857–868.

- Buckingham, M., and Rigby, P.W.J. (2014). Gene regulatory networks and transcriptional mechanisms that control myogenesis. *Dev. Cell* 28, 225–238.
- Burkin, D.J., Wallace, G.Q., Nicol, K.J., Kaufman, D.J., and Kaufman, S.J. (2001). Enhanced expression of the alpha 7 beta 1 integrin reduces muscular dystrophy and restores viability in dystrophic mice. *J. Cell Biol.* 152, 1207–1218.
- Burkin, D.J., Wallace, G.Q., Milner, D.J., Chaney, E.J., Mulligan, J.A., and Kaufman, S.J. (2005). Transgenic expression of $\alpha 7\beta 1$ integrin maintains muscle integrity, increases regenerative capacity, promotes hypertrophy, and reduces cardiomyopathy in dystrophic mice. *Am. J. Pathol.* 166, 253–263.
- Burridge, K., and Mangeat, P. (1984). An interaction between vinculin and talin. *Nature* 308, 744–746.
- Bushby, K.M.D., and Beckmann, J.S. (1995). The limb-girdle muscular dystrophies--proposal for a new nomenclature. *Neuromuscul. Disord. NMD* 5, 337–343.
- Bushby, K.M.D., and Beckmann, J.S. (2003). The 105th ENMC sponsored workshop: pathogenesis in the non-sarcoglycan limb-girdle muscular dystrophies, Naarden, April 12-14, 2002. *Neuromuscul. Disord. NMD* 13, 80–90.
- Cai, D., Frantz, J.D., Tawa, N.E., Melendez, P.A., Oh, B.-C., Lidov, H.G.W., Hasselgren, P.-O., Frontera, W.R., Lee, J., Glass, D.J., et al. (2004). IKK β /NF- κ B activation causes severe muscle wasting in mice. *Cell* 119, 285–298.
- Campbell, K.P. (1995). Three muscular dystrophies: loss of cytoskeleton-extracellular matrix linkage. *Cell* 80, 675–679.
- Campbell, R.L., and Davies, P.L. (2012). Structure-function relationships in calpains. *Biochem. J.* 447, 335–351.
- Carlson, C.G., Rutter, J., Bledsoe, C., Singh, R., Hoff, H., Bruemmer, K., Sesti, J., Gatti, F., Berge, J., and McCarthy, L. (2010). A simple protocol for assessing inter-trial and inter-examiner reliability for two noninvasive measures of limb muscle strength. *J. Neurosci. Methods* 186, 226–230.
- Carter, S.L., Rennie, C.D., Hamilton, S.J., and Tarnopolsky, null (2001). Changes in skeletal muscle in males and females following endurance training. *Can. J. Physiol. Pharmacol.* 79, 386–392.
- Cashman, N.R., Covault, J., Wollman, R.L., and Sanes, J.R. (1987). Neural cell adhesion molecule in normal, denervated, and myopathic human muscle. *Ann. Neurol.* 21, 481–489.
- Cen, S., Zhang, J., Huang, F., Yang, Z., and Xie, H. (2008). Effect of IGF-1 on proliferation and differentiation of primary human embryonic myoblasts. *Zhongguo Xiu Fu Chong Jian Wai Ke Za Zhi Zhongguo Xiu fu Chongjian Waike Zazhi Chin. J. Reparative Reconstr. Surg.* 22, 84–87.
- Chae, J., Minami, N., Jin, Y., Nakagawa, M., Murayama, K., Igarashi, F., and Nonaka, I. (2001). Calpain 3 gene mutations: genetic and clinico-pathologic findings in limb-girdle muscular dystrophy. *Neuromuscul. Disord. NMD* 11, 547–555.
- Chan-Ling, T., Page, M.P., Gardiner, T., Baxter, L., Rosinova, E., and Hughes, S. (2004). Desmin ensheathment ratio as an indicator of vessel stability. *Am. J. Pathol.* 165, 1301–1313.

- Chang, R.S.M. (1954). Continuous subcultivation of epithelial-like cells from normal human tissues. *Proc. Soc. Exp. Biol. Med. Soc. Exp. Biol. Med. N. Y.* N 87, 440–443.
- Chargé, S.B.P., and Rudnicki, M.A. (2004). Cellular and molecular regulation of muscle regeneration. *Physiol. Rev.* 84, 209–238.
- Charrasse, S., Comunale, F., Grumbach, Y., Poulat, F., Blangy, A., and Gauthier-Rouvière, C. (2006). RhoA GTPase regulates M-cadherin activity and myoblast fusion. *Mol. Biol. Cell* 17, 749–759.
- Charrin, S., Latil, M., Soave, S., Polesskaya, A., Chrétien, F., Boucheix, C., and Rubinstein, E. (2013). Normal muscle regeneration requires tight control of muscle cell fusion by tetraspanins CD9 and CD81. *Nat. Commun.* 4, 1674.
- Charton, K., Sarparanta, J., Vihola, A., Milic, A., Jonson, P.H., Suel, L., Luque, H., Boumela, I., Richard, I., and Udd, B. (2015). CAPN3-mediated processing of C-terminal titin replaced by pathological cleavage in titinopathy. *Hum. Mol. Genet.* 24, 3718–3731.
- Chen, J.-F., Tao, Y., Li, J., Deng, Z., Yan, Z., Xiao, X., and Wang, D.-Z. (2010). microRNA-1 and microRNA-206 regulate skeletal muscle satellite cell proliferation and differentiation by repressing Pax7. *J. Cell Biol.* 190, 867–879.
- Chen, M., Wang, J., Lu, J., Bond, M.C., Ren, X.-R., Lyerly, H.K., Barak, L.S., and Chen, W. (2009). The anti-helminthic niclosamide inhibits Wnt/frizzled1 signaling. *Biochemistry (Mosc.)* 48, 10267–10274.
- Chevallier, A. (1979). Role of the somitic mesoderm in the development of the thorax in bird embryos. II. Origin of thoracic and appendicular musculature. *J. Embryol. Exp. Morphol.* 49, 73–88.
- Choy, C.T., Kim, H., Lee, J.-Y., Williams, D.M., Palethorpe, D., Fellows, G., Wright, A.J., Laing, K., Bridges, L.R., Howe, F.A., et al. (2013). Anosmin-1 contributes to brain tumor malignancy through integrin signal pathways. *Endocr. Relat. Cancer* 21, 85–99.
- Chrobáková, T., Hermanová, M., Kroupová, I., Vondráček, P., Maříková, T., Mazanec, R., Zámečník, J., Staněk, J., Havlová, M., and Fajkusová, L. (2004). Mutations in Czech LGMD2A patients revealed by analysis of calpain 3 mRNA and their phenotypic outcome. *Neuromuscul. Disord.* 14, 659–665.
- Chua, K.H., Aminuddin, B.S., Fuzina, N.H., and Ruszymah, B.H.I. (2007). Basic fibroblast growth factor with human serum supplementation: enhancement of human chondrocyte proliferation and promotion of cartilage regeneration. *Singapore Med. J.* 48, 324–332.
- Chung, S.Y., Huang, W.C., Su, C.W., Lee, K.W., Chi, H.C., Lin, C.T., Chen, S., Huang, K.M., Tsai, M.S., Yu, H.P., et al. (2013). FoxO6 and PGC-1 α form a regulatory loop in myogenic cells. *Biosci. Rep.* 33, 485–497.
- Cobo, A.M., Sáenz, A., Poza, J.J., Urtasun, M., Indakoetxea, B., Urtizberea, J.A., López de Munain, A., and Calafell, F. (2004). A common haplotype associated with the Basque 2362AG --> TCATCT mutation in the muscular calpain-3 gene. *Hum. Biol.* 76, 731–741.
- Cohen, P., and Goedert, M. (2004). GSK3 inhibitors: development and therapeutic potential. *Nat. Rev. Drug Discov.* 3, 479–487.

- Comai, G., and Tajbakhsh, S. (2014). Molecular and cellular regulation of skeletal myogenesis. In *current topics in developmental biology*, (Elsevier), pp. 1–73.
- Conboy, I.M., and Rando, T.A. (2002). The regulation of Notch signaling controls satellite cell activation and cell fate determination in postnatal myogenesis. *Dev. Cell* 3, 397–409.
- Cornelison, D.D.W., and Wold, B.J. (1997). Single-cell analysis of regulatory gene expression in quiescent and activated mouse skeletal muscle satellite cells. *Dev. Biol.* 191, 270–283.
- Corrick, K.L., Stec, M.J., Merritt, E.K., Windham, S.T., Thomas, S.J., Cross, J.M., and Bamman, M.M. (2015). Serum from human burn victims impairs myogenesis and protein synthesis in primary myoblasts. *Front. Physiol.* 6.
- Crisan, M., Yap, S., Casteilla, L., Chen, C.-W., Corselli, M., Park, T.S., Andriolo, G., Sun, B., Zheng, B., Zhang, L., et al. (2008). A perivascular origin for mesenchymal stem cells in multiple human organs. *Cell Stem Cell* 3, 301–313.
- Crist, C.G., Montarras, D., and Buckingham, M. (2012). Muscle satellite cells are primed for myogenesis but maintain quiescence with sequestration of Myf5 mRNA targeted by microRNA-31 in mRNP granules. *Cell Stem Cell* 11, 118–126.
- Croall, D.E., and DeMartino, G.N. (1991). Calcium-activated neutral protease (calpain) system: structure, function, and regulation. *Physiol. Rev.* 71, 813–847.
- Cross, D.A.E., Alessi, D.R., Cohen, P., Andjelkovich, M., and Hemmings, B.A. (1995). Inhibition of glycogen synthase kinase-3 by insulin mediated by protein kinase B. *Nature* 378, 785–789.
- Dang, K., Li, Y.-Z., Gong, L.-C., Xue, W., Wang, H.-P., Goswami, N., and Gao, Y.-F. (2016). Stable atrogen-1 (Fbxo32) and MuRF1 (Trim63) gene expression is involved in the protective mechanism in soleus muscle of hibernating Daurian ground squirrels (*Spermophilus dauricus*). *Biol. Open* 5, 62–71.
- Danowski, B.A., Imanaka-Yoshida, K., Sanger, J.M., and Sanger, J.W. (1992). Costameres are sites of force transmission to the substratum in adult rat cardiomyocytes. *J. Cell Biol.* 118, 1411–1420.
- Darabi, R., Arpke, R.W., Irion, S., Dimos, J.T., Grskovic, M., Kyba, M., and Perlingeiro, R.C.R. (2012). Human ES- and iPS-derived myogenic progenitors restore dystrophin and improve contractility upon transplantation in dystrophic mice. *Cell Stem Cell* 10, 610–619.
- Daude, N., Wohlgemuth, S., Brown, R., Pitstick, R., Gapeshtina, H., Yang, J., Carlson, G.A., and Westaway, D. (2012). Knockout of the prion protein (PrP)-like Sprn gene does not produce embryonic lethality in combination with PrPC-deficiency. *Proc. Natl. Acad. Sci.* 109, 9035–9040.
- Davis, R.L., Weintraub, H., and Lassar, A.B. (1987). Expression of a single transfected cDNA converts fibroblasts to myoblasts. *Cell* 51, 987–1000.
- De Angelis, L., Berghella, L., Coletta, M., Lattanzi, L., Zanchi, M., Cusella-De Angelis, M.G., Ponzetto, C., and Cossu, G. (1999). Skeletal myogenic progenitors originating from embryonic dorsal aorta coexpress endothelial and myogenic markers and contribute to postnatal muscle growth and regeneration. *J. Cell Biol.* 147, 869–878.

- De la Torre, C., Illa, I., Faulkner, G., Soria, L., Robles-Cedeño, R., Dominguez-Perles, R., De Luna, N., and Gallardo, E. (2009). Proteomics identification of differentially expressed proteins in the muscle of dysferlin myopathy patients. *Proteomics - Clin. Appl.* 3, 486–497.
- De Luca, A. (2003). Enhanced dystrophic Progression in *mdx* mice by exercise and beneficial effects of taurine and insulin-like growth factor-1. *J. Pharmacol. Exp. Ther.* 304, 453–463.
- De Paula, F., Vainzof, M., Passos-Bueno, M.R., de Cássia M Pavanello, R., Matioli, S.R., V B Anderson, L., Nigro, V., and Zatz, M. (2002). Clinical variability in calpainopathy: What makes the difference? *Eur. J. Hum. Genet.* 10, 825–832.
- De Souza, A.T., Dai, X., Spencer, A.G., Reppen, T., Menzie, A., Roesch, P.L., He, Y., Caguyong, M.J., Bloomer, S., Herweijer, H., et al. (2006). Transcriptional and phenotypic comparisons of Ppara knockout and siRNA knockdown mice. *Nucleic Acids Res.* 34, 4486–4494.
- De Tullio, R., Stifanese, R., Salamino, F., Pontremoli, S., and Melloni, E. (2003). Characterization of a new p94-like calpain form in human lymphocytes. *Biochem. J.* 375, 689–696.
- Dear, T.N., Matena, K., Vingron, M., and Boehm, T. (1997). A new subfamily of vertebrate calpains lacking a calmodulin-like domain: implications for calpain regulation and evolution. *Genomics* 45, 175–184.
- Dear, T.N., Möller, A., and Boehm, T. (1999). CAPN11: A calpain with high mRNA levels in testis and located on chromosome 6. *Genomics* 59, 243–247.
- Dear, T.N., and Boehm, T. (1999). Diverse mRNA expression patterns of the mouse calpain genes *Capn5*, *Capn6* and *Capn11* during development. *Mech. Dev.* 89, 201–209.
- Dear, T.N., Meier, N.T., Hunn, M., and Boehm, T. (2000). Gene structure, chromosomal localization, and expression pattern of *Capn12*, a new member of the calpain large subunit gene family. *Genomics* 68, 152–160.
- Dear, T.N., and Boehm, T. (2001). Identification and characterization of two novel calpain large subunit genes. *Gene* 274, 245–252.
- Degardin, A., Morillon, D., Lacour, A., Cotten, A., Vermersch, P., and Stojkovic, T. (2010). Morphologic imaging in muscular dystrophies and inflammatory myopathies. *Skeletal Radiol.* 39, 1219–1227.
- Dellavalle, A., Sampaolesi, M., Tonlorenzi, R., Tagliafico, E., Sacchetti, B., Perani, L., Innocenzi, A., Galvez, B.G., Messina, G., Morosetti, R., et al. (2007). Pericytes of human skeletal muscle are myogenic precursors distinct from satellite cells. *Nat. Cell Biol.* 9, 255–267.
- Demonbreun, A.R., Fahrenbach, J.P., Deveaux, K., Earley, J.U., Pytel, P., and McNally, E.M. (2011). Impaired muscle growth and response to insulin-like growth factor 1 in dysferlin-mediated muscular dystrophy. *Hum. Mol. Genet.* 20, 779–789.
- Dey, B.K., Gagan, J., and Dutta, A. (2011). miR-206 and -486 induce myoblast differentiation by downregulating *Pax7*. *Mol. Cell. Biol.* 31, 203–214.
- DiFranco, M., Kramerova, I., Vergara, J.L., and Spencer, M.J. (2016). Attenuated Ca²⁺ release in a mouse model of limb girdle muscular dystrophy 2A. *Skelet. Muscle* 6.

- Dihlmann, S., Kloor, M., Fallsehr, C., and von Knebel Doeberitz, M. (2005). Regulation of AKT1 expression by beta-catenin/Tcf/Lef signaling in colorectal cancer cells. *Carcinogenesis* 26, 1503–1512.
- Dijkers, P.F., Medema, R.H., Lammers, J.W., Koenderman, L., and Coffey, P.J. (2000). Expression of the pro-apoptotic Bcl-2 family member Bim is regulated by the forkhead transcription factor FKHR-L1. *Curr. Biol. CB* 10, 1201–1204.
- Ding, V.W., Chen, R.-H., and McCormick, F. (2000). Differential regulation of glycogen synthase kinase 3 β by insulin and Wnt signaling. *J. Biol. Chem.* 275, 32475–32481.
- Dowling, J.J., Vreede, A.P., Kim, S., Golden, J., and Feldman, E.L. (2008). Kindlin-2 is required for myocyte elongation and is essential for myogenesis. *BMC Cell Biol.* 9, 36.
- Drummond, M.J., Conlee, R.K., Mack, G.W., Sudweeks, S., Schaalje, G.B., and Parcell, A.C. (2010). Myogenic regulatory factor response to resistance exercise volume in skeletal muscle. *Eur. J. Appl. Physiol.* 108, 771–778.
- Du, W.J., Li, J.K., Wang, Q.Y., Hou, J.B., and Yu, B. (2009). Lithium chloride preconditioning optimizes skeletal myoblast functions for cellular cardiomyoplasty *in vitro* via glycogen synthase kinase-3beta/beta-catenin signaling. *Cells Tissues Organs* 190, 11–19.
- Duchen, L.W., Excell, B.J., Patel, R., and Smith, B. (1973). Proceedings: Light and electron microscopic changes in mouse muscle fibres and motor end-plates caused by the depolarizing fraction (cardiotoxin) of the venom of *Dendroaspis jamesoni*. *J. Physiol.* 234, 1P-2P.
- Dunø, M., Colding-Jørgensen, E., Grønnet, M., Jespersen, T., Vissing, J., and Schwartz, M. (2004). Difference in allelic expression of the CLCN1 gene and the possible influence on the myotonia congenita phenotype. *Eur. J. Hum. Genet.* 12, 738–743.
- Durigan, J.L.Q., Peviani, S.M., Russo, T.L., Silva, A.C.D., Vieira, R.P., Martins, M.A., Carvalho, C.R.F., and Salvini, T.F. (2009). Effects of exercise training on atrophy gene expression in skeletal muscle of mice with chronic allergic lung inflammation. *Braz. J. Med. Biol. Res. Rev. Bras. Pesqui. Medicas E Biol.* 42, 339–345.
- Edelman, G.M. (1986). Cell adhesion molecules in the regulation of animal form and tissue pattern. *Annu. Rev. Cell Biol.* 2, 81–116.
- Edmondson, D.G., and Olson, E.N. (1990). A gene with homology to the myc similarity region of MyoD1 is expressed during myogenesis and is sufficient to activate the muscle differentiation program. *Genes Dev.* 4, 1450.
- Ehnert, S., Seeliger, C., Vester, H., Schmitt, A., Saidy-Rad, S., Lin, J., Neumaier, M., Gillen, S., Kleeff, J., Friess, H., et al. (2011). Autologous serum improves yield and metabolic capacity of monocyte-derived hepatocyte-like cells: possible implication for Cell transplantation. *Cell Transplant.* 20, 1465–1478.
- Eijkelenboom, A., and Burgering, B.M.T. (2013). FOXOs: signalling integrators for homeostasis maintenance. *Nat. Rev. Mol. Cell Biol.* 14, 83–97.
- Emery, A.E. (2002). The muscular dystrophies. *The Lancet* 359, 687–695.

- Ennion, S., Sant'ana Pereira, J., Sargeant, A.J., Young, A., and Goldspink, G. (1995). Characterization of human skeletal muscle fibres according to the myosin heavy chains they express. *J. Muscle Res. Cell Motil.* 16, 35–43.
- Ermolova, N., Kramerova, I., and Spencer, M.J. (2015). Autolytic activation of calpain 3 proteinase is facilitated by calmodulin protein. *J. Biol. Chem.* 290, 996–1004.
- Ervasti, J.M. (2003). Costameres: the Achilles' heel of Herculean muscle. *J. Biol. Chem.* 278, 13591–13594.
- Essers, M.A.G., de Vries-Smits, L.M.M., Barker, N., Polderman, P.E., Burgering, B.M.T., and Korswagen, H.C. (2005). Functional interaction between beta-catenin and FOXO in oxidative stress signaling. *Science* 308, 1181–1184.
- Estrella, N.L., and Naya, F.J. (2014). Transcriptional networks regulating the costamere, sarcomere, and other cytoskeletal structures in striated muscle. *Cell. Mol. Life Sci.* 71, 1641–1656.
- Evenson, A.R., Fareed, M.U., Menconi, M.J., Mitchell, J.C., and Hasselgren, P.-O. (2005). GSK-3 β inhibitors reduce protein degradation in muscles from septic rats and in dexamethasone-treated myotubes. *Int. J. Biochem. Cell Biol.* 37, 2226–2238.
- Ewen, E.P., Snyder, C.M., Wilson, M., Desjardins, D., and Naya, F.J. (2011). The Mef2A transcription factor coordinately regulates a costamere gene program in cardiac muscle. *J. Biol. Chem.* 286, 29644–29653.
- Fanin, M., Nascimbeni, A.C., Fulizio, L., Trevisan, C.P., Meznaric-Petrusa, M., and Angelini, C. (2003). Loss of calpain-3 autocatalytic activity in LGMD2A patients with normal protein expression. *Am. J. Pathol.* 163, 1929–1936.
- Fanin, M., Fulizio, L., Nascimbeni, A.C., Spinazzi, M., Piluso, G., Ventriglia, V.M., Ruzza, G., Siciliano, G., Trevisan, C.P., Politano, L., et al. (2004). Molecular diagnosis in LGMD2A: Mutation analysis or protein testing? *Hum. Mutat.* 24, 52–62.
- Fanin, M., Benedicenti, F., Fritegotto, C., Nascimbeni, A., Peterle, E., Stanzial, F., Cristofolletti, A., Castellani, C., and Angelini, C. (2012). An intronic mutation causes severe LGMD2A in a large inbred family belonging to a genetic isolate in the Alps. *Clin. Genet.* 82, 601–602.
- Fanin, M., and Angelini, C. (2015). Protein and genetic diagnosis of limb girdle muscular dystrophy type 2A: The yield and the pitfalls: Protein and Genetic Diagnosis of LGMD2A. *Muscle Nerve* 52, 163–173.
- Fardeau, M., Hillaire, D., Mignard, C., Feingold, N., Feingold, J., Mignard, D., de Ubeda, B., Collin, H., Tome, F.M., Richard, I., et al. (1996a). Juvenile limb-girdle muscular dystrophy. Clinical, histopathological and genetic data from a small community living in the Reunion Island. *Brain J. Neurol.* 119 (Pt 1), 295–308.
- Fardeau, M., Eymard, B., Mignard, C., Tomé, F.M., Richard, I., and Beckmann, J.S. (1996b). Chromosome 15-linked limb-girdle muscular dystrophy: clinical phenotypes in Reunion Island and French metropolitan communities. *Neuromuscul. Disord.* NMD 6, 447–453.

- Farina, L., De Santis, A., Morelli, G., and Ruberti, I. (2007). Dynamic measure of gene co-regulation. *IET Syst. Biol.* 1, 10–17.
- Feero, W., Li, S., Rosenblatt, J., Sirianni, N., Morgan, J., Partridge, T., Huang, L., and Hoffman, E. (1997). Selection and use of ligands for receptor-mediated gene delivery to myogenic cells. *Gene Ther.* 4, 664–674.
- Feng, X., Adiarte, E.G., and Devoto, S.H. (2006). Hedgehog acts directly on the zebrafish dermomyotome to promote myogenic differentiation. *Dev. Biol.* 300, 736–746.
- Figarella-Branger, D., Nedelec, J., Pellissier, J.F., Boucraut, J., Bianco, N., and Rougon, G. (1990). Expression of various isoforms of neural cell adhesive molecules and their highly polysialylated counterparts in diseased human muscles. *J. Neurol. Sci.* 98, 21–36.
- Fleckenstein, J.L., Watumull, D., Conner, K.E., Ezaki, M., Greenlee, R.G., Bryan, W.W., Chason, D.P., Parkey, R.W., Peshock, R.M., and Purdy, P.D. (1993). Denervated human skeletal muscle: MR imaging evaluation. *Radiology* 187, 213–218.
- Foley, A.R., Hu, Y., Zou, Y., Columbus, A., Shoffner, J., Dunn, D.M., Weiss, R.B., and Bönnemann, C.G. (2009). Autosomal recessive inheritance of classic Bethlem myopathy. *Neuromuscul. Disord.* 19, 813–817.
- Fougerousse, F., Durand, M., Suel, L., Pourquié, O., Delezoide, A.-L., Romero, N.B., Abitbol, M., and Beckmann, J.S. (1998). Expression of genes (CAPN3, SGCA, SGCB, and TTN) involved in progressive muscular dystrophies during early human development. *Genomics* 48, 145–156.
- Fougerousse, F., Anderson, L.V., Delezoide, A.L., Suel, L., Durand, M., and Beckmann, J.S. (2000). Calpain 3 expression during human cardiogenesis. *Neuromuscul. Disord.* NMD 10, 251–256.
- Franke, J., Abs, V., Zizzadoro, C., and Abraham, G. (2014). Comparative study of the effects of fetal bovine serum versus horse serum on growth and differentiation of primary equine bronchial fibroblasts. *BMC Vet. Res.* 10, 119.
- Franz, T., Vingron, M., Boehm, T., and Dear, T.N. (1999). Capn7: a highly divergent vertebrate calpain with a novel C-terminal domain. *Mamm. Genome Off. J. Int. Mamm. Genome Soc.* 10, 318–321.
- Franzini-Armstrong, C., and Jorgensen, A.O. (1994). Structure and development of E-C coupling units in skeletal muscle. *Annu. Rev. Physiol.* 56, 509–534.
- Frost, R.A., Lang, C.H., and Gelato, M.C. (1997). Transient exposure of human myoblasts to tumor necrosis factor- α inhibits serum and insulin-like growth factor-I stimulated protein synthesis. *Endocrinology* 138, 4153–4159.
- Fukada, S., Uezumi, A., Ikemoto, M., Masuda, S., Segawa, M., Tanimura, N., Yamamoto, H., Miyagoe-Suzuki, Y., and Takeda, S. (2007). Molecular signature of quiescent satellite cells in adult skeletal muscle. *Stem Cells Dayt. Ohio* 25, 2448–2459.
- Fukumoto, S., Hsieh, C.-M., Maemura, K., Layne, M.D., Yet, S.-F., Lee, K.-H., Matsui, T., Rosenzweig, A., Taylor, W.G., Rubin, J.S., et al. (2001). Akt participation in the Wnt signaling pathway through dishevelled. *J. Biol. Chem.* 276, 17479–17483.

- Fürst, D.O., Osborn, M., and Weber, K. (1989). Myogenesis in the mouse embryo: differential onset of expression of myogenic proteins and the involvement of titin in myofibril assembly. *J. Cell Biol.* 109, 517–527.
- Furukawa-Hibi, Y., Yoshida-Araki, K., Ohta, T., Ikeda, K., and Motoyama, N. (2002). FOXO forkhead transcription factors Induce G(2)-M checkpoint in response to oxidative stress. *J. Biol. Chem.* 277, 26729–26732.
- Furuyama, T., Nakazawa, T., Nakano, I., and Mori, N. (2000). Identification of the differential distribution patterns of mRNAs and consensus binding sequences for mouse DAF-16 homologues. *Biochem. J.* 349, 629–634.
- García Díaz, B.E., Gauthier, S., and Davies, P.L. (2006). Ca²⁺ dependency of calpain 3 (p94) activation. *Biochemistry (Mosc.)* 45, 3714–3722.
- García-González, D., Murcia-Belmonte, V., Esteban, P.F., Ortega, F., Díaz, D., Sánchez-Vera, I., Lebrón-Galán, R., Escobar-Castañondo, L., Martínez-Millán, L., Weruaga, E., et al. (2016). Anosmin-1 over-expression increases adult neurogenesis in the subventricular zone and neuroblast migration to the olfactory bulb. *Brain Struct. Funct.* 221, 239–260.
- Geiger, R.S., and Garvin, J.S. (1957). Pattern of regeneration of muscle from progressive muscular dystrophy patients cultivated *in vitro* as compared to normal human skeletal muscle. *J. Neuropathol. Exp. Neurol.* 16, 523–543.
- George, T., Velloso, C.P., Alsharidah, M., Lazarus, N.R., and Harridge, S.D.R. (2010). Sera from young and older humans equally sustain proliferation and differentiation of human myoblasts. *Exp. Gerontol.* 45, 875–881.
- Gerhardt, H., and Betsholtz, C. (2003). Endothelial-pericyte interactions in angiogenesis. *Cell Tissue Res.* 314, 15–23.
- Glinka, A., Wu, W., Delius, H., Monaghan, A.P., Blumenstock, C., and Niehrs, C. (1998). Dickkopf-1 is a member of a new family of secreted proteins and functions in head induction. *Nature* 391, 357–362.
- Goljanek-Whysall, K., Sweetman, D., Abu-Elmagd, M., Chapnik, E., Dalmay, T., Hornstein, E., and Munsterberg, A. (2011). MicroRNA regulation of the paired-box transcription factor Pax3 confers robustness to developmental timing of myogenesis. *Proc. Natl. Acad. Sci.* 108, 11936–11941.
- Goll, D.E., Thompson, V.F., Li, H., Wei, W., and Cong, J. (2003). The calpain system. *Physiol. Rev.* 83, 731–801.
- Goodyear, L.J., Chang, P.Y., Sherwood, D.J., Dufresne, S.D., and Moller, D.E. (1996). Effects of exercise and insulin on mitogen-activated protein kinase signaling pathways in rat skeletal muscle. *Am. J. Physiol.* 271, E403–408.
- Goto, H., Kawano, K., Kobayashi, I., Sakai, H., and Yanagisawa, S. (2002). Expression of cyclin D1 and GSK-3beta and their predictive value of prognosis in squamous cell carcinomas of the tongue. *Oral Oncol.* 38, 549–556.

- Granchelli, J.A., Pollina, C., and Hudecki, M.S. (2000). Pre-clinical screening of drugs using the *mdx* mouse. *Neuromuscul. Disord.* NMD 10, 235–239.
- Green, H.J., Thomson, J.A., Daub, W.D., Houston, M.E., and Ranney, D.A. (1979). position, fiber size and enzyme activities in vastus lateralis of elite athletes involved in high intensity exercise. *Eur. J. Appl. Physiol.* 41, 109–117.
- Grefte, S., Vullingsh, S., Kuijpers-Jagtman, A.M., Torensma, R., and Von den Hoff, J.W. (2012). Matrigel, but not collagen I, maintains the differentiation capacity of muscle derived cells *in vitro*. *Biomed. Mater.* 7, 055004.
- Gressner, A.M., and Wool, I.G. (1974). The phosphorylation of liver ribosomal proteins *in vivo*. Evidence that only a single small subunit protein (S6) is phosphorylated. *J. Biol. Chem.* 249, 6917–6925.
- Griffin, D.A., Johnson, R.W., Whitlock, J.M., Pozsgai, E.R., Heller, K.N., Grose, W.E., Arnold, W.D., Sahenk, Z., Hartzell, H.C., and Rodino-Klapac, L.R. (2016). Defective membrane fusion and repair in Anoctamin5-deficient muscular dystrophy. *Hum. Mol. Genet.* 25, 1900–1911.
- Groen, E.J., Charlton, R., Barresi, R., Anderson, L.V., Eagle, M., Hudson, J., Koref, M.S., Straub, V., and Bushby, K.M.D. (2007). Analysis of the UK diagnostic strategy for limb girdle muscular dystrophy 2A. *Brain J. Neurol.* 130, 3237–3249.
- Guerard, M.J., Sewry, C.A., and Dubowitz, V. (1985). Lobulated fibers in neuromuscular diseases. *J. Neurol. Sci.* 69, 345–356.
- Guglieri, M., Magri, F., D'Angelo, M.G., Prella, A., Morandi, L., Rodolico, C., Cagliani, R., Mora, M., Fortunato, F., Bordoni, A., et al. (2008). Clinical, molecular, and protein correlations in a large sample of genetically diagnosed Italian limb girdle muscular dystrophy patients. *Hum. Mutat.* 29, 258–266.
- Guteski-Hamblin, A.M., Greeb, J., and Shull, G.E. (1988). A novel Ca^{2+} pump expressed in brain, kidney, and stomach is encoded by an alternative transcript of the slow-twitch muscle sarcoplasmic reticulum Ca-ATPase gene. Identification of cDNAs encoding Ca^{2+} and other cation-transporting ATPases using an oligonucleotide probe derived from the ATP-binding site. *J. Biol. Chem.* 263, 15032–15040.
- Guo, Y., Xiao, L., Sun, L., and Liu, F. (2012). Wnt/beta-catenin signaling: a promising new target for fibrosis diseases. *Physiol. Res.* 61, 337–346.
- Guroff, G. (1964). A neutral, calcium-activated proteinase from the soluble fraction of rat brain. *J. Biol. Chem.* 239, 149–155.
- Gussoni, E., Soneoka, Y., Strickland, C.D., Buzney, E.A., Khan, M.K., Flint, A.F., Kunkel, L.M., and Mulligan, R.C. (1999). Dystrophin expression in the *mdx* mouse restored by stem cell transplantation. *Nature* 401, 390–394.
- Hackman, P., Vihola, A., Haravuori, H., Marchand, S., Sarparanta, J., de Seze, J., Labeit, S., Witt, C., Peltonen, L., Richard, I., et al. (2002). Tibial muscular dystrophy is a titinopathy caused by mutations in *TTN*, the gene encoding the giant skeletal-muscle protein titin. *Am. J. Hum. Genet.* 71, 492–500.

- Hamers, F.P.T., Lankhorst, A.J., van Laar, T.J., Veldhuis, W.B., and Gispen, W.H. (2001). Automated quantitative gait analysis during overground locomotion in the rat: its application to spinal cord contusion and transection injuries. *J. Neurotrauma* 18, 187–201.
- Hammond, C.L., Hinits, Y., Osborn, D.P.S., Minchin, J.E.N., Tettamanti, G., and Hughes, S.M. (2007). Signals and myogenic regulatory factors restrict Pax3 and Pax7 expression to dermomyotome-like tissue in zebrafish. *Dev. Biol.* 302, 504–521.
- Han, J.W., Pearson, R.B., Dennis, P.B., and Thomas, G. (1995). Rapamycin, wortmannin, and the methylxanthine SQ20006 inactivate p70s6k by inducing dephosphorylation of the same subset of sites. *J. Biol. Chem.* 270, 21396–21403.
- Hanna, R.A., Campbell, R.L., and Davies, P.L. (2008). Calcium-bound structure of calpain and its mechanism of inhibition by calpastatin. *Nature* 456, 409–412.
- Hanson, J., and Huxley, H.E. (1953). Structural basis of the cross-striations in muscle. *Nature* 172, 530–532.
- Hanson, J., and Lowy, J. (1963). The structure of F-actin and of actin filaments isolated from muscle. *J. Mol. Biol.* 6, 46–IN5.
- Hashimoto, T., Masuda, S., Taguchi, S., and Brooks, G.A. (2005). Immunohistochemical analysis of MCT1, MCT2 and MCT4 expression in rat plantaris muscle: MCT expression in rat skeletal muscle fibres. *J. Physiol.* 567, 121–129.
- Hasty, P., Bradley, A., Morris, J.H., Edmondson, D.G., Venuti, J.M., Olson, E.N., and Klein, W.H. (1993). Muscle deficiency and neonatal death in mice with a targeted mutation in the myogenin gene. *Nature* 364, 501–506.
- Hata, S., Abe, M., Suzuki, H., Kitamura, F., Toyama-Sorimachi, N., Abe, K., Sakimura, K., and Sorimachi, H. (2010). Calpain 8/nCL-2 and calpain 9/nCL-4 constitute an active protease complex, G-calpain, involved in gastric mucosal Defense. *PLoS Genet.* 6, e1001040.
- Hauerslev, S., Sveen, M.-L., Duno, M., Angelini, C., Vissing, J., and Krag, T.O. (2012). Calpain 3 is important for muscle regeneration: Evidence from patients with limb girdle muscular dystrophies. *BMC Musculoskelet. Disord.* 13.
- Hawke, T.J., and Garry, D.J. (2001). Myogenic satellite cells: physiology to molecular biology. *J. Appl. Physiol.* 91, 534–551.
- He, T.C., Sparks, A.B., Rago, C., Hermeking, H., Zawel, L., da Costa, L.T., Morin, P.J., Vogelstein, B., and Kinzler, K.W. (1998). Identification of c-MYC as a target of the APC pathway. *Science* 281, 1509–1512.
- Heanue, T.A., Reshef, R., Davis, R.J., Mardon, G., Oliver, G., Tomarev, S., Lassar, A.B., and Tabin, C.J. (1999). Synergistic regulation of vertebrate muscle development by Dach2, Eya2, and Six1, homologs of genes required for Drosophila eye formation. *Genes Dev.* 13, 3231–3243.
- Hedgepeth, C.M., Conrad, L.J., Zhang, J., Huang, H.C., Lee, V.M., and Klein, P.S. (1997). Activation of the Wnt signaling pathway: a molecular mechanism for lithium action. *Dev. Biol.* 185, 82–91.

- Hellström, M., Kalén, M., Lindahl, P., Abramsson, A., and Betsholtz, C. (1999). Role of PDGF-B and PDGFR-beta in recruitment of vascular smooth muscle cells and pericytes during embryonic blood vessel formation in the mouse. *Dev. Camb. Engl.* 126, 3047–3055.
- Hermanová, M., Zapletalová, E., Sedláčková, J., Chrobáková, T., Letocha, O., Kroupová, I., Zámečník, J., Vondráček, P., Mazanec, R., Maříková, T., et al. (2006). Analysis of histopathologic and molecular pathologic findings in Czech LGMD2A patients. *Muscle Nerve* 33, 424–432.
- Hirai, H., Verma, M., Watanabe, S., Tastad, C., Asakura, Y., and Asakura, A. (2010). MyoD regulates apoptosis of myoblasts through microRNA-mediated down-regulation of Pax3. *J. Cell Biol.* 191, 347–365.
- Hiramatsu, L., Kay, J.C., Thompson, Z., Singleton, J.M., Claghorn, G.C., Albuquerque, R.L., Ho, B., Ho, B., Sanchez, G., and Garland, T. (2017). Maternal exposure to western diet affects adult body composition and voluntary wheel running in a genotype-specific manner in mice. *Physiol. Behav.* 179, 235–245.
- Hiyama, A., Sakai, D., Arai, F., Nakajima, D., Yokoyama, K., and Mochida, J. (2011). Effects of a glycogen synthase kinase-3 β inhibitor (LiCl) on c-myc protein in intervertebral disc cells. *J. Cell. Biochem.* 112, 2974–2986.
- Hodges, B.L., Hayashi, Y.K., Nonaka, I., Wang, W., Arahata, K., and Kaufman, S.J. (1997). Altered expression of the $\alpha 7\beta 1$ integrin in human and murine muscular dystrophies. *J. Cell Sci.* 110 (Pt 22), 2873–2881.
- Hofer, T., Marzetti, E., Seo, A.Y., Xu, J., and Knutson, M.D. (2008). Free radicals in biology and medicine.
- Hoogewijs, D., Ebner, B., Germani, F., Hoffmann, F.G., Fabrizius, A., Moens, L., Burmester, T., Dewilde, S., Storz, J.F., Vinogradov, S.N., et al. (2012). Androglobin: a chimeric globin in metazoans that is preferentially expressed in mammalian testes. *Mol. Biol. Evol.* 29, 1105–1114.
- Hoppler, S., Brown, J.D., and Moon, R.T. (1996). Expression of a dominant-negative Wnt blocks induction of MyoD in *Xenopus* embryos. *Genes Dev.* 10, 2805–2817.
- Horikawa, Y., Oda, N., Cox, N.J., Li, X., Orho-Melander, M., Hara, M., Hinokio, Y., Lindner, T.H., Mashima, H., Schwarz, P.E., et al. (2000). Genetic variation in the gene encoding calpain-10 is associated with type 2 diabetes mellitus. *Nat. Genet.* 26, 163–175.
- Horton, M.J., Brandon, C.A., Morris, T.J., Braun, T.W., Yaw, K.M., and Sciote, J.J. (2001). Abundant expression of myosin heavy-chain IIB RNA in a subset of human masseter muscle fibres. *Arch. Oral Biol.* 46, 1039–1050.
- Hosaka, Y., Yokota, T., Miyagoe-Suzuki, Y., Yuasa, K., Imamura, M., Matsuda, R., Ikemoto, T., Kameya, S., and Takeda, S. (2002). $\alpha 1$ -syntrophin-deficient skeletal muscle exhibits hypertrophy and aberrant formation of neuromuscular junctions during regeneration. *J. Cell Biol.* 158, 1097–1107.
- Hosfield, C.M. (1999). Crystal structure of calpain reveals the structural basis for Ca²⁺-dependent protease activity and a novel mode of enzyme activation. *EMBO J.* 18, 6880–6889.

- Hu, P., Geles, K.G., Paik, J.-H., DePinho, R.A., and Tjian, R. (2008). Codependent activators direct myoblast-specific MyoD transcription. *Dev. Cell* 15, 534–546.
- Hughes, S., and Chan-Ling, T. (2004). Characterization of smooth muscle cell and pericyte differentiation in the rat retina *in vivo*. *Investig. Ophthalmology Vis. Sci.* 45, 2795.
- Huxley, A.F., and Niedergerke, R. (1954). Structural changes in muscle during contraction: interference microscopy of living muscle fibres. *Nature* 173, 971–973.
- Huxley, H.E. (1953). Electron microscope studies of the organisation of the filaments in striated muscle. *Biochim. Biophys. Acta* 12, 387–394.
- Huxley, H.E., and Hanson, J. (1954). Changes in the cross-striations of muscle during contraction and stretch and their structural interpretation. *Nature* 173, 973–976.
- Huxley, H.E., and Brown, W. (1967). The low-angle x-ray diagram of vertebrate striated muscle and its behaviour during contraction and rigor. *J. Mol. Biol.* 30, 383–434.
- Huynh, K.M., Kim, G., Kim, D.-J., Yang, S.-J., Park, S., Yeom, Y.-I., Fisher, P.B., and Kang, D. (2009). Gene expression analysis of terminal differentiation of human melanoma cells highlights global reductions in cell cycle-associated genes. *Gene* 433, 32–39.
- Hynes, R.O. (1992). Integrins: versatility, modulation, and signaling in cell adhesion. *Cell* 69, 11–25.
- Ibraghimov-Beskrovnaya, O., Ervasti, J.M., Leveille, C.J., Slaughter, C.A., Sernett, S.W., and Campbell, K.P. (1992). Primary structure of dystrophin-associated glycoproteins linking dystrophin to the extracellular matrix. *Nature* 355, 696–702.
- Illa, I., Leon-Monzon, M., and Dalakas, M.C. (1992). Regenerating and denervated human muscle fibers and satellite cells express neural cell adhesion molecule recognized by monoclonal antibodies to natural killer cells. *Ann. Neurol.* 31, 46–52.
- Ingber, D. (1991). Extracellular matrix and cell shape: Potential control points for inhibition of angiogenesis. *J. Cell. Biochem.* 47, 236–241.
- Isaac, C., Mattos, C.N. de, Rêgo, F.M.P. do, Cardim, L.N., Altran, S.C., Paggiaro, A.O., Tutihashi, R.M.C., Mathor, M.B., and Ferreira, M.C. (2011). Replacement of fetal calf serum by human serum as supplementation for human fibroblast culture. *Rev. Bras. Cir. Plástica Impresso* 26, 379–384.
- Ivaska, J., Nissinen, L., Immonen, N., Eriksson, J.E., Kähäri, V.-M., and Heino, J. (2002). Integrin alpha 2 beta 1 promotes activation of protein phosphatase 2A and dephosphorylation of Akt and glycogen synthase kinase 3 beta. *Mol. Cell. Biol.* 22, 1352–1359.
- Jacob, M., Christ, B., and Jacob, H.J. (1979). The migration of myogenic cells from the somites into the leg region of avian embryos. An ultrastructural study. *Anat. Embryol. (Berl.)* 157, 291–309.
- Jacquemin, V., Furling, D., Bigot, A., Butler-Browne, G., and Mouly, V. (2004). IGF-1 induces human myotube hypertrophy by increasing cell recruitment. *Exp. Cell Res.* 299, 148–158.
- Jackson, J.R., Kirby, T.J., Fry, C.S., Cooper, R.L., McCarthy, J.J., Peterson, C.A., and Dupont-Versteegden, E.E. (2015). Reduced voluntary running performance is associated with impaired coordination as a result of muscle satellite cell depletion in adult mice. *Skelet. Muscle* 5.

- Jaka, O., Kramerova, I., Azpitarte, M., López de Munain, A., Spencer, M., and Sáenz, A. (2012). C3KO mouse expression analysis: downregulation of the muscular dystrophy Ky protein and alterations in muscle aging. *Neurogenetics* 13, 347–357.
- Jaka, O. (2014). Aplicación del análisis de expresión en el diagnóstico y en la caracterización fisiopatológica de la distrofia muscular de cinturas tipo 2A en un modelo murino y en modelos celulares humanos. Universidad del País Vasco.
- Jaka, O., Casas-Fraile, L., Azpitarte, M., Aiastui, A., López de Munain, A., and Sáenz, A. (2017). FRZB and melusin, overexpressed in LGMD2A, regulate integrin β 1D isoform replacement altering myoblast fusion and the integrin-signalling pathway. *Expert Rev. Mol. Med.* 19.
- Jia, Z., Petrounevitch, V., Wong, A., Moldoveanu, T., Davies, P.L., Elce, J.S., and Beckmann, J.S. (2001). Mutations in calpain 3 associated with limb girdle muscular dystrophy: analysis by molecular modeling and by mutation in m-calpain. *Biophys. J.* 80, 2590–2596.
- Joe, A.W.B., Yi, L., Natarajan, A., Le Grand, F., So, L., Wang, J., Rudnicki, M.A., and Rossi, F.M.V. (2010). Muscle injury activates resident fibro/adipogenic progenitors that facilitate myogenesis. *Nat. Cell Biol.* 12, 153–163.
- Johnson, R.L., Laufer, E., Riddle, R.D., and Tabin, C. (1994). Ectopic expression of Sonic hedgehog alters dorsal-ventral patterning of somites. *Cell* 79, 1165–1173.
- Jones, A.E., Price, F.D., Le Grand, F., Soleimani, V.D., Dick, S.A., Megeney, L.A., and Rudnicki, M.A. (2015). Wnt/ β -catenin controls follistatin signalling to regulate satellite cell myogenic potential. *Skelet. Muscle* 5.
- Jones, N.C., Tyner, K.J., Nibarger, L., Stanley, H.M., Cornelison, D.D.W., Fedorov, Y.V., and Olwin, B.B. (2005). The p38 α / β MAPK functions as a molecular switch to activate the quiescent satellite cell. *J. Cell Biol.* 169, 105–116.
- Jones, S.W., Parr, T., Sensky, P.L., Scothern, G.P., Bardsley, R.G., and Buttery, P.J. (1999). Fibre type-specific expression of p94, a skeletal muscle-specific calpain. *J. Muscle Res. Cell Motil.* 20, 417–424.
- Judge, S.M., Wu, C.-L., Beharry, A.W., Roberts, B.M., Ferreira, L.F., Kandarian, S.C., and Judge, A.R. (2014). Genome-wide identification of FoxO-dependent gene networks in skeletal muscle during C26 cancer cachexia. *BMC Cancer* 14.
- Junion, G., Jagla, T., Duplant, S., Tapin, R., Da Ponte, J.-P., and Jagla, K. (2005). Mapping Dmef2-binding regulatory modules by using a ChIP-enriched in silico targets approach. *Proc. Natl. Acad. Sci.* 102, 18479–18484.
- Kamei, M., Webb, G.C., Young, I.G., and Campbell, H.D. (1998). SOLH, a human homologue of the drosophila melanogaster small optic lobes gene is a member of the calpain and zinc-finger gene families and maps to human chromosome 16p13.3 near CATM (cataract with microphthalmia). *Genomics* 51, 197–206.
- Kamei, Y., Miura, S., Suzuki, M., Kai, Y., Mizukami, J., Taniguchi, T., Mochida, K., Hata, T., Matsuda, J., Aburatani, H., et al. (2004). Skeletal muscle FOXO1 (FKHR) transgenic mice have less skeletal

- muscle mass, down-regulated type I (slow twitch/red muscle) fiber genes, and impaired glycemic control. *J. Biol. Chem.* 279, 41114–41123.
- Kammoun, M., Cassar-Malek, I., Meunier, B., and Picard, B. (2014). A simplified immunohistochemical classification of skeletal muscle fibres in mouse. *Eur. J. Histochem.* 58.
- Kanagawa, M., and Toda, T. (2006). The genetic and molecular basis of muscular dystrophy: roles of cell–matrix linkage in the pathogenesis. *J. Hum. Genet.* 51, 915–926.
- Karakas, B., Weeraratna, A.T., Abukhdeir, A.M., Konishi, H., Gustin, J.P., Vitolo, M.I., Bachman, K.E., and Park, B.H. (2007). P21 gene knock down does not identify genetic effectors seen with gene knock out. *Cancer Biol. Ther.* 6, 1025–1030.
- Kassar-Duchossoy, L., Gayraud-Morel, B., Gomès, D., Rocancourt, D., Buckingham, M., Shinin, V., and Tajbakhsh, S. (2004). *Mrf4* determines skeletal muscle identity in *Myf5:Myod* double-mutant mice. *Nature* 431, 466–471.
- Kawabata, Y., Hata, S., Ono, Y., Ito, Y., Suzuki, K., Abe, K., and Sorimachi, H. (2003). Newly identified exons encoding novel variants of p94/calpain 3 are expressed ubiquitously and overlap the alpha-glucosidase C gene. *FEBS Lett.* 555, 623–630.
- Kawai, H., Akaike, M., Kunishige, M., Inui, T., Adachi, K., Kimura, C., Kawajiri, M., Nishida, Y., Endo, I., Kashiwagi, S., et al. (1998). Clinical, pathological, and genetic features of limb-girdle muscular dystrophy type 2A with new calpain 3 gene mutations in seven patients from three Japanese families. *Muscle Nerve* 21, 1493–1501.
- Keira, Y., Noguchi, S., Kurokawa, R., Fujita, M., Minami, N., Hayashi, Y.K., Kato, T., and Nishino, I. (2007). Characterization of lobulated fibers in limb girdle muscular dystrophy type 2A by gene expression profiling. *Neurosci. Res.* 57, 513–521.
- Kephart, J.J.G., Tiller, R.G.J., Crose, L.E.S., Slemmons, K.K., Chen, P.-H., Hinson, A.R., Bentley, R.C., Chi, J.-T.A., and Linardic, C.M. (2015). Secreted frizzled-related protein 3 (SFRP3) is required for tumorigenesis of PAX3-FOXO1-positive alveolar rhabdomyosarcoma. *Clin. Cancer Res.* 21, 4868–4880.
- Kho, A.T., Kang, P.B., Kohane, I.S., and Kunkel, L.M. (2006). Transcriptome-scale similarities between mouse and human skeletal muscles with normal and myopathic phenotypes. *BMC Musculoskelet. Disord.* 7.
- Khodabukus, A., and Baar, K. (2014). The effect of serum origin on tissue engineered skeletal muscle function. *J. Cell. Biochem.* 115, 2198–2207.
- Kinbara, K., Sorimachi, H., Ishiura, S., and Suzuki, K. (1997). Muscle-specific calpain, p94, interacts with the extreme C-terminal region of connectin, a unique region flanked by two immunoglobulin C2 motifs. *Arch. Biochem. Biophys.* 342, 99–107.
- Kinbara, K., Ishiura, S., Tomioka, S., Sorimachi, H., Jeong, S.Y., Amano, S., Kawasaki, H., Kolmerer, B., Kimura, S., Labeit, S., et al. (1998). Purification of native p94, a muscle-specific calpain, and characterization of its autolysis. *Biochem. J.* 335 (Pt 3), 589–596.

- King, W.G., Mattaliano, M.D., Chan, T.O., Tschlis, P.N., and Brugge, J.S. (1997). Phosphatidylinositol 3-kinase is required for integrin-stimulated AKT and Raf-1/mitogen-activated protein kinase pathway activation. *Mol. Cell. Biol.* 17, 4406–4418.
- Klein, P.S., and Melton, D.A. (1996). A molecular mechanism for the effect of lithium on development. *Proc. Natl. Acad. Sci. U. S. A.* 93, 8455–8459.
- Kloos, A., Fisher, L., Detloff, M., Hassenzahl, D., and Basso, D. (2005). Stepwise motor and all-or-none sensory recovery is associated with nonlinear sparing after incremental spinal cord injury in rats. *Exp. Neurol.* 191, 251–265.
- König, N., Raynaud, F., Feane, H., Durand, M., Mestre-Francès, N., Rossel, M., Ouali, A., and Benyamin, Y. (2003). Calpain 3 is expressed in astrocytes of rat and microcebus brain. *J. Chem. Neuroanat.* 25, 129–136.
- van der Kooi, A.J., Barth, P.G., Busch, H.F., de Haan, R., Ginjaar, H.B., van Essen, A.J., van Hooff, L.J., Höweler, C.J., Jennekens, F.G., Jongen, P., et al. (1996). The clinical spectrum of limb girdle muscular dystrophy. A survey in The Netherlands. *Brain J. Neurol.* 119 (Pt 5), 1471–1480.
- Kops, G.J., de Ruiter, N.D., De Vries-Smits, A.M., Powell, D.R., Bos, J.L., and Burgering, B.M. (1999). Direct control of the Forkhead transcription factor AFX by protein kinase B. *Nature* 398, 630–634.
- Kops, G.J.P.L., Dansen, T.B., Polderman, P.E., Saarloos, I., Wirtz, K.W.A., Coffey, P.J., Huang, T.-T., Bos, J.L., Medema, R.H., and Burgering, B.M.T. (2002). Forkhead transcription factor FOXO3a protects quiescent cells from oxidative stress. *Nature* 419, 316–321.
- Kottyan, L.C., Davis, B.P., Sherrill, J.D., Liu, K., Rochman, M., Kaufman, K., Weirauch, M.T., Vaughn, S., Lazaro, S., Rupert, A.M., et al. (2014). Genome-wide association analysis of eosinophilic esophagitis provides insight into the tissue specificity of this allergic disease. *Nat. Genet.* 46, 895–900.
- Kraemer, W.J., Patton, J.F., Gordon, S.E., Harman, E.A., Deschenes, M.R., Reynolds, K., Newton, R.U., Triplett, N.T., and Dziados, J.E. (1995). Compatibility of high-intensity strength and endurance training on hormonal and skeletal muscle adaptations. *J. Appl. Physiol.* 78, 976–989.
- Krahn, M., Lopez de Munain, A., Streichenberger, N., Bernard, R., Pécheux, C., Testard, H., Pena-Segura, J.L., Yoldi, E., Cabello, A., Romero, N.B., et al. (2006a). CAPN3 mutations in patients with idiopathic eosinophilic myositis. *Ann. Neurol.* 59, 905–911.
- Krahn, M., Bernard, R., Pecheux, C., Hammouda, E.H., Eymard, B., Lopez de Munain, A., Cobo, A.M., Romero, N., Urtizberea, A., Leturcq, F., et al. (2006b). Screening of the CAPN3 gene in patients with possible LGMD2A. *Clin. Genet.* 69, 444–449.
- Krahn, M., Goicoechea, M., Hanisch, F., Groen, E., Bartoli, M., Pécheux, C., Garcia-Bragado, F., Leturcq, F., Jeannet, P.-Y., Lobrinus, J., et al. (2011). Eosinophilic infiltration related to CAPN3 mutations: a pathophysiological component of primary calpainopathy? *Clin. Genet.* 80, 398–402.

- Kramerova, I., Kudryashova, E., Tidball, J. G., and Spencer, M.J. (2004). Null mutation of calpain 3 (p94) in mice causes abnormal sarcomere formation *in vivo* and *in vitro*. *Hum. Mol. Genet.* 13, 1373–1388.
- Kramerova, I., Kudryashova, E., Wu, B., and Spencer, M.J. (2006). Regulation of the M-cadherin- beta-catenin complex by calpain 3 during terminal stages of myogenic differentiation. *Mol. Cell. Biol.* 26, 8437–8447.
- Kramerova, I., Kudryashova, E., Venkatraman, G., and Spencer, M.J. (2007). Calpain 3 participates in sarcomere remodeling by acting upstream of the ubiquitin-proteasome pathway. *Hum. Mol. Genet.* 16, 1006.
- Kramerova, I., Kudryashova, E., Wu, B., Ottenheijm, C., Granzier, H., and Spencer, M.J. (2008). Novel role of calpain-3 in the triad-associated protein complex regulating calcium release in skeletal muscle. *Hum. Mol. Genet.* 17, 3271–3280.
- Kramerova, I., Kudryashova, E., Wu, B., Germain, S., Vandenborne, K., Romain, N., Haller, R.G., Verity, M.A., and Spencer, M.J. (2009). Mitochondrial abnormalities, energy deficit and oxidative stress are features of calpain 3 deficiency in skeletal muscle. *Hum. Mol. Genet.* 18, 3194–3205.
- Kramerova, I., Kudryashova, E., Ermolova, N., Saenz, A., Jaka, O., López de Munain, A., and Spencer, M.J. (2012). Impaired calcium calmodulin kinase signaling and muscle adaptation response in the absence of calpain 3. *Hum. Mol. Genet.* 21, 3193–3204.
- Kramerova, I., Ermolova, N., Eskin, A., Hevener, A., Quehenberger, O., Armando, A.M., Haller, R., Romain, N., Nelson, S.F., and Spencer, M.J. (2016). Failure to up-regulate transcription of genes necessary for muscle adaptation underlies limb girdle muscular dystrophy 2A (calpainopathy). *Hum. Mol. Genet.* 25, 2194–2207.
- Krauss, R.S. (2005). Close encounters: regulation of vertebrate skeletal myogenesis by cell-cell contact. *J. Cell Sci.* 118, 2355–2362.
- Ku, N.O., Zhou, X., Toivola, D.M., and Omary, M.B. (1999). The cytoskeleton of digestive epithelia in health and disease. *Am. J. Physiol.* 277, G1108-1137.
- Kuang, S., Kuroda, K., Le Grand, F., and Rudnicki, M.A. (2007). Asymmetric self-renewal and commitment of satellite stem cells in muscle. *Cell* 129, 999–1010.
- Kubica, N., Bolster, D.R., Farrell, P.A., Kimball, S.R., and Jefferson, L.S. (2005). Resistance exercise increases muscle protein synthesis and translation of eukaryotic initiation factor 2Be mRNA in a mammalian target of rapamycin-dependent manner. *J. Biol. Chem.* 280, 7570–7580.
- Kunkel, L.M., Monaco, A.P., Bertelson, C.J., and Colletti, C.A. (1986). Molecular genetics of Duchenne muscular dystrophy. *Cold Spring Harb. Symp. Quant. Biol.* 51, 349–351.
- Kuroda, K., Kuang, S., Taketo, M.M., and Rudnicki, M.A. (2013). Canonical Wnt signaling induces BMP-4 to specify slow myofibrogenesis of fetal myoblasts. *Skelet. Muscle* 3, 5.
- Kuznetsov, S.A., Mankani, M.H., and Robey, P.G. (2000). Effect of serum on human bone marrow stromal cells: ex vivo expansion and *in vivo* bone formation. *Transplantation* 70, 1780–1787.

- LaFramboise, W.A., Guthrie, R.D., Scalise, D., Elborne, V., Bombach, K.L., Armanious, C.S., and Magovern, J.A. (2003). Effect of muscle origin and phenotype on satellite cell muscle-specific gene expression. *J. Mol. Cell. Cardiol.* 35, 1307–1318.
- Lahoria, R., and Milone, M. (2016). Rhabdomyolysis featuring muscular dystrophies. *J. Neurol. Sci.* 361, 29–33.
- Lamminen, A.E., Tantt, J.I., Sepponen, R.E., Suramo, I.J.I., and Pinko, H. (1990). Magnetic resonance of diseased skeletal muscle: combined T1 measurement and chemical shift imaging. *Br. J. Radiol.* 63, 591–596.
- Lang, J.M., Esser, K.A., and Dupont-Versteegden, E.E. (2004). Altered activity of signaling pathways in diaphragm and tibialis anterior muscle of dystrophic mice. *Exp. Biol. Med.* Maywood NJ 229, 503–511.
- Lanier, L.L., Le, A.M., Phillips, J.H., Warner, N.L., and Babcock, G.F. (1983). Subpopulations of human natural killer cells defined by expression of the Leu-7 (HNK-1) and Leu-11 (NK-15) antigens. *J. Immunol. Baltim. Md* 1950 131, 1789–1796.
- Lanier, L.L., Testi, R., Bindl, J., and Phillips, J.H. (1989). Identity of Leu-19 (CD56) leukocyte differentiation antigen and neural cell adhesion molecule. *J. Exp. Med.* 169, 2233–2238.
- Lau, P., Bailey, P., Dowhan, D.H., and Muscat, G.E. (1999). Exogenous expression of a dominant negative RORalpha1 vector in muscle cells impairs differentiation: RORalpha1 directly interacts with p300 and myoD. *Nucleic Acids Res.* 27, 411–420.
- Lau, P., Nixon, S.J., Parton, R.G., and Muscat, G.E.O. (2004). RORalpha regulates the expression of genes involved in lipid homeostasis in skeletal muscle cells: caveolin-3 and CPT-1 are direct targets of ROR. *J. Biol. Chem.* 279, 36828–36840.
- Lau, P., Fitzsimmons, R.L., Pearen, M.A., Watt, M.J., and Muscat, G.E.O. (2011). Homozygous staggerer (sg/sg) mice display improved insulin sensitivity and enhanced glucose uptake in skeletal muscle. *Diabetologia* 54, 1169–1180.
- Laure, L., Suel, L., Roudaut, C., Bourg, N., Ouali, A., Bartoli, M., Richard, I., and Danièle, N. (2009). Cardiac ankyrin repeat protein is a marker of skeletal muscle pathological remodelling: Cardiac ankyrin repeat protein in muscle plasticity. *FEBS J.* 276, 669–684.
- Lawrence, J.C., Skurat, A.V., Roach, P.J., Azpiazu, I., and Manchester, J. (1997). Glycogen synthase: activation by insulin and effect of transgenic overexpression in skeletal muscle. *Biochem. Soc. Trans.* 25, 14–19.
- Le Grand, F., and Rudnicki, M.A. (2007). Skeletal muscle satellite cells and adult myogenesis. *Curr. Opin. Cell Biol.* 19, 628–633.
- Lee, J.M., Kim, I.S., Kim, H., Lee, J.S., Kim, K., Yim, H.Y., Jeong, J., Kim, J.H., Kim, J.-Y., Lee, H., et al. (2010). ROR α attenuates Wnt/ β -catenin signaling by PKC α -dependent phosphorylation in colon cancer. *Mol. Cell* 37, 183–195.

- Lee, K., Shin, Y., Cheng, R., Park, K., Hu, Y., McBride, J., He, X., Takahashi, Y., and Ma, J. -x. (2014). Receptor heterodimerization as a novel mechanism for the regulation of Wnt/ β -catenin signaling. *J. Cell Sci.* 127, 4857–4869.
- Legate, K.R., Montañez, E., Kudlacek, O., and Füssler, R. (2006). ILK, PINCH and parvin: the tIPP of integrin signalling. *Nat. Rev. Mol. Cell Biol.* 7, 20–31.
- Léger, B., Cartoni, R., Praz, M., Lamon, S., Dériaz, O., Crettenand, A., Gobelet, C., Rohmer, P., Konzelmann, M., Luthi, F., et al. (2006). Akt signalling through GSK-3 β , mTOR and Foxo1 is involved in human skeletal muscle hypertrophy and atrophy: Akt signalling in muscle hypertrophy and atrophy. *J. Physiol.* 576, 923–933.
- Leyns, L., Bouwmeester, T., Kim, S.H., Piccolo, S., and De Robertis, E.M. (1997). Frzb-1 is a secreted antagonist of Wnt signaling expressed in the spemann organizer. *Cell* 88, 747–756.
- L'Honoré, A., Coulon, V., Marcil, A., Lebel, M., Lafrance-Vanasse, J., Gage, P., Camper, S., and Drouin, J. (2007). Sequential expression and redundancy of Pitx2 and Pitx3 genes during muscle development. *Dev. Biol.* 307, 421–433.
- Li, Z., Mericskay, M., Agbulut, O., Butler-Browne, G., Carlsson, L., Thornell, L.E., Babinet, C., and Paulin, D. (1997). Desmin is essential for the tensile strength and integrity of myofibrils but not for myogenic commitment, differentiation, and fusion of skeletal muscle. *J. Cell Biol.* 139, 129–144.
- Lilly, B., Zhao, B., Ranganayakulu, G., Paterson, B.M., Schulz, R.A., and Olson, E.N. (1995). Requirement of MADS domain transcription factor D-MEF2 for muscle formation in *Drosophila*. *Science* 267, 688–693.
- Liu, F., Zhang, G., Sheng, X., Liu, S., Cui, M., Guo, H., Xue, J., and Zhang, L. (2018). Effects of hereditary moderate high fat diet on metabolic performance and physical endurance capacity in C57BL/6 offspring. *Mol. Med. Rep.*
- Liu, Y., Heinichen, M., Wirth, K., Schmidtbleicher, D., and Steinacker, J.M. (2008). Response of growth and myogenic factors in human skeletal muscle to strength training. *Br. J. Sports Med.* 42, 989–993.
- Lodewyckx, L., Cailotto, F., Thysen, S., Luyten, F.P., and Lories, R.J. (2012). Tight regulation of wingless-type signaling in the articular cartilage - subchondral bone biomechanical unit: transcriptomics in Frzb-knockout mice. *Arthritis Res. Ther.* 14, R16.
- Lories, R.J.U., Peeters, J., Bakker, A., Tylzanowski, P., Derese, I., Schrooten, J., Thomas, J.T., and Luyten, F.P. (2007). Articular cartilage and biomechanical properties of the long bones in Frzb-knockout mice. *Arthritis Rheum.* 56, 4095–4103.
- Lories, R.J.U., Peeters, J., Szlufcik, K., Hespel, P., and Luyten, F.P. (2009). Deletion of frizzled-related protein reduces voluntary running exercise performance in mice. *Osteoarthritis Cartilage* 17, 390–396.
- Lu, M.H., DiLullo, C., Schultheiss, T., Holtzer, S., Murray, J.M., Choi, J., Fischman, D.A., and Holtzer, H. (1992). The vinculin/sarcomeric- α -actinin/ α -actin nexus in cultured cardiac myocytes. *J. Cell Biol.* 117, 1007–1022.

- Ma, H., Shih, M., Hata, I., Fukiage, C., Azuma, M., and Shearer, T.R. (2000). Lp85 calpain is an enzymatically active rodent-specific isozyme of lens Lp82. *Curr. Eye Res.* 20, 183–189.
- Macqueen, D.J., Delbridge, M.L., Manthri, S., and Johnston, I.A. (2010). A newly classified vertebrate calpain protease, directly ancestral to CAPN1 and 2, episodically evolved a restricted physiological function in placental mammals. *Mol. Biol. Evol.* 27, 1886–1902.
- Magri, F., Nigro, V., Angelini, C., Mongini, T., Mora, M., Moroni, I., Toscano, A., D'angelo, M.G., Tomelleri, G., Siciliano, G., et al. (2017). The italian limb girdle muscular dystrophy registry: Relative frequency, clinical features, and differential diagnosis: LGMD Italian registry. *Muscle Nerve* 55, 55–68.
- Mah, J.K., Korngut, L., Fiest, K.M., Dykeman, J., Day, L.J., Pringsheim, T., and Jette, N. (2016). A systematic review and meta-analysis on the epidemiology of the muscular dystrophies. *Can. J. Neurol. Sci. J. Can. Sci. Neurol.* 43, 163–177.
- Mahalingam, M., and Templeton, D.J. (1996). Constitutive activation of S6 kinase by deletion of amino-terminal autoinhibitory and rapamycin sensitivity domains. *Mol. Cell. Biol.* 16, 405–413.
- Maki, M., Narayana, S.V., and Hitomi, K. (1997). A growing family of the Ca²⁺-binding proteins with five EF-hand motifs. *Biochem. J.* 328 (Pt 2), 718–720.
- Malik, M.N., Fenko, M.D., Iqbal, K., and Wisniewski, H.M. (1983). Purification and characterization of two forms of Ca²⁺-activated neutral protease from calf brain. *J. Biol. Chem.* 258, 8955–8962.
- Mammucari, C., Milan, G., Romanello, V., Masiero, E., Rudolf, R., Del Piccolo, P., Burden, S.J., Di Lisi, R., Sandri, C., Zhao, J., et al. (2007). FoxO3 controls autophagy in skeletal muscle *in vivo*. *Cell Metab.* 6, 458–471.
- Manabe, Y., Ogino, S., Ito, M., Furuichi, Y., Takagi, M., Yamada, M., Goto-Inoue, N., Ono, Y., and Fujii, N.L. (2016). Evaluation of an *in vitro* muscle contraction model in mouse primary cultured myotubes. *Anal. Biochem.* 497, 36–38.
- Mann, B., Gelos, M., Siedow, A., Hanski, M.L., Gratchev, A., Ilyas, M., Bodmer, W.F., Moyer, M.P., Riecken, E.O., Buhr, H.J., et al. (1999). Target genes of beta-catenin-T cell-factor/lymphoid-enhancer-factor signaling in human colorectal carcinomas. *Proc. Natl. Acad. Sci. U. S. A.* 96, 1603–1608.
- Mansour, H. (2004). Restoration of resting sarcomere length after uniaxial static strain is regulated by protein kinase C and focal adhesion kinase. *Circ. Res.* 94, 642–649.
- Marden, F.A., Connolly, A.M., Siegel, M.J., and Rubin, D.A. (2005). Compositional analysis of muscle in boys with Duchenne muscular dystrophy using MR imaging. *Skeletal Radiol.* 34, 140–148.
- Marechal, G., Coulton, G.R., and Beckers-Bleukx, G. (1995). Mechanical power and myosin composition of soleus and extensor digitorum longus muscles of ky mice. *Am. J. Physiol. -Cell Physiol.* 268, C513–C519.
- Maricelli, J.W., Lu, Q.L., Lin, D.C., and Rodgers, B.D. (2016). Trendelenburg-like gait, instability and altered step patterns in a mouse model for limb girdle muscular dystrophy 2i. *PLoS ONE* 11, e0161984.

- Markuns, J.F., Wojtaszewski, J.F., and Goodyear, L.J. (1999). Insulin and exercise decrease glycogen synthase kinase-3 activity by different mechanisms in rat skeletal muscle. *J. Biol. Chem.* 274, 24896–24900.
- Martinez-Thompson, J.M., Niu, Z., Tracy, J.A., Moore, S.A., Swenson, A., Wieben, E.D., and Milone, M. (2018). Autosomal dominant calpainopathy due to heterozygous CAPN3 C.643_663del121. *Muscle Nerve* 57, 679–683.
- Martin-Pérez, J., and Thomas, G. (1983). Ordered phosphorylation of 40S ribosomal protein S6 after serum stimulation of quiescent 3T3 cells. *Proc. Natl. Acad. Sci. U. S. A.* 80, 926–930.
- Mathew, S.J., Hansen, J.M., Merrell, A.J., Murphy, M.M., Lawson, J.A., Hutcheson, D.A., Hansen, M.S., Angus-Hill, M., and Kardon, G. (2011). Connective tissue fibroblasts and Tcf4 regulate myogenesis. *Development* 138, 371–384.
- Matsumura, K., and Campbell, K.P. (1994). Dystrophin-glycoprotein complex: Its role in the molecular pathogenesis of muscular dystrophies. *Muscle Nerve* 17, 2–15.
- Mauro, A. (1961). Satellite cell of skeletal muscle fibers. *J. Biophys. Biochem. Cytol.* 9, 493–495.
- McCarthy, J.P., Agre, J.C., Graf, B.K., Pozniak, M.A., and Vailas, A.C. (1995). Compatibility of adaptive responses with combining strength and endurance training. *Med. Sci. Sports Exerc.* 27, 429–436.
- McCartney, N., Moroz, D., Garner, S.H., and McComas, A.J. (1988). The effects of strength training in patients with selected neuromuscular disorders. *Med. Sci. Sports Exerc.* 20, 362–368.
- McDaniel, J.D., Ulmer, J.L., Prost, R.W., Franczak, M.B., Jaradeh, S., Hamilton, C.A., and Mark, L.P. (1999). Magnetization transfer imaging of skeletal muscle in autosomal recessive limb girdle muscular dystrophy. *J. Comput. Assist. Tomogr.* 23, 609–614.
- McJunkin, K., Mazurek, A., Premsrirut, P.K., Zuber, J., Dow, L.E., Simon, J., Stillman, B., and Lowe, S.W. (2011). Reversible suppression of an essential gene in adult mice using transgenic RNA interference. *Proc. Natl. Acad. Sci.* 108, 7113–7118.
- McLoughlin, T.J., Smith, S.M., DeLong, A.D., Wang, H., Unterman, T.G., and Esser, K.A. (2009). FoxO1 induces apoptosis in skeletal myotubes in a DNA-binding-dependent manner. *Am. J. Physiol.-Cell Physiol.* 297, C548–C555.
- Medema, R.H., Kops, G.J.P.L., Bos, J.L., and Burgering, B.M.T. (2000). AFX-like Forkhead transcription factors mediate cell-cycle regulation by Ras and PKB through p27kip1. *Nature* 404, 782–787.
- Mercuri, E., Bushby, K., Ricci, E., Birchall, D., Pane, M., Kinali, M., Allsop, J., Nigro, V., Sáenz, A., Nascimbeni, A., et al. (2005). Muscle MRI findings in patients with limb girdle muscular dystrophy with calpain 3 deficiency (LGMD2A) and early contractures. *Neuromuscul. Disord.* 15, 164–171.
- Miano, J.M. (2010). Role of serum response factor in the pathogenesis of disease. *Lab. Investig. J. Tech. Methods Pathol.* 90, 1274–1284.

- Miller, P.J., Dietz, K.N., and Hollenbach, A.D. (2008). Identification of serine 205 as a site of phosphorylation on Pax3 in proliferating but not differentiating primary myoblasts. *Protein Sci.* 17, 1979–1986.
- Minasi, M.G., Riminucci, M., De Angelis, L., Borello, U., Berarducci, B., Innocenzi, A., Caprioli, A., Sirabella, D., Baiocchi, M., De Maria, R., et al. (2002). The meso-angioblast: a multipotent, self-renewing cell that originates from the dorsal aorta and differentiates into most mesodermal tissues. *Dev. Camb. Engl.* 129, 2773–2783.
- Miner, J.H., and Wold, B. (1990). Herculín, a fourth member of the MyoD family of myogenic regulatory genes. *Proc. Natl. Acad. Sci. U. S. A.* 87, 1089–1093.
- Miranda, A.F., Babiss, L.E., and Fisher, P.B. (1983). Transformation of human skeletal muscle cells by simian virus 40. *Proc. Natl. Acad. Sci. U. S. A.* 80, 6581–6585.
- Mitchell, K.J., Pannérec, A., Cadot, B., Parlakian, A., Besson, V., Gomes, E.R., Marazzi, G., and Sassoon, D.A. (2010). Identification and characterization of a non-satellite cell muscle resident progenitor during postnatal development. *Nat. Cell Biol.*
- Moldoveanu, T., Gehring, K., and Green, D.R. (2008). Concerted multi-pronged attack by calpastatin to occlude the catalytic cleft of heterodimeric calpains. *Nature* 456, 404–408.
- Molkentin, J.D., Black, B.L., Martin, J.F., and Olson, E.N. (1995). Cooperative activation of muscle gene expression by MEF2 and myogenic bHLH proteins. *Cell* 83, 1125–1136.
- Monaco, A.P., Neve, R.L., Colletti-Feener, C., Bertelson, C.J., Kurnit, D.M., and Kunkel, L.M. (1986). Isolation of candidate cDNAs for portions of the Duchenne muscular dystrophy gene. *Nature* 323, 646–650.
- Montarras, D., Morgan, J., Collins, C., Relaix, F., Zaffran, S., Cumano, A., Partridge, T., and Buckingham, M. (2005). Direct isolation of satellite cells for skeletal muscle regeneration. *Science* 309, 2064–2067.
- Moore, U.R., Jacobs, M., Fernandez-Torron, R., Jang, J., James, M.K., Mayhew, A., Rufibach, L., Mittal, P., Eagle, M., Cnaan, A., et al. (2018). Teenage exercise is associated with earlier symptom onset in dysferlinopathy: a retrospective cohort study. *J. Neurol. Neurosurg. Psychiatry* jnnp-2017-317329.
- Moretti, D., Del Bello, B., Cosci, E., Biagioli, M., Miracco, C., and Maellaro, E. (2009). Novel variants of muscle calpain 3 identified in human melanoma cells: cisplatin-induced changes *in vitro* and differential expression in melanocytic lesions. *Carcinogenesis* 30, 960–967.
- Morgens, D.W., Deans, R.M., Li, A., and Bassik, M.C. (2016). Systematic comparison of CRISPR/Cas9 and RNAi screens for essential genes. *Nat. Biotechnol.* 34, 634–636.
- Mori-Yoshimura, M., Segawa, K., Minami, N., Oya, Y., Komaki, H., Nonaka, I., Nishino, I., and Murata, M. (2017). Cardiopulmonary dysfunction in patients with limb-girdle muscular dystrophy 2A. *Muscle Nerve* 55, 465–469.
- Morosetti, R., Mirabella, M., Gliubizzi, C., Broccolini, A., De Angelis, L., Tagliafico, E., Sampaolesi, M., Gidaro, T., Papacci, M., Roncaglia, E., et al. (2006). MyoD expression restores defective

- myogenic differentiation of human mesoangioblasts from inclusion-body myositis muscle. *Proc. Natl. Acad. Sci.* 103, 16995–17000.
- Mukhopadhyay, N.K., Price, D.J., Kyriakis, J.M., Pelech, S., Sanghera, J., and Avruch, J. (1992). An array of insulin-activated, proline-directed serine/threonine protein kinases phosphorylate the p70 S6 kinase. *J. Biol. Chem.* 267, 3325–3335.
- Munirah, S., Ruszymah, B., Samsudin, O., Badrul, A., Azmi, B., and Aminuddin, B. (2008). Autologous versus pooled human serum for articular chondrocyte growth. *J. Orthop. Surg.* 16, 220–229.
- Münsterberg, A.E., Kitajewski, J., Bumcrot, D.A., McMahon, A.P., and Lassar, A.B. (1995). Combinatorial signaling by Sonic hedgehog and Wnt family members induces myogenic bHLH gene expression in the somite. *Genes Dev.* 9, 2911–2922.
- Murphy, M.M., Lawson, J.A., Mathew, S.J., Hutcheson, D.A., and Kardon, G. (2011). Satellite cells, connective tissue fibroblasts and their interactions are crucial for muscle regeneration. *Development* 138, 3625–3637.
- Nadruzjr, W., Corat, M., Marin, T., Guimaraespereira, G., and Franchini, K. (2005). Focal adhesion kinase mediates MEF2 and c-Jun activation by stretch: Role in the activation of the cardiac hypertrophic genetic program. *Cardiovasc. Res.* 68, 87–97.
- Nagata, Y., Partridge, T.A., Matsuda, R., and Zammit, P.S. (2006). Entry of muscle satellite cells into the cell cycle requires sphingolipid signaling. *J. Cell Biol.* 174, 245–253.
- Nakashima, K., and Yakabe, Y. (2007). AMPK activation stimulates myofibrillar protein degradation and expression of atrophy-related ubiquitin ligases by increasing FOXO transcription factors in C2C12 myotubes. *Biosci. Biotechnol. Biochem.* 71, 1650–1656.
- Nemes, A., Dézsi, L., Domsik, P., Kalapos, A., Forster, T., and Vécsei, L. (2017). Left ventricular deformation abnormalities in a patient with calpainopathy—a case from the three-dimensional speckle-tracking echocardiographic MAGYAR-Path Study. *Quant. Imaging Med. Surg.* 7, 685–690.
- Nemoto, S., and Finkel, T. (2002). Redox regulation of forkhead proteins through a p66shc-dependent signaling pathway. *Science* 295, 2450–2452.
- Niehrs, C. (2012). The complex world of WNT receptor signalling. *Nat. Rev. Mol. Cell Biol.* 13, 767–779.
- Nigro, V., and Savarese, M. (2014). Genetic basis of limb-girdle muscular dystrophies: the 2014 update. *Acta Myol. Myopathies Cardiomyopathies Off. J. Mediterr. Soc. Myol.* 33, 1–12.
- Niida, A., Hiroko, T., Kasai, M., Furukawa, Y., Nakamura, Y., Suzuki, Y., Sugano, S., and Akiyama, T. (2004). DKK1, a negative regulator of Wnt signaling, is a target of the β -catenin/TCF pathway. *Oncogene* 23, 8520–8526.
- Nilsson, M.I., Macneil, L.G., Kitaoka, Y., Alqarni, F., Suri, R., Akhtar, M., Haikalis, M.E., Dhaliwal, P., Saeed, M., and Tarnopolsky, M.A. (2014). Redox state and mitochondrial respiratory chain function in skeletal muscle of LGMD2A patients. *PLoS ONE* 9, e102549.

- Ogg, S., Paradis, S., Gottlieb, S., Patterson, G.I., Lee, L., Tissenbaum, H.A., and Ruvkun, G. (1997). The Fork head transcription factor DAF-16 transduces insulin-like metabolic and longevity signals in *C. elegans*. *Nature* 389, 994–999.
- Ohno, S., Emori, Y., Imajoh, S., Kawasaki, H., Kisaragi, M., and Suzuki, K. (1984). Evolutionary origin of a calcium-dependent protease by fusion of genes for a thiol protease and a calcium-binding protein? *Nature* 312, 566–570.
- Ohno, S., Minoshima, S., Kudoh, J., Fukuyama, R., Shimizu, Y., Ohmi-Imajohs, S., Shimizu, N., and Suzuki, K. (1990). Four genes for the calpain family locate on four distinct human chromosomes. *Cytogenet. Genome Res.* 53, 225–229.
- Ojima, K., Ono, Y., Hata, S., Koyama, S., Doi, N., and Sorimachi, H. (2006). Possible functions of p94 in connectin-mediated signaling pathways in skeletal muscle cells. *J. Muscle Res. Cell Motil.* 26, 409–417.
- Ojima, K., Ono, Y., Doi, N., Yoshioka, K., Kawabata, Y., Labeit, S., and Sorimachi, H. (2007). Myogenic stage, sarcomere length, and protease activity modulate localization of muscle-specific calpain. *J. Biol. Chem.* 282, 14493–14504.
- Ojima, K., Kawabata, Y., Nakao, H., Nakao, K., Doi, N., Kitamura, F., Ono, Y., Hata, S., Suzuki, H., Kawahara, H., et al. (2010). Dynamic distribution of muscle-specific calpain in mice has a key role in physical-stress adaptation and is impaired in muscular dystrophy. *J. Clin. Invest.* 120, 2672–2683.
- Ojima, K., Ono, Y., Ottenheijm, C., Hata, S., Suzuki, H., Granzier, H., and Sorimachi, H. (2011). Non-proteolytic functions of calpain-3 in sarcoplasmic reticulum in skeletal muscles. *J. Mol. Biol.* 407, 439–449.
- Ojima, K., Ono, Y., Hata, S., Noguchi, S., Nishino, I., and Sorimachi, H. (2014). Muscle-specific calpain-3 is phosphorylated in its unique insertion region for enrichment in a myofibril fraction. *Genes Cells Devoted Mol. Cell. Mech.* 19, 830–841.
- Okada, K., Naito, A.T., Higo, T., Nakagawa, A., Shibamoto, M., Sakai, T., Hashimoto, A., Kuramoto, Y., Sumida, T., Nomura, S., et al. (2015). Wnt/ β -catenin signaling contributes to skeletal myopathy in heart failure via direct interaction With forkhead Box O clinical perspective. *Circ. Heart Fail.* 8, 799–808.
- Olejniczak, M., Galka, P., and Krzyzosiak, W.J. (2010). Sequence-non-specific effects of RNA interference triggers and microRNA regulators. *Nucleic Acids Res.* 38, 1–16.
- Olejniczak, M., Urbanek, M.O., Jaworska, E., Witucki, L., Szczesniak, M.W., Makalowska, I., and Krzyzosiak, W.J. (2016). Sequence-non-specific effects generated by various types of RNA interference triggers. *Biochim. Biophys. Acta BBA - Gene Regul. Mech.* 1859, 306–314.
- Olson, L.E., and Soriano, P. (2009). Increased PDGFR α activation disrupts connective tissue development and drives systemic fibrosis. *Dev. Cell* 16, 303–313.
- Omary, M. (2002). Keratins: Guardians of the liver. *Hepatology* 35, 251–257.

- Ono, Y., Kakinuma, K., Torii, F., Irie, A., Nakagawa, K., Labeit, S., Abe, K., Suzuki, K., and Sorimachi, H. (2004). Possible regulation of the conventional calpain system by skeletal muscle-specific calpain, p94/calpain 3. *J. Biol. Chem.* 279, 2761–2771.
- Ono, Y., Torii, F., Ojima, K., Doi, N., Yoshioka, K., Kawabata, Y., Labeit, D., Labeit, S., Suzuki, K., Abe, K., et al. (2006). Suppressed disassembly of autolyzing p94/CAPN3 by N2A connectin/titin in a genetic reporter system. *J. Biol. Chem.* 281, 18519–18531.
- Ono, Y., and Sorimachi, H. (2012). Calpains — An elaborate proteolytic system. *Biochim. Biophys. Acta BBA - Proteins Proteomics* 1824, 224–236.
- Ono, Y., Iemura, S., Novak, S.M., Doi, N., Kitamura, F., Natsume, T., Gregorio, C.C., and Sorimachi, H. (2013). PLEIAD/SIMC1/C5orf25, a novel autolysis regulator for a skeletal-muscle-specific calpain, CAPN3, scaffolds a CAPN3 substrate, CTBP1. *J. Mol. Biol.* 425, 2955–2972.
- Ono, Y., Ojima, K., Shinkai-Ouchi, F., Hata, S., and Sorimachi, H. (2016). An eccentric calpain, CAPN3/p94/calpain-3. *Biochimie* 122, 169–187.
- Ørngreen, M.C., Dunø, M., Ejstrup, R., Christensen, E., Schwartz, M., Sacchetti, M., and Vissing, J. (2005). Fuel utilization in subjects with carnitine palmitoyltransferase 2 gene mutations: CPT2 Gene Mutations and Fuel Use. *Ann. Neurol.* 57, 60–66.
- Ott, M.O., Bober, E., Lyons, G., Arnold, H., and Buckingham, M. (1991). Early expression of the myogenic regulatory gene, myf-5, in precursor cells of skeletal muscle in the mouse embryo. *Dev. Camb. Engl.* 111, 1097–1107.
- Otto, A., Schmidt, C., Luke, G., Allen, S., Valasek, P., Muntoni, F., Lawrence-Watt, D., and Patel, K. (2008). Canonical Wnt signalling induces satellite-cell proliferation during adult skeletal muscle regeneration. *J. Cell Sci.* 121, 2939–2950.
- Ozawa, E., Noguchi, S., Mizuno, Y., Hagiwara, Y., and Yoshida, M. (1998). From dystrophinopathy to sarcoglycanopathy: evolution of a concept of muscular dystrophy. *Muscle Nerve* 21, 421–438.
- Pallafacchina, G., Calabria, E., Serrano, A.L., Kalhovde, J.M., and Schiaffino, S. (2002). A protein kinase B-dependent and rapamycin-sensitive pathway controls skeletal muscle growth but not fiber type specification. *Proc. Natl. Acad. Sci.* 99, 9213–9218.
- Paniagua, R., Nistal, R., Sesma, P., Álvarez-Uría, M., Fraile, B., Anadón, R., and Sáez, F.J. (2007). *Citología e histología vegetal y animal* (McGraw-Hill - Interamericana).
- Pankov, R., Cukierman, E., Clark, K., Matsumoto, K., Hahn, C., Poulin, B., and Yamada, K.M. (2003). Specific β 1 Integrin site selectively regulates Akt/protein kinase B signaling via local activation of protein phosphatase 2A. *J. Biol. Chem.* 278, 18671–18681.
- Pannerec, A., Formicola, L., Besson, V., Marazzi, G., and Sassoon, D.A. (2013). Defining skeletal muscle resident progenitors and their cell fate potentials. *Development* 140, 2879–2891.
- Pansters, N.A.M., van der Velden, J.L.J., Kelders, M.C.J.M., Laeremans, H., Schols, A.M.W.J., and Langen, R.C.J. (2011). Segregation of myoblast fusion and muscle-specific gene expression by distinct ligand-dependent inactivation of GSK-3 β . *Cell. Mol. Life Sci.* 68, 523–535.

- Pardo, J.V., Siliciano, J.D., and Craig, S.W. (1983). A vinculin-containing cortical lattice in skeletal muscle: transverse lattice elements ("costameres") mark sites of attachment between myofibrils and sarcolemma. *Proc. Natl. Acad. Sci. U. S. A.* 80, 1008–1012.
- Park, I.-H., and Chen, J. (2005). Mammalian target of rapamycin (mTOR) signaling is required for a late-stage fusion process during skeletal myotube maturation. *J. Biol. Chem.* 280, 32009–32017.
- Parr, B.A., Shea, M.J., Vassileva, G., and McMahon, A.P. (1993). Mouse Wnt genes exhibit discrete domains of expression in the early embryonic CNS and limb buds. *Dev. Camb. Engl.* 119, 247–261.
- Partha, S.K., Ravulapalli, R., Allingham, J.S., Campbell, R.L., and Davies, P.L. (2014). Crystal structure of calpain-3 penta-EF-hand (PEF) domain - a homodimerized PEF family member with calcium bound at the fifth EF-hand. *FEBS J.* 281, 3138–3149.
- Pearson, R.B., Dennis, P.B., Han, J.W., Williamson, N.A., Kozma, S.C., Wettenhall, R.E., and Thomas, G. (1995). The principal target of rapamycin-induced p70s6k inactivation is a novel phosphorylation site within a conserved hydrophobic domain. *EMBO J.* 14, 5279–5287.
- Pende, M., Um, S.H., Mieulet, V., Sticker, M., Goss, V.L., Mestan, J., Mueller, M., Fumagalli, S., Kozma, S.C., and Thomas, G. (2004). S6K1(-/-)/S6K2(-/-) mice exhibit perinatal lethality and rapamycin-sensitive 5'-terminal oligopyrimidine mRNA translation and reveal a mitogen-activated protein kinase-dependent S6 kinase pathway. *Mol. Cell. Biol.* 24, 3112–3124.
- Pénisson-Besnier, I., Richard, I., Dubas, F., Beckmann, J.S., and Fardeau, M. (1998). Pseudometabolic expression and phenotypic variability of calpain deficiency in two siblings. *Muscle Nerve* 21, 1078–1080.
- Perdiguerro, E., Ruiz-Bonilla, V., Gresh, L., Hui, L., Ballestar, E., Sousa-Victor, P., Baeza-Raja, B., Jardí, M., Bosch-Comas, A., Esteller, M., et al. (2007). Genetic analysis of p38 MAP kinases in myogenesis: fundamental role of p38 α in abrogating myoblast proliferation. *EMBO J.* 26, 1245–1256.
- Pereira Sant'Ana, J.A.A., Ennion, S., Sargeant, A.J., Moorman, A.F.M., and Goldspink, G. (1997). Comparison of the molecular, antigenic and ATPase determinants of fast myosin heavy chains in rat and human: a single-fibre study. *Eur. J. Physiol.* 435, 151–163.
- Person, A.D., Garriock, R.J., Krieg, P.A., Runyan, R.B., and Klewer, S.E. (2005). Frzb modulates Wnt-9a-mediated β -catenin signaling during avian atrioventricular cardiac cushion development. *Dev. Biol.* 278, 35–48.
- Peter, J.B., Barnard, R.J., Edgerton, V.R., Gillespie, C.A., and Stempel, K.E. (1972). Metabolic profiles of three fiber types of skeletal muscle in guinea pigs and rabbits. *Biochemistry (Mosc.)* 11, 2627–2633.
- Pfister, R., Acksteiner, C., Baumgarth, J., Burst, V., Geissler, H.J., Margulies, K.B., Houser, S., Bloch, W., and Fleisch, M. (2007). Loss of β 1D-integrin function in human ischemic cardiomyopathy. *Basic Res. Cardiol.* 102, 257–264.

- Pierantozzi, E., Vezzani, B., Badin, M., Curina, C., Severi, F.M., Petraglia, F., Randazzo, D., Rossi, D., and Sorrentino, V. (2016). Tissue-specific cultured human pericytes: perivascular cells from smooth muscle tissue have restricted mesodermal differentiation ability. *Stem Cells Dev.* 25, 674–686.
- Pierobon-Bormioli, S. (1981). Transverse sarcomere filamentous systems: “Z- and M-cables.” *J. Muscle Res. Cell Motil.* 2, 401–413.
- Piluso, G. (2005). Extensive scanning of the calpain-3 gene broadens the spectrum of LGMD2A phenotypes. *J. Med. Genet.* 42, 686–693.
- Pinson, K.I., Brennan, J., Monkley, S., Avery, B.J., and Skarnes, W.C. (2000). An LDL-receptor-related protein mediates Wnt signalling in mice. *Nature* 407, 535–538.
- Pisconti, A., Brunelli, S., Di Padova, M., De Palma, C., Deponti, D., Baesso, S., Sartorelli, V., Cossu, G., and Clementi, E. (2006). Follistatin induction by nitric oxide through cyclic GMP: a tightly regulated signaling pathway that controls myoblast fusion. *J. Cell Biol.* 172, 233–244.
- Pogogeff, I.A., and Murray, M.R. (1946). Form and behavior of adult mammalian skeletal muscle *in vitro*. *Anat. Rec.* 95, 321–335.
- Polakis, P. (1999). The oncogenic activation of beta-catenin. *Curr. Opin. Genet. Dev.* 9, 15–21.
- Pollitt, C., Anderson, L.V., Pogue, R., Davison, K., Pyle, A., and Bushby, K.M. (2001). The phenotype of calpainopathy: diagnosis based on a multidisciplinary approach. *Neuromuscul. Disord. NMD* 11, 287–296.
- Porter, G.A., Dmytrenko, G.M., Winkelmann, J.C., and Bloch, R.J. (1992). Dystrophin colocalizes with beta-spectrin in distinct subsarcolemmal domains in mammalian skeletal muscle. *J. Cell Biol.* 117, 997–1005.
- Potthoff, M.J., Wu, H., Arnold, M.A., Shelton, J.M., Backs, J., McAnally, J., Richardson, J.A., Bassel-Duby, R., and Olson, E.N. (2007). Histone deacetylase degradation and MEF2 activation promote the formation of slow-twitch myofibers. *J. Clin. Invest.* 117, 2459–2467.
- Pourquié, O., Coltey, M., Bréant, C., and Le Douarin, N.M. (1995). Control of somite patterning by signals from the lateral plate. *Proc. Natl. Acad. Sci. U. S. A.* 92, 3219–3223.
- Price, D.J., Mukhopadhyay, N.K., and Avruch, J. (1991). Insulin-activated protein kinases phosphorylate a pseudosubstrate synthetic peptide inhibitor of the p70 S6 kinase. *J. Biol. Chem.* 266, 16281–16284.
- Prieve, M.G., and Moon, R.T. (2003). Stromelysin-1 and mesothelin are differentially regulated by Wnt-5a and Wnt-1 in C57mg mouse mammary epithelial cells. *BMC Dev. Biol.* 3, 2.
- Przewoźniak, M., Czaplicka, I., Czerwińska, A.M., Markowska-Zagrajek, A., Moraczewski, J., Stremińska, W., Jańczyk-Ilach, K., Ciemerych, M.A., and Brzoska, E. (2013). Adhesion proteins--an impact on skeletal myoblast differentiation. *PLoS ONE* 8, e61760.
- Pullen, N., and Thomas, G. (1997). The modular phosphorylation and activation of p70s6k. *FEBS Lett.* 410, 78–82.

- Pullen, N., Dennis, P.B., Andjelkovic, M., Dufner, A., Kozma, S.C., Hemmings, B.A., and Thomas, G. (1998). Phosphorylation and activation of p70s6k by PDK1. *Science* 279, 707–710.
- Qaisar, R., Bhaskaran, S., and Van Remmen, H. (2016). Muscle fiber type diversification during exercise and regeneration. *Free Radic. Biol. Med.* 98, 56–67.
- Qian, D., Jones, C., Rzadzinska, A., Mark, S., Zhang, X., Steel, K.P., Dai, X., and Chen, P. (2007). Wnt5a functions in planar cell polarity regulation in mice. *Dev. Biol.* 306, 121–133.
- Qin, S., Zhang, Z., Li, J., and Zang, L. (2014). FRZB knockdown upregulates β -catenin activity and enhances cell aggressiveness in gastric cancer. *Oncol. Rep.* 31, 2351–2357.
- Qu, Y., Li, J., Cai, Q., Wang, Y., Gu, Q., Zhu, Z., and Liu, B. (2008). Over-expression of FRZB in gastric cancer cell suppresses proliferation and induces differentiation. *J. Cancer Res. Clin. Oncol.* 134, 353–364.
- Quach, N.L., and Rando, T.A. (2006). Focal adhesion kinase is essential for costamereogenesis in cultured skeletal muscle cells. *Dev. Biol.* 293, 38–52.
- Quattrocchi, M., Palazzolo, G., Perini, I., Crippa, S., Cassano, M., and Sampaolesi, M. (2012). Mouse and human mesoangioblasts: isolation and characterization from adult skeletal muscles. *Methods Mol. Biol. Clifton NJ* 798, 65–76.
- Quick, S., Schaefer, J., Waessnig, N., Schultheiss, T., Reuner, U., Schoen, S., Reichmann, H., Strasser, R., and Speiser, U. (2015). Evaluation of heart involvement in calpainopathy (LGMD2A) using cardiovascular magnetic resonance: Short Reports. *Muscle Nerve* 52, 661–663.
- Rajakumar, D., Alexander, M., and Oommen, A. (2013). Oxidative stress, NF- κ B and the ubiquitin proteasomal pathway in the pathology of calpainopathy. *Neurochem. Res.* 38, 2009–2018.
- Rasmussen, B.B., and Richter, E.A. (2009). The balancing act between the cellular processes of protein synthesis and breakdown: exercise as a model to understand the molecular mechanisms regulating muscle mass. *J. Appl. Physiol.* 106, 1365–1366.
- Rattner, A., Hsieh, J.C., Smallwood, P.M., Gilbert, D.J., Copeland, N.G., Jenkins, N.A., and Nathans, J. (1997). A family of secreted proteins contains homology to the cysteine-rich ligand-binding domain of frizzled receptors. *Proc. Natl. Acad. Sci. U. S. A.* 94, 2859–2863.
- Raught, B., Peiretti, F., Gingras, A.-C., Livingstone, M., Shahbazian, D., Mayeur, G.L., Polakiewicz, R.D., Sonenberg, N., and Hershey, J.W. (2004). Phosphorylation of eucaryotic translation initiation factor 4B Ser422 is modulated by S6 kinases. *EMBO J.* 23, 1761–1769.
- Ravulapalli, R., Diaz, B.G., Campbell, R.L., and Davies, P.L. (2005). Homodimerization of calpain 3 penta-EF-hand domain. *Biochem. J.* 388, 585–591.
- Ravulapalli, R., Campbell, R.L., Gauthier, S.Y., Dhe-Paganon, S., and Davies, P.L. (2009). Distinguishing between calpain heterodimerization and homodimerization. *FEBS J.* 276, 973–982.
- Raymond, F., Métaïron, S., Kussmann, M., Colomer, J., Nascimento, A., Mormeneo, E., García-Martínez, C., and Gómez-Foix, A.M. (2010). Comparative gene expression profiling between human cultured myotubes and skeletal muscle tissue. *BMC Genomics* 11, 125.

- Reed, S.A., Sandesara, P.B., Senf, S.M., and Judge, A.R. (2012). Inhibition of FoxO transcriptional activity prevents muscle fiber atrophy during cachexia and induces hypertrophy. *FASEB J.* 26, 987–1000.
- Relaix, F., Rocancourt, D., Mansouri, A., and Buckingham, M. (2005). A Pax3/Pax7-dependent population of skeletal muscle progenitor cells. *Nature* 435, 948–953.
- Relaix, F., Montarras, D., Zaffran, S., Gayraud-Morel, B., Rocancourt, D., Tajbakhsh, S., Mansouri, A., Cumano, A., and Buckingham, M. (2006). Pax3 and Pax7 have distinct and overlapping functions in adult muscle progenitor cells. *J. Cell Biol.* 172, 91–102.
- Relaix, F., Demignon, J., Laclef, C., Pujol, J., Santolini, M., Niro, C., Lagha, M., Rocancourt, D., Buckingham, M., and Maire, P. (2013). Six homeoproteins directly activate Myod expression in the gene regulatory networks that control early myogenesis. *PLoS Genet.* 9, e1003425.
- Renner, G., Noulet, F., Mercier, M.-C., Choulier, L., Etienne-Selloum, N., Gies, J.-P., Lehmann, M., Lelong-Rebel, I., Martin, S., and Dontenwill, M. (2016). Expression/activation of $\alpha 5\beta 1$ integrin is linked to the β -catenin signaling pathway to drive migration in glioma cells. *Oncotarget* 7.
- Rey, M.A., and Davies, P.L. (2002). The protease core of the muscle-specific calpain, p94, undergoes Ca^{2+} -dependent intramolecular autolysis. *FEBS Lett.* 532, 401–406.
- Rhodes, S.J., and Konieczny, S.F. (1989). Identification of MRF4: a new member of the muscle regulatory factor gene family. *Genes Dev.* 3, 2050–2061.
- Richard, I., Broux, O., Allamand, V., Fougerousse, F., Chiannikulchai, N., Bourg, N., Brenguier, L., Devaud, C., Pasturaud, P., and Roudaut, C. (1995). Mutations in the proteolytic enzyme calpain 3 cause limb-girdle muscular dystrophy type 2A. *Cell* 81, 27–40.
- Richard, I., Roudaut, C., Saenz, A., Pogue, R., Grimbergen, J.E.M.A., Anderson, L.V.B., Beley, C., Cobo, A.-M., de Diego, C., Eymard, B., et al. (1999). Calpainopathy—A survey of mutations and polymorphisms. *Am. J. Hum. Genet.* 64, 1524–1540.
- Richard, I., Roudaut, C., Marchand, S., Baghdiguian, S., Herasse, M., Stockholm, D., Ono, Y., Suel, L., Bourg, N., Sorimachi, H., et al. (2000). Loss of calpain 3 proteolytic activity leads to muscular dystrophy and to apoptosis-associated I κ B α /nuclear factor κ B pathway perturbation in mice. *J. Cell Biol.* 151, 1583–1590.
- Robert, V., Massimino, M.L., Tosello, V., Marsault, R., Cantini, M., Sorrentino, V., and Pozzan, T. (2001). Alteration in calcium handling at the subcellular level in *mdx* myotubes. *J. Biol. Chem.* 276, 4647–4651.
- Robu, M.E., Larson, J.D., Nasevicius, A., Beiraghi, S., Brenner, C., Farber, S.A., and Ekker, S.C. (2007). p53 activation by knockdown technologies. *PLoS Genet.* 3, e78.
- Rochat, A., Fernandez, A., Vandromme, M., Molès, J.-P., Bouschet, T., Carnac, G., and Lamb, N.J.C. (2004). Insulin and Wnt1 pathways cooperate to induce reserve cell activation in differentiation and myotube hypertrophy. *Mol. Biol. Cell* 15, 4544–4555.
- Roperto, S., De Tullio, R., Raso, C., Stifanese, R., Russo, V., Gaspari, M., Borzacchiello, G., Averna, M., Paciello, O., Cuda, G., et al. (2010). Calpain 3 is expressed in a proteolitically active form in

- papillomavirus-associated urothelial tumors of the urinary bladder in cattle. *PLoS ONE* 5, e10299.
- Rosales, X.Q., Malik, V., Sneh, A., Chen, L., Lewis, S., Kota, J., Gastier-Foster, J.M., Astbury, C., Pyatt, R., Reshmi, S., et al. (2013). Impaired regeneration in LGMD2A supported by increased PAX7-positive satellite cell content and muscle-specific microRNA dysregulation: Impaired Regeneration in LGMD2A. *Muscle Nerve* 47, 731–739.
- Ross, S.E., Hemati, N., Longo, K.A., Bennett, C.N., Lucas, P.C., Erickson, R.L., and MacDougald, O.A. (2000). Inhibition of adipogenesis by Wnt signaling. *Science* 289, 950–953.
- Rossi, A., Kontarakis, Z., Gerri, C., Nolte, H., Hölper, S., Krüger, M., and Stainier, D.Y.R. (2015). Genetic compensation induced by deleterious mutations but not gene knockdowns. *Nature* 524, 230–233.
- Roudaut, C., Le Roy, F., Suel, L., Poupiot, J., Charton, K., Bartoli, M., and Richard, I. (2013). Restriction of calpain 3 expression to the skeletal muscle prevents cardiac toxicity and corrects pathology in a murine model of limb-girdle muscular dystrophy. *Circulation* 128, 1094–1104.
- Roux, P.P., Shahbazian, D., Vu, H., Holz, M.K., Cohen, M.S., Taunton, J., Sonenberg, N., and Blenis, J. (2007). RAS/ERK signaling promotes site-specific ribosomal protein S6 phosphorylation via RSK and stimulates cap-dependent translation. *J. Biol. Chem.* 282, 14056–14064.
- Roy, M., Li, Z., and Sacks, D.B. (2005). IQGAP1 is a scaffold for mitogen-activated protein kinase signaling. *Mol. Cell. Biol.* 25, 7940–7952.
- Rudnicki, M.A., Schnegelsberg, P.N., Stead, R.H., Braun, T., Arnold, H.H., and Jaenisch, R. (1993). MyoD or Myf-5 is required for the formation of skeletal muscle. *Cell* 75, 1351–1359.
- Ruffini, F., Tentori, L., Dorio, A.S., Arcelli, D., D’Amati, G., D’Atri, S., Graziani, G., and Licalo, P.M. (2013). Platelet-derived growth factor C and calpain-3 are modulators of human melanoma cell invasiveness. *Oncol. Rep.* 30, 2887–2896.
- Ruvinsky, I. (2005). Ribosomal protein S6 phosphorylation is a determinant of cell size and glucose homeostasis. *Genes Dev.* 19, 2199–2211.
- Ruvinsky, I., and Meyuhas, O. (2006). Ribosomal protein S6 phosphorylation: from protein synthesis to cell size. *Trends Biochem. Sci.* 31, 342–348.
- Ruvinsky, I., Katz, M., Dreazen, A., Gielchinsky, Y., Saada, A., Freedman, N., Mishani, E., Zimmerman, G., Kasir, J., and Meyuhas, O. (2009). Mice deficient in ribosomal protein S6 phosphorylation suffer from muscle weakness that reflects a growth defect and energy deficit. *PLoS ONE* 4, e5618.
- Sacchetto, R., Margreth, A., Pelosi, M., and Carafoli, E. (1996). Colocalization of the dihydropyridine receptor, the plasma-membrane calcium ATPase isoform 1 and the sodium/calcium exchanger to the junctional-membrane domain of transverse tubules of rabbit skeletal muscle. *Eur. J. Biochem.* 237, 483–488.
- Sáenz, A., and López de Munain, A. (2017). Dominant LGMD2A: alternative diagnosis or hidden digenism? *Brain J. Neurol.* 140, e7.

- Sáenz, A., Leturcq, F., Cobo, A.M., Poza, J.J., Ferrer, X., Otaegui, D., Camaño, P., Urtasun, M., Vílchez, J., Gutiérrez-Rivas, E., et al. (2005). LGMD2A: genotype–phenotype correlations based on a large mutational survey on the calpain 3 gene. *Brain* 128, 732–742.
- Sáenz, A., Azpitarte, M., Armañanzas, R., Leturcq, F., Alzualde, A., Inza, I., García-Bragado, F., De la Herran, G., Corcuera, J., Cabello, A., et al. (2008). Gene expression profiling in limb-girdle muscular dystrophy 2A. *PLoS ONE* 3, e3750.
- Sáenz, A., Ono, Y., Sorimachi, H., Goicoechea, M., Leturcq, F., Blázquez, L., García-Bragado, F., Marina, A., Poza, J.J., Azpitarte, M., et al. (2011). Does the severity of the LGMD2A phenotype in compound heterozygotes depend on the combination of mutations? *Muscle Nerve* 44, 710–714.
- Saini, A., Rullman, E., Lilja, M., Mandić, M., Melin, M., Olsson, K., and Gustafsson, T. (2018). Asymmetric cellular responses in primary human myoblasts using sera of different origin and specification. *PLoS ONE* 13, e0192384.
- Sakai, H., Kimura, M., Isa, Y., Yabe, S., Maruyama, A., Tsuruno, Y., Kai, Y., Sato, F., Yumoto, T., Chiba, Y., et al. (2017). Effect of acute treadmill exercise on cisplatin-induced muscle atrophy in the mouse. *Pflüg. Arch. - Eur. J. Physiol.* 469, 1495–1505.
- Sakakima, H., Yoshida, Y., Suzuki, S., and Morimoto, N. (2004). The effects of aging and treadmill running on soleus and gastrocnemius muscle morphology in the senescence-accelerated mouse (SAMP1). *J. Gerontol. A. Biol. Sci. Med. Sci.* 59, 1015–1021.
- Sambasivan, R., Yao, R., Kissenpfennig, A., Van Wittenberghe, L., Paldi, A., Gayraud-Morel, B., Guenou, H., Malissen, B., Tajbakhsh, S., and Galy, A. (2011). Pax7-expressing satellite cells are indispensable for adult skeletal muscle regeneration. *Development* 138, 3647–3656.
- Sampaolesi, M. (2003). Cell therapy of -sarcoglycan null dystrophic mice through intra-arterial delivery of mesoangioblasts. *Science* 301, 487–492.
- Sanchez, A.M.J., Candau, R.B., and Bernardi, H. (2014). FoxO transcription factors: their roles in the maintenance of skeletal muscle homeostasis. *Cell. Mol. Life Sci.* 71, 1657–1671.
- Sandmann, T., Jensen, L.J., Jakobsen, J.S., Karzynski, M.M., Eichenlaub, M.P., Bork, P., and Furlong, E.E.M. (2006). A temporal map of transcription factor activity: Mef2 directly regulates target genes at All stages of muscle development. *Dev. Cell* 10, 797–807.
- Sandri, M., Sandri, C., Gilbert, A., Skurk, C., Calabria, E., Picard, A., Walsh, K., Schiaffino, S., Lecker, S.H., and Goldberg, A.L. (2004). Foxo transcription factors induce the atrophy-related ubiquitin ligase atrogin-1 and cause skeletal muscle atrophy. *Cell* 117, 399–412.
- Sanger, J.W., Chowrashi, P., Shaner, N.C., Spalthoff, S., Wang, J., Freeman, N.L., and Sanger, J.M. (2002). Myofibrillogenesis in skeletal muscle cells. *Clin. Orthop.* S153-162.
- Schiaffino, S., and Reggiani, C. (2011). Fiber types in mammalian skeletal muscles. *Physiol. Rev.* 91, 1447–1531.
- Schultz, E., Gibson, M.C., and Champion, T. (1978). Satellite cells are mitotically quiescent in mature mouse muscle: An EM and radioautographic study. *J. Exp. Zool.* 206, 451–456.

- Schwander, M., Leu, M., Stumm, M., Dorchies, O.M., Ruegg, U.T., Schittny, J., and Müller, U. (2003). Beta1 integrins regulate myoblast fusion and sarcomere assembly. *Dev. Cell* 4, 673–685.
- Sczesny-Kaiser, M., Kowalewski, R., Schildhauer, T.A., Aach, M., Jansen, O., Grasmücke, D., Güttsches, A.-K., Vorgerd, M., and Tegenthoff, M. (2017). Treadmill training with HAL exoskeleton—A novel approach for symptomatic therapy in patients with limb-girdle muscular dystrophy—preliminary study. *Front. Neurosci.* 11.
- Seale, P., Sabourin, L.A., Girgis-Gabardo, A., Mansouri, A., Gruss, P., and Rudnicki, M.A. (2000). Pax7 is required for the specification of myogenic satellite cells. *Cell* 102, 777–786.
- Senf, S.M., Dodd, S.L., and Judge, A.R. (2010). FOXO signaling is required for disuse muscle atrophy and is directly regulated by Hsp70. *Am. J. Physiol.-Cell Physiol.* 298, C38–C45.
- Shear, C.R., and Bloch, R.J. (1985). Vinculin in subsarcolemmal densities in chicken skeletal muscle: localization and relationship to intracellular and extracellular structures. *J. Cell Biol.* 101, 240–256.
- Shimo, T., Hosoki, K., Nakatsuji, Y., Yokota, T., and Obika, S. (2018). A novel human muscle cell model of Duchenne muscular dystrophy created by CRISPR/Cas9 and evaluation of antisense-mediated exon skipping. *J. Hum. Genet.* 63, 365–375.
- Shin, D., Kim, I.S., Lee, J.M., Shin, S.-Y., Lee, J.-H., Baek, S.H., and Cho, K.-H. (2014). The hidden switches underlying ROR α -mediated circuits that critically regulate uncontrolled cell proliferation. *J. Mol. Cell Biol.* 6, 338–348.
- Sipilä, S., Elorinne, M., Alen, M., Suominen, H., and Kovanen, V. (1997). Effects of strength and endurance training on muscle fibre characteristics in elderly women. *Clin. Physiol. Oxf. Engl.* 17, 459–474.
- Slusarski, D.C., Corces, V.G., and Moon, R.T. (1997). Interaction of Wnt and a Frizzled homologue triggers G-protein-linked phosphatidylinositol signalling. *Nature* 390, 410–413.
- Smerdu, V., Karsch-Mizrachi, I., Campione, M., Leinwand, L., and Schiaffino, S. (1994). Type IIx myosin heavy chain transcripts are expressed in type IIb fibers of human skeletal muscle. *Am. J. Physiol.* 267, C1723-1728.
- Smith, C.K., Janney, M.J., and Allen, R.E. (1994). Temporal expression of myogenic regulatory genes during activation, proliferation, and differentiation of rat skeletal muscle satellite cells. *J. Cell. Physiol.* 159, 379–385.
- Smolina, N., Kostareva, A., Bruton, J., Karpushev, A., Sjoberg, G., and Sejersen, T. (2015). Primary murine myotubes as a model for investigating muscular dystrophy. *BioMed Res. Int.* 2015, 594751.
- Snoeck, M., van Engelen, B.G.M., Küsters, B., Lammens, M., Meijer, R., Molenaar, J.P.F., Raaphorst, J., Verschuuren-Bemelmans, C.C., Straathof, C.S.M., Sie, L.T.L., et al. (2015). RYR1-related myopathies: a wide spectrum of phenotypes throughout life. *Eur. J. Neurol.* 22, 1094–1112.
- Soleimani, V.D., Punch, V.G., Kawabe, Y., Jones, A.E., Palidwor, G.A., Porter, C.J., Cross, J.W., Carvajal, J.J., Kockx, C.E.M., van IJcken, W.F.J., et al. (2012). Transcriptional dominance of Pax7 in adult

- myogenesis due to high-affinity recognition of homeodomain motifs. *Dev. Cell* 22, 1208–1220.
- Song, W.K., Wang, W., Sato, H., Bielser, D.A., and Kaufman, S.J. (1993). Expression of alpha 7 integrin cytoplasmic domains during skeletal muscle development: alternate forms, conformational change, and homologies with serine/threonine kinases and tyrosine phosphatases. *J. Cell Sci.* 106 (Pt 4), 1139–1152.
- Sorcini, D., Bruscoli, S., Frammartino, T., Cimino, M., Mazzon, E., Galuppo, M., Bramanti, P., Al-Banchaabouchi, M., Farley, D., Ermakova, O., et al. (2017). Wnt/ β -catenin signaling induces integrin $\alpha 4\beta 1$ in T cells and promotes a progressive neuroinflammatory disease in mice. *J. Immunol.* 199, 3031–3041.
- Sorimachi, H., Imajoh-Ohmi, S., Emori, Y., Kawasaki, H., Ohno, S., Minami, Y., and Suzuki, K. (1989). Molecular cloning of a novel mammalian calcium-dependent protease distinct from both m- and mu-types. Specific expression of the mRNA in skeletal muscle. *J. Biol. Chem.* 264, 20106–20111.
- Sorimachi, H., Ishiura, S., and Suzuki, K. (1993a). A novel tissue-specific calpain species expressed predominantly in the stomach comprises two alternative splicing products with and without Ca^{2+} -binding domain. *J. Biol. Chem.* 268, 19476–19482.
- Sorimachi, H., Toyama-Sorimachi, N., Saido, T.C., Kawasaki, H., Sugita, H., Miyasaka, M., Arahata, K., Ishiura, S., and Suzuki, K. (1993b). Muscle-specific calpain, p94, is degraded by autolysis immediately after translation, resulting in disappearance from muscle. *J. Biol. Chem.* 268, 10593–10605.
- Sorimachi, H., Kinbara, K., Kimura, S., Takahashi, M., Ishiura, S., Sasagawa, N., Sorimachi, N., Shimada, H., Tagawa, K., and Maruyama, K. (1995). Muscle-specific calpain, p94, responsible for limb girdle muscular dystrophy type 2A, associates with connectin through IS2, a p94-specific sequence. *J. Biol. Chem.* 270, 31158–31162.
- Sorimachi, H., Hata, S., and Ono, Y. (2011a). Impact of genetic insights into calpain biology. *J. Biochem. (Tokyo)* 150, 23–37.
- Sorimachi, H., Hata, S., and Ono, Y. (2011b). Calpain chronicle--an enzyme family under multidisciplinary characterization. *Proc. Jpn. Acad. Ser. B Phys. Biol. Sci.* 87, 287–327.
- Spitz, F., Demignon, J., Porteu, A., Kahn, A., Concordet, J.P., Daegelen, D., and Maire, P. (1998). Expression of myogenin during embryogenesis is controlled by Six/sine oculis homeoproteins through a conserved MEF3 binding site. *Proc. Natl. Acad. Sci. U. S. A.* 95, 14220–14225.
- Stehlíková, K., Zapletalová, E., Sedláčková, J., Hermanová, M., Vondráček, P., Maříková, T., Mazanec, R., Zámečník, J., Voháňka, S., Fajkus, J., et al. (2007). Quantitative analysis of CAPN3 transcripts in LGMD2A patients: Involvement of nonsense-mediated mRNA decay. *Neuromuscul. Disord.* 17, 143–147.
- Stitt, T.N., Drujan, D., Clarke, B.A., Panaro, F., Timofeyeva, Y., Kline, W.O., Gonzalez, M., Yancopoulos, G.D., and Glass, D.J. (2004). The IGF-1/PI3K/Akt pathway prevents expression of muscle atrophy-induced ubiquitin ligases by inhibiting FOXO transcription factors. *Mol. Cell* 14, 395–403.

- Street, S.F. (1983). Lateral transmission of tension in frog myofibers: A myofibrillar network and transverse cytoskeletal connections are possible transmitters. *J. Cell. Physiol.* 114, 346–364.
- Strobl, S., Fernandez-Catalan, C., Braun, M., Huber, R., Masumoto, H., Nakagawa, K., Irie, A., Sorimachi, H., Bourenkow, G., Bartunik, H., et al. (2000). The crystal structure of calcium-free human m-calpain suggests an electrostatic switch mechanism for activation by calcium. *Proc. Natl. Acad. Sci. U. S. A.* 97, 588–592.
- Stuelsatz, P., Pouzoulet, F., Lamarre, Y., Dargelos, E., Poussard, S., Leibovitch, S., Cottin, P., and Veschambre, P. (2010). Down-regulation of MyoD by calpain 3 promotes generation of reserve cells in C2C12 myoblasts. *J. Biol. Chem.* 285, 12670–12683.
- Stutzmann, G.E., and Mattson, M.P. (2011). Endoplasmic reticulum Ca²⁺ handling in excitable cells in health and disease. *Pharmacol. Rev.* 63, 700–727.
- Sun, L., Zhao, M., Liu, M., Su, P., Zhang, J., Li, Y., Yang, X., and Wu, Z. (2018). Suppression of FoxO3a attenuates neurobehavioral deficits after traumatic brain injury through inhibiting neuronal autophagy. *Behav. Brain Res.* 337, 271–279.
- Suzuki, A., Yoshida, M., Hayashi, K., Mizuno, Y., Hagiwara, Y., and Ozawa, E. (1994). Molecular organization at the glycoprotein-complex-binding site of dystrophin. Three dystrophin-associated proteins bind directly to the carboxy-terminal portion of dystrophin. *Eur. J. Biochem.* 220, 283–292.
- Suzuki, A., Pelikan, R.C., and Iwata, J. (2015). WNT/ β -catenin signaling regulates multiple steps of myogenesis by regulating step-specific targets. *Mol. Cell. Biol.* 35, 1763–1776.
- Suzuki, K., Hata, S., Kawabata, Y., and Sorimachi, H. (2004). Structure, activation, and biology of calpain. *Diabetes* 53 Suppl 1, S12-18.
- Sveen, M.L., Andersen, S.P., Ingelsrud, L.H., Blichter, S., Olsen, N.E., Jønck, S., Krag, T.O., and Vissing, J. (2013). Resistance training in patients with limb-girdle and becker muscular dystrophies. *Muscle Nerve* 47, 163–169.
- Sweeney, H.L., and Hammers, D.W. (2018). Muscle contraction. *Cold Spring Harb. Perspect. Biol.* 10.
- Swim, H.E., and Parker, R.F. (1957). Culture characteristics of human fibroblasts propagated serially. *Am. J. Hyg.* 66, 235–243.
- Taelman, V.F., Dobrowolski, R., Plouhinec, J.-L., Fuentealba, L.C., Vorwald, P.P., Gumper, I., Sabatini, D.D., and De Robertis, E.M. (2010). Wnt signaling requires sequestration of glycogen synthase kinase 3 inside multivesicular endosomes. *Cell* 143, 1136–1148.
- Tagliafico, E. (2004). TGF β /BMP activate the smooth muscle/bone differentiation programs in mesoangioblasts. *J. Cell Sci.* 117, 4377–4388.
- Tajbakhsh, S., Rocancourt, D., and Buckingham, M. (1996). Muscle progenitor cells failing to respond to positional cues adopt non-myogenic fates in myf-5 null mice. *Nature* 384, 266–270.
- Tajbakhsh, S., Borello, U., Vivarelli, E., Kelly, R., Papkoff, J., Duprez, D., Buckingham, M., and Cossu, G. (1998). Differential activation of Myf5 and MyoD by different Wnts in explants of mouse

- paraxial mesoderm and the later activation of myogenesis in the absence of Myf5. *Dev. Camb. Engl.* 125, 4155–4162.
- Tajbakhsh, S. (2009). Skeletal muscle stem cells in developmental versus regenerative myogenesis. *J. Intern. Med.* 266, 372–389.
- Takaishi, H., Konishi, H., Matsuzaki, H., Ono, Y., Shirai, Y., Saito, N., Kitamura, T., Ogawa, W., Kasuga, M., Kikkawa, U., et al. (1999). Regulation of nuclear translocation of forkhead transcription factor AFX by protein kinase B. *Proc. Natl. Acad. Sci. U. S. A.* 96, 11836–11841.
- Tallheden, T., van der Lee, J., Brantsing, C., Månsson, J.-E., Sjögren-Jansson, E., and Lindahl, A. (2005). Human serum for culture of articular chondrocytes. *Cell Transplant.* 14, 469–479.
- Talmadge, R.J. (2000). Myosin heavy chain isoform expression following reduced neuromuscular activity: potential regulatory mechanisms. *Muscle Nerve* 23, 661–679.
- Tapscott, S.J. (2005). The circuitry of a master switch: MyoD and the regulation of skeletal muscle gene transcription. *Development* 132, 2685–2695.
- Tagawa, K., Taya, C., Hayashi, Y., Nakagawa, M., Ono, Y., Fukuda, R., Karasuyama, H., Toyama-Sorimachi, N., Katsui, Y., Hata, S., et al. (2000). Myopathy phenotype of transgenic mice expressing active site-mutated inactive p94 skeletal muscle-specific calpain, the gene product responsible for limb girdle muscular dystrophy type 2A. *Hum. Mol. Genet.* 9, 1393–1402.
- Templeton, D.J. (2001). Protein kinases: getting NEKed for S6K activation. *Curr. Biol.* CB 11, R596-599.
- Tintignac, L.A., Lagirand, J., Batonnet, S., Sirri, V., Leibovitch, M.P., and Leibovitch, S.A. (2005). Degradation of MyoD mediated by the SCF (MAFbx) ubiquitin ligase. *J. Biol. Chem.* 280, 2847–2856.
- Todd, B., Moore, D., Deivanayagam, C.C.S., Lin, G., Chattopadhyay, D., Maki, M., Wang, K.K.W., and Narayana, S.V.L. (2003). A structural model for the inhibition of calpain by calpastatin: crystal structures of the native domain VI of calpain and its complexes with calpastatin peptide and a small molecule inhibitor. *J. Mol. Biol.* 328, 131–146.
- Tomlinson, A., Strapps, W.R., and Heemskerk, J. (1997). Linking Frizzled and Wnt signaling in *Drosophila* development. *Dev. Camb. Engl.* 124, 4515–4521.
- Toral-Ojeda, I., Aldanondo, G., Lasa-Elgarresta, J., Lasa-Fernández, H., Fernández-Torrón, R., López de Munain, A., and Vallejo-Illarramendi, A. (2016). Calpain 3 deficiency affects SERCA expression and function in the skeletal muscle. *Expert Rev. Mol. Med.* 18.
- Tran, H. (2002). DNA repair pathway stimulated by the forkhead transcription factor FOXO3a through the Gadd45 protein. *Science* 296, 530–534.
- Trimarchi, F., Favaloro, A., Fulle, S., Magaudo, L., Puglielli, C., and Di Mauro, D. (2006). Culture of human skeletal muscle myoblasts: timing appearance and localization of dystrophin-glycoprotein complex and vinculin-talin-integrin complex. *Cells Tissues Organs* 183, 87–98.
- Udd, B., Vihola, A., Sarparanta, J., Richard, I., and Hackman, P. (2005). Titinopathies and extension of the M-line mutation phenotype beyond distal myopathy and LGMD2J. *Neurology* 64, 636–642.

- Uezumi, A., Ojima, K., Fukada, S., Ikemoto, M., Masuda, S., Miyagoe-Suzuki, Y., and Takeda, S. (2006). Functional heterogeneity of side population cells in skeletal muscle. *Biochem. Biophys. Res. Commun.* 341, 864–873.
- Uezumi, A., Fukada, S., Yamamoto, N., Takeda, S., and Tsuchida, K. (2010). Mesenchymal progenitors distinct from satellite cells contribute to ectopic fat cell formation in skeletal muscle. *Nat. Cell Biol.* 12, 143–152.
- Urtasun, M., Sáenz, A., Roudaut, C., Poza, J.J., Urtizberea, J.A., Cobo, A.M., Richard, I., García Bragado, F., Leturcq, F., Kaplan, J.C., et al. (1998). Limb-girdle muscular dystrophy in Guipúzcoa (Basque Country, Spain). *Brain J. Neurol.* 121 (Pt 9), 1735–1747.
- Ussar, S., Wang, H.-V., Linder, S., Fässler, R., and Moser, M. (2006). The Kindlins: Subcellular localization and expression during murine development. *Exp. Cell Res.* 312, 3142–3151.
- Uzvölgyi, E., Kiss, I., Pitt, A., Arsenian, S., Ingvarsson, S., Udvardy, A., Hamada, M., Klein, G., and Sümegi, J. (1988). *Drosophila* homolog of the murine *Int-1* protooncogene. *Proc. Natl. Acad. Sci. U. S. A.* 85, 3034–3038.
- Vandeputte, C., Taymans, J.-M., Casteels, C., Coun, F., Ni, Y., Van Laere, K., and Baekelandt, V. (2010). Automated quantitative gait analysis in animal models of movement disorders. *BMC Neurosci.* 11, 92.
- Vannoy, C.H., Zhou, H., Qiao, C., Xiao, X., Bang, A.G., and Lu, Q.L. (2017). Adeno-associated virus-mediated mini-agrin delivery is unable to rescue disease phenotype in a mouse model of limb girdle muscular dystrophy type 2I. *Am. J. Pathol.* 187, 431–440.
- van der Velden, J.L.J., Schols, A.M.W.J., Willems, J., Kelders, M.C.J.M., and Langen, R.C.J. (2008). Glycogen synthase kinase 3 β suppresses myogenic differentiation through negative regulation of NFATc3. *J. Biol. Chem.* 283, 358–366.
- Vieira, N.M., Elvers, I., Alexander, M.S., Moreira, Y.B., Eran, A., Gomes, J.P., Marshall, J.L., Karlsson, E.K., Verjovski-Almeida, S., Lindblad-Toh, K., et al. (2015). Jagged 1 rescues the Duchenne muscular dystrophy phenotype. *Cell* 163, 1204–1213.
- Vignos, P.J., and Watkins, M.P. (1966). The effect of exercise in muscular dystrophy. *JAMA* 197, 843–848.
- Vissing, J. (2016). Limb girdle muscular dystrophies: classification, clinical spectrum and emerging therapies. *Curr. Opin. Neurol.* 29, 635–641.
- Vissing, J., and Duno, M. (2017). Reply: Dominant LGMD2A: alternative diagnosis or hidden digenism? *Brain J. Neurol.* 140, e8.
- Vissing, J., Barresi, R., Witting, N., Van Ghelue, M., Gammelgaard, L., Bindoff, L.A., Straub, V., Lochmüller, H., Hudson, J., Wahl, C.M., et al. (2016). A heterozygous 21-bp deletion in *CAPN3* causes dominantly inherited limb girdle muscular dystrophy. *Brain* 139, 2154–2163.
- Vitucci, D., Imperlini, E., Arcone, R., Alfieri, A., Canciello, A., Russomando, L., Martone, D., Cola, A., Labruna, G., Orrù, S., et al. (2018). Serum from differently exercised subjects induces myogenic differentiation in LHCN-M2 human myoblasts. *J. Sports Sci.* 36, 1630–1639.

- Wagner, K.R., Cohen, J.B., and Haganir, R.L. (1993). The 87K postsynaptic membrane protein from Torpedo is a protein-tyrosine kinase substrate homologous to dystrophin. *Neuron* 10, 511–522.
- Walton, J.N., and Natrass, F.J. (1954). On the classification, natural history and treatment of the myopathies. *Brain J. Neurol.* 77, 169–231.
- Wang, X. (2001). Regulation of elongation factor 2 kinase by p90RSK1 and p70 S6 kinase. *EMBO J.* 20, 4370–4379.
- Wang, P., Zhou, Z., Hu, A., Ponte de Albuquerque, C., Zhou, Y., Hong, L., Sierecki, E., Ajiro, M., Kruhlak, M., Harris, C., et al. (2014). Both decreased and increased SRPK1 levels promote cancer by interfering with PHLPP-mediated dephosphorylation of Akt. *Mol. Cell* 54, 378–391.
- Wang, S., Krinks, M., Lin, K., Luyten, F.P., and Moos, M. (1997). Frzb, a secreted protein expressed in the Spemann organizer, binds and inhibits Wnt-8. *Cell* 88, 757–766.
- Wang, Y., Schnegelsberg, P.N., Dausman, J., and Jaenisch, R. (1996). Functional redundancy of the muscle-specific transcription factors Myf5 and myogenin. *Nature* 379, 823–825.
- Wang, Y., Hao, Y., and Alway, S.E. (2011). Suppression of GSK-3 activation by M-cadherin protects myoblasts against mitochondria-associated apoptosis during myogenic differentiation. *J. Cell Sci.* 124, 3835–3847.
- Warhol, M.J., Siegel, A.J., Evans, W.J., and Silverman, L.M. (1985). Skeletal muscle injury and repair in marathon runners after competition. *Am. J. Pathol.* 118, 331–339.
- Watkins, S.C., Cullen, M.J., Hoffman, E.P., and Billington, L. (2000). Plasma membrane cytoskeleton of muscle: a fine structural analysis. *Microsc. Res. Tech.* 48, 131–141.
- Wernig, A., Irintchev, A., and Weisshaupt, P. (1990). Muscle injury, cross-sectional area and fibre type distribution in mouse soleus after intermittent wheel-running. *J. Physiol.* 428, 639–652.
- Wettenhall, R.E., Erikson, E., and Maller, J.L. (1992). Ordered multisite phosphorylation of Xenopus ribosomal protein S6 by S6 kinase II. *J. Biol. Chem.* 267, 9021–9027.
- White, J., Barro, M.V., Makarenkova, H.P., Sanger, J.W., and Sanger, J.M. (2014). Localization of sarcomeric proteins during myofibril assembly in cultured mouse primary skeletal myotubes. *Anat. Rec. Hoboken NJ* 2007 297, 1571–1584.
- Winbanks, C.E., Wang, B., Beyer, C., Koh, P., White, L., Kantharidis, P., and Gregorevic, P. (2011). TGF- β regulates miR-206 and miR-29 to control myogenic differentiation through regulation of HDAC4. *J. Biol. Chem.* 286, 13805–13814.
- Winokur, S.T. (2003). Expression profiling of FSHD muscle supports a defect in specific stages of myogenic differentiation. *Hum. Mol. Genet.* 12, 2895–2907.
- Wozniak, A.C., and Anderson, J.E. (2007). Nitric oxide-dependence of satellite stem cell activation and quiescence on normal skeletal muscle fibers. *Dev. Dyn.* 236, 240–250.

- Wu, Y.Z., Crumley, R.L., Armstrong, W.B., and Caiozzo, V.J. (2000). New perspectives about human laryngeal muscle: single-fiber analyses and interspecies comparisons. *Arch. Otolaryngol. Head Neck Surg.* 126, 857–864.
- Yaffe, D., and Saxel, O. (1977). A myogenic cell line with altered serum requirements for differentiation. *Differ. Res. Biol. Divers.* 7, 159–166.
- Yalvac, M.E., Amornvit, J., Braganza, C., Chen, L., Hussain, S.-R.A., Shontz, K.M., Montgomery, C.L., Flanigan, K.M., Lewis, S., and Sahenk, Z. (2017). Impaired regeneration in calpain-3 null muscle is associated with perturbations in mTORC1 signaling and defective mitochondrial biogenesis. *Skelet. Muscle* 7.
- Yamaguchi, H., Hsu, J.L., and Hung, M.-C. (2012). Regulation of ubiquitination-mediated protein degradation by survival kinases in cancer. *Front. Oncol.* 2, 15.
- Yamamoto, N., Isobe, M., Negishi, A., Yoshimasu, H., Shimokawa, H., Ohya, K., Amagasa, T., and Kasugai, S. (2003). Effects of autologous serum on osteoblastic differentiation in human bone marrow cells. *J. Med. Dent. Sci.* 50, 63–69.
- Yamazaki, Y., Kamei, Y., Sugita, S., Akaike, F., Kanai, S., Miura, S., Hirata, Y., Troen, B.R., Kitamura, T., Nishino, I., et al. (2010). The cathepsin L gene is a direct target of FOXO1 in skeletal muscle. *Biochem. J.* 427, 171–178.
- Yang, X., Yang, C., Farberman, A., Rideout, T.C., de Lange, C.F.M., France, J., and Fan, M.Z. (2008). The mammalian target of rapamycin-signaling pathway in regulating metabolism and growth. *J. Anim. Sci.* 86, E36-50.
- Yuan, H., Mao, J., Li, L., and Wu, D. (1999). Suppression of glycogen synthase kinase activity is not sufficient for leukemia enhancer factor-1 activation. *J. Biol. Chem.* 274, 30419–30423.
- Yuan, Y., Shi, X., Liu, Y., and Yang, G. (2011). FoxO1 regulates muscle fiber-type specification and inhibits calcineurin signaling during C2C12 myoblast differentiation. *Mol. Cell. Biochem.* 348, 77–87.
- Yuasa, K., Hagiwara, Y., Ando, M., Nakamura, A., Takeda, S., and Hijikata, T. (2008). MicroRNA-206 is highly expressed in newly formed muscle fibers: implications regarding potential for muscle regeneration and maturation in muscular dystrophy. *Cell Struct. Funct.* 33, 163–169.
- Zammit, P.S. (2017). Function of the myogenic regulatory factors Myf5, MyoD, Myogenin and MRF4 in skeletal muscle, satellite cells and regenerative myogenesis. *Semin. Cell Dev. Biol.* 72, 19–32.
- Zassadowski, F., Pokorna, K., Ferre, N., Guidez, F., Llopis, L., Chourbagi, O., Chopin, M., Poupon, J., Fenaux, P., Ann Padua, R., et al. (2015). Lithium chloride antileukemic activity in acute promyelocytic leukemia is GSK-3 and MEK/ERK dependent. *Leukemia* 29, 2277–2284.
- Zatz, M., and Starling, A. (2005). Calpains and disease. *N. Engl. J. Med.* 352, 2413–2423.
- Zatz, M., Vainzof, M., and Passos-Bueno, M.R. (2000). Limb-girdle muscular dystrophy: one gene with different phenotypes, one phenotype with different genes. *Curr. Opin. Neurol.* 13, 511–517.
- Zeschnigk, M., Kozian, D., Kuch, C., Schmoll, M., and Starzinski-Powitz, A. (1995). Involvement of M-cadherin in terminal differentiation of skeletal muscle cells. *J. Cell Sci.* 108 (Pt 9), 2973–2981.

Zhang, J., Zhang, L.-L., Shen, L., Xu, X.-M., and Yu, H.-G. (2013). Regulation of AKT gene expression by cisplatin. *Oncol. Lett.* 5, 756–760.

Zhao, J., Brault, J.J., Schild, A., Cao, P., Sandri, M., Schiaffino, S., Lecker, S.H., and Goldberg, A.L. (2007). FoxO3 coordinately activates protein degradation by the autophagic/lysosomal and proteasomal pathways in atrophying muscle cells. *Cell Metab.* 6, 472–483.

(2012). *The Big Picture: Medical Biochemistry* (McGraw-Hill Education).